



Durham E-Theses

An N.Q.R. study of some inorganic compounds

Gilmore, P.

How to cite:

Gilmore, P. (1980) *An N.Q.R. study of some inorganic compounds*, Durham theses, Durham University.
Available at Durham E-Theses Online: <http://etheses.dur.ac.uk/7962/>

Use policy

The full-text may be used and/or reproduced, and given to third parties in any format or medium, without prior permission or charge, for personal research or study, educational, or not-for-profit purposes provided that:

- a full bibliographic reference is made to the original source
- a [link](#) is made to the metadata record in Durham E-Theses
- the full-text is not changed in any way

The full-text must not be sold in any format or medium without the formal permission of the copyright holders.

Please consult the [full Durham E-Theses policy](#) for further details.

P. GILMORE B.Sc.

AN N.Q.R. STUDY OF SOME INORGANIC COMPOUNDS

Declaration

Subject to the provisions of the regulations for higher degrees of the University of Durham, I agree to this thesis being made available through the University Library for study or photocopy.

September, 1980.

AN E.S.R. STUDY OF SOME
INORGANIC COMPOUNDS.

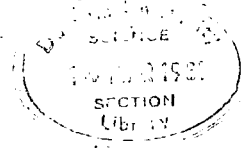
by

P. Gilmore B.Sc.
University College

A thesis submitted for the degree of Doctor of Philosophy
in the University of Durham.

The copyright of this thesis rests with the author.
No quotation from it should be published without
his prior written consent and information derived
from it should be acknowledged.

September, 1980.



To those I love
To those I loved

The copyright of this thesis rests with the author.
No quotation from it should be published without his
prior written consent and information derived from it
should be acknowledged.

Acknowledgements

I should like to express my gratitude to Dr. R.J. Lynch and Professor T.C. Waddington with whose help and guidance this research was carried out.

I also wish to thank the technical staff and many other members of the Department of Chemistry for their practical support and useful discussion.

I am indebted to the Science Research Council for a maintenance grant and for assistance to attend the Third International Symposium on Nuclear Quadrupole Resonance.

The work described in this thesis was carried out in the University of Durham between 1973 and 1976. It has not been submitted for any other degree and is the original work of the author, except where acknowledged by reference.

CONTENTS

	page
CHAPTER 1: THEORY OF THE NUCLEAR QUADRUPOLE INTERACTION	
Introduction	1
Electric field gradient and asymmetry parameter	4
The quadrupole Hamiltonian	5
Zeeman splitting of nuclear quadrupole resonances	14
Introduction	14
Single crystal studies	15
Polycrystalline sample studies	17
Temperature dependence of n.q.r.	24
Introduction	24
The Bayer theory	24
CHAPTER 2: THE INTERPRETATION OF N.Q.R. SPECTROSCOPY	
General theory	32
Approximate methods	39
The Townes and Dailey method	43
Temperature effect on n.q.r.	51
CHAPTER 3: EXPERIMENTAL DETECTION OF N.Q.R.	
Introduction	53
Marginal oscillator	54
Robinson oscillator	55
Super-regenerative oscillator	58
Signal enhancements	
a) Locked s.r.o.	61
b) Synchroniser	63
c) Computer of average transients	64
d) Sinusoidal Zeeman modulation	71

CHAPTER 3 (contd.)

Zeeman n.q.r. spectroscopy	77
Pulse n.q.r. and double - resonance n.q.r. spectroscopy							
Pulse n.q.r. spectrometer	79
Double resonance n.q.r. spectroscopy	82

CHAPTER 4: ^{35}Cl N.Q.R. INVESTIGATION OF S-Cl BOND IN VARIOUS
INORGANIC COMPOUNDS

Introduction	84
Background	85
The reaction of SCl_2 with various Lewis acids	89
Sulphur dichloride and antimony pentachloride	90
Sulphur monochloride and antimony pentachloride	92
Sulphur dichloride and aluminium trichloride	93
Sulphur dichloride and titanium tetrachloride	96
Trichlorosulphonium tetrachloroiodate	98
Sulphur dichloride and boron trichloride	99
Sulphur dichloride and tin tetrachloride	100
Discussion of ^{35}Cl n.q.r. results	102
a) number of n.q.r. lines	102
b) temperature dependence of n.q.r. signals	103
Structure SCl_3^{\oplus} complexes	105
Thionyl chloride	109
Di-t-butyl ketimino thionyl chloride	113
Pentafluoro sulphur VI chloride	114
Appendix to Chapter 4							
SCl_2 and SbCl_5	116
S_2Cl_2 and SbCl_5	116
SCl_2 and AlCl_3	117
SCl_2 and TiCl_4	118
Methods of analysis used	119

CHAPTER 5: ^{35}Cl N.Q.R. INVESTIGATION OF ZnCl_2 AND SOME OF
ITS COMPLEXES

Introduction	120
Zinc chloride and ether - donor adducts	121
Preparation	124
Structures of ZnCl_2 . ether complexes	133
Zinc chloride.tetrahydrofuran adduct	133
Zinc chloride.1,4 dioxan adduct	135
Zinc chloride.monoglyme adduct	136
Structure of ZnCl_2 .ether complexes	138
Zinc chloride. amine complexes	139

CHAPTER 6: N.Q.R. INVESTIGATION OF GROUP IV TETRACHLORIDES

Introduction	142
Silicon tetrachloride	155
Germanium tetrachloride	159
Discussion	161

CHAPTER 7: MISCELLANEOUS INVESTIGATIONS

1) The asymmetry parameter in the P-Cl bond	167
Introduction	167
Discussion	170
2) The ^{59}Co n.q.r. of π -cyclopentadienyl-cobalt-dicarbonyl	172
Introduction	172
Discussion	172
3) ^{35}Cl n.q.r. investigation of asymmetry in the C-Cl bond of	175
chloromethanes	175
Introduction	175
Methylene chloride	175
Discussion	177

REFERENCES

AN N.Q.R. STUDY OF SOME INORGANIC COMPOUNDS

F. GILMORE B.Sc.

ABSTRACT

Nuclear quadrupole resonance (n.q.r.) spectroscopy is a solid state technique which, when applied to samples containing quadrupolar nuclei, can elucidate fine structural differences and internal electronic distribution. It has been applied to a variety of inorganic compounds containing the quadrupolar nuclei, chlorine and cobalt, (i.e. ^{35}Cl and ^{59}Co). In order to remove spurious responses on a Robinson type n.q.r. spectrometer, apparatus has been constructed to generate sinusoidal magnetic modulation.

Monomeric and chain- structures have been proposed for members of a series of complexes between zinc chloride and ethers.

Marked asymmetry in the electric field gradient at chlorine has been reported for tetrachlorides of group IV. Although distortion of the molecules in the solid and disorder in the lattice are likely to produce some asymmetry, it is suggested that $p\pi-d\pi$ bonding makes a major contribution. Such bonding is postulated for the tetrachlorides above carbon tetrachloride.

Zeeman lineshape studies on thionyl chloride and tetrachlorophenyl phosphorane have yielded estimates for π -bonding in the bonds to chlorine.

A variable temperature study of the ^{59}Co quadrupole resonances of π -cyclopentadienyl cobalt dicarbonyl has revealed the absence of phase changes between 77K and 260K.

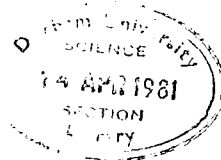
Introduction

All forms of spectroscopy involve the observation of transitions between different energy levels. The presence of different energy levels associated with a nucleus may be appreciated by considering the properties of a nucleus. Formed of neutrons and protons, a nucleus possesses positive charge. It may also possess a second property, spin angular momentum. Unless this is zero, the nucleus is considered to spin about an axis through its centre. Some nuclei are known to have spin because they exhibit magnetic properties which can be associated with the magnetic field generated by the spinning of the charged nucleus. This spinning is quantified as nuclear spin angular momentum and is denoted by the vector \vec{I} . The scalar part of \vec{I} is related to the dimensionless nuclear spin quantum number, I , by

$$\sqrt{I(I+1)} \hbar^2 \quad (1)$$

where \hbar is Planck's constant divided by 2π and I is the maximum projection of \vec{I} . There are $(2I + 1)$ possible energy levels for a nucleus.

The nuclear spin quantum number, I , is of further importance because it provides information on the "shape" of the nucleus. If I is greater than $\frac{1}{2}$, the nucleus appears to possess a non-spherical charge distribution i.e. it is extended or compressed along a certain direction. If non-spherical, the distribution of charge in the nucleus



gives rise to an electric quadrupole moment, Q . This quantity can be either positive or negative, as shown in Fig. 1.

Being an electrical property, the nuclear electric quadrupole moment, Q , will interact with an electric field. However, no net effect is observed in a uniform electric field because the turning forces exerted on the nucleus are equal. If the field is non-uniform, however, that is, if it can be represented as an electric field gradient (e.f.g.), the torques experienced by the anti-parallel dipoles of the nucleus are not equal and so the nucleus tends to assume a particular orientation of lower potential energy. Due to the spin of the nucleus, this orientation takes the form of a precessional motion about the direction of the e.f.g. as in Fig. 2a. This direction is taken as defining one of the principal axes of the e.f.g. The $(2I + 1)$ energy levels allowed for a nucleus correspond to different orientations about it. The levels are labelled by the magnetic quantum numbers, m , which are themselves projections of \vec{I} on to this axis. They take the values $I, I - 1, \dots -I$.

The electric field gradient (e.f.g.) experienced by a quadrupolar nucleus is generated by the local electronic distribution and no external field need be applied to a sample in order that these energy levels be produced. The observation of transitions between the different m levels is termed (pure) nuclear quadrupole resonance (n.q.r.) spectroscopy. Because of the very fast molecular motion

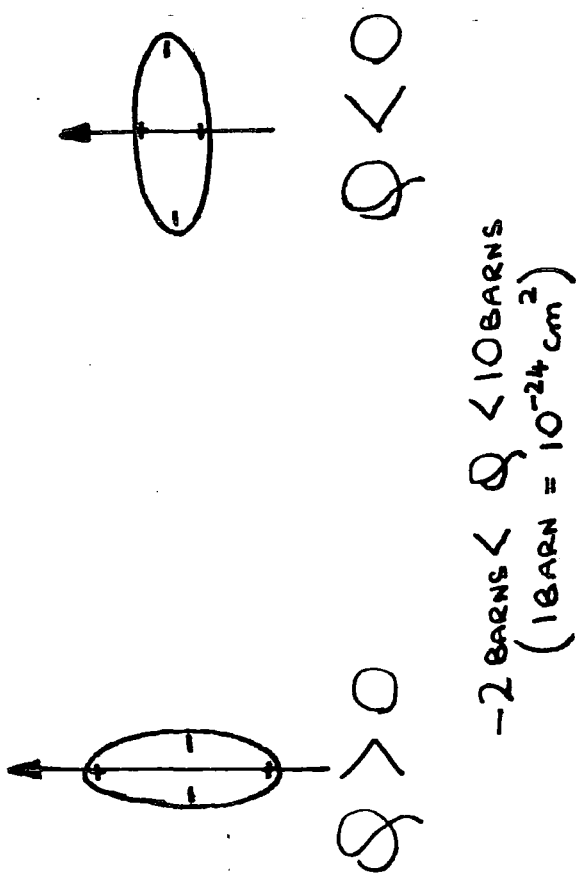


Fig.1. The electric quadrupole moment, Q , of a nucleus

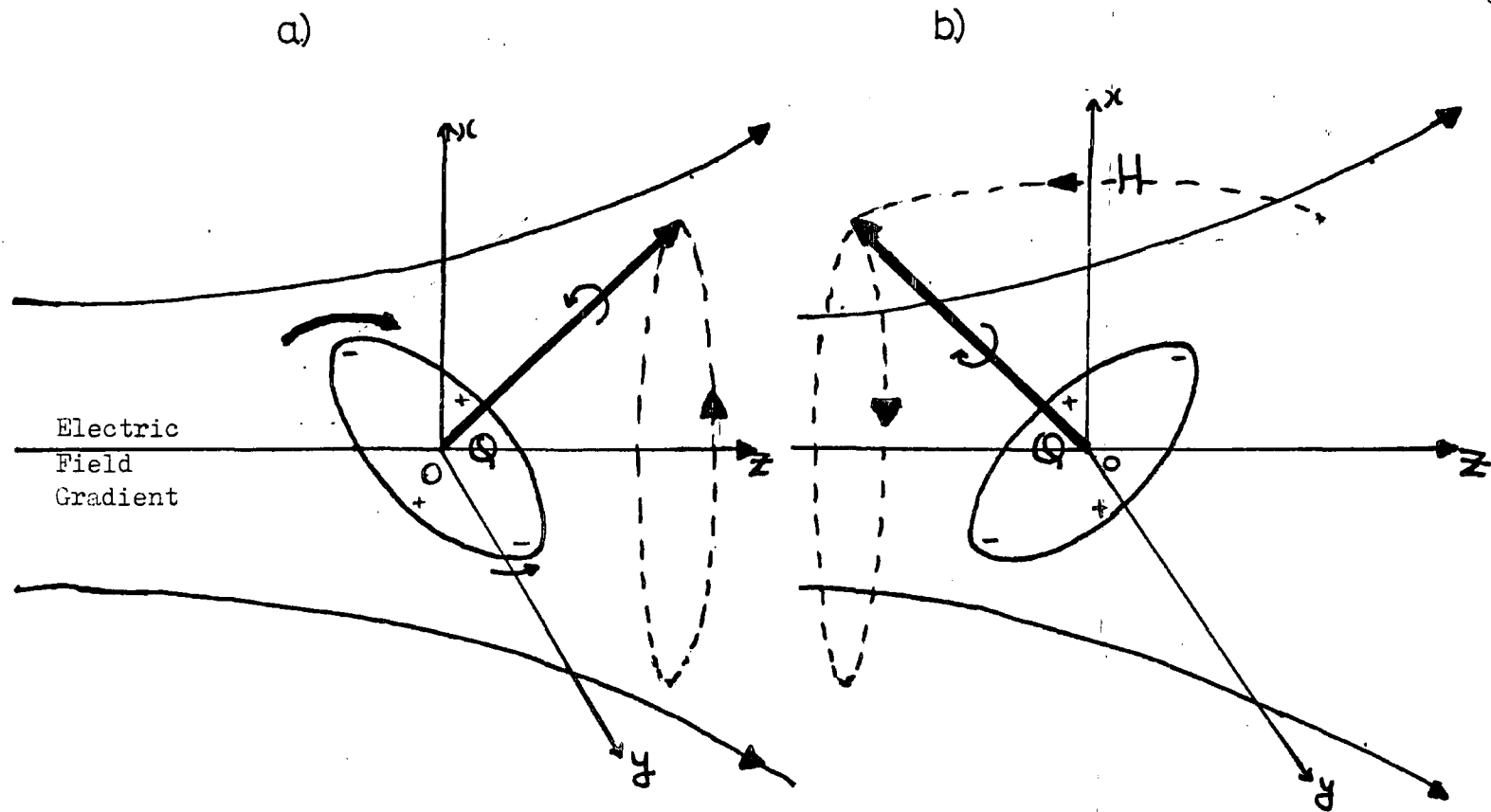


Fig2 Effect of r.f. field (in x direction) upon precession of quadrupole moment (Q) of nucleus.

and high collision rates in liquids and gases which would tend to average to zero the e.f.g. at the nucleus, n.q.r. spectroscopy is a solid state technique. If the e.f.g. is symmetrical about the direction Oz in Fig. 2a, the torques experienced by the nucleus are clearly proportional to the strength of the field gradient and to the extent to which the nucleus' charge distribution departs from spherical symmetry, that is to Q. By convention, the quantity Q appears in the interaction expression as eQ and the electric field gradient as -eq. Continuing with this convention, the torque is proportional to $[e^2qQ]$ which is termed the nuclear quadrupole coupling constant.

In order that the transitions between the quadrupolar energy levels may be observed, excitation from lower levels to less populated levels of higher potential energy must be effected by absorption of energy at a resonant frequency. Resonance occurs when

$$\Delta E = h\nu \quad (2)$$

where h is Planck's constant, ΔE is the energy difference between the two levels and ν is the frequency of electromagnetic (e.m.) radiation. The frequencies (ν) required for n.q.r. spectroscopy lie in the radio-frequency region of the e.m. spectrum. The absorption of the oscillating radio frequency field is through the interaction of its magnetic component with the nuclear magnetic dipole moment of the nucleus.(Fig.2b). The oscillating electric component has no effect because the nucleus does not possess an electric dipole. Although nuclei with higher spin quantum numbers possess nuclear multipole moments of higher order than

those already mentioned, the magnitude of their effect diminishes rapidly with increasing order and only the nuclear magnetic octupole and the nuclear electric hexadecapole are of any importance. (5,6).

Electric field gradient and asymmetry parameter

The formation of a chemical bond between atoms causes a strong non-uniform electric field along the direction of the bond. This produces an e.f.g. at each of the bonded nuclei which may be represented by a tensor having nine components in the Cartesian (x,y,z) co-ordinate system. For monodentate quadrupolar nuclei e.g. ^{35}Cl , the direction Oz of Fig. 2a (the z axis of the e.f.g.) is usually taken as lying along the bond axis. The e.f.g. experienced by such a nucleus is due to the change in electrostatic potential (V) at the nucleus, created by all the surrounding charges - nuclear and electronic. The z component of the e.f.g. is therefore:

$$-\frac{\partial^2 V}{\partial z^2} = V_{zz} \quad (3)$$

which is defined as $e q$, (e is the electronic charge).

As the e.f.g. is produced entirely by charges external to the nucleus (1) the components of the electrostatic potential (V) fulfill the Laplace condition and the e.f.g. tensor is

symmetric and traceless. i.e.

$$V_{xx} + V_{yy} + V_{zz} = 0 \quad (4)$$

where these are the diagonal terms of the e.f.g. tensor and represent the gradients along the three principal axes in Cartesian co-ordinates. The axes are labelled such that

$|V_{zz}| \geq |V_{yy}| \geq |V_{xx}|$. The nuclear quadrupole coupling constant, $|e^2qQ|$, contains the term eQ , which is V_{zz} from equation (3).

Another parameter, η , is defined as

$$\eta = \frac{|V_{xx} - V_{yy}|}{V_{zz}} \quad (5)$$

called the asymmetry parameter. The value of the asymmetry parameter (η) describes the deviation from axial symmetry of the e.f.g. It can take values in the range $0 \leq \eta \leq 1$. Taken with the Eulerian angles (discussed on p.14), $|e^2qQ|$ and η fully describe the diagonalised e.f.g. In chapter 2, their values are related to bonding characteristics and other information of structure. A fuller semi-classical description of the quantum mechanical derivation of the quadrupole interaction is now given but reference to Abragam (2) and Slichter (3) may be made for a rigorous approach.

The Quadrupole Hamiltonian

Let $V(X)$ be the electrostatic potential produced by all the charges (both electronic and nuclear) around a quadrupolar nucleus situated at point X in the crystal lattice. (Fig. 3).

The point X is represented in Cartesian co-ordinates by

(x_1, x_2, x_3) whose origin is set at the nucleus' centre. Also,

let Ze be the nuclear charge with a density of $\rho(x)$ at the point X .

The nuclear volume element $d\tau_N = dx_1 dx_2 dx_3$ has a charge

$(\rho(X).d\tau_N)$ which interacts with the electrostatic potential

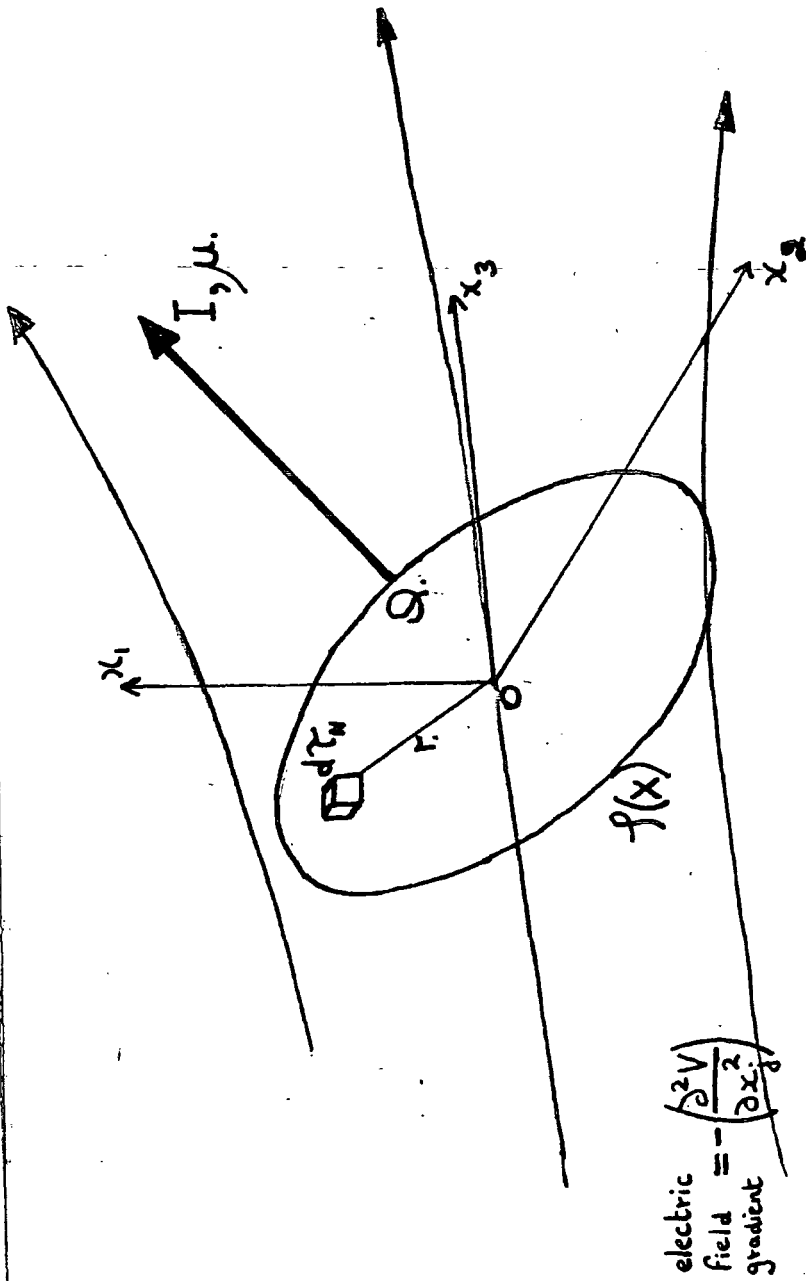


Fig. 3. Interaction of nucleus with electric field gradient.

$V(X)$. The potential energy, dE , is then

$$dE = - \rho(X) \cdot d\tau_N \cdot V(X) \quad (6)$$

By integration, the total energy of interaction (E) of the nucleus with the electrostatic potential field is thus

$$E = - \int_{\text{space}} \rho(X) V(X) d\tau_N \quad (7)$$

To take account of its variation over the nuclear volume,

$V(X)$ can be expanded as a Taylor's series about the origin,

0.

$$\begin{aligned} V(X) = V_0 + \left\{ x_1 \left(\frac{\partial V}{\partial x_1} \right)_0 + x_2 \left(\frac{\partial V}{\partial x_2} \right)_0 + x_3 \left(\frac{\partial V}{\partial x_3} \right)_0 \right\} \\ + \frac{1}{2!} \left\{ x_1^2 \left(\frac{\partial^2 V}{\partial x_1^2} \right)_0 + x_2^2 \left(\frac{\partial^2 V}{\partial x_2^2} \right)_0 + x_3^2 \left(\frac{\partial^2 V}{\partial x_3^2} \right)_0 \right. \\ \left. + x_1 x_2 \left(\frac{\partial^2 V}{\partial x_1 \partial x_2} \right)_0 + x_1 x_3 \left(\frac{\partial^2 V}{\partial x_1 \partial x_3} \right)_0 + x_2 x_3 \dots \dots \right\} \end{aligned} \quad (8)$$

Equation (8) can be re-stated in terms using j and k to

index the co-ordinates which when substituted in equation

(7) gives

$$E = - \int_{\text{space}} \rho(X) \left\{ V_0 + \sum_{j=1}^3 \left(\frac{\partial V}{\partial x_j} \right)_0 x_j + \frac{1}{2!} \sum_{j=1, k=1}^{3,3} \left(\frac{\partial^2 V}{\partial x_j \partial x_k} \right)_0 x_j x_k + \frac{1}{3!} [\dots] \right\} d\tau_N \quad (9)$$

By defining

$$\int_{\text{space}} \rho(X) x_j d\tau_N = D_j, \quad \text{the nuclear electric dipole moment} \quad (10)$$

$$\text{and } \int_{\text{space}} \rho(X) x_j x_k d\tau_N = Q'_{jk}, \quad \text{the nuclear electric quadrupole moment tensor} \quad (11)$$

equation (9) becomes

$$E = V_0 \int_{\text{space}} \rho(X) d\tau_N + \sum_{j=1}^3 D_j \left(\frac{\partial V}{\partial x_j} \right)_0 + \frac{1}{2} \sum_{j=1, k=1}^{3,3} Q'_{jk} \left(\frac{\partial^2 V}{\partial x_j \partial x_k} \right)_0 + \text{higher terms} \quad (12)$$

The first term integrates the nuclear charge density and

therefore becomes $V_0 \cdot Ze$ and is a constant which is unaffected

by the nuclear shape or orientation. It is therefore of

no importance in the generation of nuclear energy levels

and is not considered further. The second term of equation (12)

involves the nuclear electric dipole moment. Experimentally and theoretically the nuclear electric dipole moment has been shown to be zero (4) so if the induced moment is also set at zero the second term vanishes. Thus in equation (12) only quadrupolar and higher terms are left. The even terms are believed to be zero on grounds of symmetry and cancellation. The fifth term, the hexadecapole term, typically represents an energy of only about 10^{-8} cm^{-1} ($\approx 1 \text{ kHz}$) (5,6). It may usually be ignored when compared to the corresponding value of about 10^{-3} cm^{-1} ($\sim 30 \text{ MHz}$) for the quadrupole term. Furthermore, when the nuclear spin quantum number, I , is less than 2, the hexadecapole is zero. Although its effects have been observed (5,6), it will be ignored here.

Hence, if we define

$$V_{jk} = \left(\frac{\partial^2 V}{\partial x_j \partial x_k} \right)_0 \quad (13)$$

and consider only the orientation dependent terms

$$E = \frac{1}{2} \sum_{\substack{j=1 \\ k=1}}^{3,3} Q'_{jk} V_{jk} \quad (14)$$

V_{jk} represents the average value of the principal components of the e.f.g. over the ground state wave function of the molecule. By generating a new co-ordinate system from x_1 , x_2 and x_3 by rotations, V_{jk} can be redefined such that (3)

$$V_{jk} = 0 \quad \text{if } j \neq k \quad (15)$$

That is, the matrix-tensor can be diagonalised and its new axes are usually referred to as the "principal axis system".

Since the e.f.g. is produced entirely by charges external to the nucleus (1), the terms of V_{jk} fulfil the Laplace condition and therefore, evaluated at the origin, give

$$\sum_{j=1}^3 V_{jj} = 0 \quad (16)$$

That is, the matrix-tensor is traceless also. In order to simplify the nuclear electric quadrupole moment tensor, Q_{jk} , it is specified as traceless, reducing the number of independent components to five. The expression used to do this is

$$Q_{jk} = \frac{2}{3} Q'_{jk} - \delta_{jk} \sum_{i=1}^3 Q'_{ii} \quad (17)$$

where i is an index on the pattern of j and k and where δ_{jk} is the Kronecker delta.

This simplification is achieved by reorientation of the principal axis system such that the maximum component of the e.f.g. and the z axis coincide. Substituting equation (17) into equation (14) gives

$$E = 1/6 \sum_{\substack{j=1 \\ k=1}}^{3,3} Q_{jk} V_{jk} + \delta_{jk} V_{jk} \sum_{i=1}^3 Q_{ii} \quad (18)$$

However, since Q_{jk} is a traceless tensor, the sum of the diagonal terms is zero and the second term in equation (18) vanishes. Thus, the total energy of interaction of the nucleus (E) is

$$E = 1/6 \sum_{\substack{j=1 \\ k=1}}^{3,3} Q_{jk} \cdot V_{jk} \quad (19)$$

To obtain the quadrupole Hamiltonian we must substitute Q_{jk} with the quantum mechanical operator \hat{Q}_{jk} , which is carried out by replacing the classical charge density

$\rho(X)$ by its operator $\hat{\rho}(X)$. Given by

$$(3) \quad \hat{\rho}(X) = \sum_n q_n \delta(X - X_n) \quad (20)$$

the sum is over all n nuclear particles of charge q_n .

The δ - function is zero for all values of X except $X = X_n$ when its value is one. Clearly, n equals the number of protons in the nucleus, i.e. the atomic number, z, whence

$$\hat{\mathcal{F}}(X) = e \sum_{\text{protons, } n=1}^z \delta(X - X_n) \quad (21)$$

By substitution of equation (11) into equation (17), replacing $\mathcal{F}(X)$ by $\hat{\mathcal{F}}(X)$, the expression for the operator \hat{Q}_{jk} is gained.

From equation (19), therefore, we can write the quadrupole Hamiltonian (H_Q) as

$$H_Q = 1/6 \sum_{\substack{j=1 \\ k=1}}^{3,3} \hat{Q}_{jk} \cdot V_{jk} \quad (22)$$

The separation of the ground state of a nucleus from an excited state is far greater than the magnitude of H_Q .

As we are only interested in the spacial reorientation of a nucleus in its ground state, the perturbation calculation need only concern a nuclear eigenstate (ground) described by the total angular moment, I, and its $(2I + 1)$ components, m. The properties of \hat{Q}_{jk} allow the use of a theorem (Wigner-Eckart) which relates matrix elements of irreducible tensor operators to other matrices. Used with a tensor defining a new quantity eQ where Q is termed the nuclear electric quadrupole moment, a new expression for the Hamiltonian is yielded.

$$eQ = \langle II | e \sum_{n=1}^z (3z^2 - r^2) | II \rangle \quad (23)$$

We can write the quadrupole Hamiltonian as

$$H_Q = \frac{eQ}{6I(2I+1)} \sum_{\substack{j=1 \\ k=1}}^{3,3} \left\{ \frac{3}{2} (I_j I_k + I_k I_j - \delta_{jk} I^2) \right\} \cdot V_{jk} \quad (24)$$

The nine components of Q_{jk} have been capable of reduction into one constant for the nucleus, Q, because its fast

rotation averages the interaction of the nuclear charge distribution with the external electrostatic field. From equation (23) it is clear that eQ is zero for a spherical nucleus, positive if the spin axis is the major axis of the ellipsoidal nucleus and negative if the spin axis is a minor axis. Q has dimensions of r^2 and is usually expressed in units of 10^{-24} cm^2 . Typical values are given in Table 1 for a series of nuclei.

Equation (24) still contains a tensor quantity V_{jk} which may be simplified by quantum mechanical means (3). Equation (23) transposes eQ to place the maximum component of the nuclear magnetic moment along the z axis, i.e. $I_z = I$.

The derivative of potential, V_{jk} , may be simplified if the small effects of charge distribution within the nucleus are ignored. This allows use of the Laplace formulation i.e. equation (4). Only two parameters are now required to describe the magnitude of the electric field gradient (e.f.g.). One is the asymmetry parameter—equation (5)

— which may take values in the range $0 \leq \eta \leq 1$. The other parameter used is the maximum principal component which is

by convention taken as $\frac{\partial^2 V}{\partial z^2}$. i.e.

$$eQ = \frac{\partial^2 V}{\partial z^2} = V_{zz} \quad (25)$$

A simplified expression for the Hamiltonian is obtained, from which Das and Hahn (32) derive solutions to the quantum mechanical expression for the potential energy. The energy levels obtained are classified according to the quantum number appropriate to the I_z operator, viz. m , the nuclear magnetic quantum number. Das and Hahn

TABLE 1

NUCLEUS	SPIN I	QUADRUPOLE MOMENT Q, ($\times 10^{24}$ cm ²)
² H	1	+ 0.0027965
¹⁴ N	1	+ 0.0166
³⁵ Cl	3/2	- 0.0802
³⁷ Cl	3/2	- 0.0632
⁷⁹ Br	3/2	+ 0.332
⁸¹ Br	3/2	+ 0.282
⁵⁹ Co	7/2	+ 0.404

show that the energy levels for the case of $\eta = 0$ are given by

$$E_m = \frac{e^2qQ}{4I(2I-1)} \left\{ 3m^2 - I(I+1) \right\} \quad (26)$$

Due to the m^2 term in equation (26) the energy levels are doubly degenerate in m . For half integral spin nuclei there are $(I + \frac{1}{2})$ doubly degenerate levels and for integral spins there are $(I + 1)$ levels where I are doubly degenerate and the $m = 0$ level is non-degenerate. Transitions between these different m levels are induced by the applied radio-frequency (r.f.) radiation. The selection rule for the magnetic dipole transitions is

$$\Delta m = \pm 1 \quad (27)$$

The absorption and reorientation of the nucleus is shown in Fig. 2b. The frequency of the r.f. radiation required to produce a transition is given by

$$\nu = \frac{E_{m+1} - E_m}{h} \quad (28)$$

where E_{m+1} and E_m represent the different energy levels and h is Planck's constant. Substitution in equation (26) for $I = 3/2$ nuclei gives

$$\text{for } m = \pm \frac{1}{2} \text{ level, } E = - \frac{e^2qQ}{4} \quad (29)$$

$$\text{for } m = \pm \frac{3}{2} \text{ level, } E = + \frac{e^2qQ}{4}$$

and so for $I = 3/2$, there is one transition of frequency,

$$\nu_{\pm\frac{3}{2} \leftrightarrow \pm\frac{1}{2}} = \frac{e^2qQ}{2h} \quad (30)$$

From frequency (ν), therefore, can be obtained $\left| \frac{e^2qQ}{h} \right|$

that is, the nuclear quadrupole coupling constant in units of frequency (MHz). Further substitutions in equation (26) yield expressions for the energy levels for nuclei of different values of I . Thus, if the asymmetry parameter is zero,

for $I = 1$

$$\nu_{0 \leftrightarrow 1} = \frac{3}{4} \frac{e^2 g Q}{h} \quad (31)$$

for $I = 5/2$

$$\begin{aligned} \nu_{\pm 1/2 \leftrightarrow \pm 3/2} &= \frac{3}{20} \frac{e^2 g Q}{h} \\ \nu_{\pm 3/2 \leftrightarrow \pm 5/2} &= \frac{3}{10} \frac{e^2 g Q}{h} \end{aligned} \quad (32)$$

and for $I = 7/2$

$$\begin{aligned} \nu_{\pm 1/2 \leftrightarrow \pm 3/2} &= \frac{1}{14} \frac{e^2 g Q}{h} \\ \nu_{\pm 3/2 \leftrightarrow \pm 5/2} &= \frac{2}{14} \frac{e^2 g Q}{h} \\ \nu_{\pm 5/2 \leftrightarrow \pm 7/2} &= \frac{3}{14} \frac{e^2 g Q}{h} \end{aligned} \quad (33)$$

The equations (30) to (33) are concerned with frequencies of transitions in the case of axial symmetry in the e.f.g. However, more usually, this is not the case and there is a non-zero η . Although for $I = 3/2$ and $I = 1$ expressions accurate in η can be produced for the transitions, other values of I give expressions in η only soluble by numerical procedures. Thus frequencies for the case of non-zero η values are:

$$I = 3/2 \quad \nu_{\pm 1/2 \leftrightarrow \pm 3/2} = \frac{e^2 g Q}{2h} \left(1 + \frac{\eta^2}{3}\right)^{1/2} \quad (34)$$

$$I = 1 \quad \nu_{0 \leftrightarrow +1} = \nu_+ = \frac{3}{4} \frac{e^2 g Q}{h} \left(1 + \frac{\eta}{3}\right) \quad (35)$$

$$\nu_{0 \leftrightarrow -1} = \nu_- = \frac{3}{4} \frac{e^2 g Q}{h} \left(1 - \frac{\eta}{3}\right)$$

$$\nu_{-1 \leftrightarrow +1} = \nu_0 = \frac{e^2 g Q}{2h} \cdot \eta$$

$I = 5/2$, and say $\eta < 0.25$

$$\nu_{\pm 1/2 \leftrightarrow \pm 3/2} = \nu_1 = \frac{3}{20} \left(\frac{e^2 g Q}{h}\right) (1 + 0.09259\eta^2 - 0.63403\eta^4) \quad (36)$$

$$\nu_{\pm 3/2 \leftrightarrow \pm 5/2} = \nu_2 = \frac{3}{10} \left(\frac{e^2 g Q}{h}\right) (1 + 0.20370\eta^2 + 0.16215\eta^4)$$

$I = 7/2$

$$\nu_{\pm 1/2 \leftrightarrow \pm 3/2} = \nu_1 = \frac{1}{14} \left(\frac{e^2 g Q}{h}\right) (1 + 3.43333\eta^2 - 7.26070\eta^4)$$

$$\nu_{\pm 3/2 \leftrightarrow \pm 5/2} = \nu_2 = \frac{2}{14} \left(\frac{e^2 g Q}{h}\right) (1 - 0.56667\eta^2 - 1.85952\eta^4) \quad (37)$$

$$\nu_{\pm 5/2 \leftrightarrow \pm 7/2} = \nu_3 = \frac{3}{14} \left(\frac{e^2 g Q}{h}\right) (1 - 0.1001\eta^2 - 0.01804\eta^4)$$

Equations (34) to (36) and equations (37) are taken from refs. (8a) and (8c). From the frequencies obtained experimentally the values of the nuclear quadrupole coupling constant and the asymmetry parameter can be calculated for nuclei with half-spins greater than $3/2$. (8 b). For spin unity (e.g. ^{14}N) e^2qQ and η are usually obtained from the ν_+ and ν_- transitions because, unless η is very large, the ν_0 transition is often of too low a frequency to be easily detected; e.g. $\eta = 0.81$ for hydrazine (52) and $\nu_0 \sim 2$ MHz. In the case of spin $3/2$ nuclei (e.g. ^{35}Cl , ^{75}As , ^{11}B , ^{81}Br and ^{79}Br) only one transition is obtained and it alone cannot yield independent values of $|e^2qQ|$ and η . Often in practice η is less than 0.1 and, as an error of only about 0.2% is introduced, $|e^2qQ|$ is frequently taken as twice the resonance frequency.

The only way to determine the value of the asymmetry parameter (η) in the spin $3/2$ case is by Zeeman studies in which the application of a small magnetic field removes the degeneracy of the $\pm m$ states. The effect of this upon the observed spectrum lineshape is characteristic of the value of η and from it η can be measured. This technique is called Zeeman splitting of nuclear quadrupole resonances and is discussed in the following section.

Introduction

As previously shown, the nuclear quadrupole interaction is characterised by the two parameters $|e^2qQ|$ and η which are dependent one upon the other. Three other parameters deserving notice are the three Eulerian angles (α , β and γ) which define the principal axes of the e.f.g. with respect to laboratory axes (or frame of reference). The knowledge of all five can yield useful information on the electron distribution and the bond type between the quadrupolar atom and its neighbour(s). This is dealt with in Chapter 2 where the interpretation of n.q.r. information is discussed. However, for such nuclei as ^{35}Cl , ^{79}Br , ^{11}B etc. with $I = 3/2$ the measurement of their single frequencies does not yield $|e^2qQ|$ nor η as do the multiple frequencies of nuclei of higher I values. It is then necessary to make further measurements which usually involve the application of a static magnetic field.

For spin $3/2$ the single frequency of the transition between the two sets of doubly degenerate quadrupole levels is given by

$$\nu = \frac{e^2qQ}{2} \left(1 + \frac{\eta^2}{3}\right)^{\frac{1}{2}} \quad (38)$$

We cannot obtain both $|e^2qQ|$ and η from this one expression; but in Z.n.q.r. spectroscopy the application of a magnetic field to the sample removes the degeneracy. This gives rise to four transitions centred about the pure n.q.r. frequency from which $|e^2qQ|$ and η are then determinable.

Z.n.q.r. spectroscopy has been used in single crystal and polycrystalline sample experiments. Single crystal applications lead to the full elucidation of the Eulerian angles (with respect to crystallographic axes) but clearly pose experimental problems in growing a single crystal of sufficient size and have, therefore, had only limited use. (9-15). Polycrystalline specimens have been investigated also (16-24), following the pioneering work of Morino and Toyama (17).

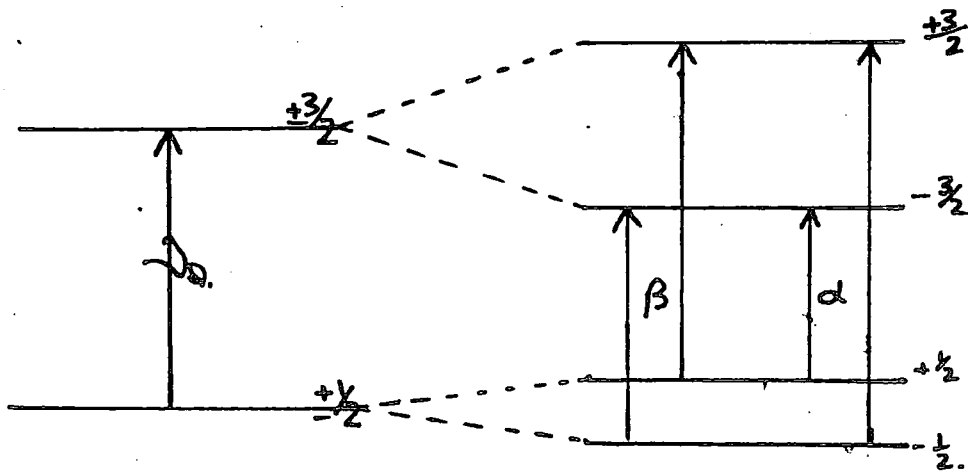
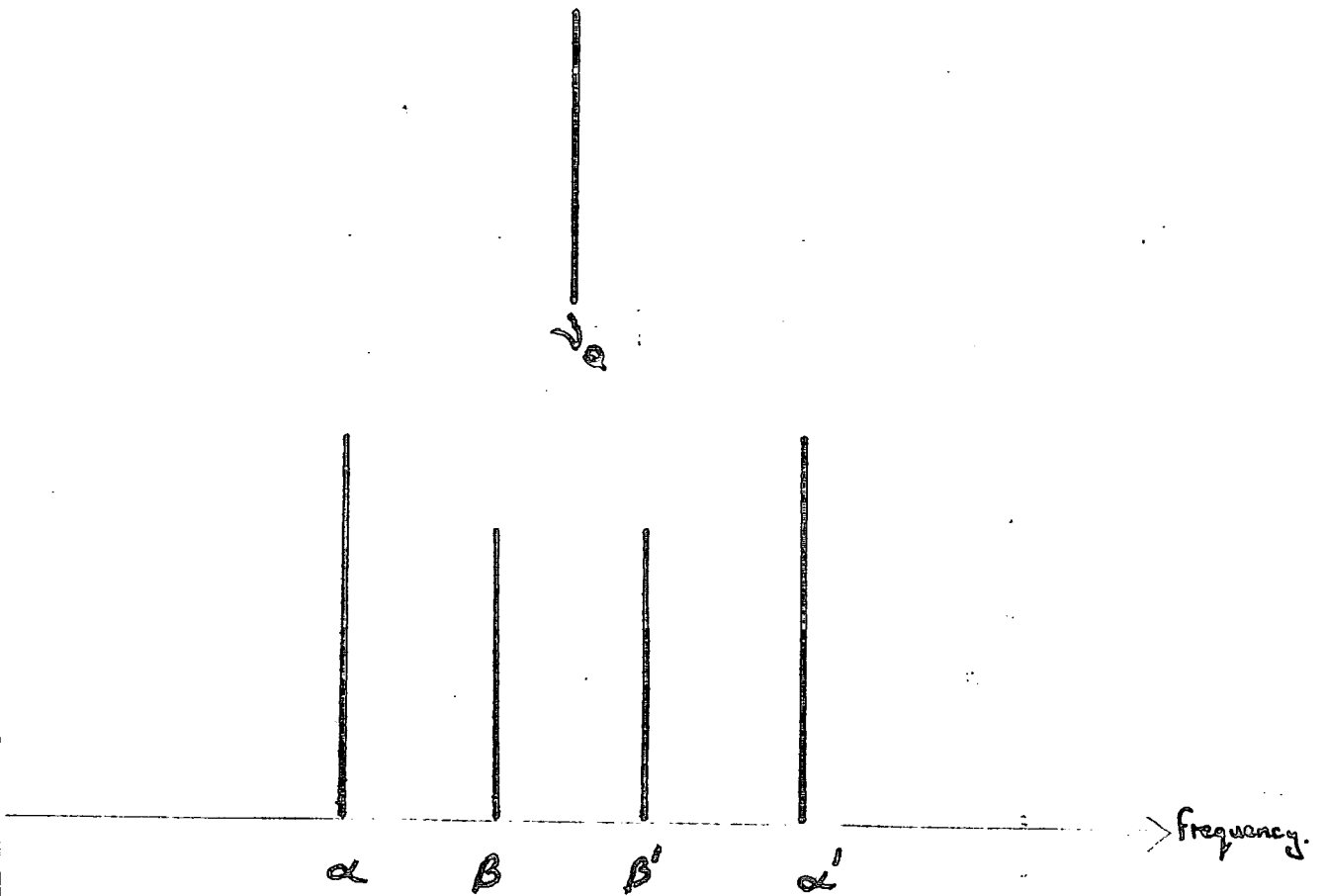
Single Crystal Studies

Although the study of the intensities of signals from a single crystal at various orientations in the radio-frequency field (H_{Rf}) would lead to an estimate of γ , the instability of the oscillator's response on moving the crystal makes this experiment difficult. The Zeeman effect is therefore indispensable for n.q.r. spectroscopy of spin $3/2$ nuclei and to continue with the single crystal treatment, the results of Dean(25) are used to describe the main methods employed. In a small static magnetic field (H_0), usually less than 150 Gauss = 0.015T, the splitting of the quadrupolar energy levels is small in comparison with their separation i.e.

$$\delta H_0 \ll e^2 q Q.$$

where δ is the gyromagnetic constant of the nuclei. The splitting leads to the production of a quadruplet as in Fig.4.

Fig.4. Splitting of a single-crystal nuclear quadrupole resonance by a magnetic field (H_0)



$H_0 = 0$

$H_0 \neq 0$
 H_0 parallel to HRF

Dean has shown that the frequencies of Z.n.q.r. singularities lie at, (25)

$$\nu = \nu_0 \pm \frac{\delta H}{2} \left\{ \sqrt{1 + \sin^2 \theta (3 - \eta^2 - 4\eta \cos 2\theta)} \pm \sqrt{9 - \sin^2 \theta (4 - \eta^2)} \right\} \quad (39)$$

From equation (39) it can be shown that the two expressions under the square root signs are equal when

$$\sin^2 \theta = \frac{2}{3 - \eta \cos 2\theta} \quad (40)$$

and clearly under this condition the two inner components (β and β') of the quadruplet coalesce at the n.q.r. resonance frequency (ν_q). The equation (40) defines the locus of points of coalescence as an elliptical cone and determination of the cone with respect to laboratory axes gives the value of η and the Eulerian angles. This, simply, is the basis of Dean's "geometrical method"(15), which allows precision measurements of these quantities. The accuracy is determined by the mechanical precision of the goniometer, the construction of the Helmholtz coils and their use.

Variations on this single crystal method have been used by V. Rehn(12), (the so-called field-frequency method) and P. Bucci, P. Cecclin and E. Scrocco (13). The authors claim to raise the accuracy of η determinations from about ± 0.01 of Dean to ± 0.001 but only gain this if critical settings of the crystal orientation are favourably established. A major problem, however, has been overcome by Bucci in using a single Helmholtz coil for the generation of the Zeeman field. This allows the almost complete investigation of the locus because of the coil's full angular freedom about the line connecting the spectrometer and probe. This geometrical method has been used for

several compounds including 1,4 - dichlorobenzene (15), 1,4 - dibromobenzene (10) and bromine (16).

The work of Kojima et al. (10) shows a possible complication of this method, since, instead of obtaining a quadruplet, a set of eight lines was observed. The Zeeman field was splitting resonances due to bromine nuclei in two molecular orientations of the 1,4 - dibromobenzene molecules. These two orientations of the molecules in the crystal give rise to different magnetic field strength components at the bromine atoms and hence two sets of lines. The problem was overcome by careful orientation of the crystal so as to apply the magnetic field parallel to the yz plane in order that the two classes of molecules experienced the same field strength thereby giving rise to the one, superimposed, quadruplet pattern. The determination of η was then made by the geometrical method.

Polycrystalline Sample Studies

Clearly for liquid samples of low freezing point or for some solid samples, single crystal growth is difficult, tedious or practically impossible and the earlier techniques cannot be used to obtain η in such samples. Consider the structure of a spectrum from a polycrystalline sample subjected to a magnetic field. We might expect the broadening

and the complete smoothing of fine structure by the superimposition of the many quadruplets from the crystallites lying in all orientations. However, calculations of transition probabilities by Dean (25) and Toyama (26) suggested that stronger than average lines would be generated for certain crystallite orientations. With the magnetic field (H_0) parallel to the radio-frequency field (H_{RF}) crystallites with their maximum e.f.g. component (q_{zz}) orientated at more than $\pm 15^\circ$ from perpendicular to H_{RF} contribute little to the overall lineshape. When Zeeman experiments upon polycrystalline (powder) samples' spin 3/2 nuclear quadrupole resonance signals were performed, a characteristic angular dependence of the two pairs of Zeeman components ($|m| = \frac{1}{2} \Rightarrow 3/2$) was observed (11) and (21).

In order to explain the technique as a probe for evaluation of the asymmetry parameter (η), consider the case of the static magnetic field (H_0), lying parallel to the inducing radio-frequency field (H_{RF}). Crystallites whose principal xy planes of the e.f.g. are parallel with the static field (i.e. whose z axes are perpendicular to H_{RF}) produce transitions comparable to the quadruplet of single crystal Zeeman experiments. Those corresponding to the inner pair of the single crystal Zeeman components (β and β') are induced by the x component of H_{RF} and those to the outer pair (α and α') by the y component. Thus, depending upon the orientation of the x and y axes to H_{RF} , the signal intensities of these lines vary in a reciprocating manner. For polycrystalline samples, therefore, a smooth spectrum of definite lineshape is observed. This behaviour of the Zeeman components

is caused by the zeroth-order effect of the asymmetry of the e.f.g. (25). Clearly, if η is non-zero the strengths of these sets of components vary and in a polycrystalline sample we expect the asymmetry to manifest itself in the envelope shape of the line, broadened by the magnetic field. The pairs of peaks are separated from the central resonance frequency (ν_Q) by approximately the Larmor frequency, ν_H . The Larmor frequency of a nucleus is calculated thus

$$\nu_H = \left| \frac{\gamma}{2\pi} H_0 \right| \quad (41)$$

where H_0 is the magnetic field strength and γ is the gyromagnetic ratio for the resonating nucleus, divided by 2π .

For a non-zero asymmetry parameter, $q_{xx} \neq q_{yy}$, therefore, changes in the lineshape for a polycrystalline powder result in the vicinity of $\nu_Q \pm \nu_H$. Their detail depends upon the value of η . With the experimental arrangement of H_{RF} parallel to H_0 , we may consider the lineshapes produced when each of the principal e.f.g. components (q_{xx} , q_{yy} and q_{zz}) lie, in turn, parallel to the magnetic field (H_0).

Transitions in the n.q.r. spectrum are, in general, induced by the component of H_{RF} perpendicular to the principal z axis, within the approximation to first order in η (25).

When H_0 is parallel to z, no absorption spectrum is observed because H_{RF} is parallel to z too. With H_0 parallel to the x axis, the outer pair of Zeeman components would lie at $\nu_Q \pm \nu_H$, and the inner pair at $\nu_Q \pm (1 - \eta)\nu_H$. However,

with this arrangement, H_{RF} is also parallel with x and therefore only the transitions corresponding to the inner pair are allowed. Thus only a pair of strong lines at $\pm (1 - \eta) \nu_H$ on either side of ν_Q are observed. With H_0 parallel to the y axis (and, therefore, with H_{RF} parallel with y), we have a similar situation, but the resulting pair of lines lie at $\pm (1 + \eta) \nu_H$ about ν_Q .

Thus for the magnetic field (H_0) parallel to the radio-frequency field (H_{RF}) no signals are seen at $\nu_Q \pm \nu_H$ but on either side of ν_Q lie pairs at

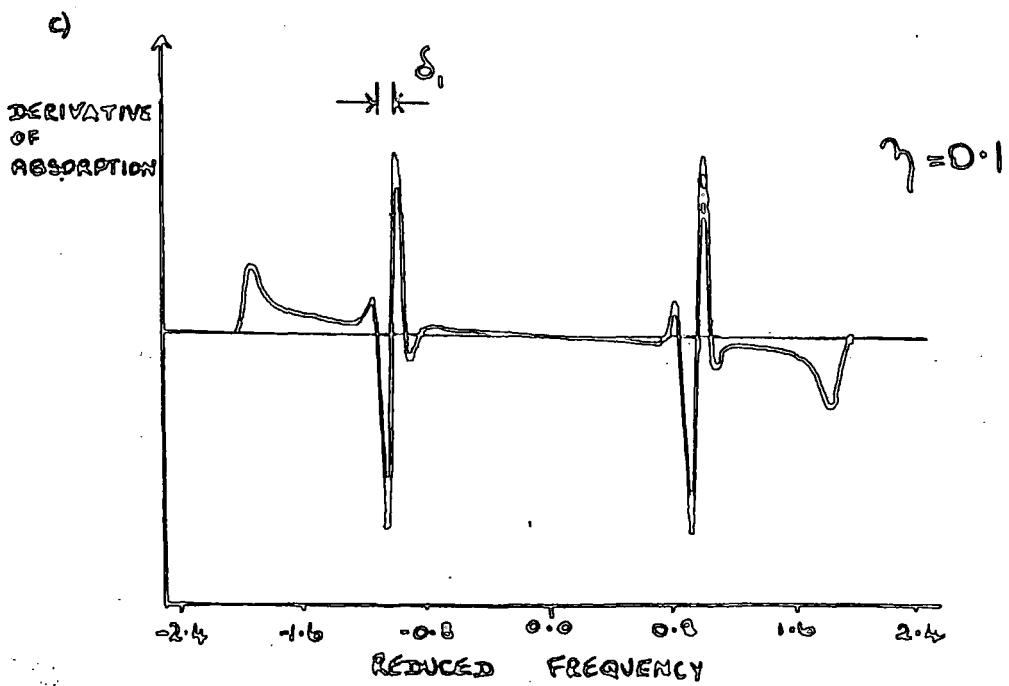
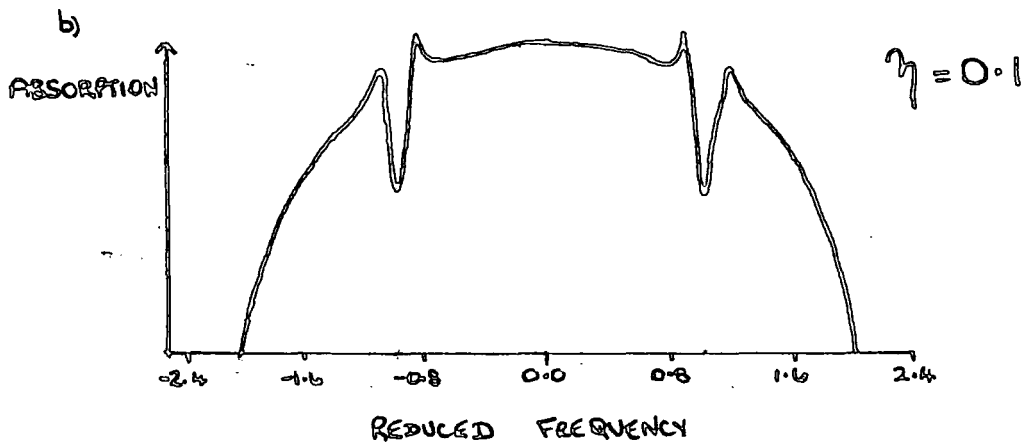
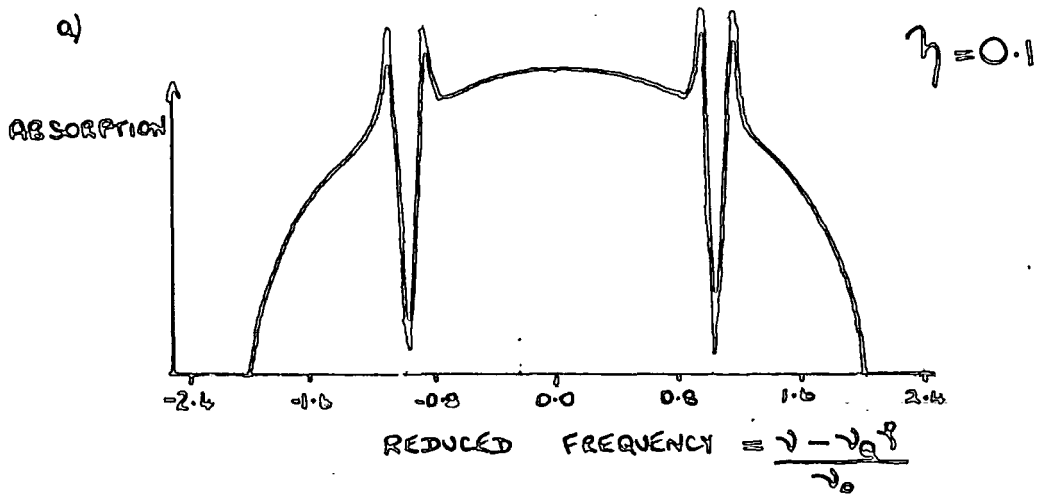
$$\begin{aligned} & \nu_Q \pm (1 + \eta) \nu_H \\ \text{and} & \nu_Q \pm (1 - \eta) \nu_H \end{aligned}$$

The development of the full lineshapes is shown in Figs. 5a)-c) which are taken from ref. (34). The scale used for the abscissa is that of reduced frequency i.e. $\frac{\nu - \nu_Q \eta}{\nu_H}$ where $\eta = (1 + \frac{\nu_Q^2}{3})^{\frac{1}{2}}$. The position of the discontinuities and their width is dependent upon the value of η ; in Figs. 5a-c), $\eta = 0.1$. The absorption represents the response of a spectrometer as the frequency is swept. The diagram 5a represents the response if the linewidth of the n.q.r. absorption is infinitely narrow. However, diagram 5b shows the more practical case of a finite linewidth, while Fig. 5c shows the likely spectrometer response - a first derivative of the absorption.

Morino and Toyama (17) observed lineshapes similar to those in Fig. 5c for Z.n.q.r. studies on 1,4 - dichlorobenzene and 1,3,5 trichlorotriazine (cyanuryl chloride). The separation between these features - δ in Fig. 5c - is given approximately by

$$\begin{aligned} \delta & \approx \left\{ (1 + \eta) \nu_H - (1 - \eta) \nu_H \right\} & (42) \\ \text{i.e.} & \delta \approx 2 \nu_H \cdot \eta \end{aligned}$$

Fig.5. Simulated Zeeman n.q.r. lineshapes



This separation (δ) is therefore characteristic of the asymmetry parameter but as the expression (42) involves the Larmor frequency (ν_H in equation (41)), its value is dependent upon the strength of the static magnetic field.

Application of a magnetic field (H_0) to the n.q.r. sample causes the loss of the degeneracy of the $\pm m$ quadrupolar energy levels. Thus the absorption of r.f. energy in order to promote transitions between these levels is possible over a wider range of frequencies. The result is a broader linewidth for the observed spectrum. The singularities at $\nu_Q \pm (1+\eta)\nu_H$ and $\nu_Q \pm (1-\eta)\nu_H$ emerge from the broadening lineshape but they are only well-defined when the separation $2\nu_H\eta$ is greater than the linewidth, $\Delta\nu$. Thus a condition for the minimum amount of broadening (equivalent to a minimum value (H_0 MIN) for H_0) required to yield the singularities can be stated as

$$\text{broadening due to asymmetry} \sim \nu_H \eta = \eta (\gamma H_0) > \Delta\nu$$

$$\text{leading to } H_0 \text{ MIN} \geq \frac{\Delta\nu}{\eta \cdot \gamma} \quad (43)$$

where $\Delta\nu$ equals the linewidth at $H_0 = 0$ (unbroadened) and where η and H_0 are as above with γ , the gyromagnetic ratio of the quadrupolar nucleus, divided by 2π .

Morino and Toyama (17) propose that the ratio

$$\frac{\delta}{2\nu_H} \quad \text{where } \nu = \text{Larmor frequency (44)}$$

$$\delta \approx 2\nu_H \cdot \eta$$

be measured at several increasing values of the field strength (H_0). This ratio is then extrapolated to infinite

field strength. Assuming that the first order analysis of the Zeeman effect holds over all field strengths, the original linewidth can be neglected in comparison with $\delta \approx 2\nu_H \cdot \lambda$ ($H_0 \rightarrow \infty$). They therefore propose that $\frac{\delta}{2\nu_H}$ converges to λ as H_0 approaches infinite values. Clearly for infinite field strengths the line would be broadened out too much to be observed. Extrapolation is therefore used. When the magnetic field (H_0) is weak in comparison to $\frac{\Delta\nu}{2\nu}$ (equation (43)), the linewidth measured is far larger than $2\nu_H \lambda$ but at stronger fields, the greater part of the separation comes from the asymmetry effect. Thus a plot of $\frac{\delta}{2\nu_H}$ versus $\frac{1}{H_0}$ has a negative gradient, tending to decrease in slope as H_0 increases. A minimum in this curve has sometimes been observed experimentally and is in agreement with a predicted curve of $\lambda - \frac{\Delta\nu}{2\nu_H}$. This is illustrated in Fig. 6a), which is taken from (17) for 1,4 dichlorobenzene. In practice, lineshapes are not as well resolved as appears from Fig. 5c). In order to improve the analysis, Morino and Toyama defined three measurements which approximated to δ and which behaved similarly. These (δ_1, δ_2 and δ_3) are illustrated in Fig. 6b). It is usual that whichever is best defined in the spectra is plotted as in Fig. 6a).

The method of Morino and Toyama has been used by various authors (16 - 24). Results are reported in this thesis for thionyl chloride, phenyl phosphorus tetrachloride, silicon tetrachloride and germanium tetrachloride.

For completeness, we must consider the alternative configuration of H_{RF} perpendicular to H_0 in which we might expect differences in lineshape. Although Morino and Toyama predicted the lineshapes, full experimental results and interpretations were furnished by R.B. Creel et al. (27) and (28). Creel compared spectra from

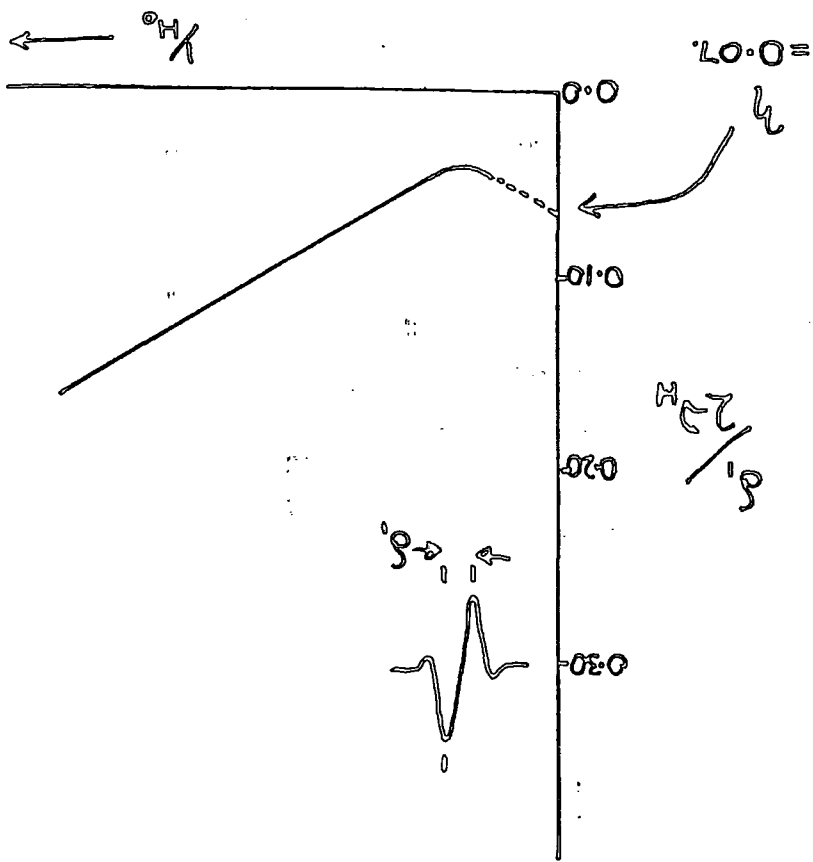


Fig. 6. a)

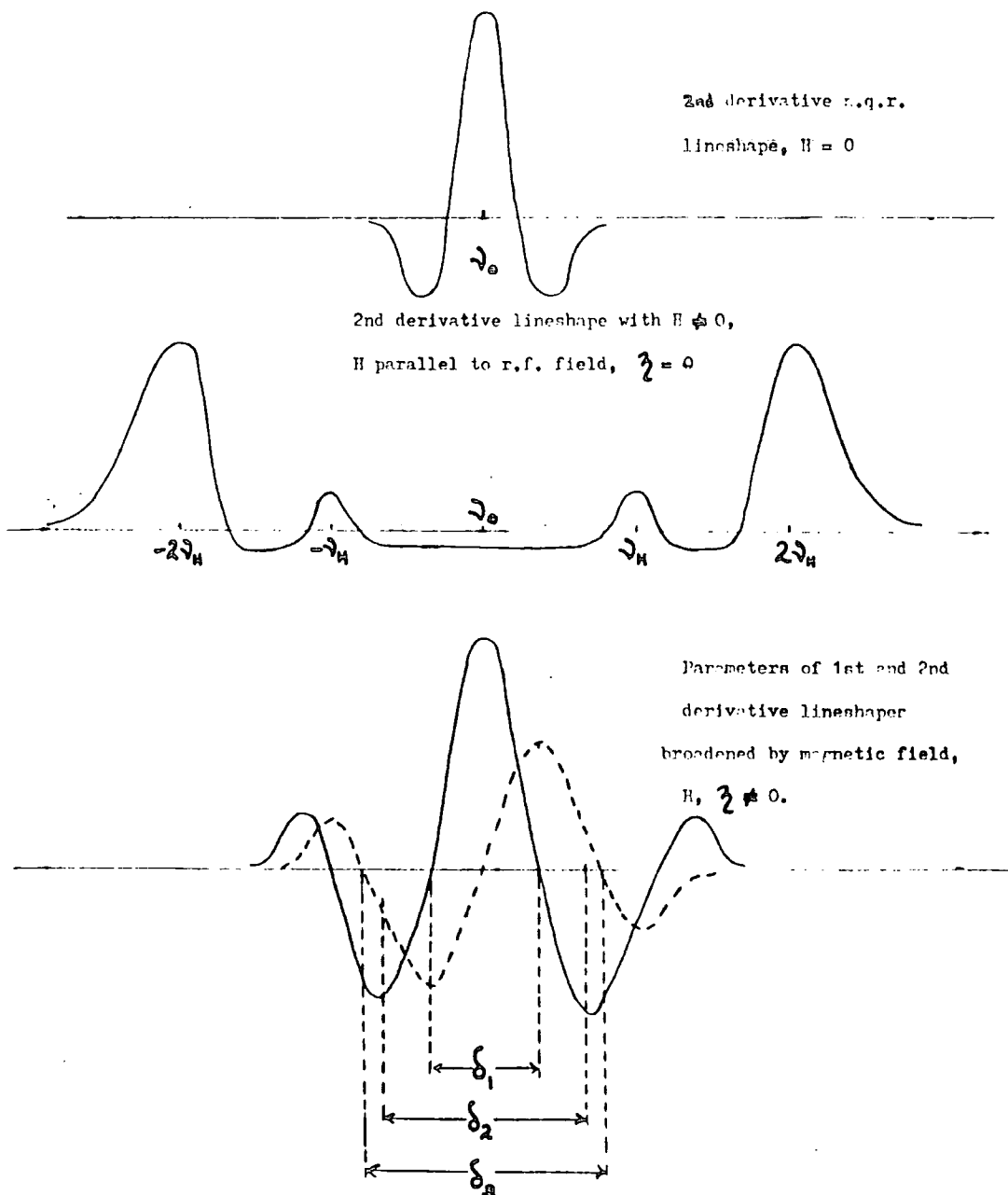
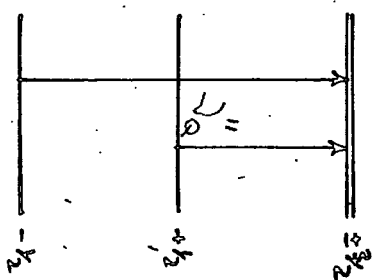
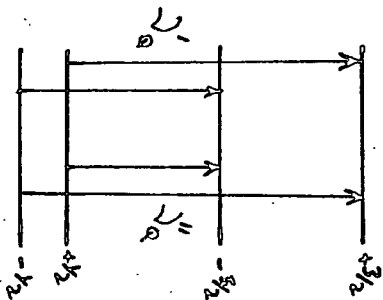
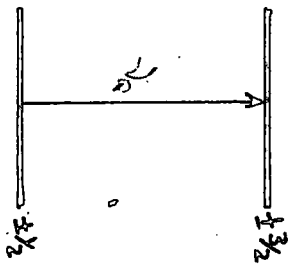


Fig. 6b) δ parameters of Zeeman n.q.r. lineshapes by Morino and Toyama analysis.



i) $H_0 = 0$
 $E \propto m^2$

ii) $H_0 \neq 0$
 $H_0 \parallel k_0 H_0$

iii) $H_0 \neq 0$
 $H_0 \perp k_0 H_0$

Fig. 7. Energy levels split by Zeeman fields of different orientations

Frequencies

i) $\nu_0 = \frac{e^2 g^2 \mu_B}{2} (1 + \frac{g^2}{3})^{1/2}$

ii) $\nu_0' = \nu_0 \pm (1 - \frac{g^2}{3}) \nu_H$

$\nu_0'' = \nu_0 \pm (1 + \frac{g^2}{3}) \nu_H$

iii) $\nu_0''' = \nu_0 \pm \nu_H$

NaClO_3 ($\eta = 0.0$ - Y. Ting et al. (29)), with those from 1,4 dichlorobenzene ($\eta = 0.08$ - Dean (25)) and mercuric chloride ($\eta = 0.08$ to 0.80 - Negita (30), Narasimham (19) and Ramakrisna (31)) but no appreciable differences were observed. The lineshapes from this configuration are therefore insensitive to η .

Morino and Toyama (17) had predicted this independence from η , showing that no Zeeman components were allowed at $\nu_a \pm (1 \pm \eta)\nu_H$. They only exist at $\nu_a \pm \nu_H$ and therefore overlap one another, giving no characteristic separations. Creel et al. (27) have shown that this behaviour is due to the dominant portion of the intensity of the resonance absorption coming from crystallites whose e.f.g. components lie parallel to H_0 i.e. q_{zz} perpendicular to H_{RF} . This is represented by $\Theta = 0$ in the expression of Das and Hahn (32). They have shown that the contribution of η to the Zeeman energy levels has as coefficient, $\sin^2 \Theta$. With $\Theta = 0$ for this experimental arrangement, the asymmetry cannot contribute to the observed lineshape. The energy levels resulting from various configurations of the magnetic field are illustrated in Fig. 7.

Temperature Dependence of n.q.r.

Introduction

Quadrupole resonances measured at various temperatures, most often reveal a negative and non-linear temperature variation. Although this dependence varies greatly for different molecules and nuclei, for a ^{35}Cl resonance, a shift to higher frequency of about 3 to 5 kHz. per degree accompanies the fall in temperature for many organo-chlorine compounds. Bayer (35) first attempted to explain this variation by proposing that torsional molecular vibrations were responsible.

The Bayer Theory

In a solid, molecular and lattice vibrations displace the nuclei. These motions are temperature dependent but some are those in which the centres of mass of the molecules (as rigid bodies) are displaced (translational modes) and some cause the orientation of the molecule as a rigid body to change (torsional modes). The translational modes do not change the resonant nucleus' quadrupole interaction with the e.f.g. but torsional modes move the e.f.g. with respect to the nucleus. The effect of torsional motion about the three principal axes of the e.f.g. is illustrated in Fig. 8 where the unprimed axes are those fixed in space and those primed are the instantaneous displaced axes. The angular displacements are given as θ_j ($j = x, y$ and z) and for small values of θ_j the instantaneous and fixed

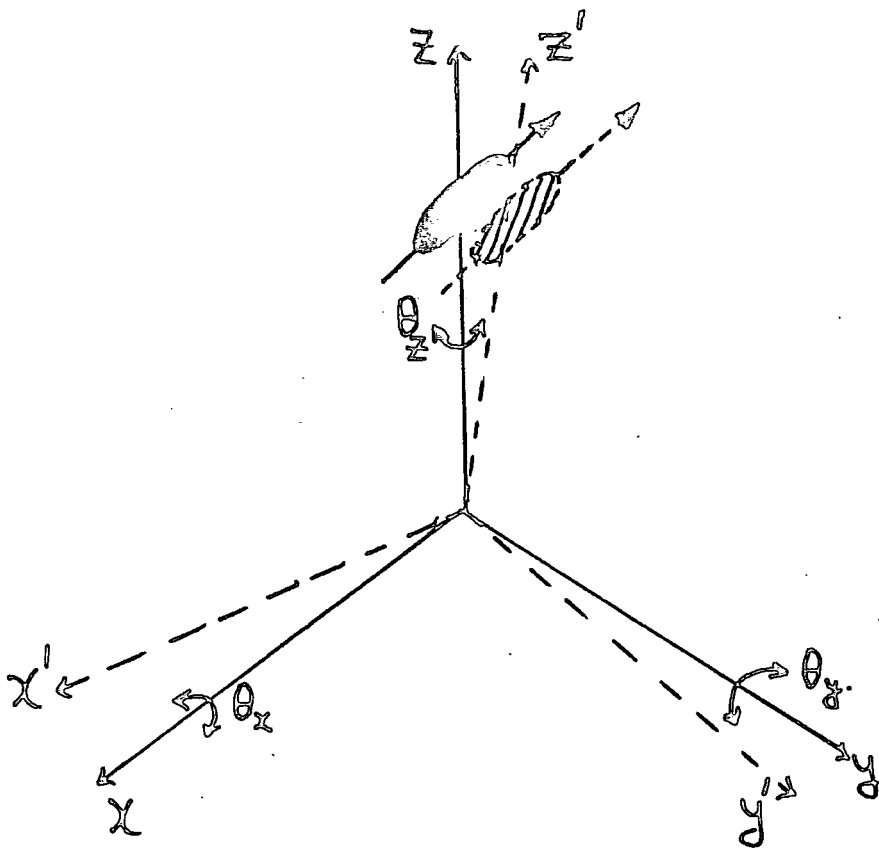


Fig. 8. The effect of torsional motion on the e.f.g. at the nucleus

axes are related by the following equations, (32):

$$V'_{xx} = (1 - \theta_y^2 - \theta_z^2)V_{xx} + \theta_z^2 V_{yy} + \theta_y^2 V_{zz} \quad (45)$$

$$V'_{yy} = \theta_z^2 V_{xx} + (1 - \theta_x^2 - \theta_z^2)V_{yy} + \theta_x^2 V_{zz} \quad (46)$$

$$V'_{zz} = \theta_y^2 V_{xx} + \theta_x^2 V_{yy} + (1 - \theta_x^2 - \theta_y^2)V_{zz} \quad (47)$$

$$V'_{xy} = \theta_z V_{xx} + (\theta_x \theta_y - \theta_z) V_{yy} - \theta_x \theta_y V_{zz} \quad (48)$$

$$V'_{yz} = -\theta_y \theta_z V_{xx} + \theta_x V_{yy} + (\theta_y \theta_z - \theta_x) V_{zz} \quad (49)$$

$$V'_{zx} = -\theta_y V_{xx} - \theta_x \theta_z V_{yy} + (\theta_x \theta_z + \theta_y) V_{zz} \quad (50)$$

Equations (45) to (50) show that the instantaneous e.f.g. tensor is time-dependent and non-diagonal. However, the torsional oscillations are of the order $30 - 100 \text{ cm}^{-1}$ representing a frequency a about 10^{12} Hz. which is much greater than the 30 MHz for a typical ^{35}Cl quadrupole resonance. The oscillations therefore average the e.f.g. and, since the expectation value of θ_j also averages to zero, i.e.

$$\langle \theta_j \rangle = 0, \quad (51)$$

the e.f.g. tensor is, on the n.q.r. time scale, diagonal.

Using the Laplace condition (equation (4)), equation (47)

then becomes

$$V'_{zz} = V_{zz} (1 - 3/2(\theta_x^2 + \theta_y^2) - 1/2(\theta_x^2 - \theta_y^2)) \quad (52)$$

Now, representing the time-averaged value of the principal component of the e.f.g., q_{zz} , by q^0 and the "stationary" value by q , equation (52) becomes

$$eq^0 = eq (1 - 3/2(\langle \theta_x^2 \rangle + \langle \theta_y^2 \rangle) - 1/2(\langle \theta_x^2 \rangle - \langle \theta_y^2 \rangle)) \quad (53)$$

where $\langle \theta_j^2 \rangle$ is the expectation value (an average) and terms in θ^4 are, as before, ignored as very small. The value of $\langle \theta_j^2 \rangle$ is termed the mean square amplitude of vibration about the j^{th} e.f.g. principal axis.

The time averaged value of the asymmetry parameter is written as η' and, ignoring terms in θ^4 , is given by

$$\eta' = \frac{e q}{e q} \left\{ \eta \left[1 - \frac{1}{2} (\langle \theta_x^2 \rangle + \langle \theta_y^2 \rangle) - 2 \langle \theta_z^2 \rangle \right] + \frac{3}{2} (\langle \theta_y^2 \rangle - \langle \theta_x^2 \rangle) \right\} \quad (54)$$

Since $\langle \theta_j^2 \rangle$ is always positive the torsional motion averaging the e.f.g. lowers $e q$ and, therefore, the nuclear quadrupole coupling constant falls. The motion about the z axis does not affect q^0 but tends to decrease η' .

The Bayer theory therefore separates the dynamical effect of torsional motion in the crystal from the static effects of the charge distribution in the vicinity of the resonant nucleus. This assumption is valid in molecular crystals where the e.f.g. is provided predominantly by the bonding electrons of the molecule.

The n.q.r. frequencies are thus temperature dependent through the mean square amplitudes $\langle \theta_j^2 \rangle$ of vibration about the e.f.g. principal axes. It is assumed that only the librations or low frequency internal torsions are important in the averaging process and that each molecule librates independently of its neighbours. In the general case of three torsional motions we can represent them by quantum mechanical oscillators thus (32)

$$\langle \theta_j^2 \rangle = \frac{\hbar}{I_j \omega_j} \left(\frac{1}{2} + \frac{1}{\left(\exp \left(\frac{\hbar \omega_j}{k T} \right) - 1 \right)} \right) \quad (55)$$

I_j and ω_j are respectively the moments of inertia of the molecule and angular oscillation frequency about the principal e.f.g. axis j ($j = x, y$ and z), h is Planck's constant divided by 2π , k is Boltzmann's constant and T is the absolute temperature.

Substitution of (55) into equation (53) gives, (32)

$$eq' = eq \left\{ 1 - \frac{3}{2} h \left[\frac{(1+\eta_3)}{2A_x \omega_x} + \frac{(1-\eta_3)}{2A_y \omega_y} \right] - \frac{3}{2} h \left[\frac{(1+\eta_3)}{A_x \omega_x (\exp(\frac{h\omega_x}{kT}) - 1)} + \frac{(1-\eta_3)}{A_y \omega_y (\exp(\frac{h\omega_y}{kT}) - 1)} \right] \right\} \quad (56)$$

The first set of bracketed terms gives the effect of zero-point vibrations on eq' , the second set contains the temperature dependent expression. For a nucleus of spin $3/2$ we may write the temperature dependent resonance frequency,

ν , as

$$\nu = \frac{e^2 q' Q}{2} \left(1 + \frac{(\eta')^2}{3} \right)^{\frac{1}{2}} \quad (57)$$

where $\eta' \approx \frac{q}{q'} \cdot (\eta)$.

Substituting in (56) yields, (32)

$$\nu' = \frac{e^2 q' Q}{2h} \left\{ 1 - \frac{3}{2} h \left[\frac{(1+\eta_3)}{2A_x \omega_x} + \frac{(1-\eta_3)}{2A_y \omega_y} \right] - \frac{3}{2} h \left[\frac{(1+\eta_3)}{A_x \omega_x (\exp(\frac{h\omega_x}{kT}) - 1)} + \frac{(1-\eta_3)}{A_y \omega_y (\exp(\frac{h\omega_y}{kT}) - 1)} \right] + \frac{\eta^2}{6} \right\} \quad (58)$$

The terms of higher order than η^2 are ignored. The first and last terms of equation (58) when summed yield ν , if multiplied by $\frac{e^2 q' Q}{2h}$. Since the first set of terms are independent of temperature, differentiation of (58)

yields

$$\frac{1}{\nu} \left(\frac{\partial \nu}{\partial T} \right) = \frac{-3h^2}{2kT^2} \left\{ \frac{(1+\eta_3) \exp(\frac{h\omega_x}{kT})}{A_x (\exp(\frac{h\omega_x}{kT}) - 1)^2} + \frac{(1-\eta_3) \exp(\frac{h\omega_y}{kT})}{A_y (\exp(\frac{h\omega_y}{kT}) - 1)^2} \right\} \left(\frac{1}{1 + \frac{\eta^2}{3}} \right) \quad (59)$$

Equation (59) can thus be simplified if β is small and can be ignored, and if $\frac{\omega_j}{kT} \ll 1$,

$$\frac{1}{\nu} \left(\frac{\partial \nu}{\partial T} \right) = - \frac{3A}{8\pi^2} \left\{ \frac{\exp\left(\frac{k\omega_x}{kT}\right)}{A_x \omega_x^2} + \frac{\exp\left(\frac{k\omega_y}{kT}\right)}{A_y \omega_y^2} \right\} \quad (60)$$

If equation (57) is replaced by the frequency equation for nuclei of spins $> 3/2$, similar derivations can be made to give an expression for their frequencies' temperature dependence.

The assumption upon which equation (55) is based, namely that we can represent the mean squared angular displacements $\langle \theta_j^2 \rangle$ as normal co-ordinates, is, however, not strictly correct since the molecule does not librate independently of its neighbours. Kushida (38) pointed out that any small amplitude external co-ordinates, θ_j , can be expanded as a linear combination of the normal co-ordinates X_i , thus

$$\theta_j = \sum_i W_{ji} X_i \quad (61)$$

where W_{ji} gives the relative weight of each normal mode contributing to molecular motion. The resulting mean square angular amplitudes can then contain contributions from all the normal modes, not only the librations.

McEnnan and Schemp (36,37) have calculated for solid chlorine the contribution of lattice mode frequencies to e.f.g. averaging by motion. They used group theory techniques to calculate the values of θ_j in equation (61).

Further, Kushida (38) showed that if only librational and torsional modes are involved and these are harmonic, then

$$\nu = \nu_0 \left\{ 1 - \frac{3}{2} \sum_{i=1}^N W_{ji} \left(\frac{h}{4\pi^2 I_i \omega_i} \right) \left(\frac{1}{2} + \frac{1}{\exp\left(\frac{h\omega_i}{kT}\right) - 1} \right) \right\} \quad (62)$$

where W_{ji} gives the relative weight made by the i^{th} mode to the nuclear motion, ω_i is the frequency of the mode and I_i is its effective moment of inertia about the axis (i) associated with the motion. N is the number of modes. ν_0 is the n.q.r. frequency that would be obtained for a rigid lattice in the absence of even its zero-point vibrations. The value of ν_0 is estimated from a plot of n.q.r. frequency against temperature - taking the extrapolated intersection with the frequency axis at $T = 0$ K. Expression (62) may be simplified if only low frequency modes (much more important in the averaging process) are used. A low frequency (ω_i) mode is one whose frequency is less than $\frac{kT_m}{h}$ (63)

where T_m is the lowest temperature used in the experiment.

Additionally if W_{ji} is taken as 1 for these modes, then

$$\nu = \nu_0 \left\{ 1 - \frac{3kT}{8\pi^2} \sum_{i=1}^N \frac{1}{I_i \omega_i^2} - \frac{k^2}{8kT} \sum_{i=1}^N \frac{1}{I_i} \right\} \quad (64)$$

Hence, when put into the form

$$\nu = a + bT + c/T,$$

equation (64) yields

$$a = \nu_0$$

$$b = - \frac{3k\nu_0}{8\pi^2} \sum_{i=1}^N \frac{1}{I_i \omega_i^2} \quad (65)$$

and

$$c = \frac{k^2}{8k} \sum_{i=1}^N \frac{1}{I_i}$$

Thus $\left(\frac{\partial \nu}{\partial T}\right)_\nu$ can be approximated by

$$\left(\frac{\partial \nu}{\partial T}\right)_\nu \approx - \frac{3k\nu_0}{8\pi^2} \sum_{i=1}^N \frac{1}{I_i \omega_i^2} \quad (66).$$

Equation (66) may be compared with equations (59) and (60).

N is the number of modes contributing to the temperature dependent averaging of eq_{zz} . However, under many practical circumstances, one or two modes make the dominant contributions.

The higher values of temperature required to make valid

the use of equations (64) and (66), i.e. $T \gg c$ in (65),

represent that part of the frequency/ temperature plot where the plotted line is closely linear and the slope almost constant. The use of a gradient measured at a temperature (T), inserted into equation (66) can yield a predicted torsional or librational frequency. It may be necessary to invoke a combination of several frequencies but these values can be compared with those observed in the far infra-red or Raman spectrum of the compound being investigated.

The different temperature dependences of various compounds are therefore explicable in terms of their varying inter-molecular (and in some cases intramolecular) interactions and of their different molecular masses and shapes producing different low-frequency librational motions. This theory has been applied by many authors (39 - 46) but a number of modifications to the theory have been proposed, each attempting to fit it more closely to physical reality.

The most commonly questioned assumption of the simple theory is that librational frequencies are constant. The lattice frequencies, not being purely harmonic, are temperature and volume dependent. When the equation of state for a solid is known, the dependence of the frequencies upon volume can be included (in the analyses by Kushida, Benedek and Bloembergen (45)) if the pressure dependence of the n.q.r. frequencies is found as well as their temperature dependence. Brown (47) has used a linear temperature dependence term of the form $\nu = \nu_0(1 - \alpha T)$ for the libration frequencies' temperature dependence which has been applied to high temperature n.q.r. studies (48). Measured temperature dependences of librational

frequencies have been incorporated in n.q.r. studies (49). Duchesne (50) has included the contribution of molecular stretching mode vibrations in the averaging of eq_{zz} . However, the contribution is very small due to their much higher frequencies.

Examples of n.q.r. temperature dependence studies are given in ref. (51). This thesis has included several, among them the cases of methylene chloride (to investigate the influence of a non-zero asymmetry parameter) and π -Cyclopentadienyl cobalt dicarbonyl.

Introduction

Of the five possible parameters n.q.r. spectroscopy can yield to describe the e.f.g. experienced by a quadrupolar nucleus in a molecule, usually only the magnitude (e^2qQ) and the symmetry of the field gradient (η) are known. Any interpretation of n.q.r. spectroscopy must attempt to relate those parameters to a description of the electronic distribution. The demands of interpretation range from those of the theoretical chemist seeking an experimental means to check simulations to the practical chemist for whom factors such as bond ionicity, degree of π -bonding, or extent of hybridisation hold appeal. This chapter deals primarily with the latter objective.

General Theory

Consider a quadrupolar nucleus lying at the origin of a set of Cartesian co-ordinates. It interacts with a volume element ($d\tau$) of charge density ρ , of vectorial distance (r) from the origin. (Fig. 1). This element produces an electrostatic potential at the origin of

$$V = \frac{\rho \cdot d\tau}{|r|} \quad (1)$$

Resolving in the Z direction gives

$$\frac{dr}{dz} = \frac{z}{r} = \cos \theta \quad (2)$$

COORDINATE AXES AT SURROUNDING NUCLEUS IN A
MOLECULAR CHARGE DISTRIBUTION.

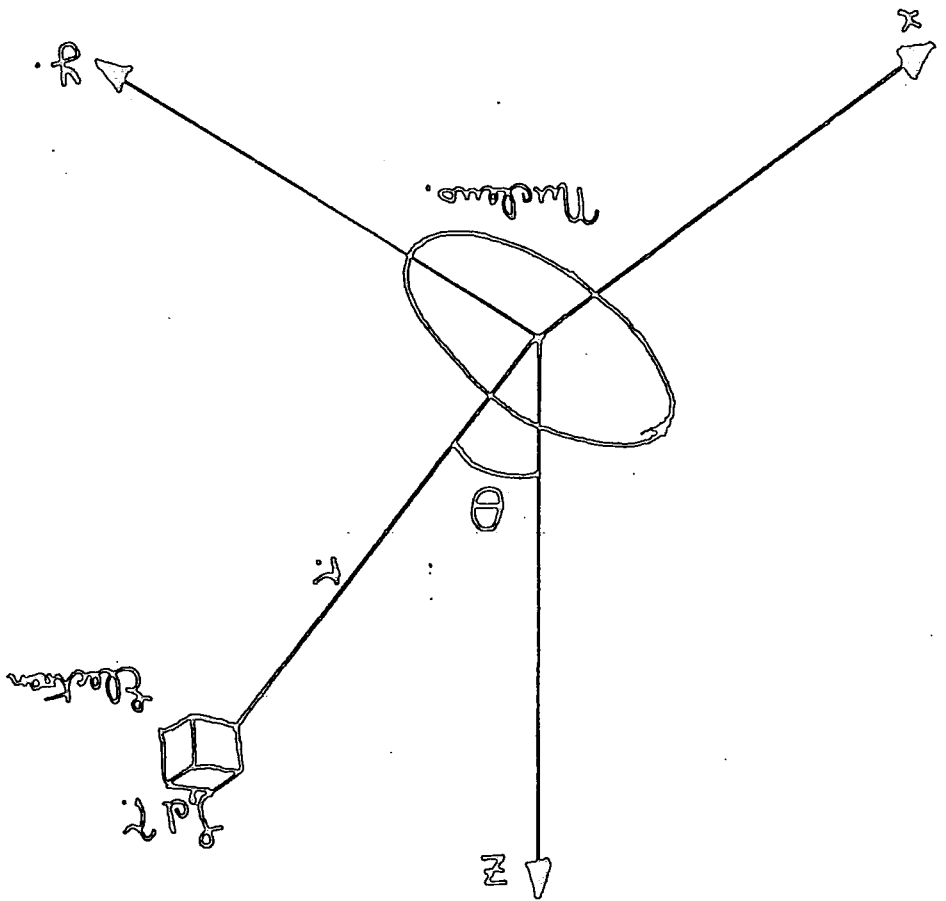


Fig. 1

and hence,

$$\frac{dV}{dz} = - \int \left(\frac{z}{r^3} \right) d\tau = - \int \left(\frac{\cos \theta}{r^2} \right) d\tau \quad (3)$$

Differentiation again gives (1),

$$\frac{d^2V}{dz^2} = \int \left\{ \frac{3 \cos^2 \theta - 1}{r^3} \right\} d\tau \quad (4)$$

Equation (4) represents the principal component (V_{zz}) of the e.f.g. tensor experienced by the nucleus due to the volume element $d\tau$. To derive the total electric field gradient, integration of (4) is required. Charge, $\rho d\tau$, is replaced in quantum mechanical terms by $\psi^* \cdot \psi d\tau$ - the expectation value (or probability) of the wave function ψ . Thus the expectation value of V_{zz} is

$$\begin{aligned} \langle V_{zz} \rangle &= e \int \psi^* \left(\frac{3 \cos^2 \theta - 1}{r^3} \right) \psi \cdot d\tau \\ &= \text{eq.} \end{aligned} \quad (5)$$

where ψ is a molecular wave function.

The Born-Oppenheimer approximation for molecular wave functions now permits the separation of ψ into nuclear and electronic components.

$$\psi = \psi_{\text{nuc.}} \cdot \psi_{\text{elec.}} \quad (6)$$

$\psi_{\text{nuc.}}$ can be further sub-divided into the translational, rotational and vibrational components.

$$\psi_{\text{nuc.}} = \psi_{\text{trans.}} \psi_{\text{rot.}} \psi_{\text{vib.}} \quad (7)$$

Because the e.f.g. is measured at a fixed point (the quadrupolar

nucleus) within the molecule Ψ trans. is of no consequence to the e.f.g., eq. The interaction between Ψ rot. and the stationary e.f.g. is evidenced in fine structure of bands in microwave spectroscopy. From this hyperfine structure values of the nuclear quadrupole coupling constant, comparable to those from n.q.r. spectroscopy, can be obtained. In the solid state however the effect of Ψ rot. on eq is not important. We are, therefore, interested in the e.f.g. of a vibrating molecule in a fixed co-ordinate system.

The observed e.f.g.'s are averaged values over the vibrational motion. The ^{35}Cl coupling constant in gaseous KCl molecules has been shown to depend strongly upon the vibrational state (2). This however is only an important effect when the values of eq and the coupling constants are small as work on methyl chloride has shown (3). In calculations of the e.f.g. at N^{14} in $\text{H-C}\equiv\text{N}$, Scrocco et al. (4) compared results obtained from a rigid equilibrium model with those averaged over the linear stretching vibration of several linear configurations. The agreement was within 1% which is much closer than is usually found for comparisons of theoretical with experimental e.f.g. values. The rigid molecule in its equilibrium configuration is therefore usually used and equation (6) becomes

$$\Psi = \Psi_{\text{fixed nuc.}} \cdot \Psi_{\text{elec.}} \quad (8)$$

From equation (5) the e.f.g. can be described in two terms. The first, representing the nuclear contribution, can be evaluated exactly irrespective of the electronic wave function. It is necessary to integrate over all nuclei in the molecule (N). The second term represents the evaluation of the average value of the function,

$$\frac{3 \cos^2 \theta - 1}{r^3}$$

over the molecular electronic wave function (and ground vibrational state). Thus;

$$eq = V_{zz} = \sum_i^N Z_i e \left(\frac{3 \cos^2 \theta_i - 1}{R_i^3} \right) - e \int \psi_{elec}^* \left(\frac{3 \cos^2 \theta - 1}{r^3} \right) \psi_{elec} d\tau \quad (9a)$$

which may be written as,

$$eq = eq_{nuc.} + eq_{elec.} \quad (9b)$$

where Z_i is the total charge (number of protons) of the other nuclei in the molecule situated at a distance R_i from the quadrupolar nucleus. Because the nuclear and electronic terms have different charges, the e.f.g. (eq) is the difference of two larger terms, one of which may be known exactly. The theoretical e.f.g. is therefore very sensitive to the accuracy of the electronic wave functions. As an example, $eq_{elec.}$ and $eq_{nuc.}$ are -2.1192 and 2.4329 cm^2 respectively for deuterium in deuterium chloride (5).

Most atomic and molecular wave functions are approximate.

Consider the effects of the various approximations on the resultant calculated e.f.g's. The variation method applied to a set of trial functions containing certain parameters is most usually used. The total electronic wave function $\psi_{elec.}$ is normally written as a set of doubly-occupied orthogonal molecular orbitals which in turn are composed of n orthogonal atomic spin orbitals, ϕ_i . These atomic spin orbitals are assumed to be products of radial ($R_{nlms}(r)$) angular (the spherical harmonics $Y^{lm}(\theta, \Phi)$) and spin (X^s) functions n, l, m, s . i.e.

$$\phi = A R_{nlms}(r) \cdot Y^{lm}(\theta, \Phi) \cdot X^s \quad (10)$$

where A is a normalising coefficient while the molecular orbitals are of the form,

$$\psi_j = \sum_i^n C_{ij} \phi_i \quad (11).$$

In equation (10) only $R_{(r)}^{nlms}$ is unknown and contains any required parameters. These parameters are selected according to the variation procedure to minimise the energy associated with the function. For atomic calculations analytical Hartree-Fock atomic wave functions are most usual which, if used in their unrestricted form, assume $R_{(r)}^{nlms}$ to be a function of all the quantum numbers. However, more often the restricted form is used making $R_{(r)}^{nlms}$ a function of n and l, the principal and azimuthal quantum numbers, only. A significant error in the calculated e.f.g. from these wave functions is introduced thereby and is one known under the collective name of Sternheimer shielding (6). This error may be seen as the consequence of the restricted form of the Hartree-Fock wave functions assigning spherical symmetry to all filled shells. The average value of $(3 \cos^2 \theta - 1)$ is zero for a spherical distribution of charge because the average value of $\cos^2 \theta$ is one third. Therefore the filled shells are set to contribute nothing to the e.f.g. In atoms, then, the calculated e.f.g. is said to arise solely from the electrons in the valence shell. However this representation of atomic e.f.g., already subject to several approximations, requires further adjustment. Under the influence of an asymmetrical valence orbital (5) and the quadrupolar nucleus the inner filled shells distort from spherical symmetry. Their distortion makes a contribution to the total e.f.g. at the nucleus of say, $-Req_{\text{valence}}$, where eq_{valence} is the e.f.g. in the absence of such distortion.

R is called the Sternheimer polarisation factor of the atom.

The observed e.f.g. (e_q) is thus,

$$e_q = (1-R)e_{q \text{ valence}} \quad (12)$$

Using perturbation theory on restricted Hartree Fock functions, Sternheimer (6) and Scozzoco (7) have evaluated values of $(1-R)$ for free atoms, e.g. for $\text{Cl}(\text{Ne}3s^23p^5)$, $(1-R)$ is estimated as 0.888 which corresponds to shielding.

The values of R usually lie between 0.0 and 0.5.

The other important component of the nuclear quadrupole coupling constant in addition to e_q is the nuclear quadrupole electric moment, eQ . We might suggest in atoms that from experimental values of e^2qQ the value of eQ could be extracted if calculated values of e_q were available. However for many-valence-electron atoms Hartree-Fock wave functions are not sufficiently reliable and so experimental values of $\langle \frac{1}{r^3} \rangle$ are obtained. Atomic emission and atomic beam resonance spectroscopy yield values of $\langle \frac{1}{r^3} \rangle$ from the magnetic coupling between the nucleus and the electrons (9,10) which are then used to obtain "empirical values" of e_q . eQ may then be calculated, this being the most reliable method as yet (9). Armed with values of eQ the e.f.g. values for molecules containing the atoms can be obtained from their nuclear quadrupole coupling constants (e^2qQ). A valuable test of molecular wave functions is then to compare theoretical with the experimental values of e_q .

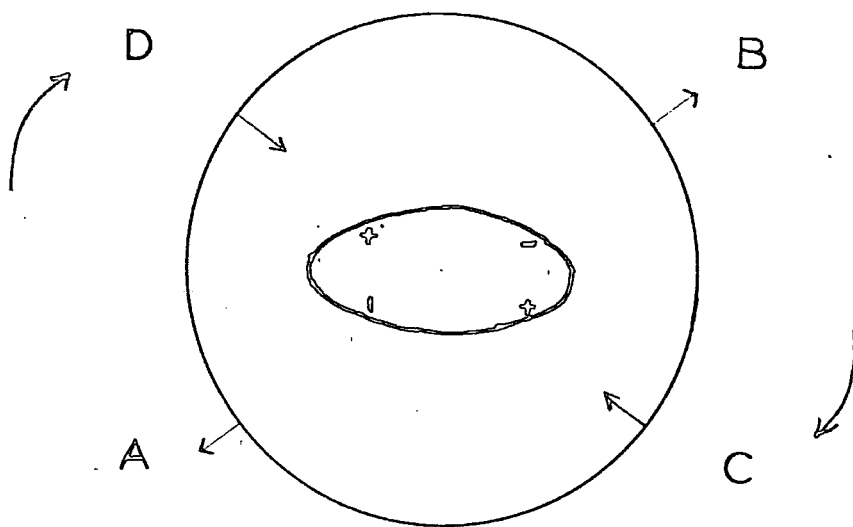
To return to Sternheimer shielding we may consider its causes and importance. The distortion from spherical symmetry of the inner shells produces an additional e.f.g. at the nucleus as shown in equation (12). The distortion or polarisation is of

two types. In the first, a radial shift of electronic charge occurs. In Fig. 2 this is represented by contraction of the shell at C and D and expansion at A and B. The main contributing electrons to the e.f.g. - the valence electrons - "feel" the quadrupolar interaction with the nucleus reinforced. This therefore is anti-shielding corresponding to a negative R. Angular distortion is the second affect and can be represented as electronic charge moving to C and D from A and B. This shields the nuclear quadrupole from the valence electrons and corresponds to a positive R.

In contrast to the generally poor theoretical values of the e.f.g. calculated for atoms, results for small molecules have proved to be closely accurate. The reason lies in that the trial wave functions used for small molecules have had few restrictions placed upon them. The use of all orbitals in self consistent field LCAO methods causes the calculation to incorporate any core orbital distortions in the final electron distribution. (Examples of the results of ab-initio calculations are given in Table 1). The polarisation effects are therefore automatically included and in such calculations on molecules the Sternheimer term can be ignored.

Still, n.q.r. data cover molecules of a far wider range than are at present amenable to theoretical evaluation by the methods above. Accurate wave functions for them cannot be expected for many years to come. Indeed the growth of experimental techniques such as n.q.r. spectroscopy has been spurred by a desire to investigate electronic structure as yet too complicated for theoretical calculations. Methods for the correlation of experimental

Fig. 2.



Sternheimer polarisation of electron shell

TABLE 1

MOLECULE	NUCLEUS	THEORETICAL FIELD GRADIENT (a.u.)	EXPERIMENTAL FIELD GRADIENT (a.u.)	REF.
Hydrogen Fluoride	^2H	-0.541	-0.52	(5)
Formaldehyde	^2H	-0.207	-0.261	(31)
Hydrogen Sulphide	^2H	-0.265, $\eta = 0.167$	-0.229, $\eta = 0.205$	(32)
Hydrogen Cyanide	^2H	-0.317	-0.310	(33)
	^{14}N	-1.204	-1.131	
Nitrogen	^{14}N	-1.35	-1.323	(34)
Hydrogen Chloride	^{35}Cl	+3.923	3.639	(8)
		+3.612	3.639	(5)
Aziridine	^{14}N	-1.008, $\eta = 0.683$	-1.038, $\eta = 0.629$	(35)
Pyrole	^{14}N	-1.480, $\eta = 0.109$	-0.752, $\eta = 0.071$	(35)
Isoxazole	^{14}N	-1.695, $\eta = 0.704$	0.3	(35)
Oxazole	^{14}N	-1.405, $\eta = 0.314$	-1.123, $\eta = 0.21$	(35)
Pyridine	^{14}N	-1.778, $\eta = 0.115$	-1.374, $\eta = 0.405$	(35)
Pyrazine	^{14}N	-1.868, $\eta = 0.048$	-1.291, $\eta = 0.536$	(35)

AN ILLUSTRATIVE LIST OF MOLECULES FOR WHICH AB INITIO
WAVE-FUNCTIONS ARE AVAILABLE.

nuclear quadrupole coupling constants with electron distributions have been developed and these techniques are now discussed.

Approximate Methods

Consider equation (9a) and ways to simplify the interactions. Townes and Dailey proposed several simplifications (12) which included,

- 1) An assumption that only valence electrons of the quadrupolar nucleus are important in generating the e.f.g. i.e. eq_{valence} .

This therefore assigns spherical symmetry to the inner shells. As seen already, this is not strictly true and so a correction factor, P, is introduced to represent the e.f.g. contribution generated by the polarised inner orbitals.

- 2). An assumption that in other nuclei of the molecule their inner shells are tightly bound and that the e.f.g. at the quadrupolar nucleus is due to them as point charges of value (Z-n) where n is their valency and Z is their nuclear charge. This contribution is written as eq_{core} . The assumption of fixed nuclei is included.

1) and 2) may therefore be summarised as, molecular e.f.g., eq :

$$eq = eq_{\text{valence}} - eq_{\text{core}} - P \quad (13)$$

$$\begin{aligned} \text{where, } eq_{\text{valence}} &= \left\langle \psi_{\text{valence elec.}} \left| \sum_i \frac{3\cos^2\theta_i - 1}{r_i^3} \right| \psi_{\text{valence elec.}} \right\rangle \\ &\equiv \left\langle \psi_{\text{valence}}^* \left| \mathcal{H}_q \right| \psi_{\text{valence}} \right\rangle \quad (14) \end{aligned}$$

The field gradient operator \mathcal{H}_q is a one electron operator and usually ψ_{valence} is written as a Slater determinant in terms of orthogonal one electron wave functions (χ_j) - molecular orbitals, M.O. i.e.

$$\psi_{\text{valence}} = \chi_1 \cdot \chi_2 \cdots \chi_j \cdots \chi_N \quad (15)$$

In the LCAO-MO approximation the M.O.'s. are written as linear combinations of atomic orbitals, A.O.'s., ϕ . i.e.

$$\psi_j = \sum_k a_{jk} \phi_k \quad (16)$$

Substituting equation (16) in equation (14) gives,

$$\begin{aligned} \text{eq valence} = \sum_j & \left\{ \sum_k a_{jk}^2 \langle \phi_k | \mathcal{H}_j | \phi_k \rangle + \sum_l a_{jl} \langle \phi_l | \mathcal{H}_j | \phi_l \rangle \right. \\ & + \sum_{k \neq l} a_{jk} a_{jl} \langle \phi_k | \mathcal{H}_j | \phi_l \rangle + \sum_{l \neq m}^{(17)} a_{jl} a_{jm} \langle \phi_l | \mathcal{H}_j | \phi_m \rangle \end{aligned}$$

where j indicates summing over the valence M.O.'s., k over the A.O.'s. of the quadrupolar nucleus, and l and m over A.O.'s. of other nuclei. Equation (17) represents (within the LCAO-MO approximation) an exact expression for the electronic e.f.g. of an isolated molecule. The approximations of Townes and Dailey allowed the separation of the observed e.f.g. (eq) into three components (equation 13). Comparison of the terms in equation (17) with those in equation (13) provided Townes and Dailey with an approximation allowing development of a method for interpreting nuclear quadrupole coupling constants (n.q.c.c.). The contribution of nuclei external to the quadrupolar nucleus (eq_{core}) and that of the inner shells of the quadrupolar nucleus (P) are set against the two-(k, l) and three-(l, m) centre terms of equation (17). Namely that the e.f.g. experienced by the nucleus is,

$$\text{eq} = \sum_j \sum_k a_{jk}^2 \langle \phi_k | \mathcal{H}_j | \phi_k \rangle \quad (18)$$

This results in treatment considering only orbitals on the

quadrupolar nucleus and those of atoms to which it is bonded.

A description of the Townes and Dailey (approximate) method for determination/interpretation of n.q.c.c.'s. is given later.

A study of exact solutions of equation (17) has however shown that eq_{core} is equal and opposite to the second term plus one half of the third term in equation (17). Cotton and Harris (13) have shown this to be closely the case in several halogen complexes.

They propose that the e.f.g. is,

$$eq = \sum_j \left\{ \sum_k a_{jk}^2 \langle \phi_k | \mathcal{H}_q | \phi_k \rangle + \frac{1}{2} \sum_{k \neq l} a_{jk} a_{jl} \langle \phi_k | \mathcal{H}_q | \phi_l \rangle \right\} + P \quad (19)$$

because the three-centre integrals (in l and m) are certainly all small and can be neglected. Cotton and Harris suggested that Mulliken type approximations (14) be made for the two-centre integral in equation (19), i.e.

$$\langle \phi_k | \mathcal{H}_q | \phi_l \rangle = S_{kl} \langle \phi_k | \mathcal{H}_q | \phi_k \rangle \quad (20)$$

where S_{kl} is the overlap integral $\langle \phi_k | \phi_l \rangle$. Therefore from (19),

$$eq = \sum_j \sum_k \left\{ \langle \phi_k | \mathcal{H}_q | \phi_k \rangle \left(a_{jk}^2 + \frac{1}{2} a_{jk} \sum_{l \neq k} a_{jl} S_{kl} \right) \right\} + P \quad (21)$$

Equation (21) may be written as,

$$eq = e \sum_k f_k v_k + P \quad (22)$$

where, $eq_k = \langle \phi_k | \mathcal{H}_q | \phi_k \rangle$

and is the e.f.g. generated by an electron in the k^{th} A.O. and, also in equation (22),

$$f_k = \sum_j \left\{ a_{jk}^2 + \frac{1}{2} a_{jk} \sum_{l \neq k} a_{jl} S_{kl} \right\} \quad (23)$$

The nuclear quadrupole coupling constant is given by,

$$|e^2 q Q| = \sum_k f_k \left\{ e^2 q_k + \frac{e^2 P Q}{\sum_k f_k} \right\} \quad (24)$$

The second term, in P, is incalculable. An approximation common to all (approximate) methods was invoked by Cotton and Harris, viz. that the polarisation effects are proportionately the same in the isolated atom as in the atom in a molecule and that they vary negligeably from molecule to molecule. The polarisation effects are said to be included in the e.f.g. due to an election in an A. O., ϕ_k . Hence,

$$|e^2qQ| = \sum_k f_k \cdot e^2q_kQ \quad (25)$$

The terms f_k are Mulliken's total (gross) atomic orbital populations (14). As will be seen later, if S_{k1} is set to zero, equation 25 reduces to the Townes and Dailey expression for the n.q.c.c..

Cotton and Harris (15) applied equation 25 to calculating e.f.g.'s at ^{35}Cl for complexes of the type MCl_n^{m-} (e.g. PtCl_4^{2-} , PtCl_6^{2-}) where the quantities needed for (25) were already estimated. For PtCl_4^{2-} , they computed a value of 34 MHz for the n.q.c.c. (expl. value 36.1 MHz). However, the predicted e^2qQ values must be viewed in the light of approximations made in deriving the eigenfunctions used in the calculation. For this reason and the general lack of sufficiently accurate eigenfunctions, the method of Cotton and Harris is not of general use. However, it retains the advantage of being based on an M.O. description of the chemical bonds in a molecule.

Kaplansky and Whitehead (37) have reported an erratum to an equation presented by Cotton and Harris. Correctly stated, the equation is

$$e^2qQ = 109.7 \sum_i \sum_k (2 - \{ N_k (C_{ik}^2 + \sum_{j>i} C_{ik} C_{jk} S_{ij}) \})$$

and represents the change in the n.q.c.c. caused by the change in occupancy of atomic orbital i due to bonding. We therefore turn to a more detailed analysis of the applications of the method of Townes and Dailey.

The Townes and Dailey Method.

In equation (18) the atomic orbitals ϕ_{nl} are written as products of a radial function and a spherical harmonic as in equation (13), i.e.

$$\phi_{nl} = A_{kl} R(r) Y^{lm}(\theta, \phi) \quad (13)$$

Here the spin functions X^S are ignored since for one electron A.O.'s they are the two usual $s = +\frac{1}{2}$ functions. Substitution of (13) in equation (18) gives the principal component of the e.f.g. generated by one electron in an A.O. (1),

$$eq_{(A.O.)} = \langle \phi | \frac{3\cos^2\theta - 1}{r^3} | \phi \rangle \quad (26)$$

$$= \left\{ \frac{3m^2 - 1(1+1)}{1(2l-1)} \right\} \left\{ \frac{2l}{2l+3} \right\} \left\langle \frac{1}{r^3} \right\rangle \quad (27)$$

where $\left\langle \frac{1}{r^3} \right\rangle$ is the average value of the function $\frac{1}{r^3}$ over

the A.O. in space.

Townes and Dailey (12) state that the e.f.g. due to p-electrons is far greater than that due to any other source. This is supported theoretically and on experimental evidence. With the knowledge that distortion (polarisation) of inner shells is accommodated already, we can say that they contribute nothing to the total e.f.g., as do the s-orbitals due to their spherical symmetry.

For a p - electron, the maximum e.f.g. arises for

a P_z electron. So from equation (27):

$$eq(p_z) = 4/5 \left\langle \frac{1}{r^3} \right\rangle \quad (28)$$

For d - electrons, however, the maximum occurs for

a d_z^2 electron (signs of e.f.g.'s are opposite) and

$$\begin{aligned} \text{eq}(d_z^2) &= 4/7 \left\langle \frac{1}{r^3} \right\rangle & (29) \\ &= -\text{eq}(d_x^2 - d_y^2, dxy) \end{aligned}$$

From these calculations on the angular terms only,

p - electrons contribute more to the e.f.g. Furthermore,

average values for $\left\langle \frac{1}{r^3} \right\rangle$ for p and d orbitals are in the

ratio 8 : 1 (same n) given by

$$\left\langle \frac{1}{r^3} \right\rangle = \frac{Z^3}{a_0^3 n^3 l^3} \quad (30)$$

where Z = nuclear charge (number of protons), a_0 is the radius of the first shell, n and l are the principal and azimuthal quantum numbers respectively. Although, of course, hydrogenic radial functions (30) are not generally applicable it is found experimentally that the e.f.g.'s produced by p - electrons are ten times those produced by d - electrons having the same principal quantum number (n). A consequence of the field gradient's dependence upon Z^3 is that the nuclear quadrupole coupling constants are likely to be higher for nuclei of high atomic number. This theory is particularly appropriate to ^{35}Cl where the e.f.g. usually lies along its bond.

With regard to the e.f.g. generated by p - electrons, it is clear that the maximum value for the e.f.g. is generated along the symmetry axis of the orbital. Hence we define eq_0 as the principal component of the e.f.g. tensor given by a p - orbital, i.e.

$$\text{eq}(p_z) = \text{eq}_0 \quad (31)$$

From the Laplace condition (Chapter 1, equation (4)),

the contributions of the other two p - orbitals can be estimated. On the other hand, equation (27) could be used for $m = 1$. This gives for an electron in the p_x and p_y ,

$$eq(p_x) = eq(p_y) = -\frac{1}{2}eq_0 \quad (32)$$

For Townes and Dailey, therefore, the e.f.g., generated by the p - orbitals is

$$\begin{aligned} eq &= a_z(eq_0) - \frac{1}{2}(a_x + a_y)(eq_0) \\ &= eq_0(a_z - \frac{1}{2}(a_x + a_y)) \end{aligned} \quad (33)$$

where a_j is the electron occupancy of the p_j orbital.

Let us consider the case of a chlorine atom. Its electronic configuration is $1s^2 2s^2 2p^6 3s^2 3p^5$ but its inner shell $1s^2 2s^2 2p^6$ is spherically symmetrical under the Townes and Dailey approximations. The shell and $3s^2$ therefore contribute nothing to the e.f.g. The p - orbitals are $3p_x^2, 3p_y^2, 3p_z$, labelling the symmetry axis the z axis. The e.f.g. along this z axis is then determined by the orbital occupancy of the Cl 3p orbitals. Thus:

<u>Orbital</u>	<u>Orbital gradient</u>	<u>Orbital population</u>	<u>Total gradient</u>
$3p_x$	$-\frac{1}{2} eq_0$	2	$-eq_0$
$3p_y$	$-\frac{1}{2} eq_0$	2	$-eq_0$
$3p_z$	eq_0	1	eq_0

For a chlorine atom, therefore, the e.f.g. is $-eq_0$. This may be related to the nuclear quadrupole coupling constant, $|e^2qQ|$ (measured by atomic spectra), 109.6 MHz. Thus the total e.f.g. is equal, but opposite in sign to that produced

by a single electron in the $3p_z$ orbital.

In the chlorine molecule the e.f.g. at the chlorine atom is generated by the electrons in the single bond involving the $3p_z$ orbital (or a $3s - 3p_z$ hybrid orbital) and those in the $3p_x$ and $3p_y$ orbitals. We may write a general s-p hybrid as:

$$\begin{aligned} \text{bonding } \phi_b &= \alpha 3s + (1 - \alpha^2)^{\frac{1}{2}} 3p_z \\ \text{non-bonding } \phi_{nb} &= (1 - \alpha^2)^{\frac{1}{2}} 3s - \alpha 3p_z \end{aligned} \quad (34)$$

The bonding A.O.'s (ϕ_b) combine to make the bonding sigma orbital, $\bar{\Phi}_b$.

$$\bar{\Phi}_\sigma = \frac{1}{\sqrt{2(1-S)}} (\phi_b^1 + \phi_b^2) \quad (35)$$

where S is the overlap integral (equation (20)) between the bonding orbitals. The e.f.g. along the z axis at one of the chlorine nuclei is therefore the sum of the $n = 3$ orbital contributions. i.e.

Orbital	Orbital gradient	Orbital population	Total gradient
$\bar{\Phi}_b$	$\frac{1-\alpha^2}{2(1+S)} \cdot eq_0$	2	$\frac{(1-\alpha^2)}{(1+S)} \cdot eq_0$
$\bar{\Phi}_{n.b.}$	$\alpha^2 eq_0$	2	$2\alpha^2 \cdot eq_0$
$3p_x$	$-\frac{1}{2} eq_0$	2	$-eq_0$
$3p_y$	$-\frac{1}{2} eq_0$	2	$-eq_0$

For the chlorine molecule the e.f.g. is therefore $eq_0(1 - \alpha^2)\left(\frac{1}{1+S} - 2\right)$ and the value of $|e^2qQ|$ measured by n.q.r. is 108.9 MHz.

The assumption by Townes and Dailey that overlap contributions may be ignored helps simplify the expression for the e.f.g. of molecular chlorine. Furthermore, the close

similarity of the coupling constant values for atomic and molecular chlorine suggests that α has a value close to zero. This is assumed and a Hückel description has subsequently been widely used. The approximations for a simplified expression also include an exclusion of d - orbital participation in bonding.

In a heteronuclear bond, R-Cl, the e.f.g. at chlorine is generated by a polarised covalent bond. If chlorine is the more electronegative atom in the molecule R-Cl we may view the bonding in a valence bond picture as being a resonance hybrid of ionic and purely covalent forms

$$\text{i.e. } \Phi = (1 - i)(R - Cl) + i(R^+Cl^-) \quad (38)$$

where i is the fractional ionic character of the bond.

Since for Cl^- all three p - orbitals are filled and the electron distribution spherically symmetric its contribution to the e.f.g. at chlorine is zero. Therefore, the total gradient is along the R-Cl bond,

$$eq = - (1 - i)(1 - \alpha^2)eq_0 \quad (39).$$

Because α^2 is usually ignored, the ionicity (i) of the R-Cl bond may therefore be calculated from equation (39).

In the case of the molecule R-Cl where chlorine is the less electronegative partner, the more likely resonance hybrid is

$$\Phi = (1 - b)(R - Cl) + b(R^-Cl^+) \quad (40)$$

The positive charge on chlorine causes a contraction in the orbitals in excess of that already allowed for, and thereby increases the e.f.g.. A correction term, ϵ , is therefore introduced, values of which are available for

various atoms (16). It is usually small, e.g. for chlorine a value of 0.14 is used. The weighted e.f.g., if s-p hybridisation is ignored ($\alpha = 0$), is then

$$\begin{aligned} eq &= -e((1 - i)q_0 - 2i(1 + \epsilon)q_0) \\ &= -eq_0(1 + i + 2i\epsilon) \end{aligned} \quad (41)$$

For chlorine involved in π -bonding the axial symmetry of the e.f.g. is disturbed, i.e. $a_x, a_y \neq 2$. The asymmetry parameter, η , is an experimentally obtainable quantity and can be related to orbital populations (a_j) thus:

$$\begin{aligned} \text{e.f.g. due to } p_z, \quad eq_z &= eq_0 \left(a_z - \frac{1}{2}(a_x + a_y) \right) \\ \text{e.f.g. due to } p_y, \quad eq_y &= eq_0 \left(a_y - \frac{1}{2}(a_x + a_z) \right) \\ \text{e.f.g. due to } p_x, \quad eq_x &= eq_0 \left(a_x - \frac{1}{2}(a_y + a_z) \right) \end{aligned} \quad (42)$$

$$\text{and, therefore, } e^2qQ = \sum_{i=x,y,z} \left(a_{zi} - \frac{1}{2}(a_{xi} + a_{yi}) \right) e^2q_0Q \quad (43)$$

From equation(5) in chapter 1, therefore:

$$\eta \left(\frac{eq_z}{eq_0} \right) = 3/2 (a_x - a_y) \quad (44a)$$

The ratio $\frac{eq_z}{eq_0}$ may be replaced by that of the coupling constants;

that is, of the compound in question to that of the chlorine molecule which has full p-orbital occupancy and $\eta = 0$. In conjugated carbon-chlorine bonds, the original application of this formula, the difference in occupancy of the p_x and p_y orbitals ($a_x - a_y$) represents the degree of π -bonding (π) present. It was obtainable from the two measurable parameters, η and e^2qQ . i.e. from equation (44a),

$$\text{differential } \pi\text{-character of bond, } (\pi) = \frac{2}{3} \eta \left(\frac{e^2qQ}{109.6} \right) \quad (44b)$$

Although the above expressions have been derived from a consideration of chlorine as the quadrupolar nucleus, the following example of pyridine illustrates their wider use - in this case for ^{14}N as the quadrupolar nucleus. Assuming that the nitrogen σ bonds in pyridine can be represented by sp^2 hybrids and that the π -electrons move in an M.O.

which, close to nitrogen, appears as a pure p - orbital, the e.f.g. contributions may be determined. From bonding wave functions (17),

$$\begin{aligned} eq_z &= eq_0(4/3 - \frac{1}{2}a - 1/6b) \\ eq_y &= eq_0(-\frac{2}{3} + a - \frac{2}{3}b) \\ eq_x &= eq_0(-\frac{2}{3} - \frac{1}{2}a + 5/6b) \end{aligned} \quad (45)$$

where b is the occupancy of the N - C σ bonds, a is the π - electron density and it is assumed that 2 electrons lie in the lone pair. This lone pair makes the greatest contribution to the e.f.g. at the nitrogen atom and so the C_{2v} axis of the molecule is chosen as the z axis. The y axis is taken perpendicular to the plane of the ring and the x axis lies in its plane.

From (45) the equations for e^2_{qQ} and η are derived and

$$\frac{e^2_{qQ}}{e^2_{q_0Q}} = 4/3 - \frac{1}{2}a - 1/6b \quad (46)$$

while
$$\eta = 3/2(b - a) \frac{e^2_{q_0Q}}{e^2_{qQ}}$$

Equations (46) can be solved for a and b using the experimental values $e^2_{qQ} = 4.584$ MHz and $\eta = 0.396$ and taking for ^{14}N $e^2_{q_0Q} = 8.4$ MHz (18). Thus,

$a = 1.145$, $b = 1.289$ and $c = 0.723$, where c is the total excess electron density on the nitrogen viz:

$$c = (a + 2b - 3).$$

As a final expression concerning π - bonding we consider the cases of (a) both p_x and p_y orbitals involved in π - bonding and (b) only one of them involved.

Thus from equation (33) for a halogen bond:

$$\begin{aligned} (a) \quad \frac{e^2_{qQ}}{109.6} &= (1 - i - \pi) \\ (b) \quad \frac{e^2_{qQ}}{109.6} &= (1 - i - \frac{\pi}{2}) \end{aligned} \quad (47)$$

neglecting any contribution of the 3d orbitals. These, then, can be used with an expression for ionicity, i ,

$$i = \frac{1}{2}(X_a - X_b) \quad (48)$$

where X_i are the electronegativities of the bonded atoms involved (19,20). Equation (48) can be used to yield from equation (44) an estimate of η if it is not already known.

Lucken has proposed that the most serious defect of the Townes and Dailey method is its failing to take account of the m (magnetic quantum number) dependence of the field gradients produced by the valence orbitals (21). He has suggested that different values of e^2q_0Q be used for the σ and π electrons. However, although it should prove worthwhile, the lack of data needed makes its development unlikely at present.

To sum up then, the Townes and Dailey approach contains many major approximations but attempts at refinements do not normally bring better agreement. This is probably caused by the fortuitous cancellation of conflicting requirements for the majority of molecules. The theory works especially well for the halogens where it is possible that the effect of d - orbital hybridisation on e^2q_0Q , acting in the opposite sense to that of s - hybridisation, effectively balance one another out in molecules of related structure, (20a).

Temperature effect on n.q.r.

The n.q.r. frequency is not always a continuous function of the temperature of a sample. Usually the discontinuity is caused by a phase change in the solid sample or by the introduction of another molecular mode of motion, causing a change in the e.f.g. experienced by the quadrupolar nucleus. An interesting example of discontinuity caused by the onset of a hindered rotation motion is transdichloroethane (22) where, after a break in the recorded signal, one returns but now lies 4.5 MHz lower in frequency. The pressure dependence of this phase transition has now been recorded (36).

The number of lines observed in the n.q.r. spectrum is indicative of the number of inequivalent sites in the crystal unit cell. Therefore, the n.q.r. data provide an aid to the information available from X - ray structural investigations. Single crystal Zeeman studies of nuclear quadrupole resonances locate the principal e.f.g. axes which thereby fix the locations of the quadrupolar nuclei in the unit cell.

^{35}Cl n.q.r. has been used to elucidate the molecular geometries of many chloro-compounds which exist in the solid state and are not readily investigated by such as n.m.r. Examples of these lie in the field of phosphorus chemistry where phosphorus V halides have received much attention (30).

Phosphorus pentachloride has a trigonal bipyramidal structure in the gas phase but the usual solid PCl_5 is known to be an ionic crystal $(\text{PCl}_4)^{\oplus}(\text{PCl}_6)^{\ominus}$. (24,25). As expected,

there are four resonances at high frequencies due to PCl_4^+ and six at lower frequencies due to PCl_6^- . (26). A metastable molecular form of PCl_5 has yielded a spectrum consisting of two low frequency lines and a single high frequency line (27). This is interpreted as indicating a trigonal bipyramidal structure with the two frequencies at low frequencies due to the axial chlorine atoms and the single higher frequency line due to the three identical equatorial chlorine atoms. A consideration of phosphorus V chlorofluorides (28,29) has shown that the more electronegative fluorine atoms prefer to occupy the axial positions which are therefore assumed to be more ionic. This is supported by their longer bond lengths and lower n.q.r. frequencies.

Finally, to illustrate the use of the asymmetry parameter (η) in structural investigations we may consider the case of some cobalt carbonyl derivatives. In the case of molecules such as $\text{Co}(\text{CO})_3\text{X.Y}$ (where $\text{X} = \text{PPh}_3, \text{AsPh}_3$ and $\text{Y} = \text{SiCl}_3$) the ^{59}Co n.q.r. frequencies show the asymmetry parameter to be zero. This therefore shows the molecules to be trigonal bipyramidal with the ligands X and Y in trans-positions.

Introduction

The first nuclear quadrupole resonance was detected in 1950 by Dehmelt and Krüger (1), since when efforts to improve and develop methods of detection have been unceasing. Among those techniques achieving wide acceptance are pulsed - (2) and double resonance - spectrometers (3) which are discussed later.

The n.q.r. spectrometers employed in this work have been the DECCA super-regenerative type and a home-built Robinson - oscillator spectrometer. This latter continuous wave (c.w.) spectrometer was originally passed to us by AEL. In addition to discussion of the basic types of spectrometer, methods of signal improvement are covered. The development and use of a computer of average transients (c.a.t.) and of a sinusoidal Zeeman modulator are also described.

Marginal oscillator

Developed by Pound and Knight (4) the marginal oscillator improved upon the separate oscillator circuits (5) which were very prone to microphonic noise. With a valve feedback circuit it has no requirement for the constant current source of the separate oscillator and is therefore a simpler circuit. The amplitude of oscillations is determined by the balancing of the (negative) conductance of the feedback circuit with the shunt resistance of the circuit. When resonance of the circuit with a nuclear absorption occurs, energy is absorbed from the radio frequency field and the effective shunt resistance increases. The amplitude of oscillation is therefore diminished and this is detected. Because the voltage on the coil is much greater than the nuclear signal voltage, almost pure absorption lineshapes are obtained from this type of oscillator.

Limitations to the range of operation of the marginal oscillator arise from instability in the mutual conductance of the (feedback) valve. Only at low levels is sensitivity satisfactory but below about 20 mV on the coil oscillation is likely to cease. It is also unlikely to sustain oscillation with the oscillator circuit of low L/C ratio. Although relatively insensitive to microphonic noise, spurious amplitude modulation due to frequency modulation breakthrough causes problems. To maintain the marginality of the oscillator, adjustments to the feedback must be made as the frequency is swept. The marginal oscillator is therefore of limited use in n.q.r. spectroscopy and is only applied to low frequency resonances with narrow linewidths e.g. ^{14}N n.q.r.

It is however widely used in n.m.r. where the feedback adjustment is not required if the field is swept.

Robinson oscillator

The Robinson oscillator (6) uses separate oscillator and limiter devices and thereby removes the disadvantages of the marginal oscillator which has a single device to provide both regeneration and limiting. The resulting circuit experiences much reduced breakthrough of frequency modulation but maintains the freedom from microphonic noise found in the marginal. This type of circuit is sometimes referred to as a limited oscillator. The relationship between regeneration and circuit loss is linear and so great changes in radio-frequency (r.f.) level do not result from slight fluctuations in regeneration. The preferred limiting device is a saturated pentode which, when coupled with the correct resistor, provides adequate limiting action for a 20:1 change in r.f. level. Improved sensitivity compared with the marginal oscillator is combined with this greater range of r.f. level. Whilst providing high enough r.f. levels for quite broad n.q.r. lines, low levels (needed for narrow lines) are obtained easily due to adequate regeneration which can sustain oscillation with circuits of a low L/C ratio. The Robinson oscillator, having a large frequency range (up to 40 MHz), may therefore be used in n.q.r. investigations of both ^{35}Cl and ^{14}N nuclei.

Edmonds and Robinson (7) have introduced a capacitive potential divider for the feedback circuit which allows a higher voltage on the oscillator coil before the amplifier is overloaded. This makes possible the use of limited oscillators like the

Robinson circuit at increased r.f. levels without losing the advantage of r.f. amplification before detection, namely high sensitivity to narrow lines. This development enables the limited oscillator to rival the super-regenerative oscillator in the lower frequency range (<40 MHz) with the advantage of a better lineshape response. The Robinson oscillator used in work reported in this thesis is shown overleaf and will now be described.

Built originally by A.E.I. (Dr. H. Barber) the oscillator comprises a resonant circuit with its coil enclosing the sample, an E180F amplifier, a diode (1K914) and a 6AK5 limiter, the output of which is fed back to the resonant circuit via a resistor. (Fig.5). The 6AK5, augmented by the 1K914, also serves as a grid-leak detector for the n.q.r. signal. The oscillator is frequency modulated using a varactor diode (VLA 721B). A 6:1 variation in r.f. level can be achieved, the range being set by varying the value of the feedback resistor or capacitor. The lower limit to r.f. is approximately 0.1V peak and is due to the limited gain of the single E180F. At the upper limit of approximately 1V peak, grid current flows and renders the circuit insensitive. Although replacement of the E180F by a higher gain valve (E810F) produced more than 10V peak to peak, the sensitivity of the circuit to n.q.r. was degraded.

The r.f. levels obtained from the spectrometer are adequate for the detection of some quadrupole resonances which are often easily saturated (Fig. 1). Although the r.f. levels are not high enough for the broader ^{35}Cl and ^{37}Cl resonances (e.g. di-*t*-butylketimineborondichloride $(\text{Bu}^t)_2\text{CNBCl}_2, \Delta\nu = 22\text{kHz}$) (Fig. 2), the narrow linewidth ($\Delta\nu$)

Fig. 1. ^{15}N n.g.r. of Hexamine ; 3.308 MHz at 296 K.

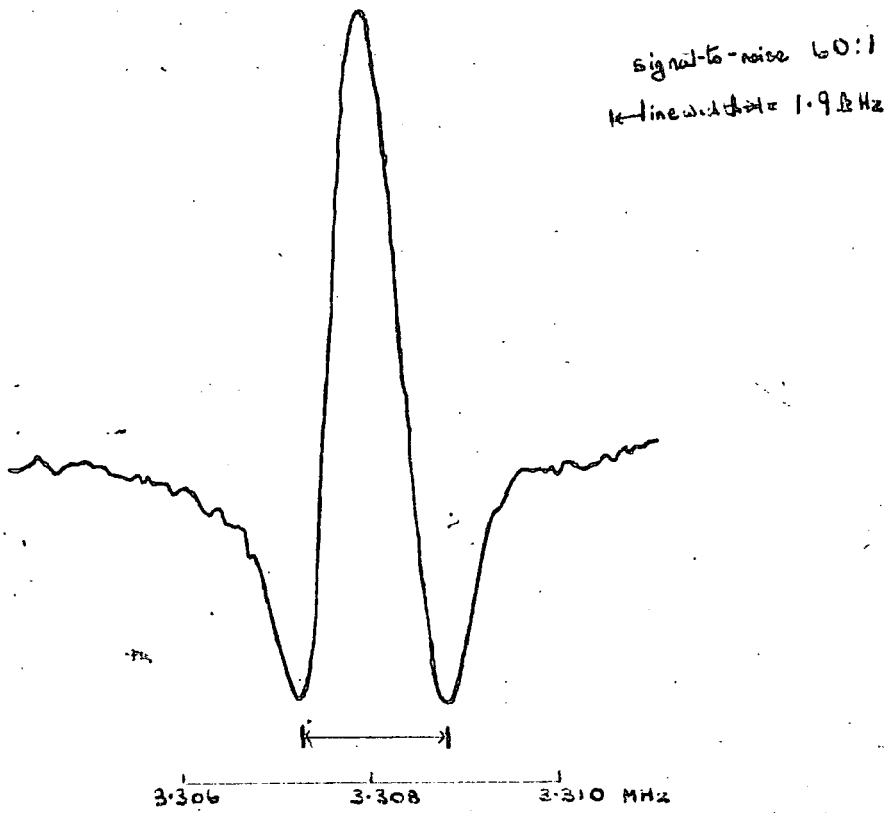
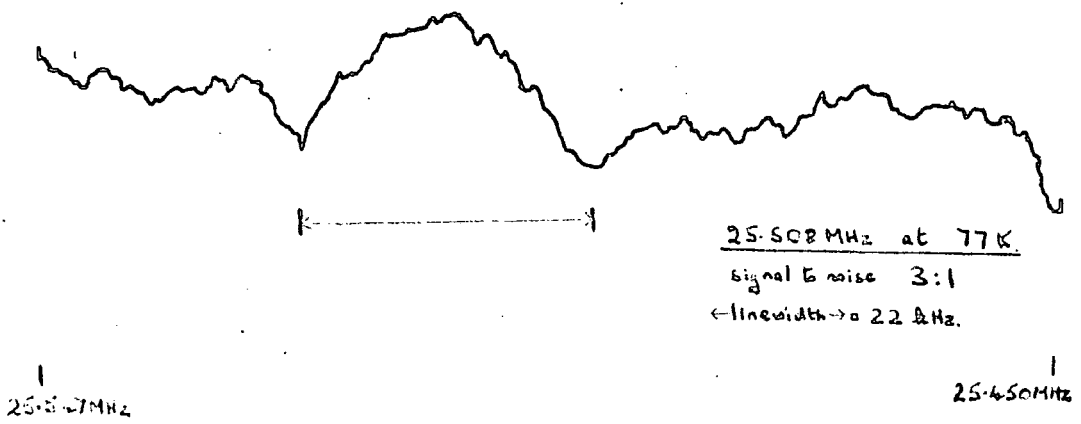
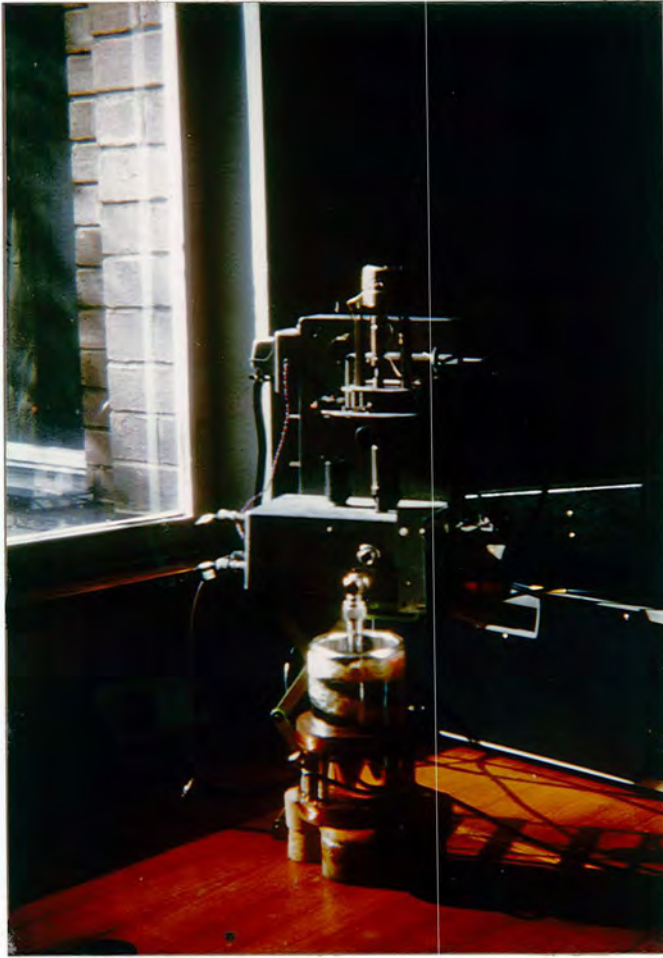


Fig. 2. ^{35}Cl n.g.r. of phenyl phosphorus tetrachloride





The probe and head of the "AEI" spectrometer

resonances of mercuric chloride and boron trichloride ($\Delta\nu = 5\text{kHz}$) are detected strongly (Fig. 3). The doublet observed for boron trichloride is worthy of comment. The separation measured in Fig. 3 is 4.95kHz and may be compared with 3.68kHz measured by Raman et al (3). The doublet was explained as due to $^{11}\text{B}-^{35}\text{Cl}$ and $^{10}\text{B}-^{35}\text{Cl}$ isotopes. The full ^{35}Cl n.q.r. spectrum of titanium tetrachloride is displayed in Fig. 4.

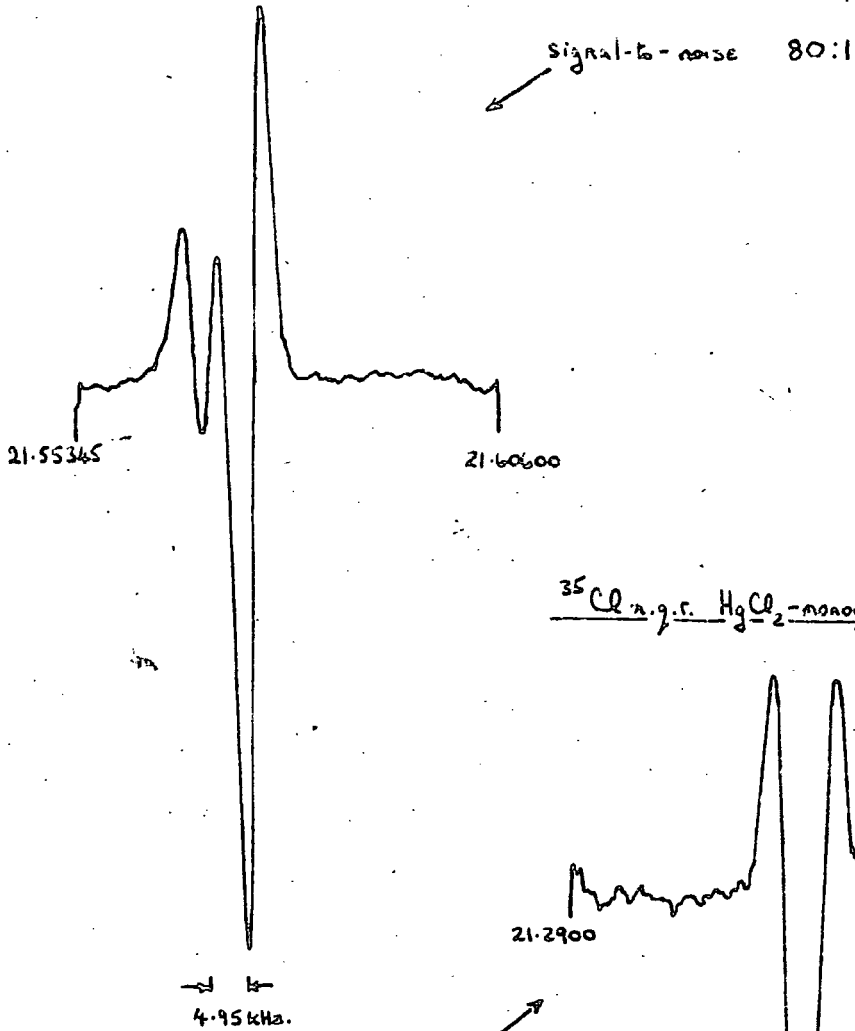
With frequency-modulation (f.m.) detection a small amplitude modulation effect accompanies the f.m. which produces a resonance in the oscillator circuit at the f.m. frequency. As its magnitude is greater than that of the n.q.r. signal, this resonance is filtered in the pre-amplifier. An op. amp. (741LN) is set to unity gain except for a sharp rejection notch at the modulation frequency of 140Hz . Any second harmonic of the spurious resonance (280Hz) cannot be removed because detection at the phase sensitive detector is at twice the f.m. frequency. It is therefore necessary in searching for a quadrupole resonance to carry out search sweeps both with the sample present and with it absent.

The frequency modulation is generated by a vibrating high-Q reed oscillating at 140Hz . The very stable sinusoidal waveform is used to modulate the r.f. oscillator and to generate a 280Hz square wave to the phase detector.

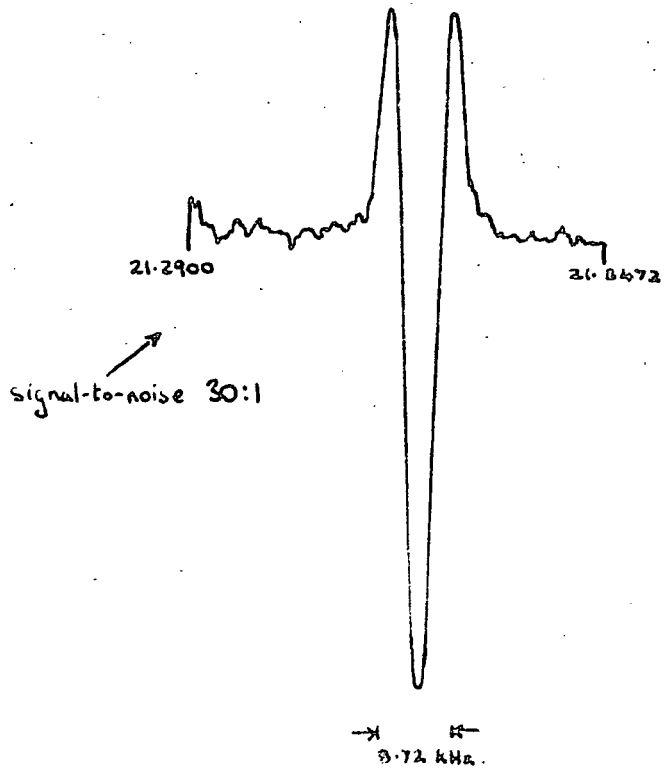
Sinusoidal Zeeman modulation using a stabilised power supply driven by a frequency generator has been employed in lineshape studies using this spectrometer. Results are reported later. The advantage of Zeeman modulation is that as its influence

Fig 3

^{35}Cl n.g.r. BCl_3 at 77K.



^{35}Cl n.g.r. HgCl_2 -monoglyme adduct at 77K.



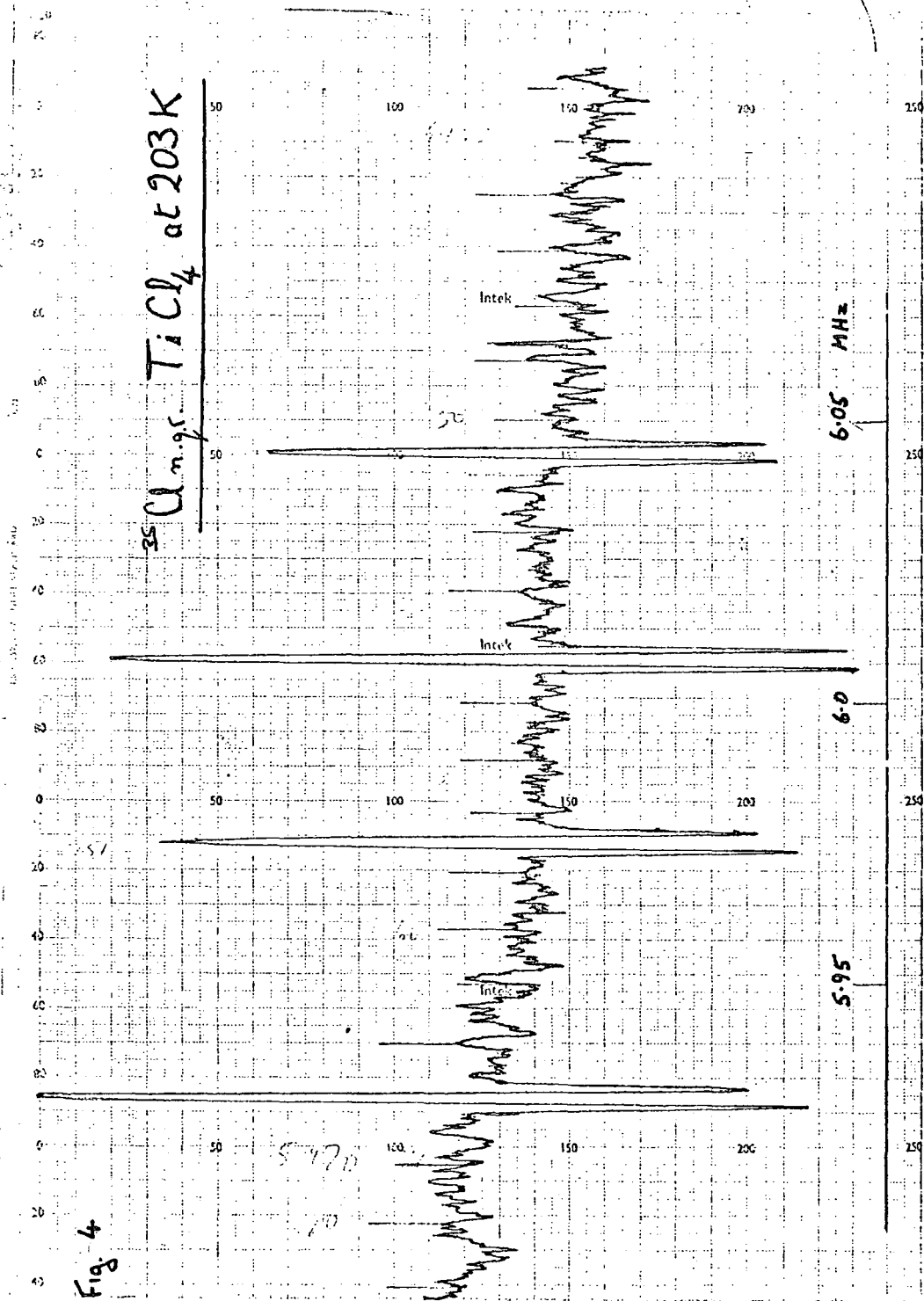


Fig 4

is directly upon the quadrupole interaction, external spurious signals are not observed.

A circuit diagram of the AEI spectrometer appears in Fig. 5. The overall preamplifier gain is approximately 200 and the signal is applied to a unity gain buffer, to high-pass filters and to a low-pass filter. Following the gain control, the signal is amplified and passed to the phase detector. After optimising the phase of the reference to give maximum n.q.r. signal, the output is amplified and fed to a chart-recorder.

Although the spectrometer does not have automatic gain control, drift of the base line is not usually a problem. The level of noise can be reduced with the use of long time constants but in practice the time constant used did not usually exceed 10 sec.

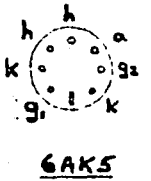
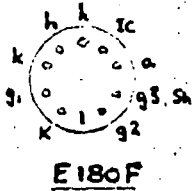
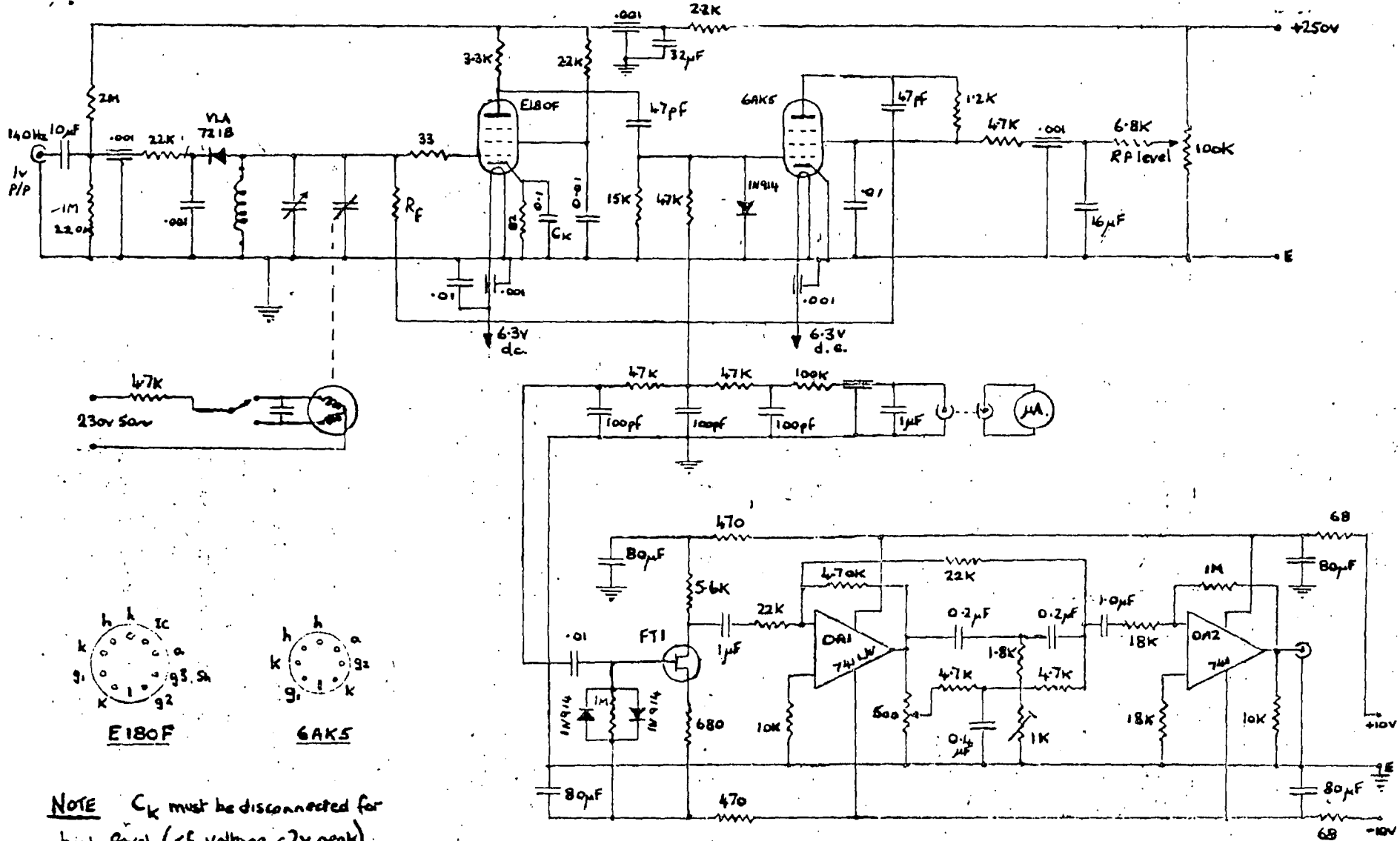
Super-regenerative oscillator

The first nuclear quadrupole resonance was detected using a super-regenerative oscillator (s.r.o.) (1). This device is one of the most widely used in n.q.r. spectroscopy because of the wide frequency ranges (5-1000MHz) and high r.f. levels (1-10V) obtainable. However, an s.r.o. is seldom satisfactory as a detector when operating below 5MHz and is therefore used for such nuclei as ^{35}Cl , ^{81}Br , ^{121}Sb , ^{59}Co .

The operation of the s.r.o. is to allow the r.f. oscillation envelope to periodically build up after which it forces the envelope to decay. This is termed "quenching" and in the DECCA spectrometer employed in this work an externally

FIG. 5.

CIRCUIT DIAGRAM OF AEI SPECTROMETER.



NOTE C_k must be disconnected for high level (r.f. voltage $\approx 2V$ peak) operation & R_f should be decreased.

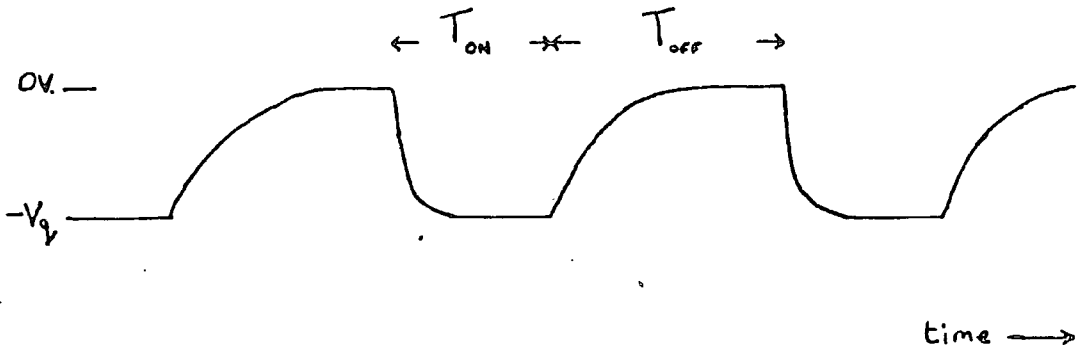
ROBINSON OSCILLATOR AND PRE-AMPLIFIER

generated waveform is used, the frequency of which is about 10^{-3} times that of the oscillator. The quenching effect is illustrated in Fig. 6. The quench voltage is applied as a bias to the active device of the oscillator, causing oscillation to be damped. When this bias is switched off, r.f. oscillation can be restored by either a random noise spike, the "tail" of the previous oscillation or by an n.q.r. signal. By the first, no phase relationship between pulses is retained and is termed the incoherent mode. In the second manner coherence or, the retention of phase, is achieved. Coherent operation of an s.r.o. results in a very narrow linewidth in the power spectrum which (in the high-Q (quality) circuit) is rarely sufficient to excite a quadrupole resonance. It is therefore usual to employ a partially-coherent mode for n.q.r. detection. Usually the s.r.o. is operated with oscillations reaching their limiting amplitude before being (periodically) quenched. This is termed the "logarithmic mode" whereby the gain of the circuit is proportional to the logarithm of the signal voltage.

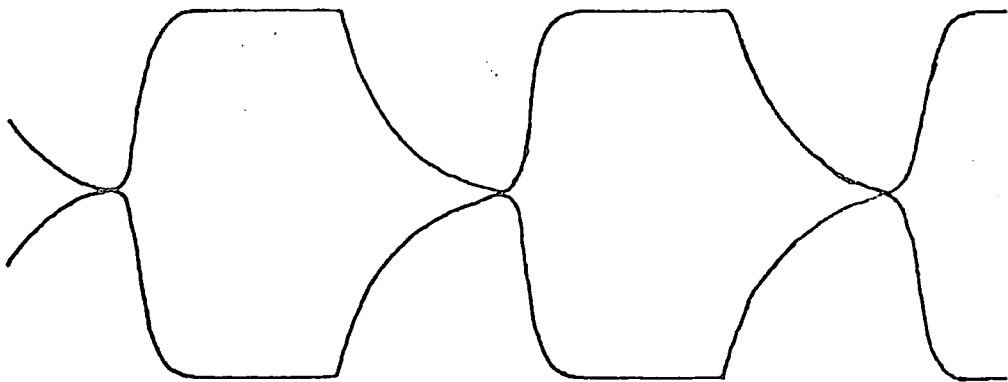
When the radio-frequency of the oscillator excites nuclear quadrupole transitions the oscillation envelope amplitude builds up earlier and a rise in the average output is detected. Further, due to the excited nuclear spins relaxing to restore the nil r.f. field Boltzmann distribution, a voltage is induced in the coil which prolongs the tail of the oscillation envelope. Detection is primarily of this nuclear induction signal but is not purely inductive and in consequence the s.r.o. suffers from poor lineshape fidelity. A mixture of first and second derivative lineshapes is usually obtained.

Fig. 6

Quench waveform



R. f envelope



The quenching action modulates the amplitude of the r.f. envelope.

As the power spectrum contains many sidebands in addition to the fundamental, any one of which may effect a quadrupole resonance, accurate measurement of the resonant frequency can be further complicated.

This latter difficulty has been greatly reduced by the use of sideband suppression. The DECCA operates sideband suppression by modulating the quench frequency at about 1Hz through about one third of its frequency. The fundamental in the power spectrum is then adjusted to be stationary in frequency. Excitations by modulated sidebands are smoothed by the detection time constant so that the spectrum recorded is due to the fundamental alone. There still remains, however, the problem of poor lineshapes from the s.r.o.. This problem is covered in the following section on enhancements.

The actual detection of an n.q.r. signal is achieved by monitoring the output of the oscillator. Changes can be observed with an oscilloscope but a phase-sensitive detector (p.s.d.) is more usual. The p.s.d. detects the component of an n.q.r. signal which has been modulated and is in phase with the audio-frequency modulation. It improves significantly the signal-to-noise ratio of the quadrupole resonance. To display the spectrum, the output of the p.s.d. is fed to a chart recorder.

The modulation used in n.q.r. spectroscopy is usually of two types. It is either frequency-modulation or magnetic-field (Zeeman) modulation. Frequency-modulation, although more sensitive, has the disadvantage of being susceptible to

resonances other than those due to n.q.r. e.g. external radio transmissions. This is not the case with Zeeman modulation as used in n.q.r. spectroscopy. This is the preferred mode when searching wide frequency ranges. A magnetic field of up to $0.02T$ is applied at a low audio-frequency (< 200 Hz). During the 'off' periods the n.q.r. signal is unaffected but, when the field is 'on' a signal is broadened. With a Zeeman field of sufficient strength, a signal from a polycrystalline sample becomes so broad as to be undetectable. The signal is therefore strongly modulated. Phase-sensitive detection of the oscillator output locates such modulated signals. Only the pure quadrupole resonances are Zeeman-modulated and additionally, this modulation does not influence measurements of frequency. The DECCA spectrometer uses a bisymmetric square waveform for Zeeman modulation. The construction and use of a sinusoidal Zeeman modulator is discussed later in this chapter.

Signal Enhancements

a) Locked s.r.o.

The s.r.o. as described has two main failings when applied to lineshape studies. These are its frequency instability and its poor lineshape. Tong (9) describes how external frequency locking of an s.r.o. can remove these problems. An incoherent s.r.o. is made coherent by the injection of an external r.f. voltage into the oscillator tank circuit. The result is a frequency - and phase- locked s.r.o. whose lineshape response can be manipulated by varying a single frequency difference.

In the locked s.r.o. the residual frequency is the normal unquenched oscillator frequency (f_o) but the exciting r.f. spectrum becomes centred upon the injected frequency (f_i). The frequency of the central component of the r.f. spectrum depends only upon f_i and not upon the quench frequency nor the resonant frequency of the s.r.o. tank circuit (f_o). The spectrometer is therefore frequency locked by an external stable source.

The lineshape response in an s.r.o. is determined by the phase difference between the residual and exciting pulses of the oscillator. Tong shows that this phase relationship can be related to the frequency difference ($f_i - f_o$). Adjustment therefore to this frequency difference will render any desired lineshape and when $f_i = f_o$ the response of the ideal locked s.r.o. will be the same as that of an ideal conventional s.r.o. Unfortunately in the practical s.r.o. changes in fundamental frequency occur during the quench cycle and thus further phase shifts occur between the exciting and residual pulses. These are accommodated by treating them as a single term, constant for each pulse. The final trimming of a line-shape when ($f_i - f_o$) has been set is to introduce small phase corrections by "pulling" the auto phase control (loop). In consequence however, the r.f. spectrum is asymmetrical in phase and amplitude about the fundamental and irregular sidebands are observed (9).

Read (10) has constructed a spectrometer upon the principles of Tong. The lineshape fidelity and frequency stability

of the locked s.r.o. were illustrated for p-dibromobenzene. An asymmetry parameter of 12% was determined from Zeeman n.q.r. spectra obtained with fields of 0.003-0.004T. Operating at 225MHz a locked sweep-width of 450kHz was achieved with this machine, the signal from which was averaged. For wider search applications, the s.r.o. could be locked to a stepped frequency synthesiser operating a signal averager.

b) Synchroniser

Brooker and Startup (11) have also produced an n.q.r. spectrometer of high lineshape fidelity and frequency stability. Adapting a limited oscillator to signal averaging techniques they have lost the higher frequency range of an s.r.o. but achieve pure lineshapes more easily. The highest reported resonance of the spectrometer is of sodium chlorate (30.525MHz). The long-term frequency instability of the Robinson oscillator makes it unsuitable for averaging purposes. The authors however make use of a synchroniser to overcome this problem. The synchroniser (Hewlett-Packard 8708A) samples the spectrometer frequency and then, by application of a voltage to a varactor diode in the oscillator tank circuit, corrects any frequency drift. To obtain a sweep of the spectrometer the synchroniser is itself stepped by a ramp voltage. Typically a sweep width of 50-80kHz at a rate of about 40Hz sec^{-1} is employed. The stability achieved with the synchroniser makes possible the use of a computer of average transients (c.a.t.). The steps of the frequency sweep are sampled into separate channels of the c.a.t. and signal enhancement

(due to noise reduction) is proportional to the square root of the number of sweeps. Like that of the Read spectrometer, the area of application of this machine has been Zeeman n.q.r.

c) Computer of Average Transients (c.a.t.)

High transfer rates for data from experimental instruments to computers via analogue-to-digital converters have made possible the real-time storage and manipulation of such data. With digital-to-analogue conversion, programmes may be written to control an instrument. One of the simplest applications of a computer is as an averager i.e. a computer of average transients or c.a.t.

As applied to a spectrum, the c.a.t. stores an array of datum points corresponding to the number of channels into which the spectrum has been divided. The spectrum is scanned in a stepped manner and the output at each step is 'written' to the corresponding channel. The computer sums and calculates the average of the entries to each channel when the spectrum is repeatedly scanned. The summing (and averaging) can be achieved by one of two methods. Either a complete array is added each time the full spectrum is swept or each channel may be sampled several times during one slower scan. This latter method is termed boxcar integration.

The principle behind the operation of a c.a.t. is that repeatedly averaging a spectrum enhances a non-random signal by suppressing the random noise. Noise produces a random output to a channel which when repeatedly sampled

tends to be self-cancelling. An n.q.r. signal will however be reinforced by repeated sampling. Compared with the signal-to-noise ratio from a single scan, averaging should give improvement by a factor of the square root of the number of sampling sweeps made. Its advantage over a long single sweep is that it is less susceptible to $1/f$ noise (12).

The c.a.t. reported in this thesis was originally constructed to improve the signal strength for Zeeman n.q.r. spectra of sulphuryl chloride at 77K. It was connected to a DECCA spectrometer because the n.q.r. frequencies required lay outside the range of the AEI oscillator. The computer used was a Varian 620L which provided 1024 channels for a full sweep. A ramp voltage (0 to 10V) of 1023 'steps' was generated via a digital-to-analogue converter and was applied to the frequency modulation (f.m.) varactors of the DECCA oscillator. The sweep time was variable in multiples of one twentieth of a second. Sampling in each channel may be varied from one-tenthousandth up to one-sixth of a second. To provide sufficient width to the c.a.t. spectrum, the original 10pF (BA1100) varactors were replaced with 47pF (HV2111) varactors. The full ramp voltage then produced a sweep width of up to 280kHz at 37.7 MHz. This sweep width could be varied by adjustment of the attenuator placed between the digital to analogue converter and the external-f.m. socket of the spectrometer.

The output of the spectrometer was sampled at two stages. The first was from the oscillator itself after r.f. filtering and amplification and the second from the phase sensitive detector (p.s.d.) output. It was soon established that instability in the oscillator following each sweep

accounted for a dramatic rise and fall in the base line of the averaged spectrum. This could obscure much spectral information and the p.s.d. output was therefore used in the c.a.t. experiments reported here. The number of sweeps was varied and sweeptimes ranging from five seconds to thirty minutes were evaluated. The most frequently used settings were of ten-minute scans with a ten second time constant. With a current of up to one ampere applied to the Zeeman coils, the coolant usually remained effective for about ten hours allowing sixty sweeps of the c.a.t.

The n.q.r. spectrum of p-dichlorobenzene was recorded at room temperature in order to check that replacement of the f.m. varactors had caused no reduction in sensitivity of the spectrometer. It was found that due to the greater capacitance, the depth of frequency modulation had increased but, when readjusted, the spectrometer sensitivity was unaffected with an estimated signal-to-noise ratio of 75:1 and an observed linewidth of 4kHz (Fig. 7). The operation of the c.a.t. was tested at room temperature with samples of p-dichlorobenzene, dichloro-bis-benzonitrile paladium II and zinc chloride. All spectra were enhanced as expected. The successful improvement in signal strength of the resonance due to zinc chloride resolves it as a broad singlet (Fig. 8). Single scans had shown some fine structure suggesting a possible triplet. (See Chapter 5).

As reported in Chapter 4 the asymmetry parameter (η) of thionyl chloride at 77K has been measured. However, the

RGZ/230/1001 Zb 271 35°C m.g.r. ¹⁷p-dichlorobenzene at room temperature

Signal-to-noise 7.5:1

Fig 7

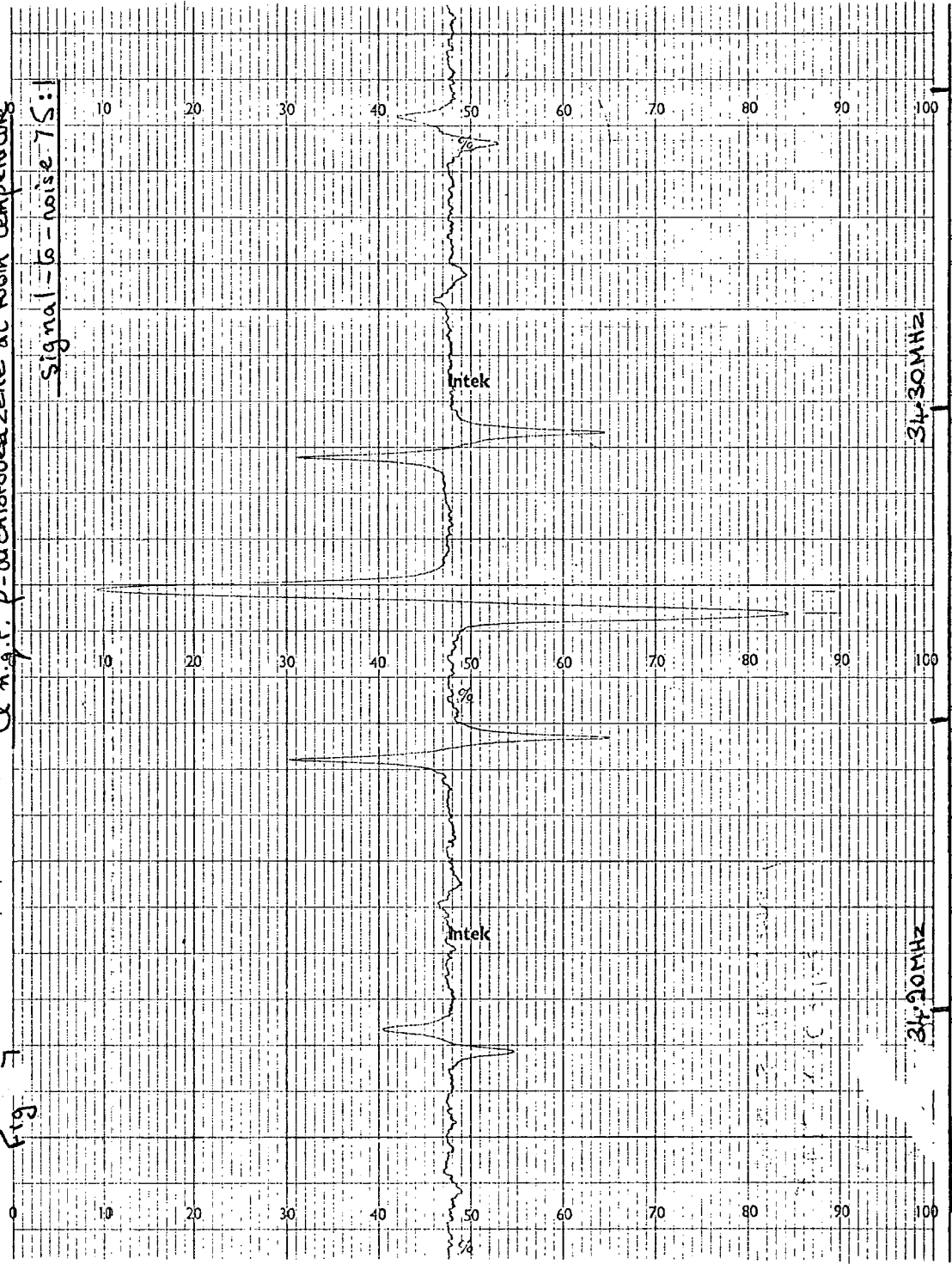
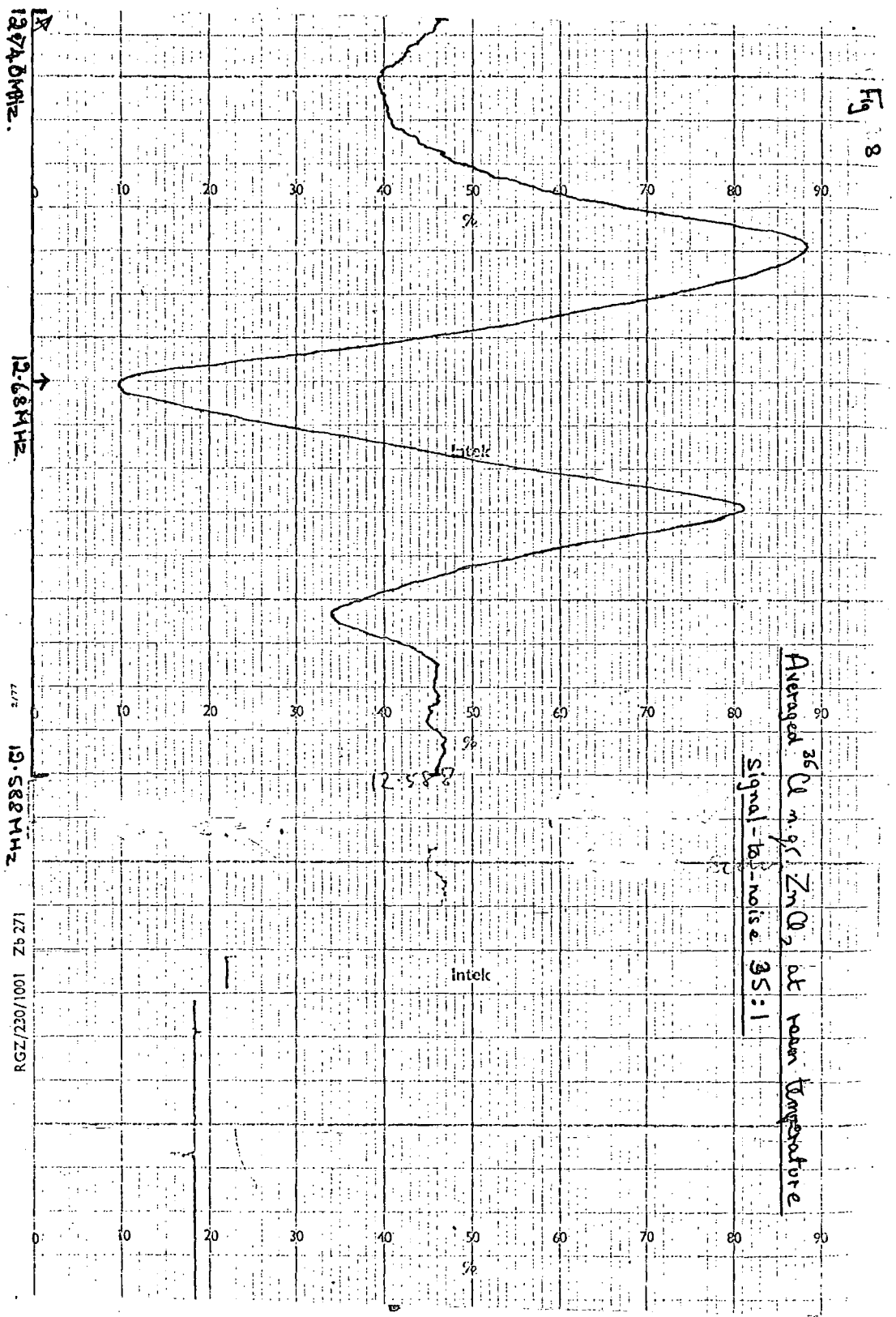


Fig 8



Averaged 36 U n.g. ZnO₂ at room temperature
Signal-to-noise 35:1

Intel

12.74 MHz

12.68 MHz

12.58 MHz

12.571 MHz

477

RGZ/230/1001 Z9 271

measurement of η in sulphuryl chloride had been prevented by the weakness of the resonances. It was hoped that averaging would reveal enough structure in Zeeman n.q.r. spectra to measure η . The quadrupole resonances of sulphuryl chloride (13) are reported at liquid nitrogen temperature and averaging at this temperature was attempted. Manipulation of the n.q.r. lineshape was required and, as with thionyl chloride, this resulted in the loss of some signal strength.

All attempts to obtain enhanced spectra at liquid nitrogen temperature led to failure. This was at first attributed to the ingress of liquid nitrogen (or of condensed oxygen) into the probe and to exclude it the probe was more tightly sealed with a greased rubber 'O' ring. As the problem persisted, probes were left in liquid nitrogen for several hours in order to equilibrate before connection to the spectrometer. Although single sweep spectra were obtainable using the system, averaging tended to smooth out any signal. It appeared that frequency drift was the cause. With liquid nitrogen as the coolant it is probably attributable to the leaking of liquid into the probe.

Cold nitrogen gas produced by bubbling nitrogen gas through liquid nitrogen achieved the temperatures required ($< 150\text{K}$) but failed to cure the problems of drift. However, powdered dry ice employed as a solid coolant was found to be a great improvement and n.q.r. signals observed at low temperatures could be averaged (e.g. $\oplus \text{SCl}_2$). No Zeeman spectra for sulphuryl chloride were obtained although at this temperature it is frozen. The application of the c.a.t.

system to broad, weak n.q.r. signals was investigated at dry ice temperature with the $^{35}\text{SbCl}_3$ signals from a sample of $[\text{SbCl}_3^+][\text{SbCl}_6^-]$. A further attempt to enhance Zeeman n.q.r. spectra was also made using the quadrupole resonances from axial chlorines in phenyl phosphorus tetrachloride.

At dry ice temperature the quadrupole resonances due to $^{35}\text{SbCl}_3$ lie at 42.230 and 41.654 MHz. At these frequencies a c.a.t. sweep width of up to 360kHz is achievable. The table below compares the c.a.t. performance at dry ice and liquid nitrogen temperatures for the 42.230 MHz resonance.

Single slow motor sweep

Four 10-minute c.a.t.

sweeps

	DRY ICE	LIQ N ₂	DRY ICE	LIQ N ₂
signal-to-noise ratio	5/1	12/1	6/1	8/1
linewidth (kHz)	15	8	17	40

The large linewidth after cutting at liquid nitrogen temperature reflects the drift experienced with sulphuryl chloride. The signal-to-noise ratio at liquid nitrogen temperature is lower than that observed for a single motor-driven sweep. This is further evidence for the

degrading influence of frequency drift.

The value of the asymmetry parameter (η) for the equatorial chlorine atoms of phenyl phosphorus tetrachloride has been determined as 0.17 and is reported in this thesis. However, the weaker intensities of ^{35}Cl quadrupole resonances due to the axial chlorine atoms prevented the determination of their asymmetry parameter (η). Fig 9 illustrates the approximately first derivative lineshape due to axial chlorine atoms which was averaged in the attempt to determine η . The linewidth is 4.5kHz and the lineshape was obtained with a centre shift compensation setting of 154. Fig (10) shows the lineshape obtained for zero magnetic field after thirty 10-minute sweeps have been averaged. Clearly an improvement has been made and so the resonance was averaged while subjecting the sample to Zeeman magnetic fields. Figs. 11A - 11D display the changes in lineshape due to magnetic fields caused by currents 0.25, 0.5, 0.6 and 0.8 amps. The averaging period was of fifty 10-minute sweeps. This period was the limit for a packed dewar of dry ice when a current of 0.8 amps was being used. Replenishing a dewar with powdered dry ice usually resulted in a drift in frequency due to the vibrations. Fig. 11D therefore represents the limit of this Zeeman n.q.r. investigation.

Although discontinuities are evident in the spectra obtained for a current of 0.6 amps (Fig 11C) these are not seen in spectra at 0.7 and 0.8 amps. The estimated width of these discontinuities is 2.5kHz which is only about

Fig 9 ^{35}Cl ngr. of PRRQ₁₁ at dry ice temperature
(25.35 MHz line at zero magnetic field)

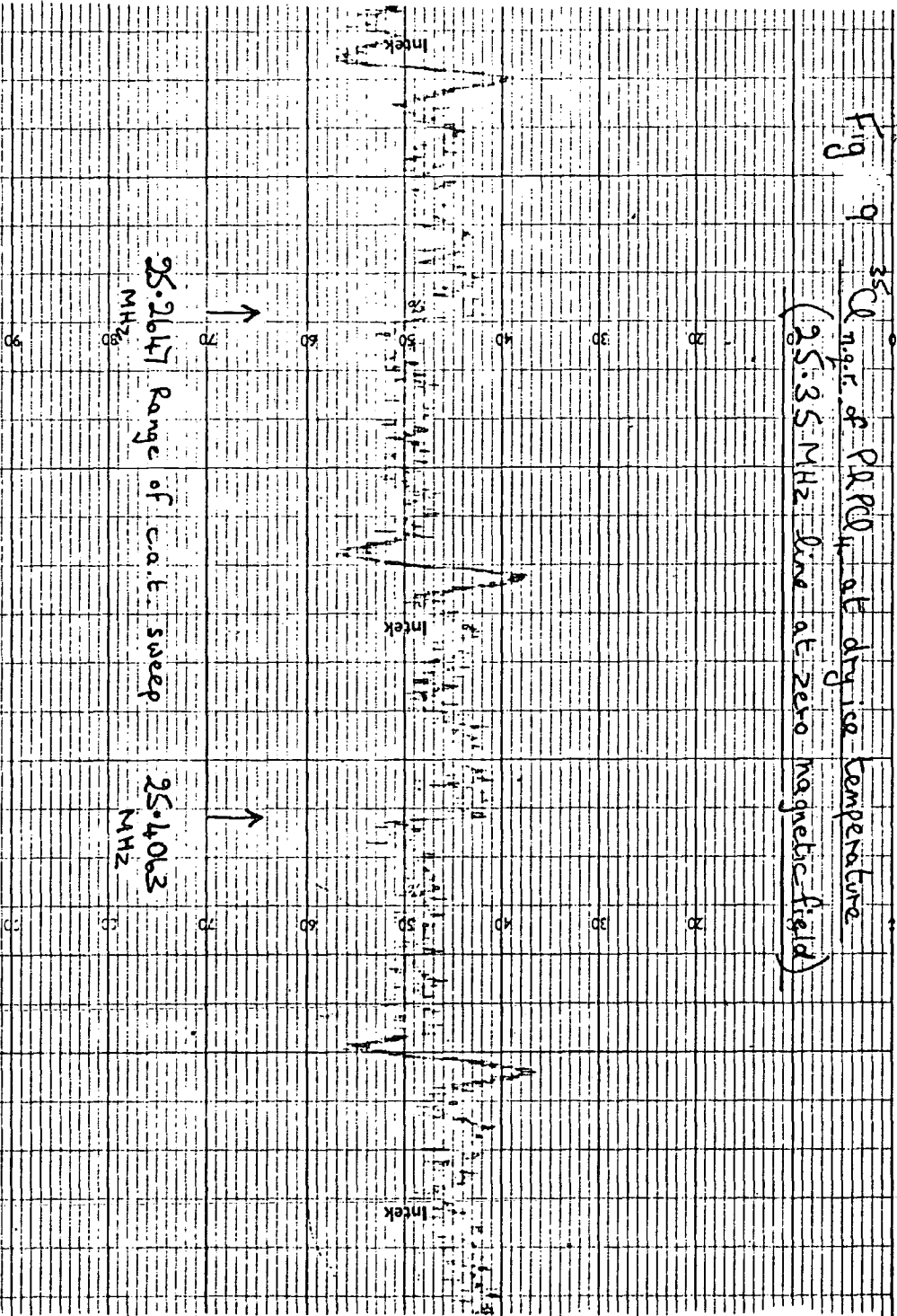
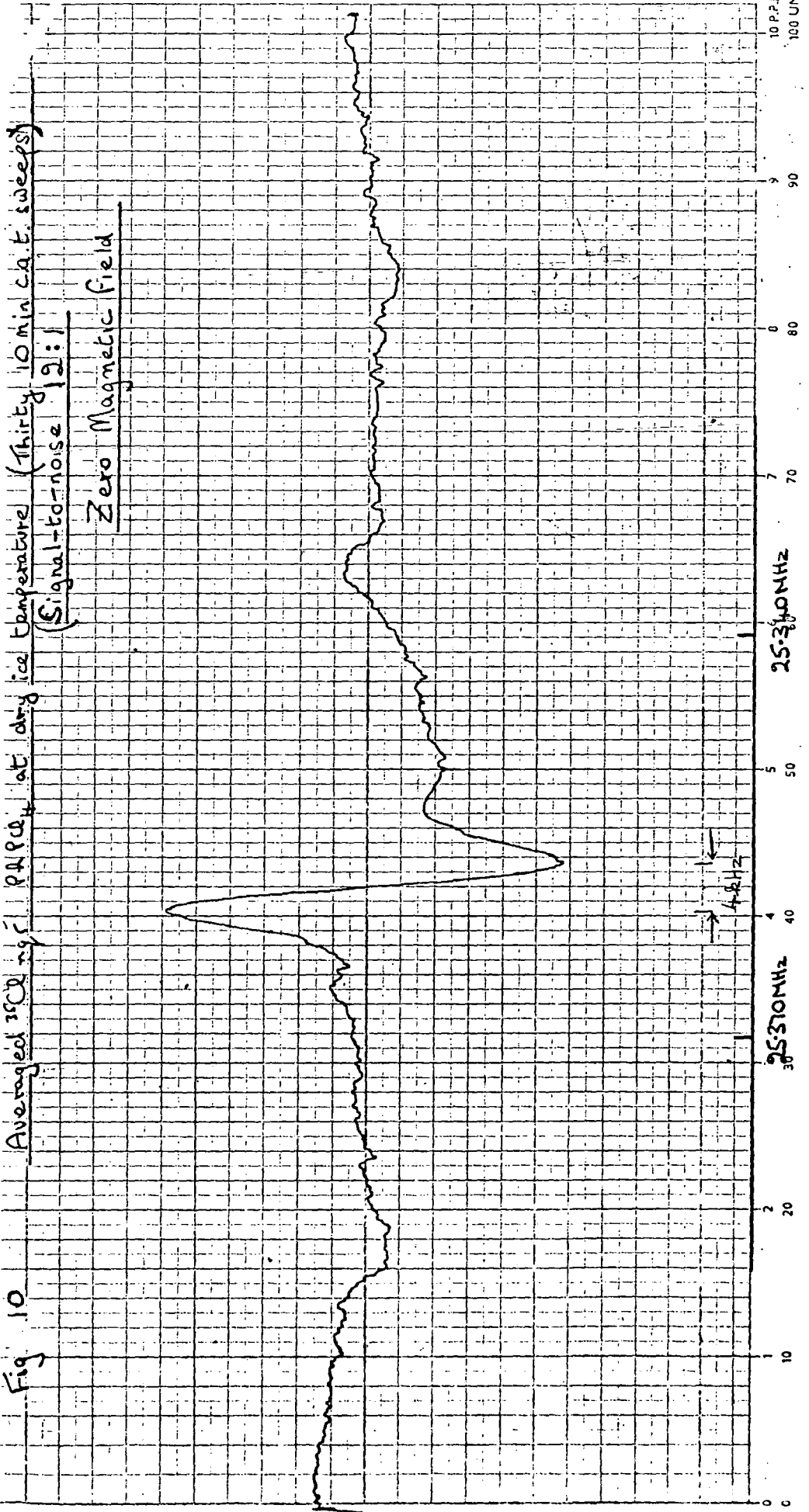


Fig. 10

Averaged ^{13}C NMR of PAPP₄ at dry ice temperature (Thirty 10 min c.a.t. sweeps)
(Signal-to-noise 12:1)

Zero Magnetic field



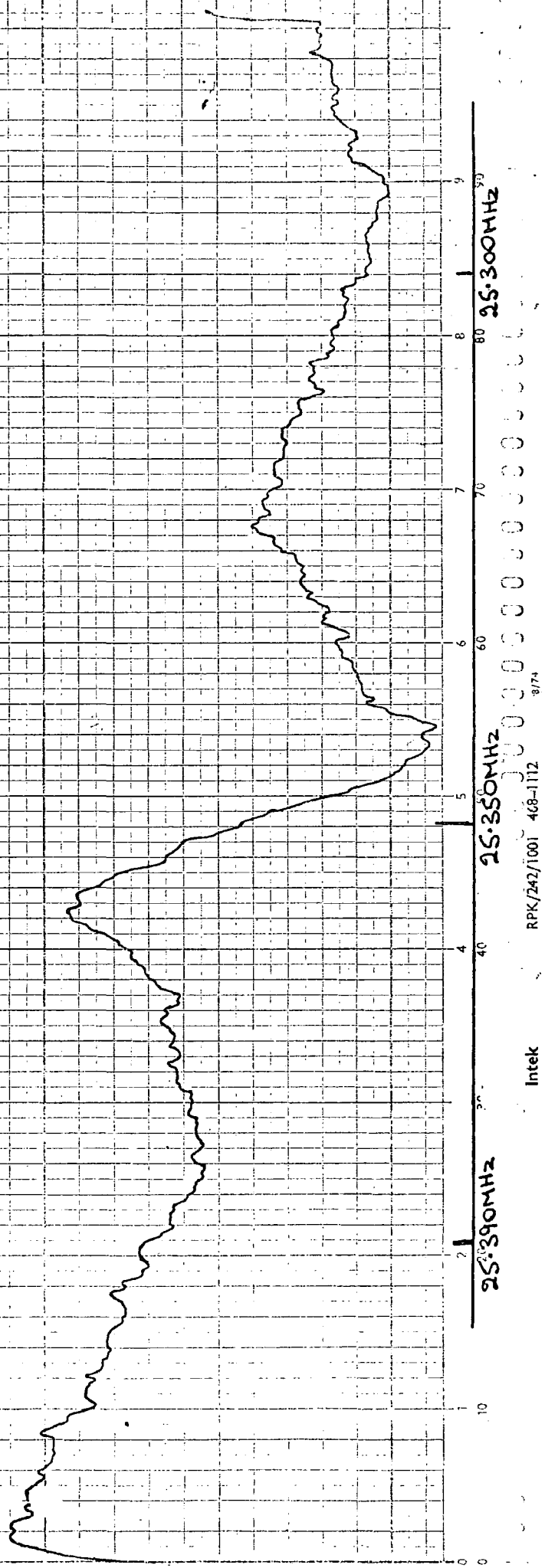
SUBMITTED BY _____
COMPOUND _____

SOLVENT _____
CONC. _____
OPERATOR _____

Fig 11A

Averaged ^{25}Cl n.g.s. EPR at dry ice temperature (fifty 10 min cat. sweeps)

Magnetic Field = 0.775 mT (0.25 amp)



25.290MHz

25.350MHz

25.300MHz

Intek

RPK/242/1001 468-1112
8/74

Fig. 11. B Averaged ^{35}Cl n.g. P.P.P. at dry ice temperature (Fifty 10 min c.a.t. sweeps)

Magnetic Field = 1.55 mT (0.50 amp)

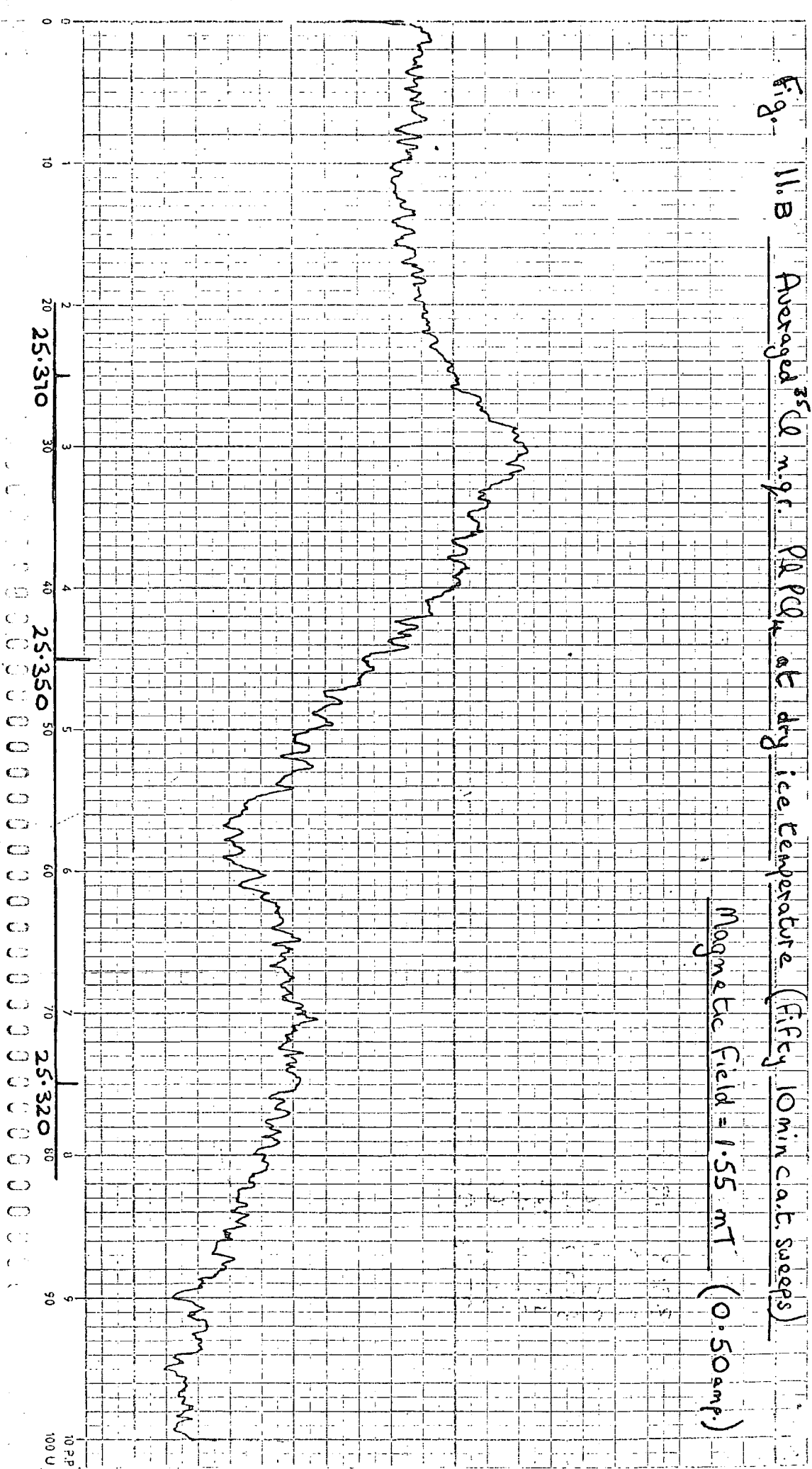


Fig. 11c Averaged ^{35}Cl n.g.r. PRPC₄ at dry ice temperature (fifty 10-min. c.o.t. sweeps)

Magnetic field = 1.86 mT. (0.6 amp.)

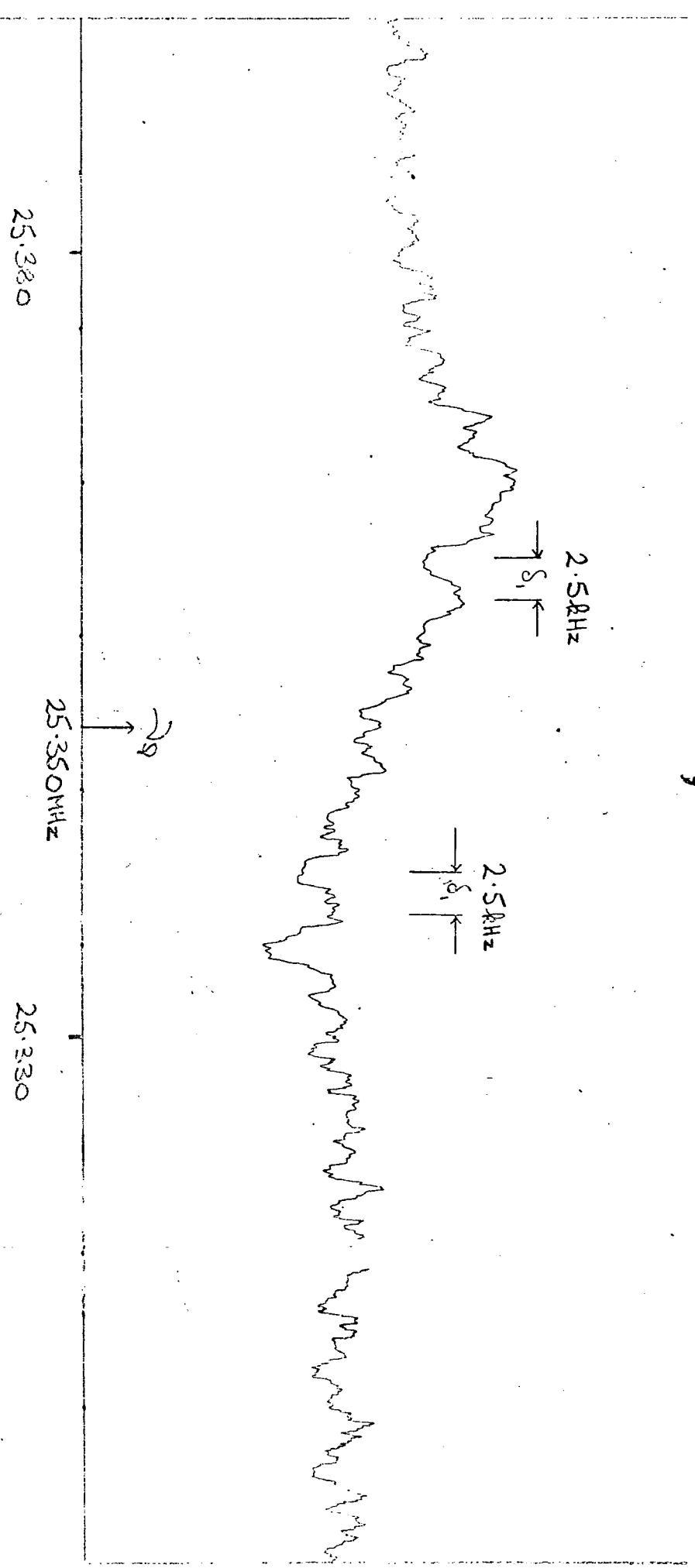
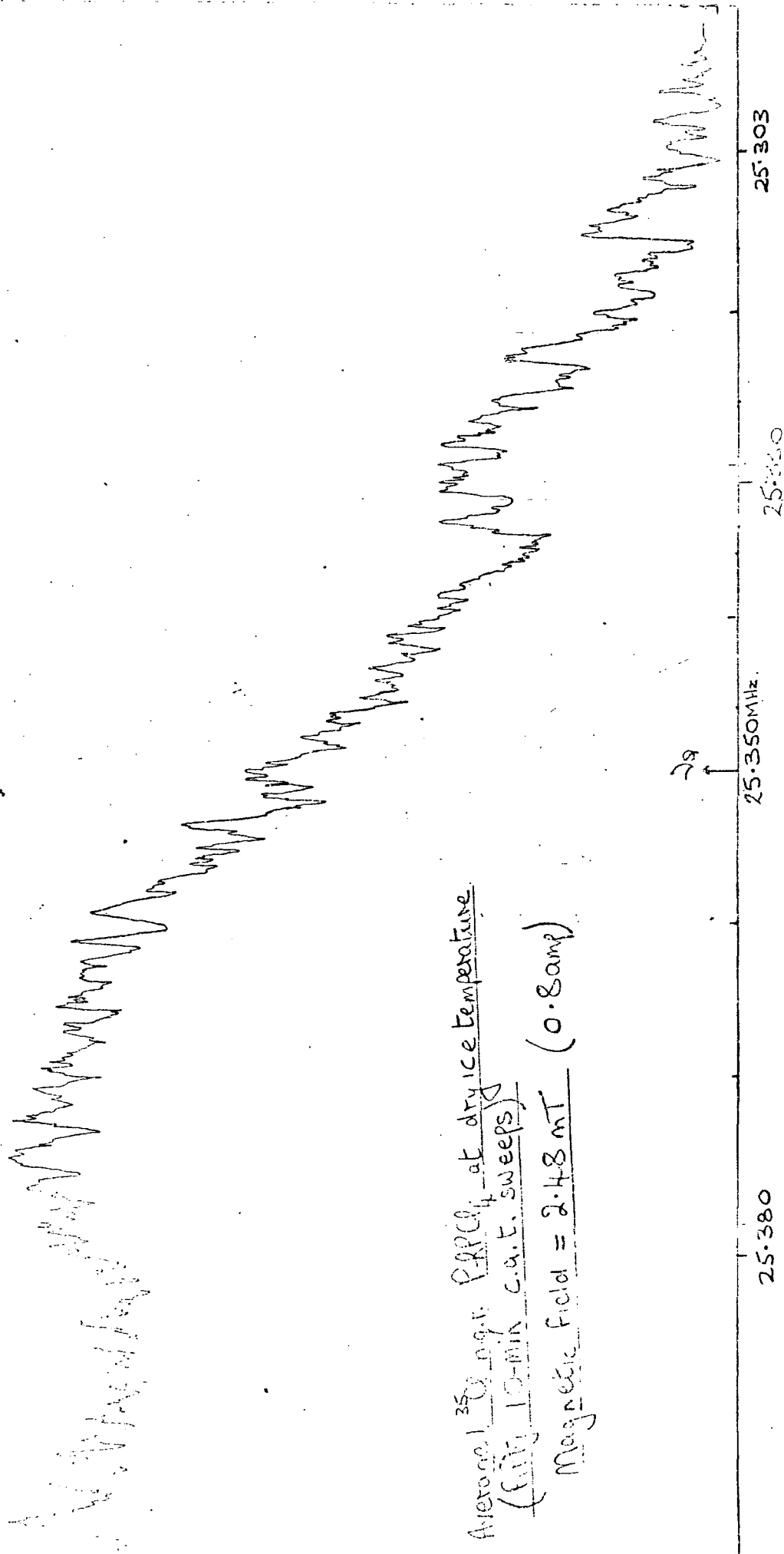


Fig. 11B



half the zero field line-width. An estimate of δ from these measurements is not possible and so only a value for the equatorial chlorine atoms of phenyl phosphorus pentachloride is reported in Chapter 7.

As noted earlier an alternative form of averaging is boxcar integration. The spectrum is sampled channel-by-channel and so only part of the total averaging period is spent upon the lineshape itself. The possibility that boxcar integration might better handle frequency drift than does multiple scan averaging was investigated. The sampling time for each channel of the output was determined by the setting of a single sweep-time (usually 10 mins.). The number of sampling periods in each channel was then set by a sweep-number function. In multiple scan mode, this determined the number of sweeps to be repeated before averaging, whereas in the boxcar mode, it determined the number of sampling periods for each channel before averaging and before "stepping" to the next channel. Forty 2-minute c.a.t. scans of the 42.230 MHz resonance of $^{35}\text{SCl}_3$ at dry ice were used in both multiple scan and boxcar modes. The resultant signal-to-noise ratios were the same ($\sim 20/1$) and the linewidths were identical (14 kHz). With boxcar integration, however, it was found that small 'spikes' were given in the output and were too numerous to remove by erasion of the data points. Although 3-point smoothing was able to remove them, the detail of the resultant spectrum was poor. Repetition and subtraction of background spectra failed to remove this problem. It was found best to continue with the multiple scan method using 10-minute scans.

d) Sinusoidal Zeeman Modulation

In a private communication from Professor Brooker (University of South Florida) it was pointed out that sinusoidal Zeeman modulation could be employed in n.q.r. spectroscopy. A single pair of coils could provide both modulation and a static magnetic field for Zeeman n.q.r. investigation. Previous attempts to use square-wave Zeeman modulation with the AEI (Robinson-type) spectrometer had met with little success due to an inability to drive the coils. It was thought that the simpler circuit required for sinusoidal magnetic modulation could remove this problem. With the aim of applying this system to the AEI spectrometer a power supply was constructed for testing, firstly with the Zeeman coils of the DECCA n.q.r. spectrometer.

A stabilized power supply with a limit of 5 amps was used with an audio-frequency signal generator modulating the current limit. The modulation was applied across the comparator resistor and the current output was modulated by the feedback loop.

A D.C. output had to be maintained for modulation by the sinusoidal input because, in principle, the power supply could not be driven below earth. It was necessary to modulate a fluctuating D.C. current in order to maintain a symmetrical sinusoidal output (Fig. 12a). The coils of the DECCA spectrometer measure three inches in depth and five inches in diameter. The three hundred turns of 18 s.w.g. copper wire produce a resistance of about three ohms. The circuit is shown schematically in Fig. 12b. All sources were either floating about the earth of the signal generator or were connected to the spectrometer earth through the p.s.d.

Fig 12a)
Current applied to Zeeman coils

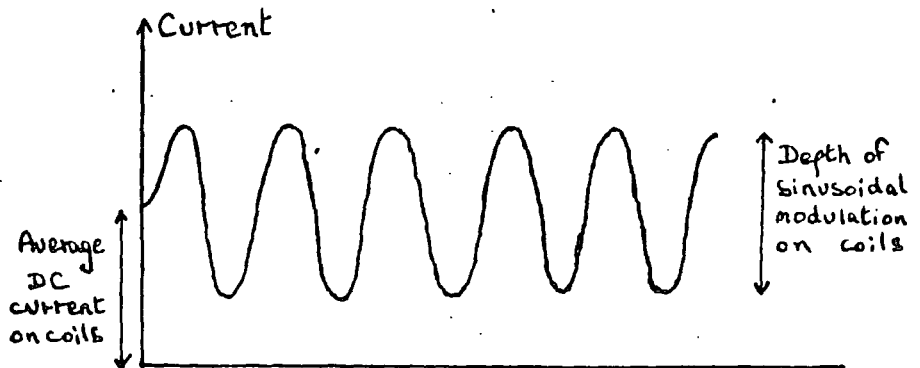
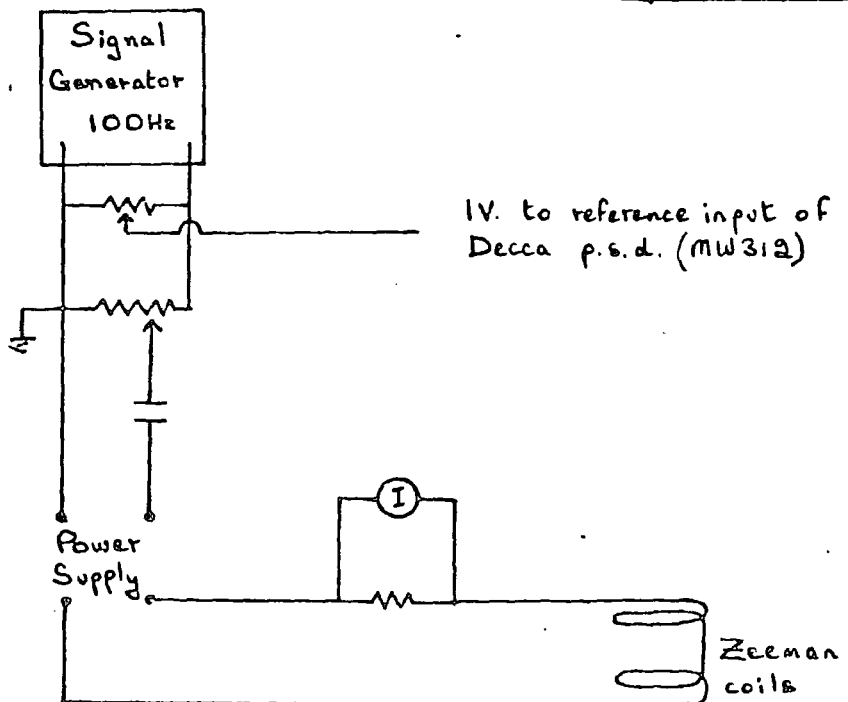


Fig 12b)
Circuit of Zeeman modulation for Decca n.g.r.
spectrometer

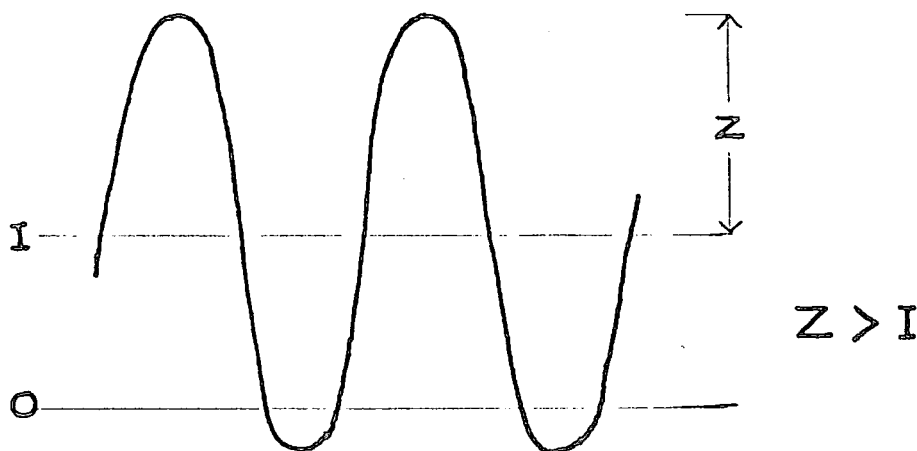


The preliminary tests were carried out at room temperature with the strong n.q.r. signal of p-dichlorobenzene with a DC offset (and therefore a static field) present.

It was found that the detected signal strength was very little sensitive to the phase of the p.s.d. reference although two positions were marginally better. Signal strength was found to be better for high levels of modulation.

This is to be expected but a limit is reached for a modulation field strength sufficient to completely erase the signal.

The effect of this depth of modulation upon n.q.r. linewidths was not noticeable when compared with the line-broadening due to the static magnetic field caused by the DC current. It is shown below that isolation of the DC current was not beneficial. Due presumably to the back e.m.f. of the collapsing field the power supply could be driven negative (below earth), thereby allowing depths of modulation (Z) greater than the DC current (I), viz:

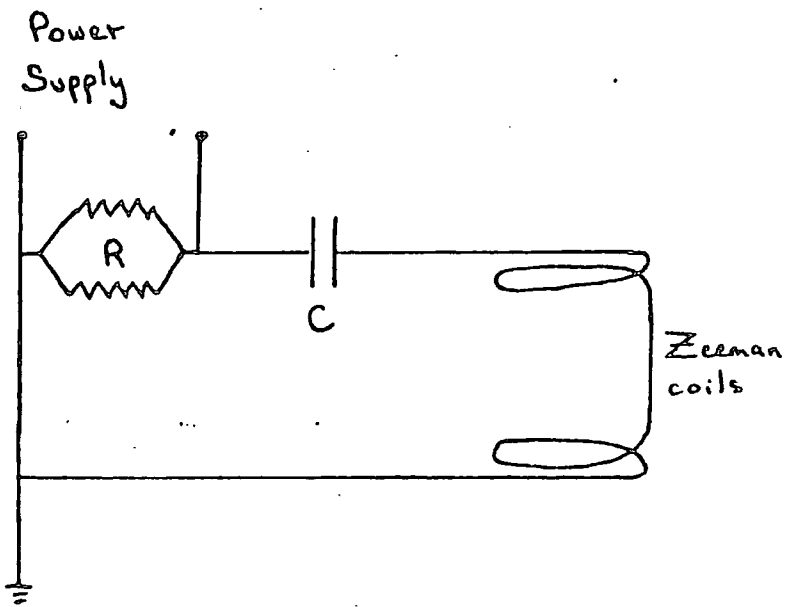


Examples to illustrate depths of modulation possible are given below.

DC OFFSET (resultant field, mT.) I amp	MAXIMUM MODULATION DEPTH Z amp
0.1 (0.31)	3I
0.5 → 1.0 (1.55 - 3.1)	2I → 1.5I
2.0 → 3.0 (6.2 - 9.3)	I

The presence of a DC current on the Seeman coils broadened the n.c.r. signals and caused a reduction in observed signal strength. In an attempt to remove this problem, the DC current was isolated from the coils by placing a 5000 μ capacitor in the circuit and by dropping the DC across resistors (Fig. 13). The result was that the sensitivity of the spectrometer fell dramatically and the output became much more phase-sensitive. It was found that the modulation was no longer sinusoidal in waveform and that the depths achievable were lowered. As examples of the reduced sensitivity, p-dichlorobenzene at room temperature generated a signal of $S/N \sim 3/1$ with modulation set at $Z = 0.3$ amp. and boron trichloride at 77° a signal of

Fig 13



$R = 2 \times 10 \Omega$ (17w) ceramic heatsink resistors.

$C = 5000 \mu\text{F}$ capacitor

Isolation of DC on Zeeman coils.

$S/N \sim 2/1$ under similar conditions. The lack of a good modulation lineshape was felt to be the likely cause of reduced sensitivity. A phase-optimised spectrum of p-dichlorobenzene is shown in Fig. 14 and is to be compared with those of Fig. 15 for which the D.C. was not isolated.

A transformer was introduced in place of the signal generator in the hope of reducing mains ripple on the modulation waveform. However, its coarseness produced a very deformed modulation waveform which resulted in a poor lineshape for the detected n.q.r. signal. The transformer, modulating at 50 Hz, was found to reduce sensitivity below that obtained using the signal generator and was therefore used no further. (Fig. 16).

Whilst accepting that D.C. isolated sinusoidal Zeeman modulation was unsatisfactory for detection purposes, it was felt that sinusoidal Zeeman modulation with a static magnetic field was of practical use, especially for Zeeman splitting experiments. To this end a pair of coils was produced for use with the probes of the Robinson-type spectrometer. The coil dimensions are given in Fig. 17a. The magnetic field produced by the coils was calibrated using a Newport Instruments magnetometer (Type H-indium arsenide Hall probe). The Hall probe was supported in the centre of the coils and the instrument output was recorded as a deflection on a Smiths Industries Servoscribe chart recorder. The deflections recorded at varying currents upon the coils were calibrated against that obtained using the standard field facility of the magnetometer. The measured magnetic fields and applied currents were plotted to calibrate the Zeeman coils (Fig. 17b). A theoretical field strength has also been calculated from the dimensions of the coil and is reported in Fig. 17a). The

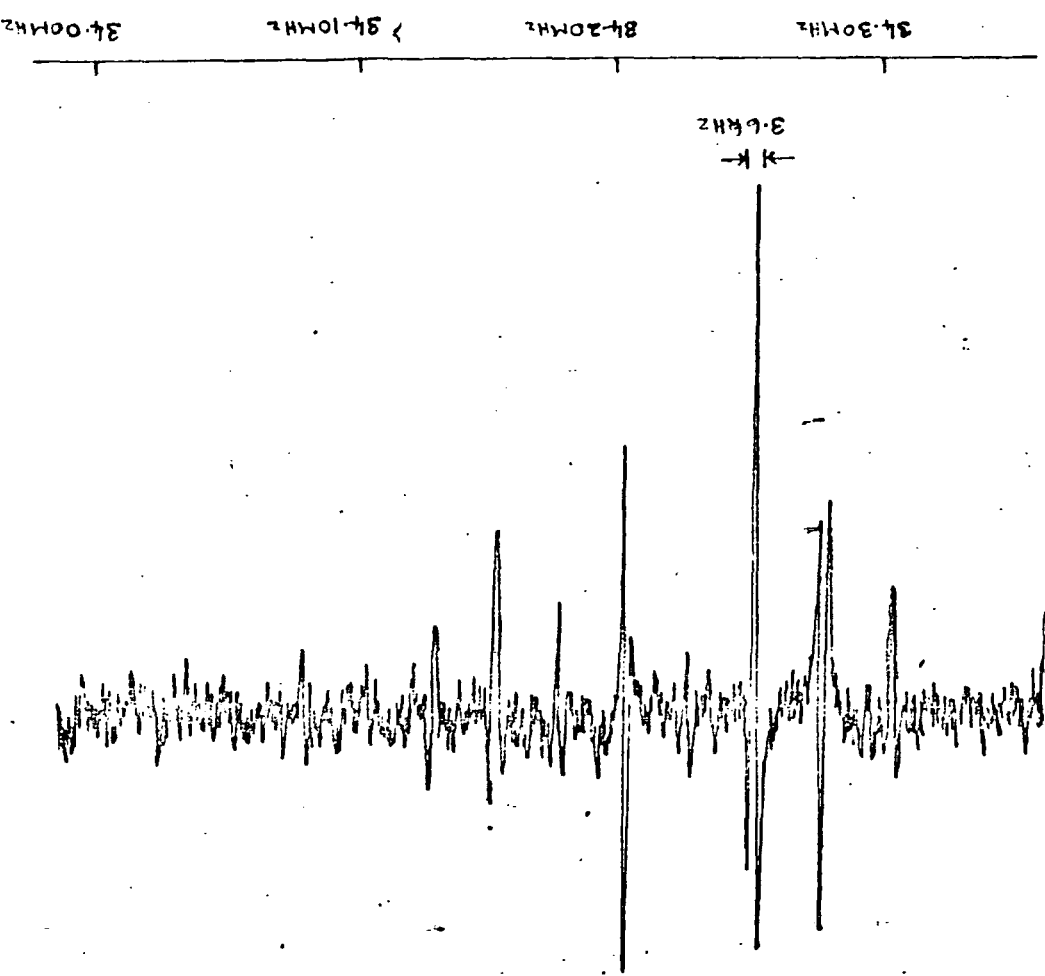
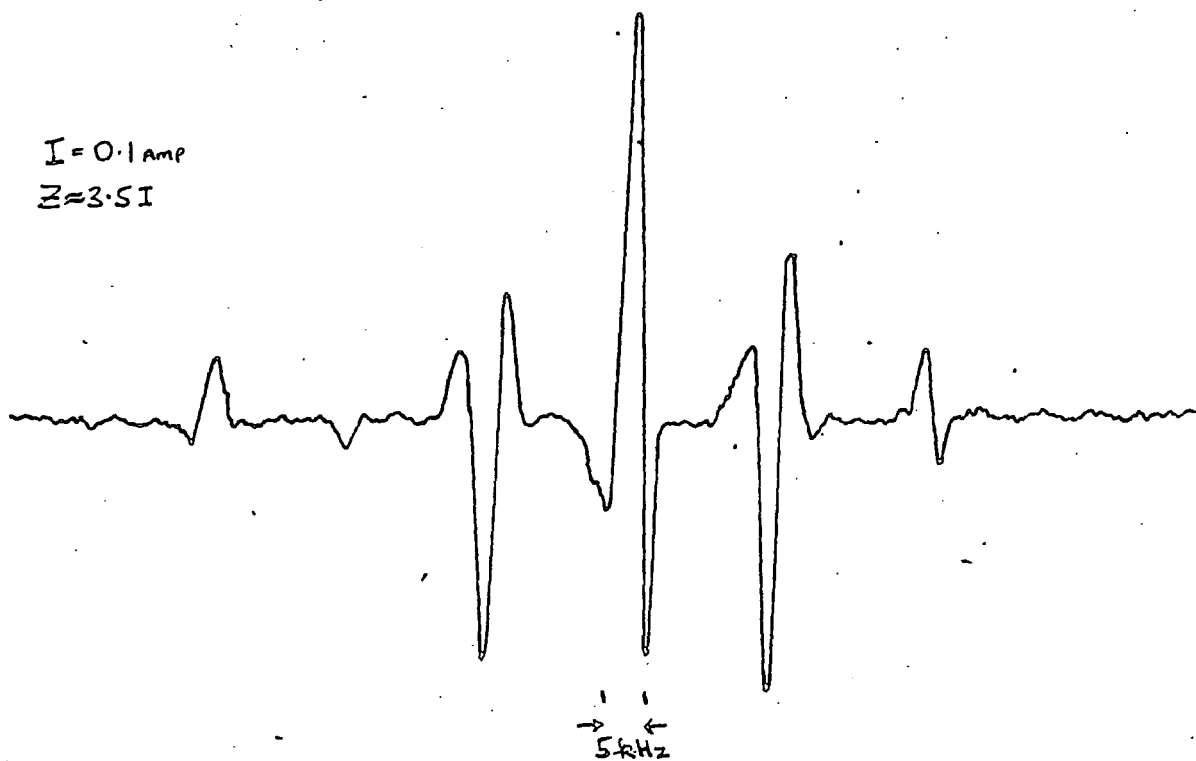


Fig. 14
 ^{35}Cl mg. r. p-dichlorobenzene at 293K using sinusoidal Zeeman modulation with D.C. isolated. Signal to noise = 9:1

Fig 15.

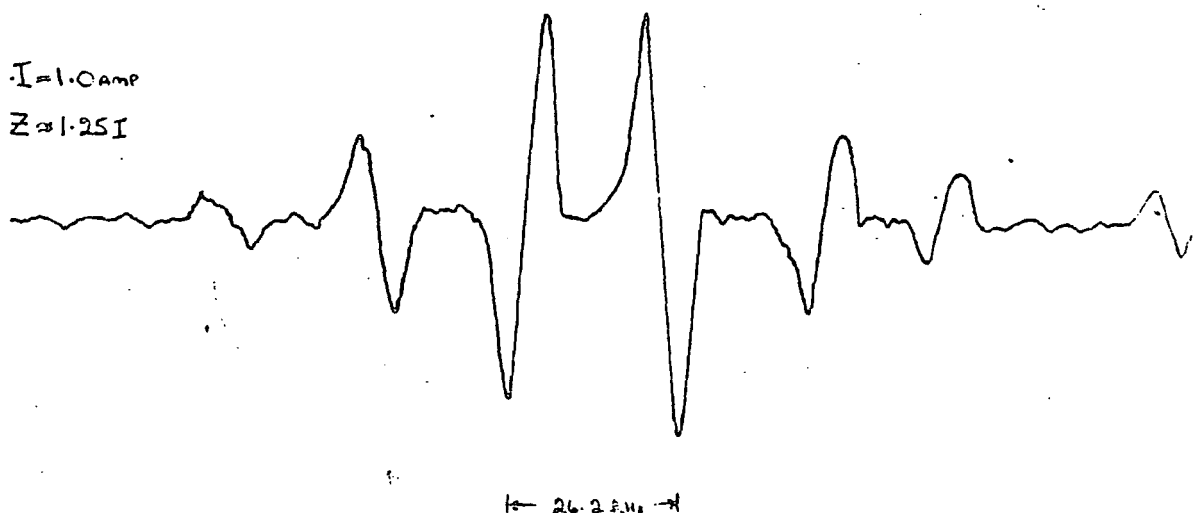
^{35}Cl n.g.r. p-dichlorobenzene at 283K using sinusoidal Zeeman modulation, D.C. current = 0.1 amp. Signal-to-noise $\geq 40:1$



34.40 MHz 34.30 MHz 34.20 MHz

^{35}Cl n.g.r. p-dichlorobenzene at 283K using sinusoidal Zeeman modulation, D.C. current = 1.0 amp. Signal-to-noise $\geq 27:1$

$I = 1.0 \text{ amp}$
 $Z \approx 1.251$



34.40 34.30 MHz 34.20 MHz

Fig. 16 ^{35}Cl p-dichlorobenzene at 283K using sinusoidal
Zeeman modulation, DC current = 0.1 amp with 50Hz
modulation from a transformer. Signal-to-noise = 25:1

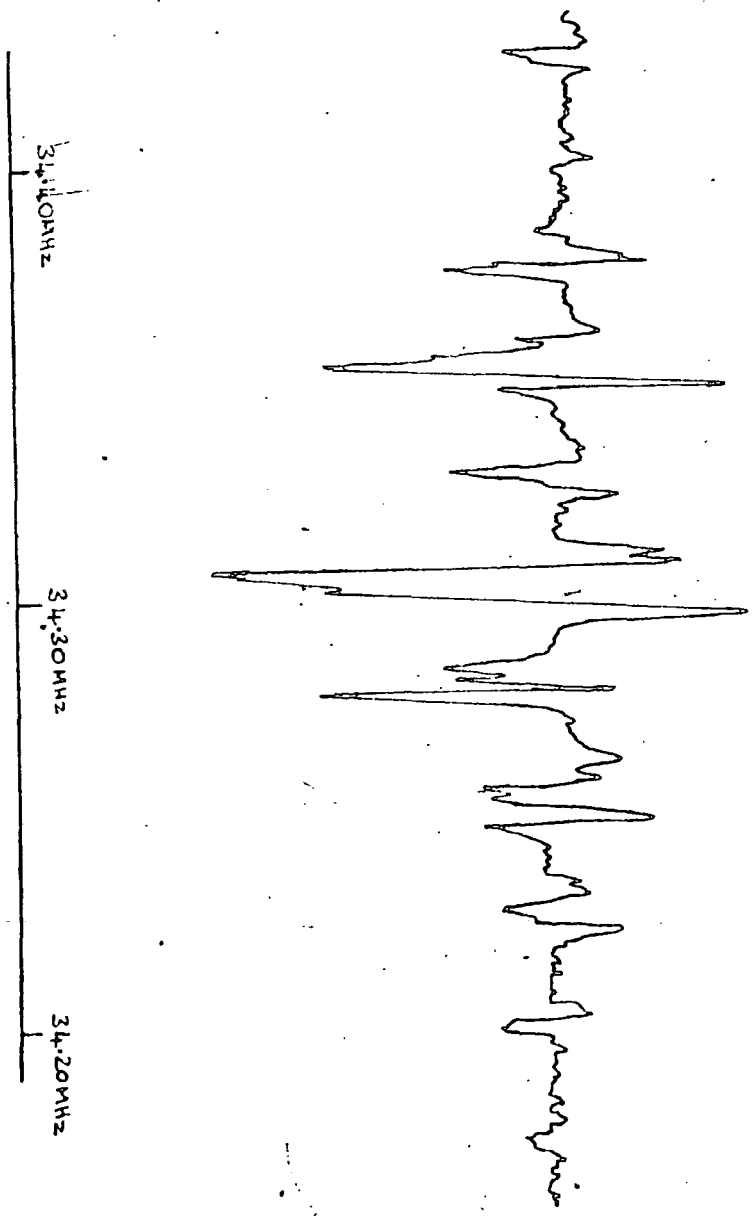
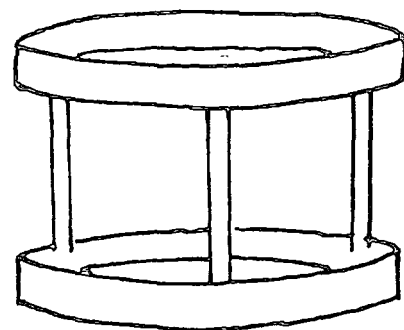


Fig 17a)

Zeeman coils for Robinson-type (AEI)

n.g.r. spectrometer.



Separation of coils = 8 cm.

Mean diam. = 11.5 cm.

No. of turns

240

Gauge of wire

20 swg

Resistance of coil

nominal

6 Ω

measured

5.9 Ω

Current measuring resistor

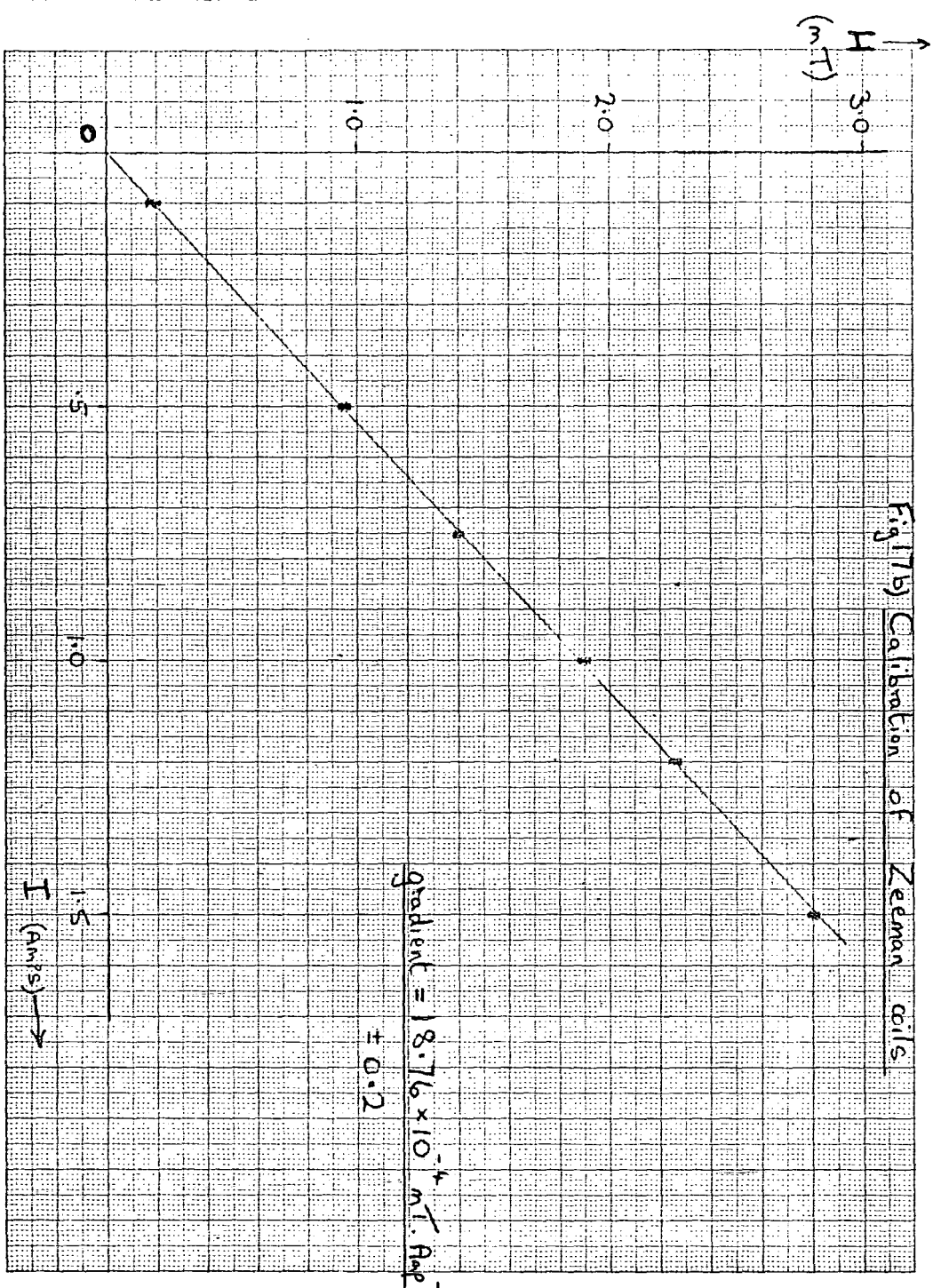
2 Ω

1.9 Ω

Calibration of Field = $(18.76 \pm 0.2) \times 10^{-4} \text{ T.A}^{-1}$

Theoretical field = $23.090 \times 10^{-4} \text{ T.A}^{-1}$

Fig 1(b) Calibration of Zeeman coils



significant difference has been resolved by the close agreement of observed values of $2 \nu_H$ in Zeeman spectra of silicon tetrachloride and those calculated from the theoretical field strength value (Chap. 6, p.155). Perhaps the difference is due to an error in the calibration and is probably due to some damage to the standard magnet.

Muha (14) recently found that a simple bidirectional Zeeman modulator using a silicon controlled rectifier circuit was only satisfactory with s.r.o.-type n.q.r. spectrometers. With marginal and limited oscillator spectrometers, pick-up appears to have been a problem. It was therefore satisfying to find that the sinusoidal Zeeman modulator operated very well with the AEI (Robinson-type) spectrometer.

The AEI spectrometer contains a notch filter set at 140 Hz which is used in conjunction with frequency modulation. Rather than remove the filter, sinusoidal Zeeman modulation was operated at 140 Hz. A Farnell (Type LFM) signal generator was used to drive the power supply and to provide a reference to the Brookdeal 9401 lock-in amplifier (p.s.d.). Detection was at 280 Hz because each sinusoidal wavelength produces two "field-off" periods of modulation. The modulator was operated without isolation of the DC offset and a static magnetic field was therefore present upon the sample coil at all times. In contrast to results with the DECCA spectrometer, sensitivity was strongly dependent upon the phase setting of the p.s.d. reference.

The amplitude of a Zeeman component is proportional to the height of the absorption line and so, as the line is swept, the absorption lineshape should be produced, (9). The spectrometer

roduced the second derivative of the absorption lineshape and adjustment of phase produced its inversion, Fig. 18. The output of the signal generator was adjusted for optimum signal strength and fidelity to a sinusoidal modulation lineshape. The best conditions proved to be at 2V (r.m.s.) which produced modulation depth of $Z = 1.5I$ for $I = 0.02$ amp. and of $Z = 2I$ for $I = 0.1$ amp. Sample spectra are shown in Figs. 19a and 19b. Fig. 19a compares the spectrometer output with frequency and sinusoidal Zeeman modulation. There is a noticeable broadening of the linewidth by the D.C. offset required by the Zeeman modulation. Fig. 19b shows the full n.q.r. spectrum of silicon tetrachloride at 77K obtained on the AEI spectrometer using sinusoidal Zeeman modulation.

Attempts to reduce the DC offset (and therefore the static magnetic field) below 0.02 amp. caused clipping of the lower limits of the sinusoidal modulation. With a zero setting for the DC current, a modulation lineshape closely resembling half-wave rectification was produced. The results of using this as modulation were very poor - Fig. 20. To obtain any signal at all, a high output was needed from the signal generator. This resulted in a sharply sloping baseline. The linewidth is slightly narrowed by the near absence of a static magnetic field but for silicon tetrachloride at 77K, the best signal obtained had a signal-to-noise ratio of only $4/1$.

Sinusoidal Zeeman modulation has been used to investigate the Zeeman n.q.r. behaviour of several Group IV tetrachlorides which is discussed in Chapter 6.

Fig. 18
 ^{35}Cl n.g.f. silicon tetrachloride at 77K. — effect
of detection phase upon spectrometer response

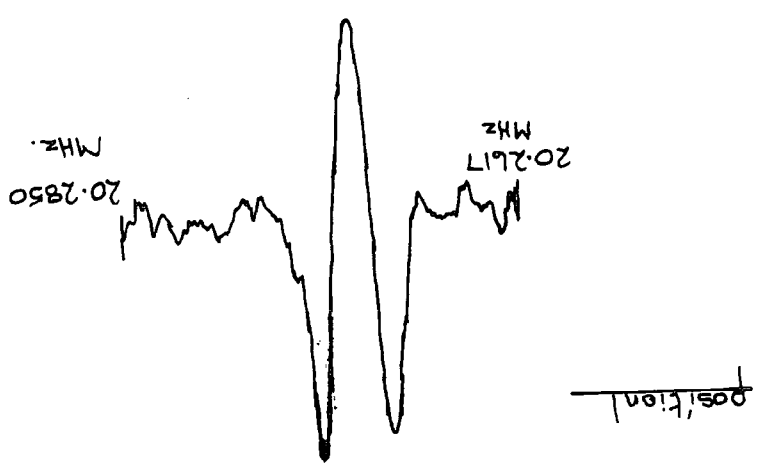
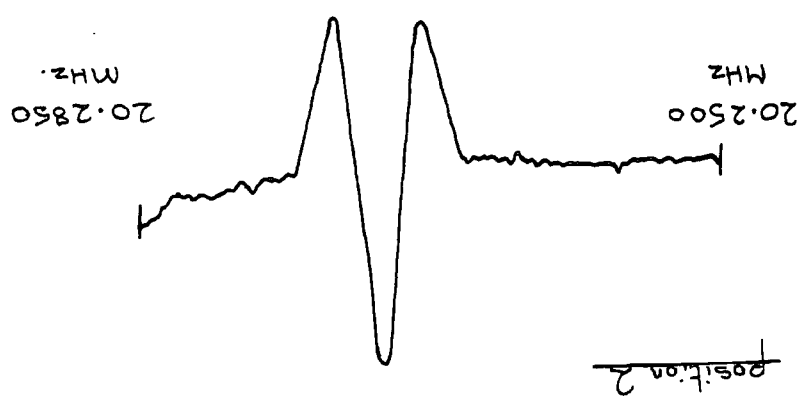
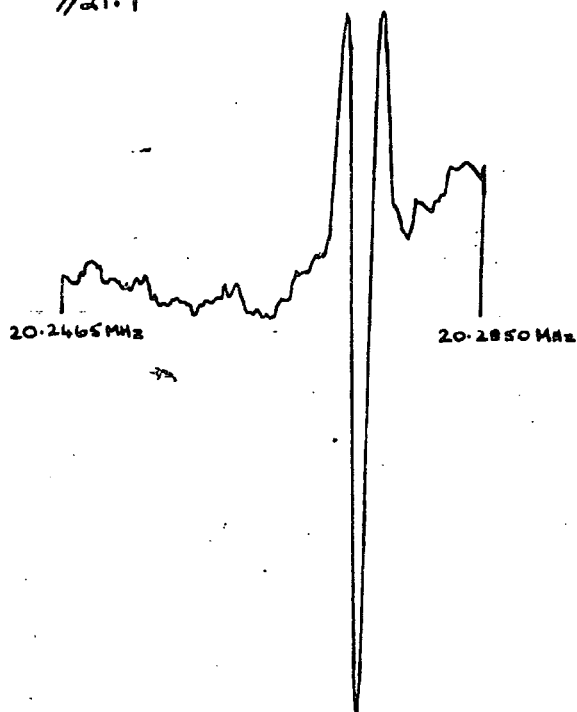


Fig. 190) ^{35}Cl n.g.r. silicon tetrachloride at 77K on AEI spectrometer using different modulation. (20.273MHz line).

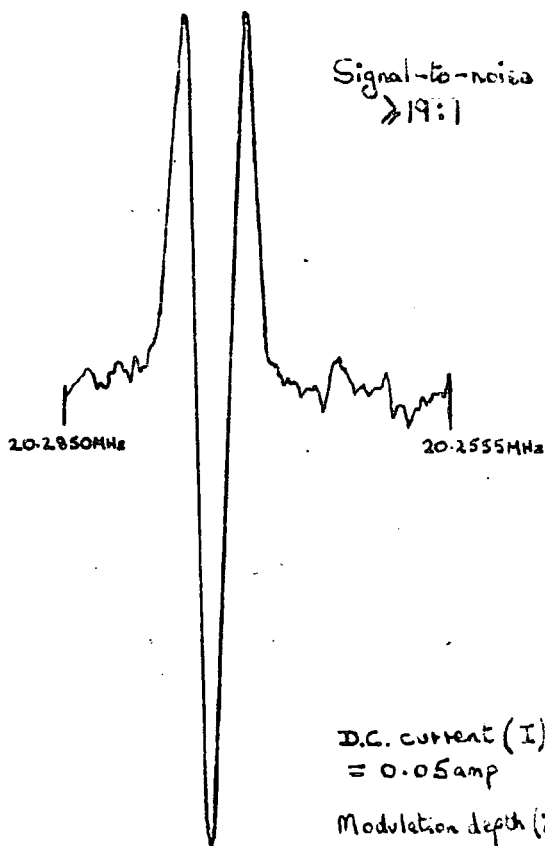
140Hz frequency modulation

140Hz sinusoidal Zeeman modulation

Signal-to-noise
 $\gg 21:1$



Signal-to-noise
 $\gg 19:1$



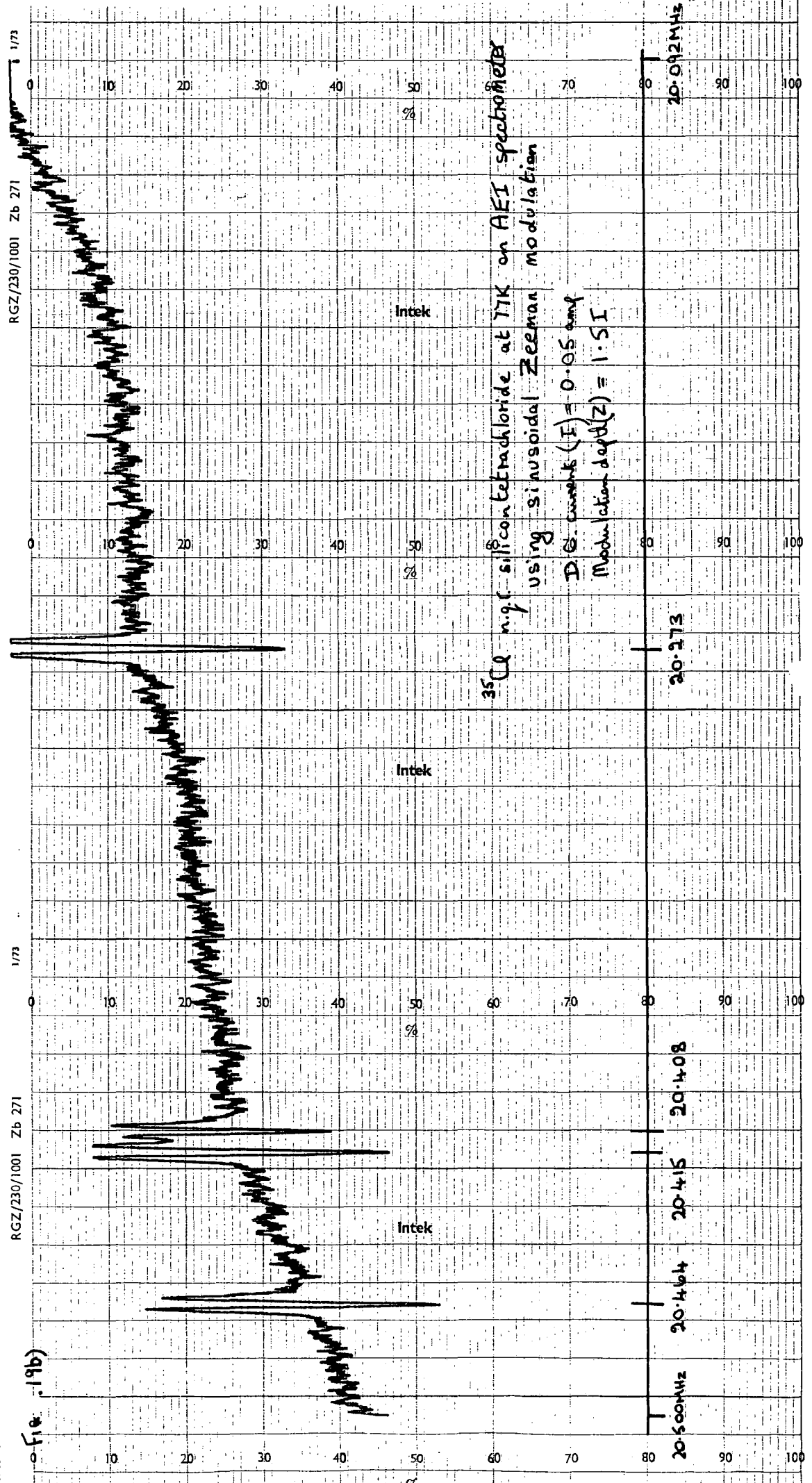
3.2024z

4.668Hz

D.C. current (I)
 $= 0.05 \text{ amp}$

Modulation depth (Z)
 $= 1.5 I$

file: 196b)



^{35}Cl n.g.c. silicon tetrachloride at 77K on AFI spectrometer
 using sinusoidal Zeeman modulation
 $D \cdot \text{currents (I)} = 0.05 \text{ amp}$
 Modulation depth(Z) = 1.5I

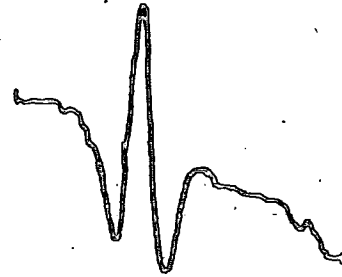
^{35}Cl n.g.r. silicon tetrachloride at 77K on AEI spectrometer

Fig. 20

using sinusoidal Zeeman modulation

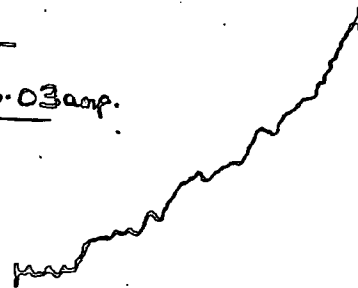
(I) D.C. current = 0.02 amp

(Z) Modulation = 1.5 I



(I) D.C. current ≈ 0.0 amp.

(Z) modulation $\approx 0.02 - 0.03$ amp.



20.2600 MHz

20.2850 MHz

Zeeman n.q.r. Spectroscopy (Z.n.q.r.)

The theory of Zeeman n.q.r. spectroscopy has been explained in Chapter 1. The determination of asymmetry parameters for chlorine in thionyl chloride has been reported in Chapter 4. A similar determination for equatorial chlorine in the trigonal bipyramidal molecule phenyl-phosphorus (V) chloride is reported in Chapter 7. In both of these cases, the DECCA spectrometer was used. In the case of PhPOCl_2 only a result for the stronger resonances from the equatorial chlorine atoms was obtained. In the case of the quadrupole resonances from the chlorine atoms in axial positions, unsuccessful attempts to enhance the signals were made using the computer of average transients. Both results reported were therefore obtained from Zeeman n.q.r. experiments upon the unenhanced spectrometer responses.

The method of Morino and Toyama (15) was used, in which measurements of splittings in the Z.n.q.r. lineshape are plotted against the inverse of magnetic field. Extrapolation to infinite field yields the value of the asymmetry parameter (η). The measurements needed to determine η are detailed in Chapter 1.

To make satisfactory measurements it was necessary to obtain a lineshape of clear definition. The two compounds investigated produced ^{35}Cl resonance lineshapes which closely approximated first derivative (dispersion) lineshape. The lineshape responses for both experiments were manipulated using the centre shift control. Sideband suppression was also applied

to rid the spectrum of sidebands.

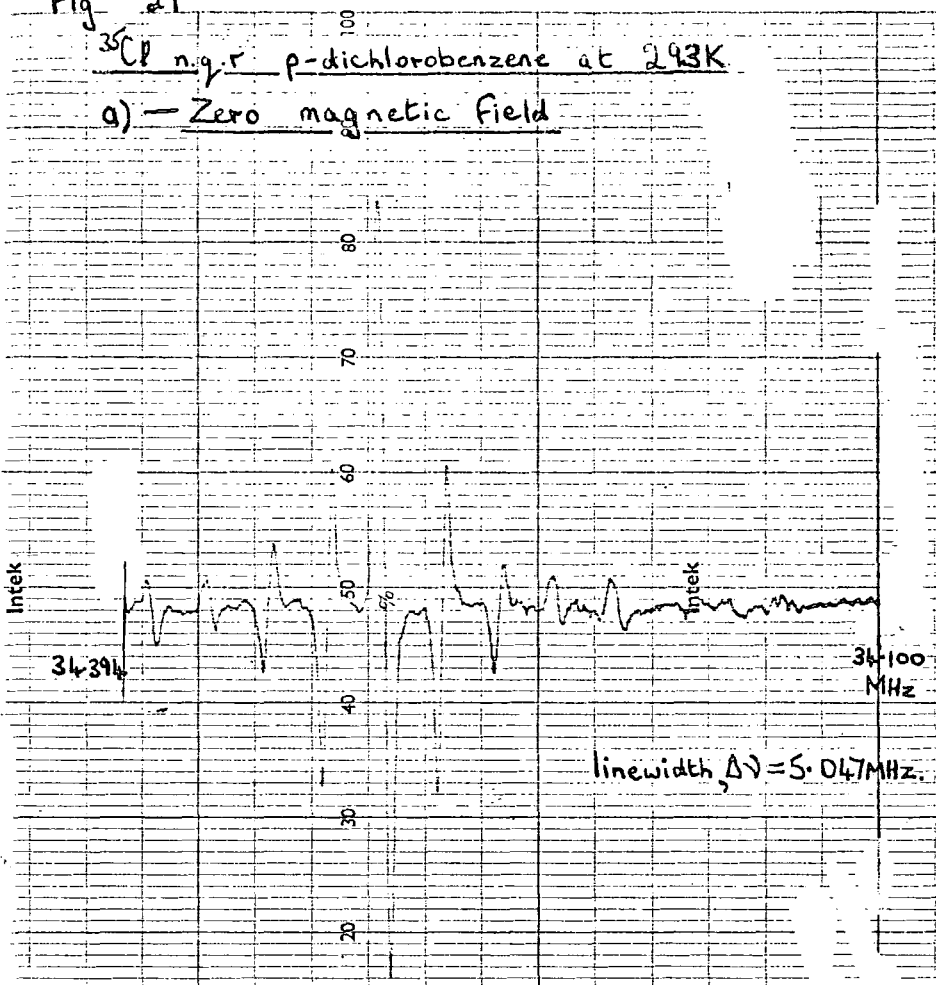
The validity of the measurements was checked by a similar determination of the asymmetry parameter of chlorine in p-dichlorobenzene. Examples of the lineshapes produced are shown in Fig. 21. From the spectra at varying field strengths, the curve shown in Fig. 22 was produced, from which a value of η was determined. The Zeeman coils of the DECCA spectrometer were calibrated at 31.7×10^{-4} Tesla amp⁻¹. The value of 0.08 agrees closely with that of Morino and Toyama themselves (15). This substantiates the reliability of the method used in evaluating η for thionyl chloride and phenyl-phosphorus (V) chloride.

A technique to avoid the use of sideband suppression was tried. The DECCA spectrometer was operated with a quench frequency of about 5 kHz which causes any sidebands to collapse into the fundamental lineshape. Unfortunately, as Smith and Tong (16) observed, the loss in sensitivity is too great for Zeeman splitting studies to be made.

Fig 21

³⁵Cl n.g.r. p-dichlorobenzene at 293K

a) — Zero magnetic field



b) — Magnetic field = 0.0064 T

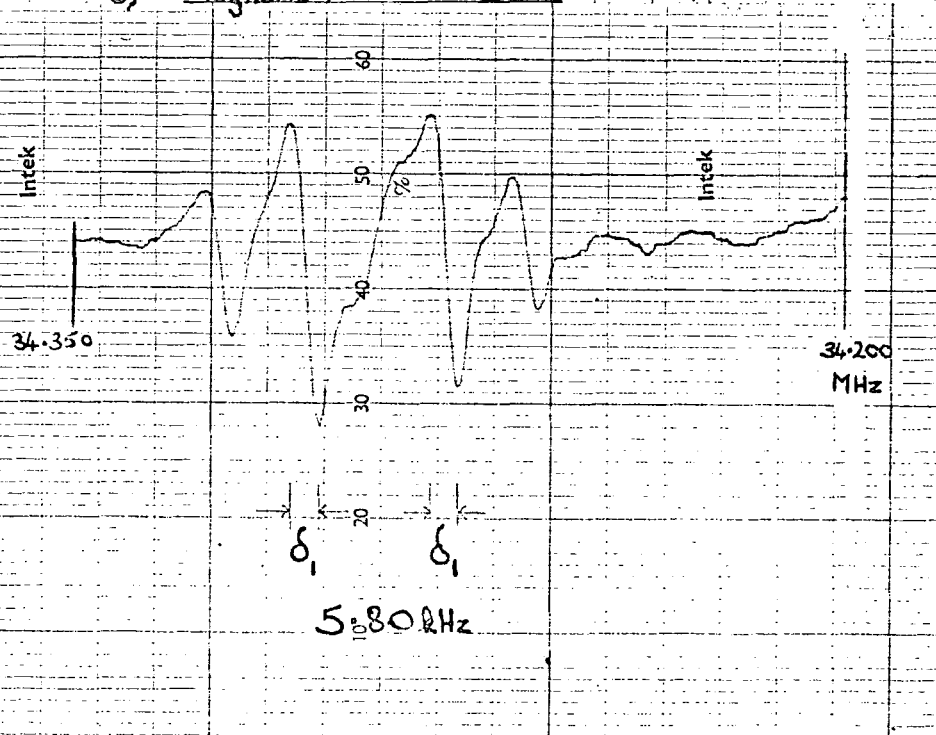
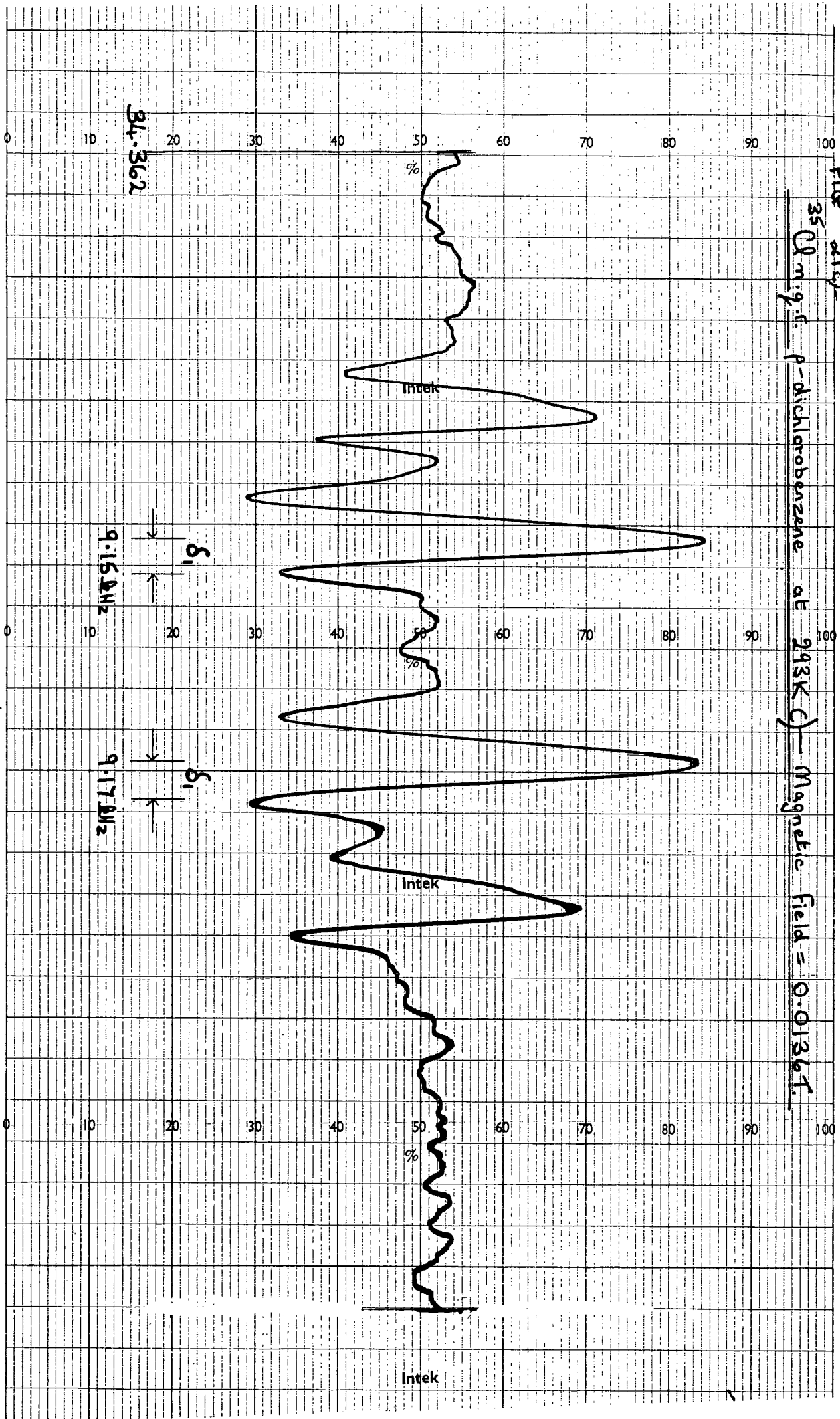


FIG 21c

³⁵Cl m.g.f. p-dichlorobenzene at 293K () - Magnetic field = 0.0136T.



$\frac{S_1}{224}$

Fig. 22 Determination of η in p-dichlorobenzene by method of Morino and Toyama.

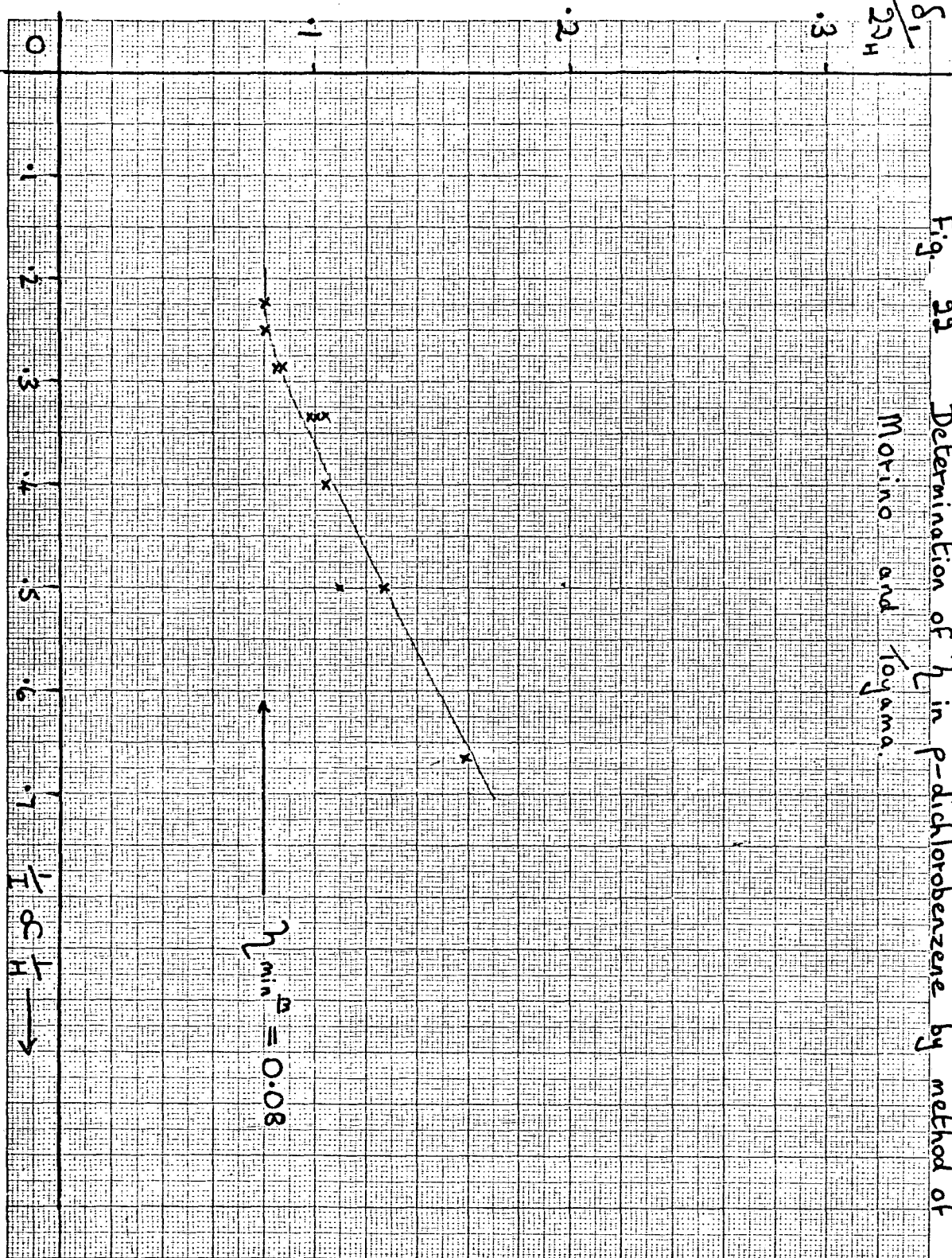


Fig. 23

TABLE FOR FIG. 22

I (amp.)	$\frac{1}{I}$ (amp ⁻¹)	δ_1 (kHz)	$\frac{\delta_1}{2\pi \nu_H}$
1.5	0.667	6.322	0.159
2.0	0.5	5.80 6.740	0.127 0.109
2.5	0.4	6.512 6.860	0.0985 0.1037
3.0	0.333	7.753 8.023 8.235	0.0977 0.101 0.104
3.5	0.286	7.931 8.046	0.0857 0.0869
4.0	0.25	8.500	0.0803
4.3	0.233	9.16	0.0802
4.5	0.222	9.529	0.0801

Pulse n.q.r. and Double-Resonance n.q.r. Spectroscopy

There remain two types of n.q.r. spectrometers as yet undiscussed. As they have not been used in the course of research reported in this thesis, their treatment will consist of short descriptions.

Pulsed n.q.r. spectrometers can provide more information than continuous-wave spectrometers. Of particular interest are nuclear relaxation times. Because linewidths in n.q.r. are typically broader than those of n.m.r., high power radio-frequency transmitters are required (1-5 kW) and high costs are therefore incurred in the circuitry. Instruments of this type have not been widely used for searching experiments because frequent retuning of the broad-band amplifiers is required to maintain sensitivity over the wide resonance frequency ranges of quadrupolar nuclei. However, such is the usefulness of information from relaxation times that this form of n.q.r. spectroscopy has achieved widespread usage, (17), (18).

In a poly-crystalline sample the direction of the principal axis of the e.f.g. (the Z axis, if the e.f.g. is axially symmetrical) covers all orientations. The nuclear quadrupole moments of the nuclei may be regarded as precessing about this direction, which we shall take as being the Z axis. When the strong r.f. field (H) of the transmitter coil is applied, the magnetic moments of the nuclei begin to precess about its axis also and at a rate of γH , (γ = the gyromagnetic constant of the

nucleus). In a poly-crystalline sample the field gradient direction is arbitrary but the pulse duration controls the amount of rotation of the macroscopic nuclear magnetic moment, M .

There are two pulse periods used. In one, M travels through 90° from the Z direction and is termed a 90° pulse. The other is the time required to move M through 180° and is termed a 180° pulse. When a pulse is switched off, M continues to precess about Z but then, under relaxation influences i) components of M disperse in the xy plane, and ii) M begins to return to the Z direction.

At the end of a pulse, the precession of M (about Z) causes an oscillating voltage to be induced in the surrounding coil. However, as process i) progresses and the macroscopic magnetisation (M) is dispersed into the components of each nucleus, the induced signal decreases progressively. This decrease is called the free induction decay (f.i.d.) from which a time constant can be calculated and which is usually represented as T_2^* , and is called the inverse linewidth parameter.

The spin-spin relaxation time, T_2 , is determined by the Carr-Purcell sequence ($90-\tau-180$) (19).

Process ii) is governed by a single rate constant if only two nuclear energy levels exist (e.g. $I=3/2$). The rate constant, T_1 , is described as the spin-lattice relaxation time. This is because energy exchanges between the nuclear spins and the lattice thermal energy levels are responsible for the return of M to the Z direction. The rate equation is due to

Bloch (20):

$$\begin{array}{l} \text{rate of return} \\ \text{to equilibrium} \end{array} , \quad \frac{dM_z}{dt} = \frac{-(M_z - M_0)}{T_1}$$

where M_0 is the original magnitude of M and M_z is the component of M in z-direction.

Determination of T_1 is usually made using the pulse sequence 180- τ -90. The initial 180° pulse turns M into the -Z direction which removes magnetisation from the Z direction. When the pulse is switched off, the magnetisation is gradually restored to the +Z direction. After an interval τ , an inspection 90° pulse is applied the free induction decay (f.i.d.) of which will be a measure of the magnetisation that has returned to the Z direction (M_z). As τ is increased the f.i.d. following the second pulse will follow the value of M_z . For the 180- τ -90 sequence the signal will initially decrease as M_z decays from a negative value to zero and then it will build up as M_z returns to its initial positive value. T_1 is obtained from the rate equation where the height of the f.i.d. replaces (M_z).

While the limitations of c.w. and super-regenerative techniques have concentrated much work on chlorine n.q.r., the intrinsically greater sensitivity of pulsed n.q.r. has allowed the investigation of, otherwise, less promising nuclei. One such nucleus is ^{14}N whose (commonly) long relaxation times and low resonance frequencies have previously made searches fruitless. It can now be probed by a technique capable of overcoming the saturation problem. The investigation of boron nuclei

(^{11}B and ^{10}E) and quadrupolar nuclei in low abundance (e.g. ^{17}C and ^{33}S) should also benefit from pulsed n.q.r. spectroscopy.

Double resonance n.q.r. spectroscopy makes use of pulsed techniques. Double resonance with level crossing (DRLC) was first demonstrated by Slusher and Hahn (21). In this technique the quadrupolar interaction of one nucleus (X) is detected by its influence upon a second nucleus (Y) to which it is either bonded or in close proximity. This second nucleus (Y) should have an easily observed pulsed - n.m.r. or-n.q.r. signal which will usually be monitored as an f.i.d. If the nucleus Y is to be observed by, say, n.m.r. the experiment consists of irradiating the sample at the magnetic resonance of Y followed by the rapid transfer of the sample to the coil of a continuous-wave (c.w.) r.f. transmitter whose frequency is slowly being swept. The sample moves between these two devices and the height of the f.i.d. of the nucleus Y is monitored. When the r.f. transmitter irradiates the sample at a quadrupole resonance of the nucleus X, absorption of energy results in a population change in the energy levels. During the transfer to the n.m.r. spectrometer, a coincidence (level-crossing) of the energy levels occurs for the two types of nuclei and, in an energy exchange ($Y \rightarrow X$), the f.i.d. of the second nucleus (Y) is changed. The detection of this change is clear evidence that the swept transmitter frequency has coincided with an n.q.r. signal of the nuclei X.

The DRLC technique has been used to detect n.q.r. signals for nuclei otherwise inaccessible to continuous-wave spectrometers

e.g. ^{14}N and ^2D . Edmonds (22) has used proton n.m.r. as the Y nuclei to detect ^{14}N n.q.r. of a variety of amino-acids and peptides. He has also studied ^2D resonances in various ice structures (24). Hertzög and Hahn (3) studied the double resonance effect of the continuous wave resonance of ^{23}Na upon the f.i.d. of ^{35}Cl in NaClO_3 i.e. the interaction of two quadrupolar nuclei.

Jones and Hartmann (23) have demonstrated a variation of double resonance n.q.r. spectroscopy. This method they call steady state nuclear double resonance. It differs from DRLC in that the second nucleus (Y) is held in a constant state of magnetisation. A continuous r.f. field is applied to nucleus Y while a second r.f. transmitter is swept for resonance of the other nucleus (X). The resonance of nucleus X is detected as a change in the magnetisation of nucleus Y. The advantage claimed for this method over DRLC is the less stringent instrument stability required.

INORGANIC COMPOUNDS

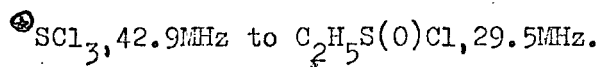
Introduction

This chapter reports n.q.r. and vibrational spectra for some compounds of $^{\oplus}\text{SCl}_3$ and the n.q.r. frequencies for pentafluoro-sulphur VI chloride and a ketimine sulphinyl chloride. The asymmetry parameter of the S-Cl bonds in thionyl chloride has been measured using the Zeeman splitting n.q.r. technique.

³⁵Cl n.q.r. Investigation of S-Cl Bond in Various Compounds.

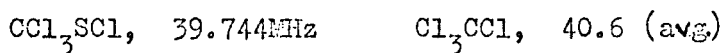
Background

Although sulphur bonded to chlorine can exist in several valence states, the range of frequencies observed in ³⁵Cl nuclear quadrupole resonance (n.q.r.) is a little less than that of chlorine bonded to carbon (1) i.e.



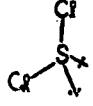
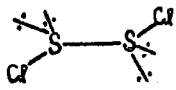
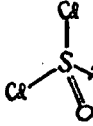
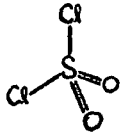
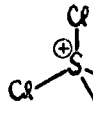
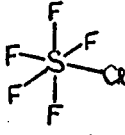
The n.q.r. frequency depends upon the presence or absence of lone pairs on, and hybridisation of, the sulphur atom. Also important are the total inductive effect of substituents and whether the sulphur is involved in d_π-bonding. This is illustrated in Table 1.

The ³⁵Cl n.q.r. frequency for trifluoromethyl sulphenyl chloride lies above that of chlorine bonded to sulphur in trichloromethyl sulphenyl chloride reflecting the normal inductive influence of a more electronegative group on the S-Cl bond. This differs from the situation observed for alkyl halides where hyperconjugation of the trifluoromethyl group causes a lowering of the ³⁵Cl quadrupole resonance frequency of trifluoromethyl chloride from that of carbon tetrachloride.



In phenyl sulphenyl chloride the ³⁵Cl n.q.r. exhibits a lowering in frequency characteristic of the inductive

TABLE 1

COMPOUND	FORMULA	STRUCTURE	³⁵ Cl n.q.r. FREQUENCIES OF S-Cl BOND AT 77K (MHZ)	REF.
Sulphur Dichloride	SCl ₂		40.250, 39.088, 39.018 39.011 (avg. 39.342)	(2)
Sulphur monochloride	S ₂ Cl ₂		35.977, 35.584	(1)
Substituted sulphenyl chlorides	R-SCl	R=CF ₃ =CCl ₃ =C ₂ H ₅ =C ₆ H ₅ =(CH ₃) ₂ H	42.196 39.744 (avg.) 36.978 37.011 36.000, 35.598	(2) (2) (2)
Thionyl Chloride	S(O)Cl ₂		32.088, 31.884 (avg 31.986)	(1)
Substituted sulphinyl chlorides	RS(O)Cl	R=C ₂ H ₅	29.477	(1)
Sulphuryl Chloride	S(O) ₂ Cl ₂		37.810, 37.597 (avg. 37.704)	(1)
Substituted Sulphonyl Chlorides	RS(O) ₂ Cl	R=CF ₃ =CCl ₃ =C ₂ H ₅	36.276 32.519	(1) (1)
Trichlorosulphonium Cation	⁺ SCl ₃		42.932, 42.185 (as hexachloroantimonate)	(1)
Pentafluoro Sulphur (VI) Chloride	SF ₅ Cl		42.680	This Thesis

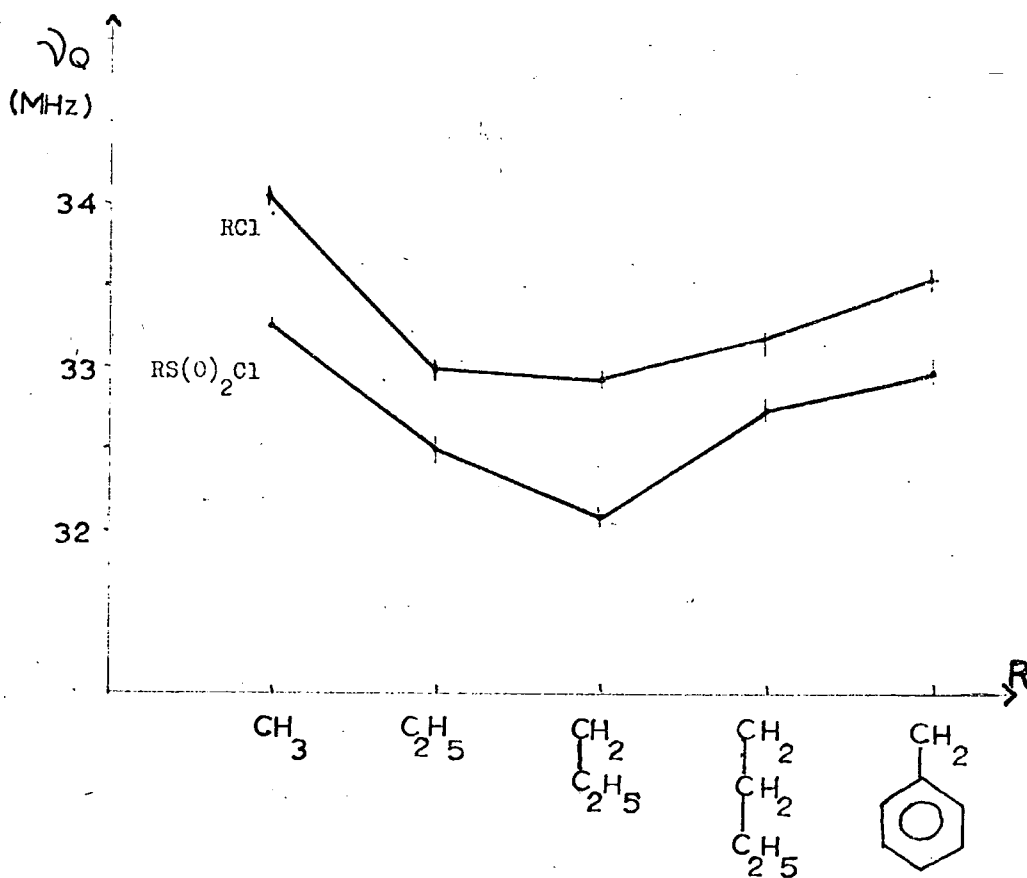
influence with an atom to which the chlorine does not conjugate. The variation in n.q.r. frequency for a limited range of sulphenyl chlorides has been explained by Whitehead and Hart as due to σ -inductive effects and re-hybridisation on the sulphur atom (1). Thus divalent sulphur transmits electronic effects similarly to the tetrahedral (-CH₂-) methylene group. Another study (2) on alkyl sulphenyl chlorides suggested that conjugative effects are more important than inductive effects. However, the hypothesis is weakened because the increase in ³⁵Cl n.q.r. frequency for trifluoromethyl sulphenyl chloride cannot then be explained. The abnormally low frequency for di-N-methylamine sulphenyl chloride (Table 1) was not commented upon either, but it is probably caused by the involvement of internal polarisation (3).

The ³⁵Cl n.q.r. frequencies of substituted phenyl sulphenyl chlorides (RSCl) are indicative of a different mechanism of electronic transmission through the sulphur to the chlorine atom (4). The inductive effect was observed to be greater than the conjugative although in this series conjugation, if possible with the sulphur atom, might have been favoured. The further observation of near random frequency shifts for other substituted phenyl sulphenyl chlorides lends added weight to the assertion that in sulphenyl chlorides, inductive effects have the major influence on the ³⁵Cl n.q.r. frequency (1).

The chlorine n.q.r. frequencies for straight chain alkyl sulphonyl chlorides, R-S(O)₂Cl, parallel the behaviour of the

Fig. 1.

Comparison of ^{35}Cl n.q.r. frequencies of straight chain alkyl sulphonyl chlorides and of corresponding alkyl chlorides. (from Ref. 1)



frequencies for alkyl chlorides, R-Cl. The frequencies of alkyl sulphonyl chlorides are lower due to the lower electronegativity of sulphur. The $-\text{SO}_2-$ group appears to transmit primarily inductive electronic effects. However, the lack of correlation of n.q.r. data on alkyl sulphonyl chlorides, $\text{R S(O)}_2\text{Cl}$, with those of alkyl halides, RCH_2Cl , shows that the $-\text{SO}_2-$ group does not act like $-\text{CH}_2-$ (5). As with sulphenyl chlorides, the n.q.r. frequency of trifluoromethyl - substituted sulphonyl chloride indicates that hyperconjugation is not transmitted through the sulphur atom (Table 1). The $-\text{SO}_2-$ group is thus mainly a transmitter of σ -bond inductive effects.

For substituted phenyl sulphonyl chlorides no relationship comparable to that of alkyl sulphonyl chlorides with alkyl chlorides was found (1). Lucken (5) has proposed that the large difference between the ^{35}Cl n.q.r. frequencies of p-nitrophenyl- and m-nitrophenyl - sulphonyl chlorides indicates conjugative coupling through the sulphur to the S-Cl bond in the case of the p-nitro-compound. π -character was therefore assigned to the bond and conjugative transmission proposed for the $-\text{SO}_2-$ group. However, no correlation between the n.q.r. frequencies of RC(O)Cl and $\text{RS(O)}_2\text{Cl}$, where allowance for π -conjugative effects is made, is found. Furthermore, inductive effects alone appear to explain the variation in frequencies for chloro-substituted phenyl sulphonyl chlorides (1).

A Scrocco-type equation (6) has been evaluated for differently substituted phenyl sulphonyl chlorides. The allowances

in frequency for the $-S(O)_2Cl$ group in the various positions σ -, m - and p - of the phenyl ring fitted well for chloro-substituted phenyl systems where, as stated above, inductive effects are expected to dominate. However, when applied to nitro-, carboxyl-, and methyl- substituted phenyl sulphonyl chlorides no satisfactory equation could be established. Since these groups can participate in π -conjugation to the ring, it is possible that they may be causing necessary variations in hybridisation of the sulphur atom or are making use of the d_{π} orbitals on it. The contrast with divalent sulphur is therefore that substitution of lone pairs by oxygen atoms on sulphur promotes its conjugative powers.

Using the United Atom Approach (7), (3), and the close comparison of ^{35}Cl n.q.r. frequencies for $RS(O)_2Cl$ and $RMCl_3$ (M = Group IV metal, i.e. Si, Ge, Sn), Hart and Whitehead conclude that the $-SO_2-$ group can be reasonably represented by its "united atom" germanium (1). This would explain the poor transmitting power for electronic effects of $-SO_2-$ and its participation in π -type bonding using the p_{π} molecular orbitals of d_{π} symmetry.

Sulphinyl chlorides, $RS(O)Cl$, probably behave in a similar manner to sulphonyl chlorides and π -conjugative effects are a possible influence on n.q.r. frequencies. Only limited n.q.r. data are available on these compounds due to their ready decomposition (1).

The Reaction of Sulphur Dichloride with Various Lewis Acids

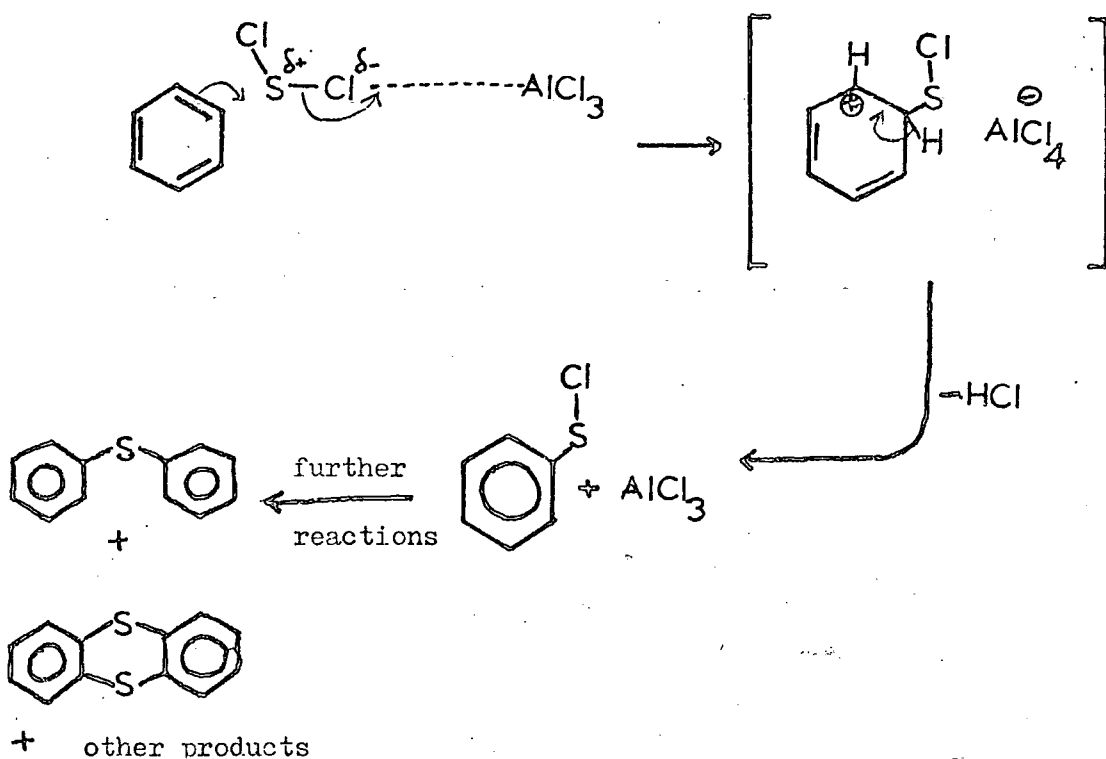
In a study of the reaction of sulphur dichloride with some Lewis acids, Nabi (9) reported the formation of solid 1 : 1 complexes. Those reported included $\text{SCl}_2 \cdot \text{SbCl}_5$, $\text{SCl}_2 \cdot \text{FeCl}_3$ and $\text{SCl}_2 \cdot \text{AlCl}_3$. The production of $(\text{SCl})^{\oplus}$ by self-ionisation of sulphur dichloride in acetone has also been reported (10). The ^{35}Cl n.q.r. and other spectra of the products of these and other reactions involving sulphur dichloride were studied in order to identify any sulphur-chlorine cations formed.

Any ^{35}Cl n.q.r. response for sulphur dichloride itself was unobserved at 77 K on the Decca spectrometer. It has been reported as a multiplet (avg. 39.342MHz) using a pulsed spectrometer (2). Possibly the formation of a glass upon freezing the sample has prevented its observation with the s.r.o. spectrometer.

Distilled sulphur dichloride was dissolved in dry "Spectrosol" grade acetone. After two days, standing at room temperature, the dark red solution had turned to a black tar in the sealed ampoule. The proposed self-ionisation was based upon conductivity measurements in which conduction was said to be due to $(\text{SCl})^{\oplus}$ and $(\text{Cl})^{\ominus}$. However a more plausible explanation is that by reaction of sulphur dichloride with the enol-form of acetone, trace quantities of hydrochloric acid are formed. This would produce the conducting species $(\text{H})^{\oplus}$ and $(\text{Cl})^{\ominus}$ and subsequently would promote reaction with the acetone. Heal and Kane (11) have studied the ionisation of sulphur dichloride and sulphur monochloride in acetonitrile but have observed the equilibrium constants to be very small ($K \sim 4 \times 10^{-7}$) and self-ionisation was

regarded as unlikely.

The assistance of Lewis acids in aromatic halogenation reactions is well known and in 1884, Friedel and Craft (12) succeeded in reacting sulphur dichloride with benzene using aluminium trichloride as catalyst. The reaction is now seen as proceeding through an activated complex involving the Lewis acid thus,



In the reactions of sulphur dichloride with Lewis acids (9), transfer of charge occurs and must therefore cause a change in the electronic populations at the chlorine atoms bonded to both the sulphur and the Lewis acids. ^{35}Cl n.q.r. spectroscopy was therefore applied to investigate the structure of the complexes.

1) Sulphur Dichloride and Antimony Pentachloride

The preparation and analysis details are included in the chapter Appendix.

The prepared solid in a sealed ampoule was used to record its ^{35}Cl n.q.r. spectrum and Raman spectrum. It was found that this compound reacted with dry Nujol. This and the other complexes prepared with strong Lewis acids were therefore milled in distilled Kelf grease. To protect caesium iodide plates polythene discs were used to separate the mull from the plates.

Spectroscopic Results

The ^{35}Cl n.q.r. spectrum of this product is almost identical with that Hart et al. obtained from a sample of $(\text{SCl}_3)^{\oplus}(\text{SbCl}_6)^{\ominus}$ prepared from SCl_4 (13). (Table 2).

Although using a similar super-regenerative oscillator spectrometer, Hart observed a signal to noise ratio of only 2/1 for the high frequency $(\text{SCl}_3)^{\oplus}$ species. It can therefore be concluded from the n.q.r. spectrum that the reaction product is $(\text{SCl}_3)^{\oplus}(\text{SbCl}_6)^{\ominus}$.

The infra-red bands of the hexachloroantimonate ion at 540 cm^{-1} and 180 cm^{-1} were observed, as were those of $(\text{SCl}_3)^{\oplus}$, in spectra recorded on Perkin Elmer 547 and Beckmann FS720 (far infra-red) machines (Table 3). A polythene support for the milled samples was used with the FS720. The broad band at about 330 cm^{-1} , which appears in spectra of this and the other trichlorosulphonium complexes, was found to also exist in the blank runs. It was therefore likely to originate in slow reaction of the samples with the polythene.

FIG. 2. ^{35}Cl nqr at 77K of
 $\ominus\text{SO}_3$ in $\ominus\text{SbCl}_6$



43MHz.

42MHz

TABLE 2. N.q.r. results observed at 77K

REACTION	OBSERVED		LITERATURE	
	³⁵ Cl	³⁷ Cl	Species (Ref)	³⁵ Cl
<u>1)</u>				
SbCl ₂ + SbCl ₅	42.900 (⁸ /1)	33.825 (⁵ /1)	⊕SbCl ₃ (1, 14)	42.932 (² /1)
1 : 1	42.160 (")	33.235 (")		42.185 (")
	25.810 (⁸ /1)	20.35 (³ /1)	⊖SbCl ₆ (1,14)	25.832 (² /1)
	24.789 (⁴ /1)	19.52 (² /1)		24.810 (")
	24.133 (¹² /1)	19.06 (⁴ /1)		24.269 (")
				24.174 (")
<u>2)</u>				
S ₂ Cl ₂ + SbCl ₅	42.932 (¹² /1)	33.825 (⁴ /1)	Compare 1)	ditto
1 : 1	42.183 (")	33.248 (")	⊕SbCl ₃	
	25.829 (⁶ /1)	20.37 (³ /1)	⊖SbCl ₆	
	24.810 (² /1)	not observed		
	24.155 (⁴ /1)	19.04 (² /1)		
<u>2)</u>				
S ₂ Cl ₂ + SbCl ₅	42.910 (⁹ /1)	33.821 (³ /1)	Compare 1)	ditto
1 : 2	42.172 (")	33.254 (")	⊕SbCl ₃	
	24.834 (⁵ /1)	20.37 (² /1)	⊖SbCl ₆	
	24.819 (² /1)	not observed		
	24.160 (⁴ /1)	19.04 (² /1)		
<u>3)</u>				
SbCl ₂ + AlCl ₃	43.376 (³ /1)	34.203 (² /1)	⊕SbCl ₃ ⊖AlCl ₄ (2)	not observed
3 : 1	42.096 (⁷ /1)	33.202 (³ /1)		
	<u>at 292K</u>			<u>at 301 K</u>
	11.000 (⁷ /1)	8.69 (² /1)	⊖AlCl ₄ (2)	11.04
	10.473 (⁷ /1)	8.25 (² /1)		10.46
	10.214 (")	8.05 (")		10.18
	9.873 (")	7.79 (")		9.91

TABLE 2.

REACTION	OBSERVED		LITERATURE	
	^{35}Cl	^{37}Cl	Species (Ref)	^{35}Cl
<u>4)</u> $\text{SCL}_2 + \text{TiCl}_4$	42.41 ($^{4/1}$)	33.44 ($^{2/1}$)	Compare 1)	
	42.05 (")	33.13 (")	$\oplus\text{SCL}_3$	
	41.87 (")	33.00 (")		
<u>5)</u> Supplied Sample	42.637 ($^{14/1}$)	33.607 ($^{5/1}$)	Compare 1)	
$\oplus\text{SCL}_3 \ominus\text{ICl}_4$ (Form 1)	42.091 (")	33.184 (")	$\oplus\text{SCL}_3$	
	41.726 (")	32.890 (")		
	28.123 ($^{5/1}$)	22.15	$\ominus\text{ICl}_4 \oplus\text{K}$ (33)	22.37
	25.895 ($^{4/1}$)	20.40		
	20.95 ($^{2/1}$)	not observed		
<u>6)</u> $\text{SCL}_2 + \text{BCl}_3$	21.515 ($^{100/1}$)	16.960 ($^{30/1}$)	BCl_3 (21)	21.582
3 : 1	21.48 (shoulder)			21.578
<u>7)</u> $\text{SCL}_2 + \text{SnCl}_4$	21.84 ($^{2/1}$)	not observed	$\ominus\text{SnCl}_5 \oplus\text{PCl}_4$ (23)	
1 : 1	21.39 (")			
(Crystals)				
$\text{SCL}_2 + \text{SnCl}_4$	24.302 ($^{6/1}$)	19.153 ($^{2/1}$)	SnCl_4 (32)	24.294
3 : 1	24.184 (")	19.070 (")		24.226
(frozen liquids	24.037 (")	18.980 (")		24.140
in ampoule)	23.702 (")	18.692 (")		23.719

TABLE 3.

SPECIES	RAMAN BANDS		SPECIES	RAMAN BANDS	
	OBSERVED cm ⁻¹	LITERATURE cm ⁻¹ (Ref.)		OBSERVED cm ⁻¹	LITERATURE cm ⁻¹ (Ref.)
1) and 2) $\overset{\oplus}{\text{SbCl}_3} \overset{\ominus}{\text{SbCl}_6}$					
$\overset{\oplus}{\text{SbCl}_3}$	{ 535 524 502 282 220	543 519 (44) 284 214 † (14)	$\overset{\ominus}{\text{SbCl}_6}$	336 277 175	337 277 (46) 172
3) $\overset{\oplus}{\text{AlCl}_3} \overset{\ominus}{\text{AlCl}_4}$					
$\overset{\oplus}{\text{AlCl}_3}$	{ 530 518 498 281 208 219	{ 533 521 498 276 (16) 208 215 +(43)	$\overset{\ominus}{\text{AlCl}_4}$	575 351 - 141	575 349 180 (46) 146 +(43)
4) $\overset{\oplus}{\text{TiCl}_3} \overset{\ominus}{\text{TiCl}_5}$					
$\overset{\oplus}{\text{TiCl}_3}$	522 492 272 208	-	$\overset{\ominus}{\text{TiCl}_5}$	{ 423 419 388 309 222	-
Also 4) lines at 143, 153(sh), 445 and 462 unassigned				90	

TABLE 3.

SPECIES	RAMAN BANDS		SPECIES	RAMAN BANDS	
	OBSERVED -1 cm	LITERATURE -1 cm (Ref)		OBSERVED -1 cm	LITERATURE -1 cm (Ref)
5) $\text{SbCl}_3\text{ICl}_4$ SbCl_3	-	{ 512 498 485 (42) 279 220 212	ICl_4	-	282 260 228 (48) 218 154 143 125

† See note 2.

TABLE 3.

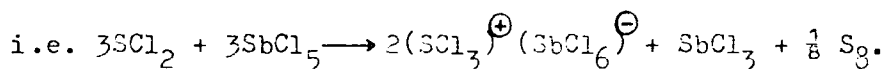
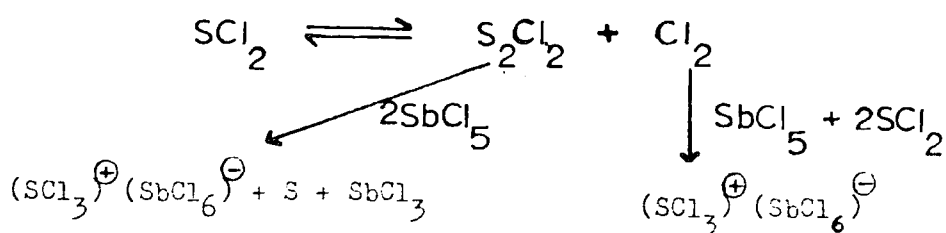
SPECIES	I.R. BANDS		SPECIES	I.R. BANDS	
	OBSERVED cm ⁻¹	LITERATURE cm ⁻¹ (Ref)		OBSERVED cm ⁻¹	LITERATURE cm ⁻¹ (Ref)
1) and 2) $\overset{\oplus}{\text{S}}\text{Cl}_3 \overset{\ominus}{\text{Sb}}\text{Cl}_6$ $\overset{\oplus}{\text{S}}\text{Cl}_3$	275 333	275 (14)	$\overset{\ominus}{\text{Sb}}\text{Cl}_6$	340 (S) 177	340 180 (14)
3) $\overset{\oplus}{\text{S}}\text{Cl}_3 \overset{\ominus}{\text{Al}}\text{Cl}_4$ $\overset{\oplus}{\text{S}}\text{Cl}_3$	274 326 broad	274 (45) 496 518	$\overset{\ominus}{\text{Al}}\text{Cl}_4$	- 178	575 180 (49)
4) $\overset{\oplus}{\text{S}}\text{Cl}_3 \overset{\ominus}{\text{Ti}}\text{Cl}_5$ $\overset{\oplus}{\text{S}}\text{Cl}_3$	271 330	-	$\overset{\ominus}{\text{Ti}}\text{Cl}_5$	385 (vw) 349 - 170 -	385 417 346 (47) 212 170 83

Notes

1. KCl discs, prepared in a hand die, were found to react with SCl_3 compounds. I.R. absorptions at 505 cm^{-1} and 530 cm^{-1} were produced which are characteristic of sulphur dichloride. Therefore, for the above results, KCl discs were replaced with caesium iodide plates protected by polythene discs.
2. Raman investigation of $\overset{\oplus}{\text{S}}\text{Cl}_3 \overset{\ominus}{\text{Sb}}\text{Cl}_6$ (ref 14) was unsuccessful due to fluorescence of sample in the red laser. A green laser was used in this work and in which the sample did not fluoresce.

Raman spectra have been recorded on a Cary 81 spectrometer. The Raman spectrum for this complex shows bands due to the trichlorosulphonium ion and the hexachloroantimonate species (Table 3). The complex is therefore confirmed as containing $(\text{SCl}_3)^{\oplus} (\text{SbCl}_6)^{\ominus}$.

While the analysis of Nabi and Khalique (9) appears to support the production of a 1:1 complex $\text{SCl}_2 \cdot \text{SbCl}_5$ it is not incompatible with a mixture containing $(\text{SCl}_3)^{\oplus} (\text{SbCl}_6)^{\ominus}$. If the 1:1 reaction mixture lost no products, the analysis could support the reaction,



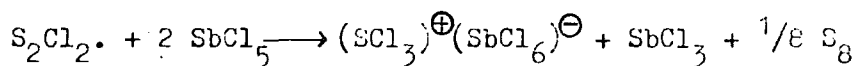
The disproportionation of sulphur dichloride proposed in the reaction mechanism is given support by the reaction of sulphur monochloride itself with antimony pentachloride. This is the subject of the next section. Investigations of complexes with other Lewis acids provide further support and are discussed below.

2) Sulphur Monochloride and Antimony Pentachloride

In a similar manner to that used in the reaction of sulphur dichloride with antimony pentachloride, sulphur monochloride was mixed in 1:1 and 1:2 molar proportions with the same Lewis acid. Reaction takes place forming yellow solid products. The ^{35}Cl n.g.r. spectrum shows the presence in both cases of

$(\text{SbCl}_6)^{\ominus}(\text{SbCl}_3)^{\oplus}$ (Table 2). The n.q.r. frequencies observed for the products of reaction with 1) sulphur dichloride and 2) sulphur monochloride differ slightly. It is probably attributable to impurity or crystallinity differences and not to a chemical difference. The greater strengths of the n.q.r. resonances for $(\text{SbCl}_3)^{\oplus}$ obtained from the monochloride cannot be easily explained but it is likely that it is due to the physical state of the samples.

Partington performed a similar reaction of sulphur monochloride with antimony pentachloride in sulphuryl chloride and obtained $\text{SbCl}_4 \cdot \text{SbCl}_5$ (15). The likely reaction is expressed by



Analysis (reported in Appendix to this chapter) of the product of the 1:2 molar reaction indicated that all reactants were absorbed. The above equation is therefore supported by a 1:2 mechanism and by the observation of spectra due to $(\text{SbCl}_3)^{\oplus}(\text{SbCl}_6)^{\ominus}$. Whilst the presence of elemental sulphur could not be demonstrated, an n.q.r. signal at 19.65 MHz was attributed to antimony trichloride at 77K (32).

It has therefore been shown that antimony pentachloride reacts with sulphur dichloride and sulphur monochloride by means of oxidation and reduction. The simple 1:1 adduct of $\text{SbCl}_2 \cdot \text{SbCl}_5$ proposed by Nabi has been shown to be a mixture containing $(\text{SbCl}_3)^{\oplus}(\text{SbCl}_6)^{\ominus}$. Similar complexes were however reported with aluminium trichloride and titanium tetrachloride where oxidation of the sulphur chlorides is less likely.

3) Sulphur Dichloride and Aluminium Trichloride

The reaction was carried out with a 1:1 molar mixture. Details

of the preparation are given in the appendix. The production of a yellow liquid distillate (removed when the mixture was pumped) indicates a possible difference in reaction mechanism from that shown for antimony pentachloride as Lewis acid.

Spectroscopic Results

Table 2 shows that the presence of $(\text{SCl}_3)^{\oplus} (\text{AlCl}_4)^{\ominus}$ is indicated by the n.q.r. spectrum. A previous study (16) of this compound failed to find the n.q.r. responses of $(\text{SCl}_3)^{\oplus}$. Two resonances are observed with an intensity ratio of about two to one. The higher frequency line is the highest recorded n.q.r. frequency for an S-Cl bond. Internal non-bonding interactions probably enhance the electric field gradient at one of the chlorine sites of $(\text{SCl}_3)^{\oplus}$. The Raman spectrum of this reaction product closely agrees with that of $(\text{SCl}_3)^{\oplus} (\text{AlCl}_4)^{\ominus}$ (16) (Table 3). The infra red spectrum, although less conclusive, is in agreement with this formula.

If the first step of the reaction with sulphur dichloride involves a disproportionation reaction thus,



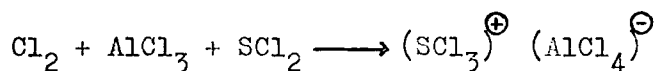
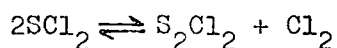
the reaction of chlorine and aluminium trichloride with sulphur dichloride will yield the product $(\text{SCl}_3)^{\oplus} (\text{AlCl}_4)^{\ominus}$.

Although reported as forming a complex $2\text{S}_2\text{Cl}_2 \cdot \text{AlCl}_3$ (17), no interaction was observed between aluminium trichloride and sulphur monochloride when sealed together in an ampoule. The n.q.r. spectrum of the mixture gave no evidence for a new species.

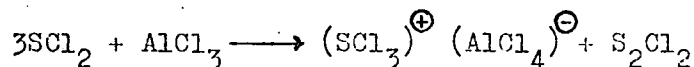
It was therefore possible that the liquid distilled off from the reaction between sulphur dichloride and aluminium trichloride was sulphur monochloride. This was investigated by using excess aluminium chloride in the reaction mixture and by taking the Raman spectrum of the distillate. The spectrum gave clear evidence that it was indeed sulphur monochloride, i.e.

cm^{-1}	$\nu_1(\text{S-S})$	Symm. $\nu_2(\text{S-Cl})$	ν_3	ν_4	Assymm $\nu_5(\text{S-Cl})$	ν_6
Observed	543	450	207	104	435	240
Literature	540	446	205	102	434	238

Thus the proposed reaction mechanism is,



i.e.



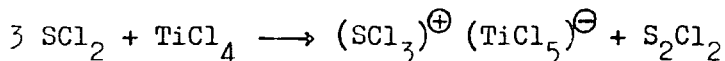
Sulphur dichloride and aluminium trichloride were reacted in the molar ratio 3:1 and were stirred to ensure complete reaction. Droplets of a yellow liquid (sulphur monochloride) collected on the flask sides and the yellow solid containing $(\text{SCl}_3)^{\oplus}$ $(\text{AlCl}_4)^{\ominus}$ was formed. After pumping at room temperature for about fifteen minutes the solid residue was analysed for aluminium, chlorine and sulphur. Details are given in the Appendix but the analysis supports the formula $(\text{SCl}_3)^{\oplus}$ $(\text{AlCl}_4)^{\ominus}$.

The reported 1:1 complex $\text{SCl}_2 \cdot \text{AlCl}_3$ (9) is therefore shown to be

unlikely. From all spectroscopic information the complex is believed to be $(\text{SCl}_3)^{\oplus} (\text{AlCl}_4)^{\ominus}$.

4) Sulphur Dichloride and Titanium Tetrachloride

The presence of a lower oxidation state for titanium means that titanium tetrachloride could react with sulphur dichloride as a weak oxidising agent and a mechanism like that with antimony pentachloride might be supposed. If, however, it remains in oxidation state four, the titanium tetrachloride could react as a Lewis acid in a mechanism like that of aluminium trichloride. In a separate experiment with sulphur monochloride, titanium tetrachloride was found not to react; the dry liquids remaining as two layers even after several days in a refrigerator. It therefore seems more likely that the reaction is



Spectroscopic Results

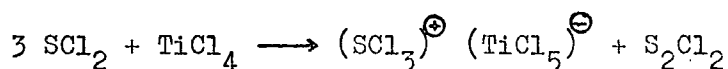
The n.q.r. spectrum reveals that $(\text{SCl}_3)^{\oplus}$ is again present but now three lines of equal intensities are observed, (Table 2). The n.q.r. frequencies observed for ^{35}Cl bonded to titanium in titanium tetrachloride are found to be very low (18) indicating a high degree of ionicity and $p_{\pi} - d_{\pi}$ interaction in the Ti-Cl bonds (5). These frequencies lie below the sensitive range of the Decca spectrometer employed and, since the n.q.r. frequencies of $(\text{TiCl}_5)^{\ominus}$ are likely to be equally low, the failure to observe them is explicable. Sweeps at room temperature and 77K between 3 and 7 MHz with the AEI spectrometer also failed to locate any signals.

In the vibrational spectra, some evidence of $(\text{TiCl}_5)^{\ominus}$ is found but

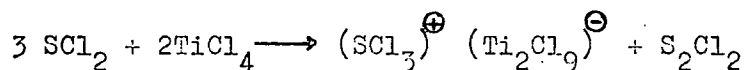
the instability of the compound is manifested by the strong band at 500cm^{-1} of titanium tetrachloride (Table 3). This explains the vapour pressure of titanium tetrachloride and the white fumes which prevented the collection of any sulphur monochloride as a distillate from the reaction mixture.

The observed Raman spectrum contains absorptions due to $(\text{SCl}_3)^{\oplus}$ and also those reported for $(\text{TiCl}_5)^{\ominus}$ including the strongest at 419cm^{-1} (Table 3). A previously unreported Raman active band, ν_2 , is given as 309cm^{-1} but Raman bands for ν_1 and ν_8 cannot be assigned. The presence of weakly complexed titanium tetrachloride is further indicated by a band at 143cm^{-1} .

The counter ion to $(\text{SCl}_3)^{\oplus}$ will be of the type $(\text{TiCl}_5)^{\ominus}$ or $(\text{Ti}_2\text{Cl}_9)^{\ominus}$ since the vapour pressure of titanium tetrachloride indicates that it can be quite readily lost. On this basis the reaction may be represented by one of the equations,



or



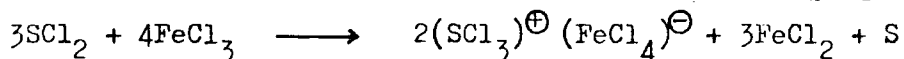
Two samples were therefore prepared in the ratios 3:1 and 3:2 of sulphur dichloride to titanium tetrachloride. After pumping on them for a short time to remove the sulphur monochloride (and some titanium tetrachloride) analysis for titanium, chlorine and sulphur was carried out on each. Details are given in the chapter appendix but the closest fit for both samples was with STiCl_3 . The counter ion is therefore probably $(\text{TiCl}_5)^{\ominus}$.

The Raman spectrum also supports the presence of $(\text{TiCl}_5)^{\ominus}$ (Table 3). However, due to other bands obscuring possible lines at either 280 cm^{-1} or 264 cm^{-1} , the presence of $(\text{TiCl}_5)^{\ominus}$ as the dimeric $(\text{Ti}_2\text{Cl}_{10})^{2\ominus}$ anion cannot be ruled out (19). The complex is therefore believed to be $(\text{SCl}_3)^{\oplus} (\text{TiCl}_5)^{\ominus}$ or $(\text{SCl}_3)^{\oplus}_2 (\text{Ti}_2\text{Cl}_{10})^{2\ominus}$.

5) $(\text{SCl}_3)^{\oplus} (\text{ICl}_4)^{\ominus}$

A sample characterised as $(\text{SCl}_3)^{\oplus} (\text{ICl}_4)^{\ominus}$ was investigated by ^{35}Cl n.q.r. spectroscopy. Prepared by the method of Jaillard (20) it was supplied by Dr. T.H. Page of Royal Holloway College and was believed to be Form I of this compound (34). The presence of $(\text{SCl}_3)^{\oplus}$ is shown by the three lines about 42 MHz (Table 3) which have equal intensities. The counter ion $(\text{ICl}_4)^{\ominus}$ is responsible for the three lines at 28.123, 25.895 and 20.95 MHz which account for three of the chlorine atoms. The difficulty in observing a line due to the fourth chlorine atom of $(\text{ICl}_4)^{\ominus}$ may be because it has a bridging position between the anion and $(\text{SCl}_3)^{\oplus}$. This aspect is discussed later. The Raman spectrum of this compound is reported in Table 3 (31).

A complex between sulphur dichloride and ferric chloride ($\text{SCl}_2 \cdot \text{FeCl}_3$) was reported by Nabi and Khaleque (9). The author did not prepare this himself but assumes it to be $(\text{SCl}_3)^{\oplus} (\text{FeCl}_4)^{\ominus}$. The reported 1:1 complex is likely to be the product from a redox reaction analogous to that involving antimony pentachloride, i.e.



When compared to the 1:1 reaction proposed by Nabi and Khaleque, the 3:4 molar ratio may explain why the analysis figures reported by Nabi are high for iron and low for chlorine and sulphur (9). The heterogeneous nature of the reaction may also obscure the true values.

However, the action of sulphur dichloride with other Lewis acids was investigated. Those used were boron trichloride and tin tetrachloride whose weaker Lewis acidities are clearly demonstrated by the results, reported below.

6) Sulphur Dichloride and Boron Trichloride

Preparation

Commercial boron trichloride was distilled on to distilled sulphur dichloride in a silica ampoule on a vacuum line. The ampoule was then sealed. No reaction appeared to occur at room temperature nor even when held at low temperatures for long periods.

Spectroscopic Results

After slow cooling, with shaking, to liquid nitrogen temperature,

the ^{35}Cl n.q.r. spectrum of the sample was investigated. No evidence of $(\text{SCl}_3)^{\oplus}$, nor of sulphur dichloride was found in the spectrum but very strong resonance occurred at 21.515 and 21.48 MHz. These resonances are assigned to boron trichloride. The n.q.r. frequencies of pure boron trichloride are 21.582 and 21.578 MHz (21) and it is therefore clear that reaction has not taken place and that the shift in n.q.r. frequency is probably due to an impurity effect. Boron trichloride is a weaker Lewis acid than the previous three used. It is probably that the disproportion of sulphur dichloride is not sufficiently aided by boron trichloride to promote reaction.

7) Sulphur Dichloride and Tin Tetrachloride

Preparation

Distilled tin tetrachloride was slowly added to sulphur dichloride in a cooled flask under nitrogen. No reaction was observed at 10°C but, on standing in a refrigerator for several days, a few pale, cubic crystals were deposited. These were filtered cold under vacuum and were then sealed under vacuum in a vial, also kept cold. The ^{35}Cl n.q.r. spectrum was taken at 77K.

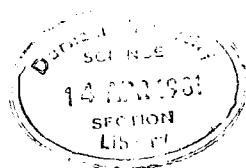
Spectroscopic results

The only resonances to be observed in the n.q.r. spectrum lie at 21.39 and 21.84 MHz (Table 2). This strongly suggests that reaction of the tin tetrachloride has occurred because its very strong resonances centred on 24.09 MHz were not present (22). Although resonances due to $(\text{SCl}_3)^{\oplus}$ were not observed, its presence may be inferred. The likely counter ion is $(\text{SnCl}_5)^{\ominus}$, the n.q.r. resonances of which have been observed previously in $(\text{PCl}_4)^{\oplus} (\text{SnCl}_5)^{\ominus}$ at 22.04, 22.08 and 20.32 MHz. The lowest

frequency resonance was observed by Lynch (23) to be weaker than the others and could be due to an axial site in the ion. This would explain why only two resonances were found here, the lowest frequency line being too weak for observation (Table 2). The greater separation of these resonances may well be due to internal non-bonding interactions. The wide ranges of the frequencies observed for $(\text{AlCl}_4)^{\ominus}$ and $(\text{SbCl}_6)^{\ominus}$ lend support to this.

An attempt to fully characterise this crystalline product failed because in warming to room temperature, the crystals decompose. A small sample decomposed during mulling for infra-red investigation but the bulk was lost during a room temperature n.q.r. spectrum run. Further attempts to prepare these crystals failed with tin tetrachloride and sulphur dichloride showing no signs of reaction and, even on scratching, no sign of crystal deposition.

An ampoule containing a 3:1 molar mixture of sulphur dichloride and tin tetrachloride was slowly cooled, with shaking, to 77K and its n.q.r. spectrum was taken. The only resonances observed were due to tin tetrachloride (Table 2), with very little shift from those of pure tin tetrachloride (22).



Discussion of ^{35}Cl n.q.r. Results

The presence of $(\text{SCl}_3)^{\oplus}$ in the products of several reactions has been shown by ^{35}Cl n.q.r. and by vibrational spectroscopy. The high n.q.r. frequency observed for $(\text{SCl}_3)^{\oplus}$ reflects the effect of a positive charge on sulphur to increase its electronegativity leading to greater covalency in the S-Cl bonds.

a) Number of n.q.r. lines

The number of resonances and the relative values of their signal-to-noise ratios are often helpful in assigning point symmetries to the resonant species. In the compound with $(\text{TiCl}_5)^{\ominus}$ as anion three resonances of equal intensity are observed near 42 MHz. Assuming one molecule per unit cell this indicates that the three chlorine atoms of $(\text{SCl}_3)^{\oplus}$ are in non-equivalent sites. The same applies to $(\text{SCl}_3)^{\oplus}$ in $(\text{SCl}_3)^{\oplus} (\text{ICl}_4)^{\ominus}$.

There are two resonances due to $(\text{SCl}_3)^{\oplus}$ in $(\text{SCl}_3)^{\oplus} (\text{AlCl}_4)^{\ominus}$ the strengths of which indicate that two sites of chlorine atoms are equivalent but not to the third site. The point symmetry of the ion is thus C_s .

Two, apparently equal, resonances are observed at 77K for the $(\text{SCl}_3)^{\oplus}$ ion in $(\text{SCl}_3)^{\oplus} (\text{SbCl}_6)^{\ominus}$. This intensity pattern is observed for all samples at 77K including that of Hart et al (14). The strongest resonance for $(\text{SCl}_3)^{\oplus}$ is observed for the 1:1 sulphur monochloride and antimony pentachloride complex. This is probably due to the sample being of fortuitously better crystallinity. The two resonances for $(\text{SCl}_3)^{\oplus}$ are insufficient to predict the number of molecules in the unit cell. However, the intensities of the lines due to $(\text{SbCl}_6)^{\ominus}$ suggest a single counter ion in the cell.

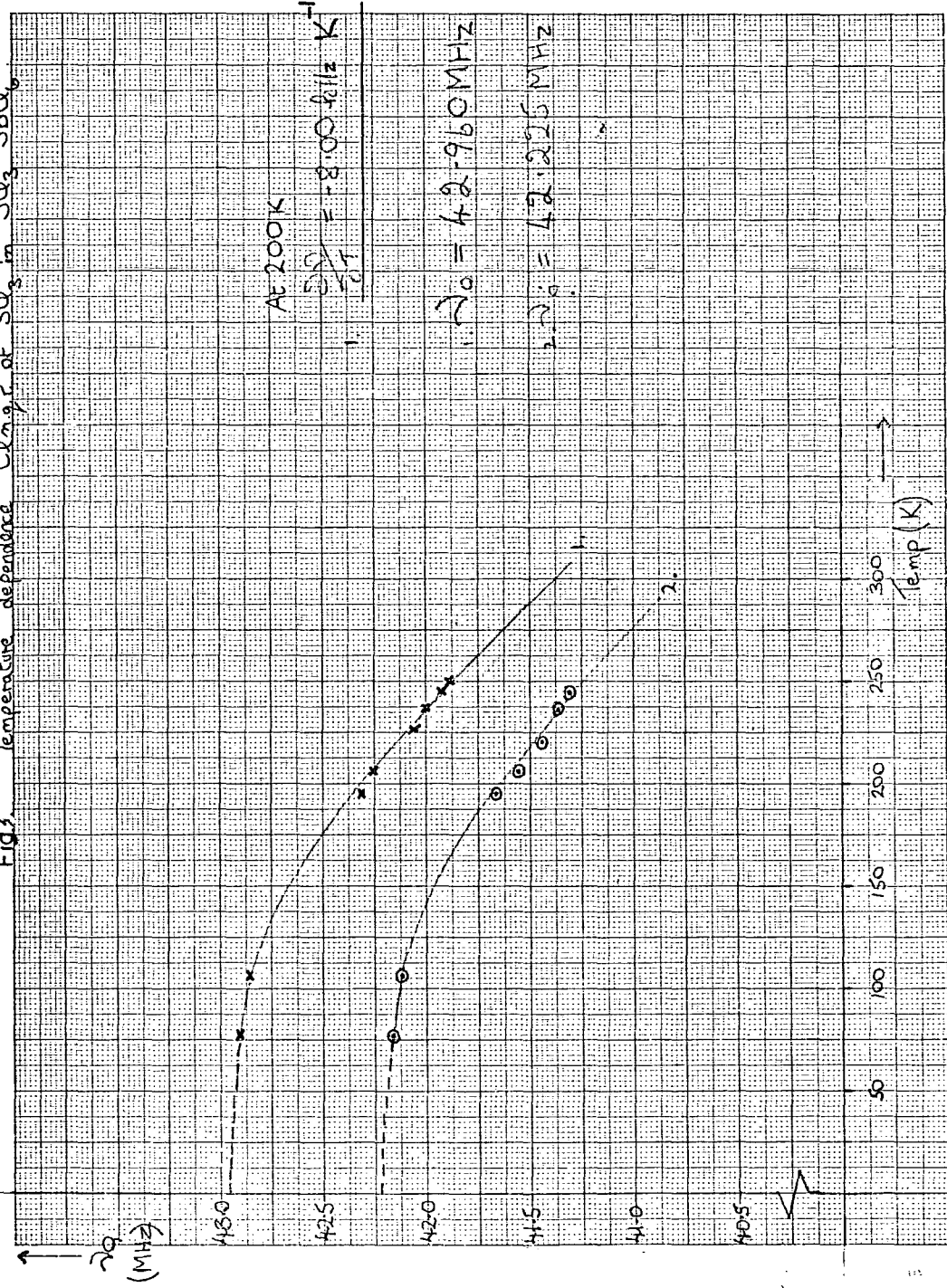
b) Temperature Dependence of n.q.r. Signals

The temperature dependence of both n.q.r. lines of $(\text{SbCl}_3)^{\oplus}$ in $(\text{SbCl}_3)^{\oplus} (\text{SbCl}_6)^{\ominus}$ was observed and is shown in Figure 3. Above 200K the two resonances due to $(\text{SbCl}_3)^{\oplus}$ are still present for the compound but their strengths are now observed to be in the ratio of 2 : 1 with the higher frequency resonance of greater intensity. This probably represents C_s or C_v point symmetry for the $(\text{SbCl}_3)^{\oplus}$ ion and indicates that two chlorine atoms lie in equivalent sites. The observed equal intensity for the resonances at 77K is accidental. A possible cause of the unreliable intensity patterns is that at 77K the relaxation times associated with the two resonances are very different while at 200K they become comparable.

Any phase changes from 77K to 250 K are unlikely because the n.q.r. frequency versus temperature plots would then show discontinuities. Resonances were not observable at temperatures above 250K probably due to fast relaxation by, say, a rotational mode broadening the line beyond detection. Both resonances exhibit the same temperature gradient so it is likely that the three chlorine atoms experience the same potential barrier to torsional motion. An average temperature gradient of $-8.00 \text{ kHz deg}^{-1}$ is found for the upper frequency resonance at 200K, where the variation of frequency with temperature is changing slowly.

Using the formula developed by Bayer and Kushida (1.35) and (1.45) for the temperature dependence of n.q.r. frequency (at constant pressure) and ignoring terms in η , an estimate of the librational frequencies causing this dependence can be made. With an estimated S-Cl bond length of 0.199 n.m. and a value of 98° for

Fig 3. Temperature dependence ^{25}Cl center of SO_3 in $\text{SO}_3 \cdot \text{SbCl}_6$

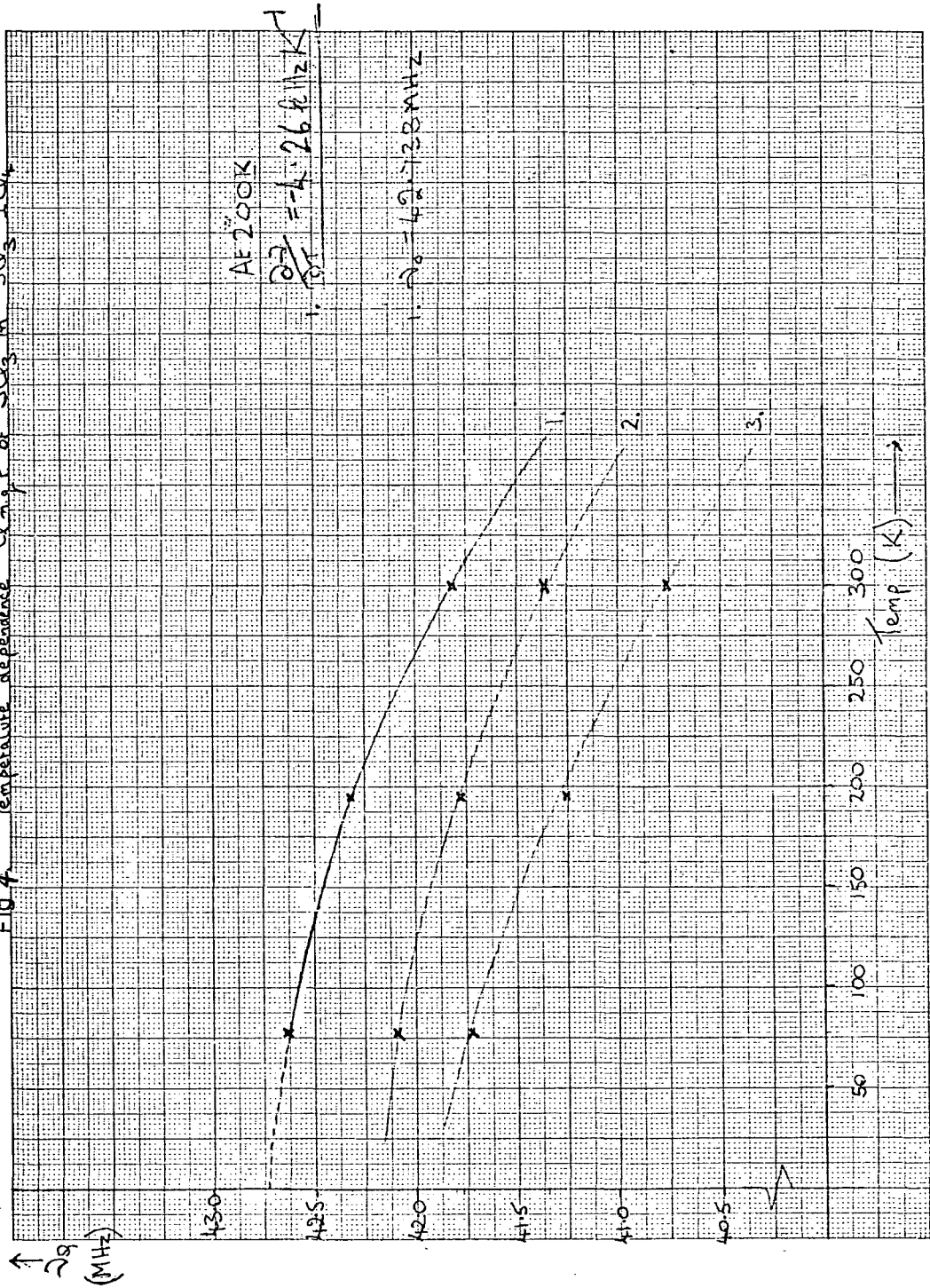


$\text{Cl } \hat{S} \text{ Cl}$, the frequency corresponding to libration about the C_3 axis is 15.2 cm^{-1} . Libration about axes perpendicular to C_{3v} corresponds to a frequency of 42.2 cm^{-1} if doubly degenerate. If all three motions (and moments of inertia) contribute, a librational mode of 44.8 cm^{-1} is calculated. However, no frequencies as low as this were observed in the Raman spectrum.

In the case of $(\text{SCl}_3)^{\oplus}$ in $(\text{SCl}_3)^{\oplus} (\text{ICl}_4)^{\ominus}$ the temperature dependence of the three quadrupole resonances was investigated and is shown in Figure 4. For the highest frequency line an average frequency/temperature gradient of $-4.30 \text{ kHz deg}^{-1}$ is observed at 200K where the gradient is changing slowly. It is therefore seen to have a gradient approximately half that of the corresponding resonance for $(\text{SCl}_3)^{\oplus}$ in $(\text{SCl}_3)^{\oplus} (\text{SbCl}_6)^{\ominus}$. This is interpreted below as evidence that association of $(\text{SCl}_3)^{\oplus}$ with $(\text{ICl}_4)^{\ominus}$ occurs. Using the same parameters as in the case of $(\text{SCl}_3)^{\oplus} (\text{SbCl}_6)^{\ominus}$ corresponding librational frequencies of 20.8 cm^{-1} (C_{3v} axis), 57.7 cm^{-1} (doubly degenerate, perpendicular to C_{3v}) and 61.3 cm^{-1} (three motions) are calculated.

These were not reported by Finch et al (31) but lattice modes in the region of $25\text{-}80 \text{ cm}^{-1}$ can be seen in the Raman spectrum illustrated in their paper.

FIG A Temperature dependence ^{35}Cl m.p.r. of SO_2 in $50\% \text{ICl}_4$



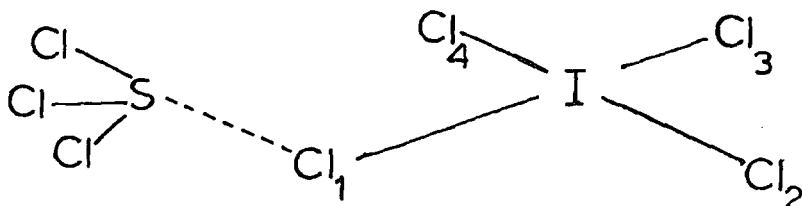
Structure of $\oplus\text{SCl}_3$ complexes.

Information on the internal structure of the $(\text{SCl}_3)^\oplus$ complexes investigated may be obtained by comparison with related group VI species and from interpretation of the n.q.r. and vibrational spectroscopy data. The variation in average frequencies and in the number of ^{35}Cl quadrupole resonances observed for $(\text{SCl}_3)^\oplus$ in the pairs $\oplus\text{SCl}_3\text{Sb}^\ominus\text{Cl}_6$, $\oplus\text{SCl}_3\text{TiCl}_5$, $\oplus\text{SCl}_3\text{ICl}_4$ indicate that differences in structure are possible.

It is proposed that in the first pair the higher ^{35}Cl n.q.r. frequencies due to $\oplus\text{SCl}_3$ and their large temperature dependence (in the hexachloroantimonate compound) indicate that the $\oplus\text{SCl}_3$ ion is not associated with the anion, whereas, in the case of the second pair, the lower average ^{35}Cl n.q.r. frequencies and lower temperature dependence (in the tetrachloroiodate compound) suggest that some form of interaction through the chlorine atoms of the anion may be occurring. For the first pair of compounds, there are two ^{35}Cl n.q.r. lines (at 77K) attributable to the trichlorosulphonium ion but there are three (at 77K) for the other pair. The difference appears significant when the n.q.r. frequencies for the anions are also considered.

The n.q.r. results for the hexachloroantimonate and tetrachloroaluminate ions are typical for these anions, indicating that strong interaction with the $\oplus\text{SCl}_3$ cation is unlikely. However, the response for the tetrachloroiodate ion differs from the singlet observed for the alkali metal tetrachloroiodates (e.g. KICl_4 , 22.37 MHz (38)). The structure of the multiplet can account for three of the four chlorine

atoms. An interpretation in terms of strong intermolecular interaction may be made thus:



If strong enough, the polarisation interaction would reduce the n.q.r. frequency of chlorine (1) well below that of the others. This, coupled with the lower detection performance of the spectrometer for bridging chlorine, would explain why only three chlorine atoms are accounted for in the reported n.q.r. spectrum. A fourth line at 14.85 MHz (77K) has since been reported and confirms this prediction (37).

The trichlorosulphonium ion acts as a strongly polarising cation but appears to have a more pronounced effect upon the tetrachloroiodate anion than upon itself. It seems likely that any charge transferred from $\text{Cl}_{(1)}$ of the tetrachloroiodate would enter the trichlorosulphonium ion through the lone pair on sulphur. If it remained on the sulphur, the increased charge might cause a closing together of the SCl_3 pyramid. It might however be distributed to the chlorine atoms. Either their increased ionicity or an extension of the S-Cl bond may explain the slight reduction in the ^{35}Cl n.q.r. frequency compared with those of the trichlorosulphonium ion in $(\text{SCl}_3)^{\oplus} (\text{SbCl}_6)^{\ominus}$; i.e. avg. 42.151 MHz versus 42.530 MHz.

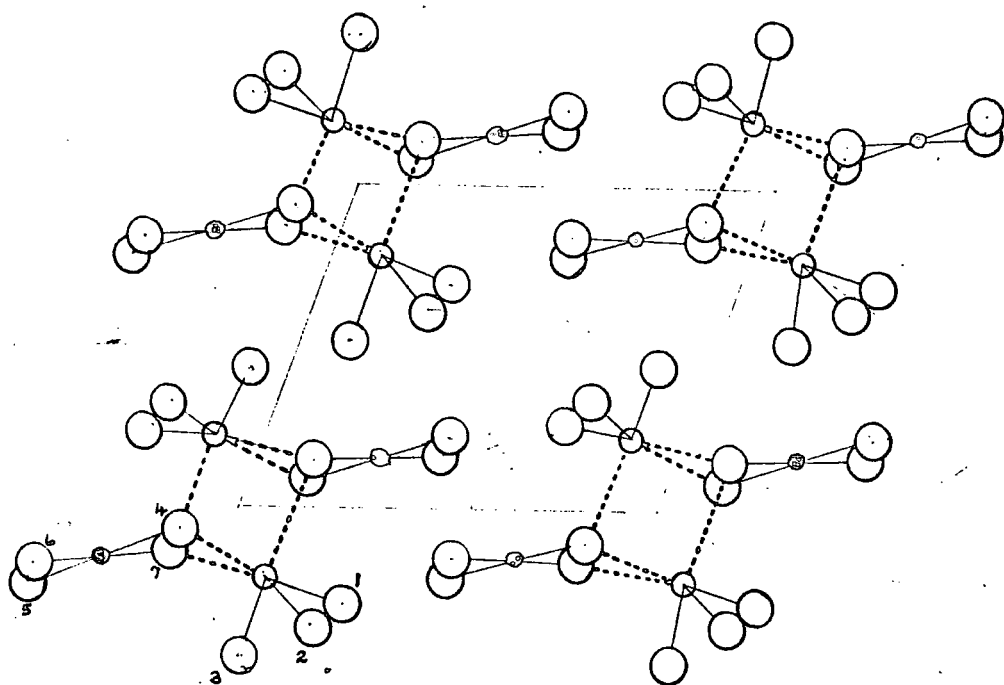
The tetrachloroiodate and tetrachloroaurate ions have been the subject of vibrational spectroscopic investigation into intermolecular interaction. The results point to the influence that smaller, polarising cations may exert on these large, square-planar anions(31). For the undistorted anion of D_{4h} symmetry,

three vibrational modes are Raman active but if the symmetry is greatly reduced (C_8 or C_1) nine deformation and stretching modes may be possible. For both $\text{SCl}_3^{\oplus}\text{AuCl}_4^{\ominus}$ and $\text{SCl}_3^{\oplus}\text{ICl}_4^{\ominus}$ the multiplicity of lines in the Raman spectra has led Finch to conclude that a reduction in the symmetry of the anions has occurred. Fokina (33) has suggested that bridging between SCl_3^{\oplus} and AuCl_4^{\ominus} occurs in trichlorosulphonium tetrachloroaurate.

A.J. Edwards (34) has determined the structure of $\text{SCl}_3^{\oplus}\text{ICl}_4^{\ominus}$ in the stable form used in this n.q.r. study. Bridging between the trichlorosulphonium and the tetraiodate ions appears to occur.

There are three non-bonding contacts to the sulphur atom by chlorine atoms of the $(\text{ICl}_4)^{\ominus}$ anions. The bond lengths of the distorted anion may be correlated with the number of bridging interactions experienced by the chlorine atom. Thus the longest I-Cl bond involves Cl₍₄₎ which makes two contacts of 0.3096 n.m. and 0.3118 n.m. to two different sulphur atoms. The intermediate I-Cl distance involves Cl₍₇₎ which makes one contact to sulphur of 0.3130 n.m. The shortest bonds of the anion involve chlorine atoms (5) and (6) which make no contacts with sulphur. The reported S-Cl bond lengths of the trichloro-sulphonium ion average 0.199 n.m. There are four "molecules" in the unit cell and the reported structure of form I of $(\text{SCl}_3)^{\oplus}(\text{ICl}_4)^{\ominus}$ is given in Fig. 5. The distortion of the tetrachloroiodate ion is very similar to that found in the structure of $\text{KICl}_4 \cdot \text{H}_2\text{O}$ in which interionic interaction was proposed (39). The close similarity of the n.q.r. spectra of the compounds supports this comparison (40).

There is a gradual reduction in the S-Cl stretching frequencies observed in the Raman spectrum of the compounds containing SCl_3^{\oplus} (Table 3). The lowest frequencies are those reported for $\text{SCl}_3^{\oplus}\text{ICl}_4^{\ominus}$ which approach those of SCl_4 (41). Because the structure of solid



- — iodine
- — sulphur
- — chlorine

----- polarisation interaction

Fig. 5. $\text{SCl}_3^+ \text{ICl}_4^-$
(after ref. (34))

SCl_4 employs bridging chlorines, this has been proposed as further evidence of significant interionic interaction (42). The variation of stretching frequencies may be a measure of the strengths of interaction between SCl_3^{\oplus} and the anion in the sequence of compounds reported in this thesis.

The two forms of $\text{SCl}_3^{\oplus} \text{ICl}_4^{\ominus}$ - I (stable) and II (metastable) - have been the subject of a study by vibrational and n.q.r. spectroscopy (42). Of special interest is the positive temperature coefficient reported for the lowest ^{35}Cl n.q.r. frequency of tetrachloriodate in form I. This is compatible with strong secondary covalent bonding interactions between the sulphur and one of the chlorines of ICl_4^{\ominus} . Such bonding appears to be much weaker in form II which displays a narrower range of n.q.r. frequencies for the anion (25.25 - 20.07 MHz at 77K), the lowest of which does not show an anomalous positive temperature coefficient.

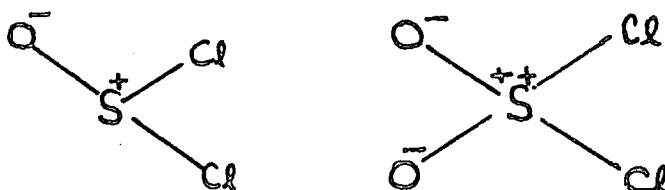
Finally, the ready loss of titanium tetrachloride from $(\text{SCl}_3^{\oplus} \text{TiCl}_5^{\ominus})$ when pumped upon, may be taken as further evidence for bridging interactions resulting in the extraction of a chloride ion from the titanium - chloride anion.

Other compounds containing the S-Cl bond were investigated using n.q.r. spectroscopy. The asymmetry parameter of thionyl chloride was determined.

Thionyl chloride.

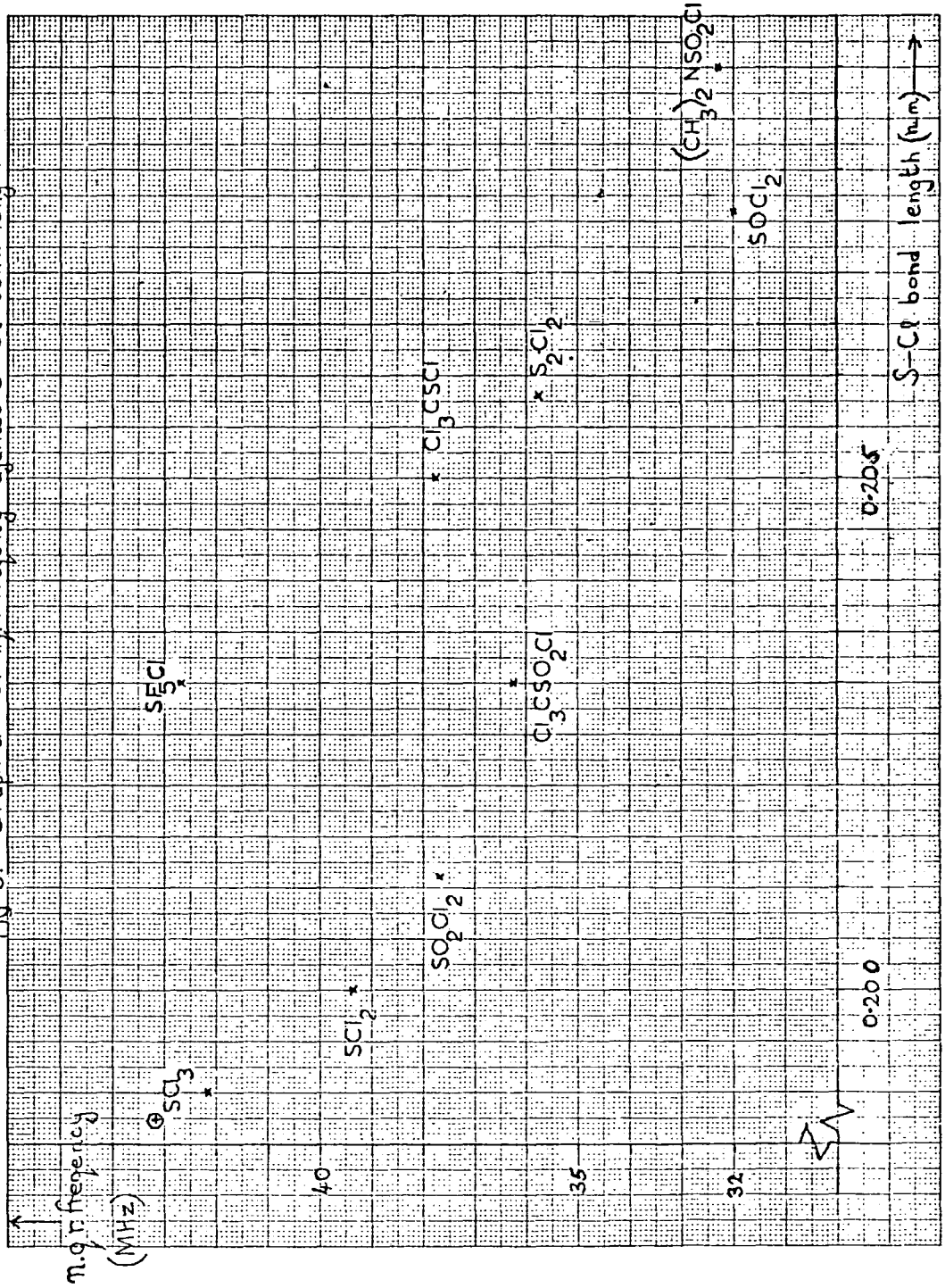
Figure 6 is a plot of ^{35}Cl n.q.r. frequency against S-Cl bond length for several compounds containing the S-Cl bond. The spread illustrates the varying influence of electronegativity and hybridisation at the sulphur atom. These, combined with bond length, help determine the electric field gradient (e.f.g.) and hence the quadrupole resonance frequency of the attached chlorine atom. The average n.q.r. frequency of chlorine in sulphur monochloride is as expected from the electronegativity of the sulphur (5). From this it appears that the n.q.r. frequency of thionyl chloride is unusually low.

Lucken (5) suggests that the large difference in ^{35}Cl n.q.r. frequencies between thionyl chloride (average 31.986 MHz) and sulphuryl chloride (average 37.704 MHz) is caused by the contributions of these canonical forms to their molecular structure.



The double positive charge on the sulphur atom of sulphuryl chloride would enhance the electronegativity of the sulphur

Fig 6. Graph of ^{35}Cl n.r. frequency against S-Cl bond length



atom and hence raise the average n.q.r. frequency of the chlorine atoms. Lucken also makes the suggestion that the raised electronegativity of the sulphur atom in thionyl and sulphuryl chlorides gives rise to extensive π back-bonding of the chlorine atoms to the sulphur.

The result of π back-bonding by a chlorine atom is to lower its n.q.r. frequency. In thionyl chloride only one oxygen atom competes with the chlorine atoms for π -bonding. This may suggest that π -bonding in thionyl chloride is greater than in sulphuryl chloride, which may help explain the lower n.q.r. frequency of the former. In support of this further ^{35}Cl n.q.r. data may be used. Compare the differences in n.q.r. frequency of the two substituted oxychlorides, when one of the chlorine atoms is replaced by an ethyl group. i.e.

SOCl_2 avg. 31.986MHz. SO_2Cl_2 avg. 37.703MHz.

EtSOCl 29.477MHz. EtSO_2Cl 32.519MHz.

$\Delta = 2.509\text{MHz.}$ $\Delta = 5.184\text{MHz.}$

The n.q.r. frequencies were reported by Whitehead and Hart (1). The marked fall in n.q.r. frequency experienced by sulphuryl chloride reflects the lower electronegativity of the ethyl group. The smaller reduction in frequency for thionyl chloride may support the presence of π -bonding in the S-Cl bond. The substitution of a chlorine atom by an ethyl group will cause S-Cl π -bonding to be reduced which may then partially compensate for the fall in frequency caused by the lower electronegativity of the ethyl group. Similarly a comparison of the differences in n.q.r. frequency

upon replacement of the sulphur atom by a selenium atom may be made. Sulphuryl chlorides have already been shown to transmit σ -induction effects primarily. Thus compare the differences:

PhSCl	37.01 MHz. (2)	SOCl ₂	31.99 (avg) (1)
		. and	
PhSeCl	30.36 (avg) (26)	SeOCl ₂	30.41 (avg) (26)

Saatszaov et al. has shown that in the series R₁R₂R₃SeCl (where R = Cl, Me and Ph) the selenium atom transmits primarily σ -inductive effects (26). The n.q.r. frequency for thionyl chloride can therefore be seen as lower than expected. This again suggests the presence of significant π -bonding.

This presence of π -bonding in thionyl chloride due to back-donation from the chlorine atoms to the sulphur results in the electric field gradient (e.f.g.) at the chlorine atoms being substantially axially asymmetric about the S-Cl bond. This asymmetry would be reflected in a non-zero asymmetry parameter (η) for the resonances. With Zeeman n.q.r. spectroscopy the asymmetry parameter was measured for thionyl chloride at 77K.

Extrapolation of the graph in Fig. 7, obtained by the method of Morino and Toyama (30), yields a value for η of 0.27. The two resonances of thionyl chloride yield similar values as would be expected if their separation in frequency were due to external crystalline effects only. More points are displayed in Fig. 7 for the line at 32.091 MHz because this one was examined in full, whereas only comparison data were recorded for the line at 31.687 MHz.

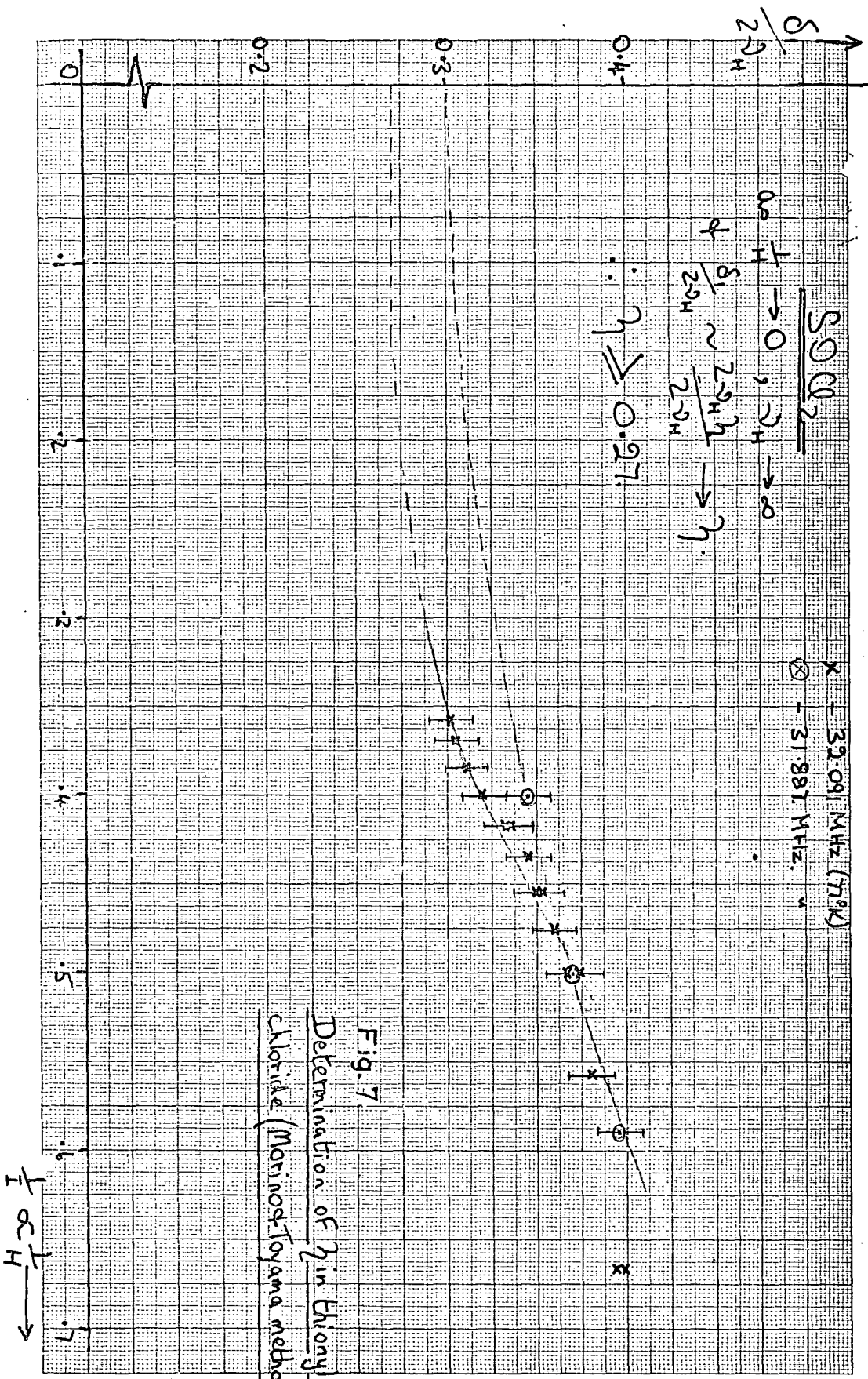


Fig. 7
 Determination of γ in Chloride
 Chloride (Morino-Toyama method)

In Figures 8, 9 and 10 respectively the line shapes of the 32.091 MHz resonance are given for magnetic fields generated by zero, 2.2 amp and 2.6 amps. The measurements of δ_s are indicated on each figure. The value of η cannot be directly related to π -character in the S-Cl bond. However its magnitude is strongly suggestive of substantial π -bonding.

The temperature dependence of the two resonances of thionyl chloride is reported in Figure 11. The quite high negative value of the temperature gradient, -6.3 kHz K^{-1} , provides no further evidence for π -bonding, however.

The proposal that π -bonding in the S-Cl bonds is much reduced in sulphuryl chloride (5) would be much enhanced if a measurement of the asymmetry parameter yielded a much lower value than 0.27. However, due to the low signal strength of the observed resonances of even large samples of distilled sulphuryl chloride this determination was prevented.

In an attempt to obtain comparable data, the preparation of common derivatives of thionyl and sulphuryl chlorides was attempted. Ketimino derivatives were prepared thus:

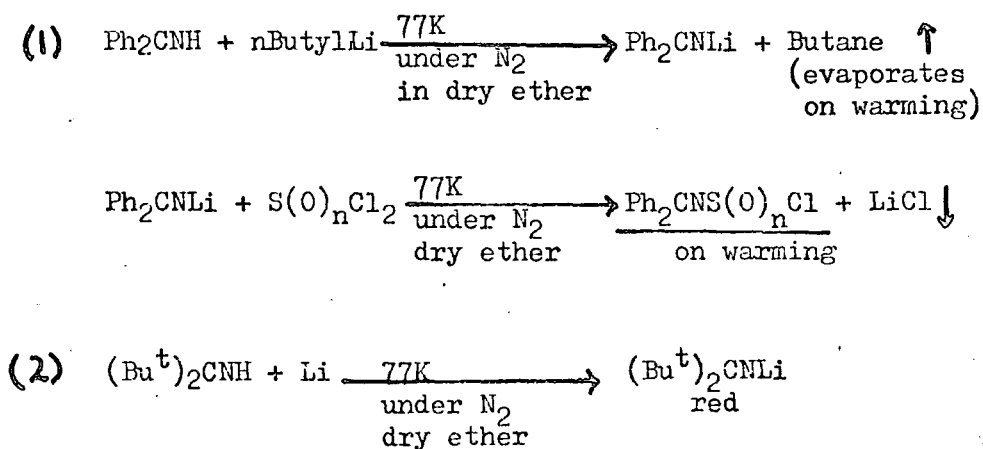


Fig 8 ^{35}Cl Zeeman nmr: SOCl_2 at 77K on Decca spectrometer

$I = 0$ amp.

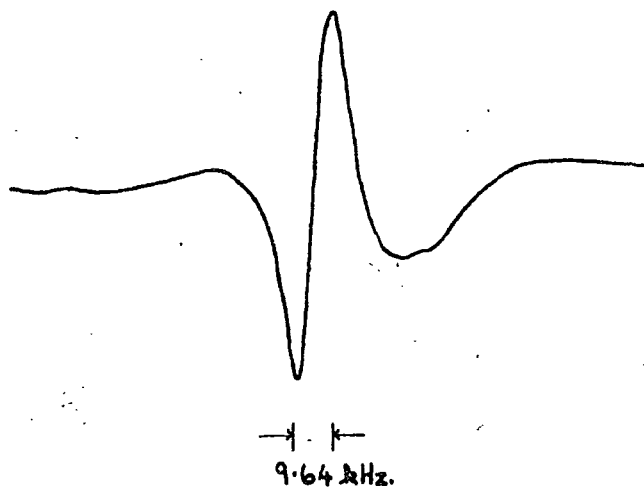


Fig. 9.

$I = 2.2$ amp. $\equiv 6.82$ mT.

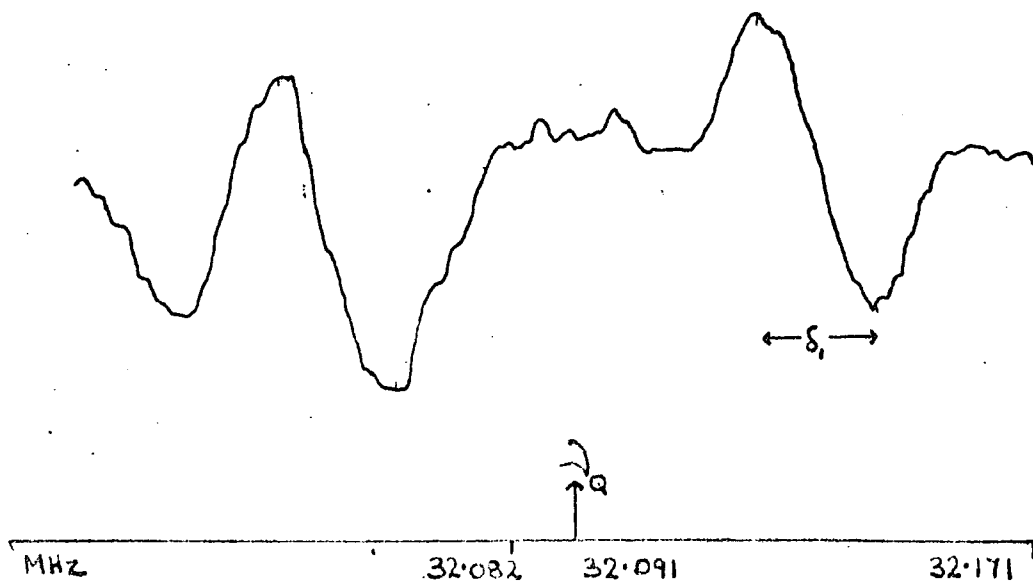
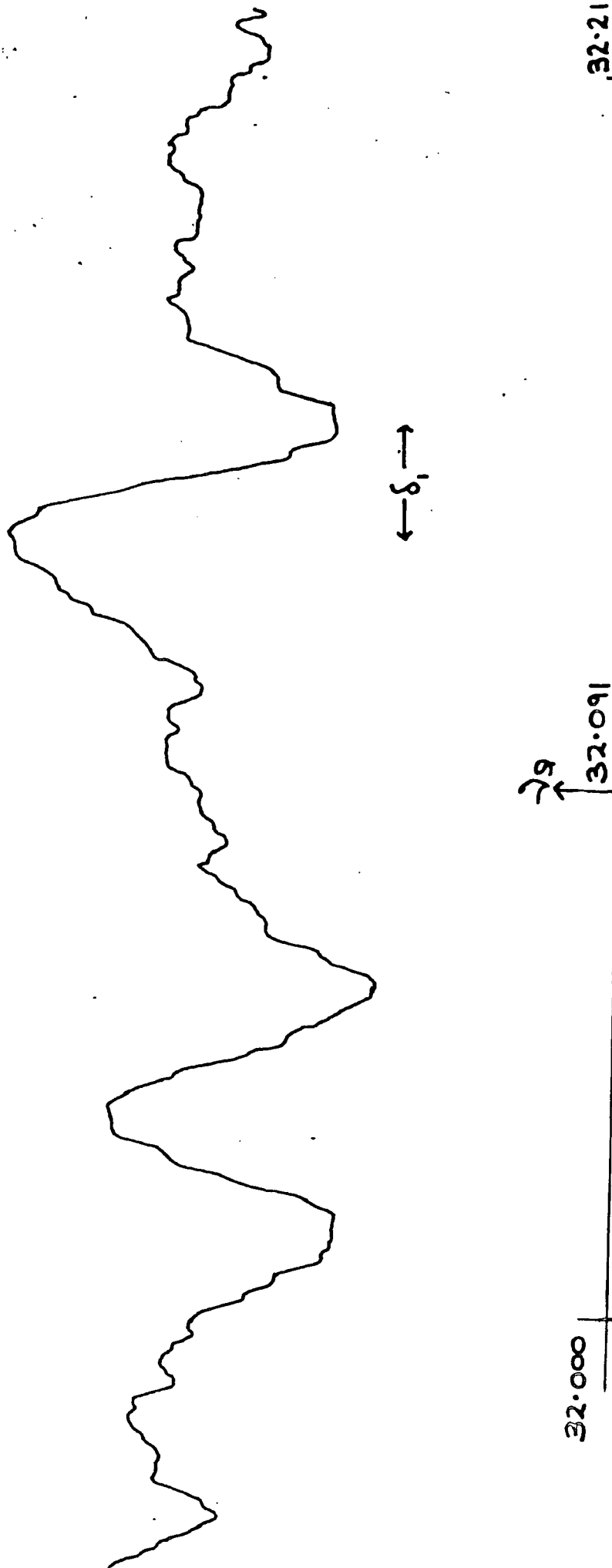


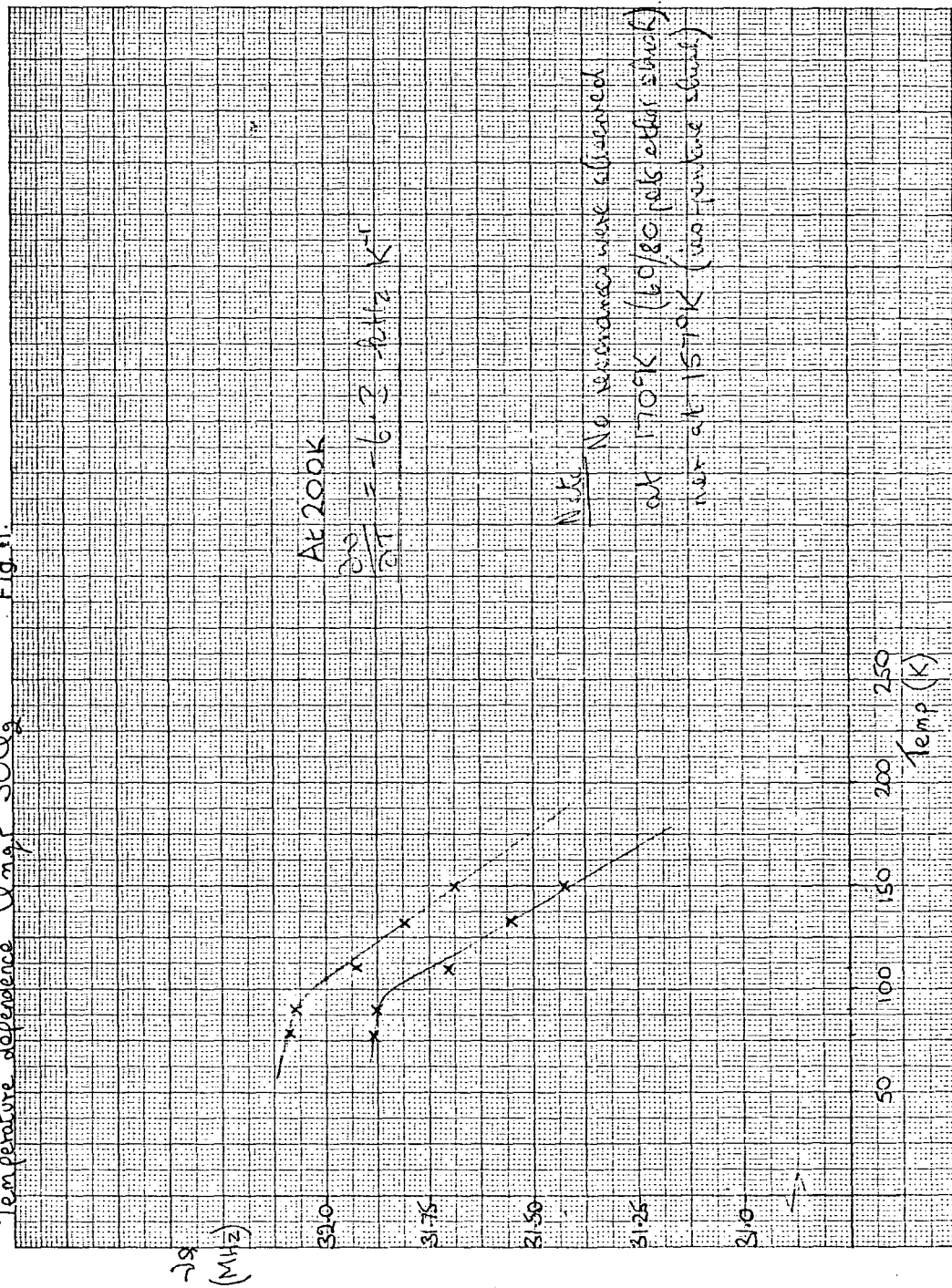
Fig. 10. Zeeman nqr. SOCl_2

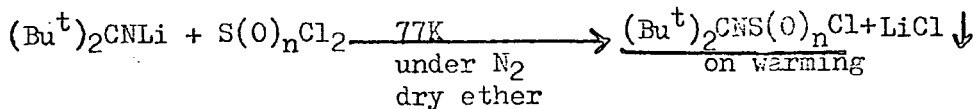
$I = 2.6 \text{ amp.} \cong 8.06 \text{ mT.}$



Temperature dependence of ν_{max} SOCl₂

Fig. 11.





$n = 1, 2.$

Of the four derivatives prepared only one, $(\text{Bu}^t)_2\text{CNSOCl}$ yielded a ^{35}Cl quadrupole resonance. Details of the n.q.r. data, infra red spectrum and analytical data are given in Table 4.

Di-t-butyl ketimino thionyl chloride

The infra-red data is compared with that of thionyl chloride and indicates the presence of a monomeric unit of di-t-butyl ketimine thionyl chloride in the solid. A probable cause for the failure to observe any ^{35}Cl quadrupole resonances for the diphenyl ketimino derivatives is that the compounds exist in dimeric units, bridged through the nitrogen atom of the ketimino group. This may cause dislocation in the lattice and broaden the n.q.r. resonances making detection by the spectrometer more difficult.

It is strongly suggested by studies of infra-red data and from bond length measurements that the ketimino group takes part in π -bonding interactions with the atom to which it is bonded. This could be an explanation of the small rise in n.q.r. frequency from that of thionyl chloride. If the ketimino group has a similar electronegativity to chlorine, it will not greatly effect the electronegativity of the sulphur atom. The cause of the rise in n.q.r. frequency may then be the preference of sulphur to π -bond through the

TABLE 4

Characterisation of Di-t-butyl-ketimino thionyl chloride $(\text{Bu}^t)_2\text{CNS}(\text{O})\text{Cl}$

2

1) n.q.r. data at 77K:

34.012 MHz	$S/N = \frac{6}{1}$
33.840	"
33.703	"

Variance on n.q.r. frequencies is 5kHz.

No signals were observed at room temperature.

2) Infra-red data:

Comparison is made with thionyl chloride.

$(\text{Bu}^t)_2\text{CNS}(\text{O})\text{Cl}$ cm^{-1}	$\text{SOCl}_2(50)$ cm^{-1}	$(\text{Bu}^t)_2\text{CNS}(\text{O})\text{Cl}$ cm^{-1}	SOCl_2 cm^{-1}
2975		872	
2200		778, 740(sh)	
1590		590	
1481		534	
1360		503	490
1227	1229	483	443
1160		408	
1053			344
973, 938(sh)			284
			194

3) Analysis:

	<u>observed</u>	<u>calculated for $\text{C}_9\text{H}_{18}\text{NSOCl}$</u>
%S	13.25	14.32
%Cl	15.40	15.88
%C	46.69	48.32
%N	5.25	6.26
%H	7.62	8.05

3d orbitals to the ketimino group instead of to the chlorine. This would then diminish the π -bonding by the chlorine atom to the sulphur and hence cause the chlorine n.q.r. frequency to rise.

The nitrogen atom of the ketimine group is of approximately sp^2 hybridisation and the bond between the sulphur and nitrogen atoms is therefore inclined at an angle of about 120° to that between the nitrogen and the carbon atom of the ketimino group. This may much reduce the degree of π -interaction transmitted from nitrogen to sulphur. The electronegativity of the ketimino group, if greater than that of chlorine, could then explain the increased n.q.r. frequency. There is insufficient data available to promote only one explanation.

Attempts to prepare N-amine derivatives of both thionyl chloride and sulphuryl chloride were unsuccessful. Piperidine gave a solid derivative with sulphuryl chloride but with thionyl chloride charring occurred. The flakes of the sulphuryl chloride derivative yielded no ^{35}Cl quadrupole resonance. Although it is reported that both oxychlorides form strong complexes with trimethylamine (27), the details of preparation are not given, and no satisfactory derivatives were obtained by the author.

Pentafluoro sulphur VI chloride.

Finally, the n.q.r. frequency at 77K is reported for pentafluoro sulphur VI chloride (Table 5). It is seen to be close to that expected from the coupling constant obtained by Kewley (28) using microwave spectroscopy. In Table 5, the n.q.r. data are compared with those estimated for pentafluoro sulphur VI bromide

obtained by Neuvar (29) for the gaseous compound. The bond between sulphur and the bromine atom is seen to have a polarity $S^{\delta-}-Br^{\delta+}$ (0.03 e^- charges) and from this an estimate of the electronegativity of the SF_5^- group is made.

The presence of π -bonding in the S-Cl bond of SF_5Cl was predicted by Hart and Whitehead (1), who expected it to cause a lowering of the n.q.r. frequency. These authors used an estimated n.q.r. frequency of 40 MHz which has now been shown to be too low. The observed ^{35}Cl resonance frequency (42.68 MHz) is comparable to that observed for $^{35}Cl_3$ (42-43 MHz) which represents the maximum of the generally narrow range found for S-Cl bonds. The high electronegativities of $(S^{VI})F_5$ and $(S^{IV})^{\oplus}$ probably account for the frequencies. In the apparent absence of a lowering of n.q.r. frequency, it seems unlikely that π -bonding plays a significant part in the S-Cl bonds.

Appendix to Chapter 4

For all the preparations sulphur dichloride was distilled from over phosphorus pentachloride which stabilises it against disproportionation. The reactions were carried out in dry conditions either in a nitrogen filled flask or in a dry glove box. Addition of reagents was made against a counter flow of nitrogen. The components were agitated and left for several hours to complete reaction. Any volatiles were pumped off before the products were transferred to glass ampoules in a glove box. The ampoules were then sealed.

1) SCL_2 and SbCl_5

To 2ml. sulphur dichloride was slowly added 4.1ml general reagent antimony pentachloride. Although the flask was cooled in a bath of water, vigorous reaction occurred immediately with the production, by an exothermic reaction, of a dark yellow solid. There appeared to be no volatiles produced.

Analysis

	observed	calc ^d . for SSbCl_7	Calc ^d . for SSbCl_7	(%)
% Cl	61.30	61.02	67.03	60.2
% S	7.91	7.90	5.72	7.0

Product is a mixture containing $(\text{SCL}_2)^{\oplus}$ $(\text{SbCl}_5)^{\ominus}$.

2) S_2Cl_2 and SbCl_5

1:1 and 1:2 molar proportions of sulphur monochloride and antimony pentachloride were mixed in flasks under dry nitrogen. In exothermic reactions a yellow solid was produced. There appeared

Table 5

PentaFluoro sulphur VI chloride.

1) ^{35}Cl n.q.r. frequency :

measured at 77K, = 42.680 MHz S/N = 5/1 (this thesis)

By molecular symmetry, $\eta = 0$, $\therefore |e^2_{qQ}| = 85.36 \text{ MHz}$

2) e^2_{qQ} from microwave :

$$\text{gaseous } \text{SF}_5^{35}\text{Cl}, e^2_{qQ} = -81.5 \pm 5 \text{ MHz} \quad (28)$$

$$\text{gaseous } \text{SF}_5^{79}\text{Br}, e^2_{qQ} = 800 \pm 5 \text{ MHz} \quad (29)$$

$$\text{and } ^{79}\text{Br}, e^2_{qQ} = -769.756$$

Hence, the $\text{F}_5\text{S} - \text{Br}$ bond is polarised $\text{SF}_5 \overset{\delta-}{\text{---}} \overset{\delta+}{\text{Br}}$.

$$3) \quad \frac{e^2_{qQ}}{e^2_{q_0Q}} = - (1 + i + 2ie) \quad (\text{Chap. 2, equation 41})$$

and for Br, $e = 0.13$

Thus, for SF_5Br , ionicity, $i = -0.03$

i.e. δ -bond population in S-Br bond = 0.97

4) For the electronegativity of $\overset{\delta+}{\text{SF}_5}$, χ_{SF_5}

$$= \frac{1}{2} (\chi_{\text{SF}_5} - \chi_{\text{Br}}) \quad (\text{Chap. 2, equation 48})$$

from which $\chi_{\text{SF}_5} = 2.86$

to be no volatiles upon pumping. The product of the 1:2 reaction was analysed.

Analysis

	observed	calc ^d for $S_2Sb_2Cl_{12}$	Calc ^d for $S SbCl_9$
% Cl	57.46	57.83	67.03
% S	8.50	8.71	6.72

If the reaction had proceeded by any mechanism other than 1:2 an excess of one reactant would have been pumped off. The observed chlorine and sulphur analyses would then have differed substantially from those calculated for $S_2Sb_2Cl_{12}$.

3) SCl_2 and $AlCl_3$

Aluminium chloride was purified by sublimation at $110^{\circ}C$ under about 0.02mmHg pressure. The aluminium chloride was powdered in a nitrogen-filled dry box and placed in a weighed flask equipped with two tap sockets. Sulphur dichloride was introduced with a syringe against a counter current of dry nitrogen. Sufficient sulphur dichloride for a 1:1 molar mixture was added whilst the aluminium chloride was continuously agitated. As before the flask was cooled in water as the reaction was significantly exothermic. A moist yellow solid was produced from which, on pumping, a yellow liquid was distilled.

An analysis of a 3:1 molar mixture of sulphur dichloride and powdered aluminium chloride was made. The results for the powdered product are given on the following page.

	observed	calc ^d for SAlCl_7
%Cl	79.38	80.80
%S	10.24	10.40
%Al	9.3	8.8

The analysis is in close agreement and justifies a formula for the product of $(\text{SCl}_3)^{\oplus}(\text{AlCl}_4)^{\ominus}$.

4) SCl_2 and TiCl_4

Distilled titanium tetrachloride was added slowly to distilled sulphur dichloride in a flask cooled to about 15°C . After a few moments of inactivity the two liquids suddenly, and quite violently, reacted producing a fine bulky bright yellow solid. Like the other solids prepared, the sample was sensitive to moisture but more so, evolving white fumes of titanium dioxide even in a dry box. Although the solid appeared to be dry, it was pumped upon for a few minutes on the vacuum line. It was found that titanium tetrachloride was being removed. It was therefore apparent that the product was less stable than those previously prepared with antimony pentachloride and aluminium chloride.

Two samples in 3:1 and 3:2 ratios of sulphur dichloride to titanium tetrachloride were prepared. The analysis figures are reported below.

Analysis

	Calc ^d for STiCl_8	Calc ^d for $\text{STi}_2\text{Cl}_{12}$	Calc ^d for $\text{S}_2\text{TiCl}_{12}$	observed	
				3:1	3:2
%Cl	78.00	76.88	79.16	77.85	78.23

%S	8.80	5.78	11.91	9.33	9.14
%Ti	13.20	17.34	8.93	12.98	13.37

From the figures it is clear that the closest agreement is with STiCl_8 , i.e. $(\text{SCl}_3)^{\oplus}(\text{TiCl}_5)^{\ominus}$.

The slightly low analysis values for chlorine and titanium in the 3:1 sample can be explained by the loss of some titanium tetrachloride on pumping. This is supported by the slight increase in the sulphur analysis.

Methods of Analysis Used

The Schöniger oxygen flask combustion method was used to bring the samples into solution.

Chloride was detected potentiometrically with silver nitrate.

Sulphur was detected as sulphate with barium perchlorate and sulphanazo 3.

Aluminium and titanium metals were measured by atomic absorption on a Perkin Elmer 403 spectrometer.

ITS COMPLEXES

Introduction

Nuclear quadrupole resonance spectroscopy is a useful tool for structural investigations of metal chlorides forming molecular crystals. There are no published n.q.r. data on zinc chloride although studies on the complex halides of zinc (1,2) illustrate the potential. This chapter reports ^{35}Cl n.q.r. and i.r. data obtained on zinc chloride and several of its ether adducts with a discussion of their likely differing structures. In addition, the ^{35}Cl n.q.r. frequency is reported for a tetrahedral amine complex of zinc chloride.

Zinc chloride and ether-donor adducts

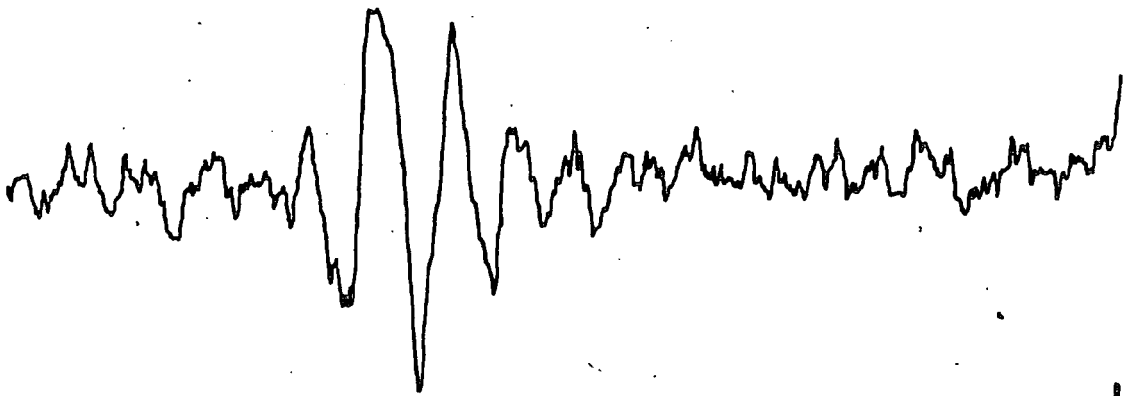
Although once thought to possess the CdCl_2 structure, zinc chloride is now known to be trimorphic. The α - and β - forms are composed of a three-dimensional framework built of ZnCl_4 tetrahedra and the δ - form has the layer structure of red mercury (II) iodide. In all three forms the zinc atom is four-coordinate and the chlorine atom two-coordinate. Commercial samples, due to their means of production, are more likely to be α -, δ - or a mixture of the two. (3). The α - form of space group $I \bar{4} 2d$ is tetragonal and has four molecules in the unit cell (4). The δ - form, also tetragonal, has space group $P4 / nmc (D_{4h}^{15})$ and has two molecules in the unit cell (46).

A broad singlet is observed in the ^{35}Cl n.q.r. spectrum at room temperature (Fig. 1). Averaging at room temperature has confirmed the line to be a singlet (Fig. 2). The temperature dependence of the ^{35}Cl quadrupole transition is shown in Fig. 3. At 195K the dependence is -0.57 kHz K^{-1} . A small negative temperature coefficient, without obvious discontinuity suggests the absence of any phase changes over the range 295 - 77K. It is compatible with a framework lattice bridged through chlorine and is about half that obtained for zinc bromide when adjusted for comparison (-1.43 kHz K^{-1}) (Fig. 4). Anhydrous zinc bromide has tetrahedral units in a tetragonal structure (42).

The single broad ^{35}Cl n.q.r. response obtained from crystalline zinc chloride is not sufficient to determine which of the three crystalline forms is present. It is shown below that introduction of ether molecules into the lattice does not produce large changes in the observed ^{35}Cl quadrupole frequencies (Table 1). It may be inferred that the lattice is of an open type. The simplicity of the quadrupole response perhaps best fits the tetragonal, layer structure of δ -zinc chloride which has only two molecules in the unit cell. i.e. it is suggested that the ^{35}Cl n.q.r. line observed at 12.67 MHz results from δ -zinc chloride.

Four samples of anhydrous zinc chloride were used and yielded a slight spread in n.q.r. frequencies.

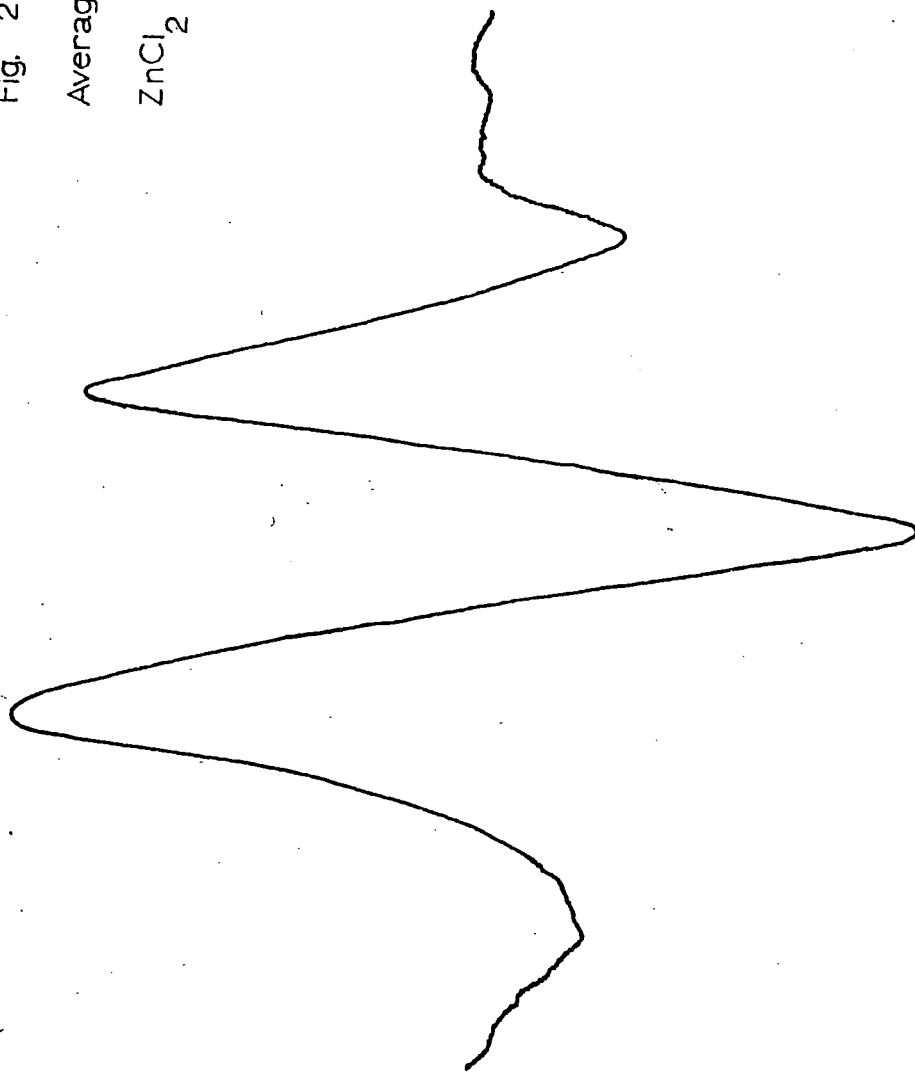
Fig. 1



12.886 MHz.

12.300 MHz.

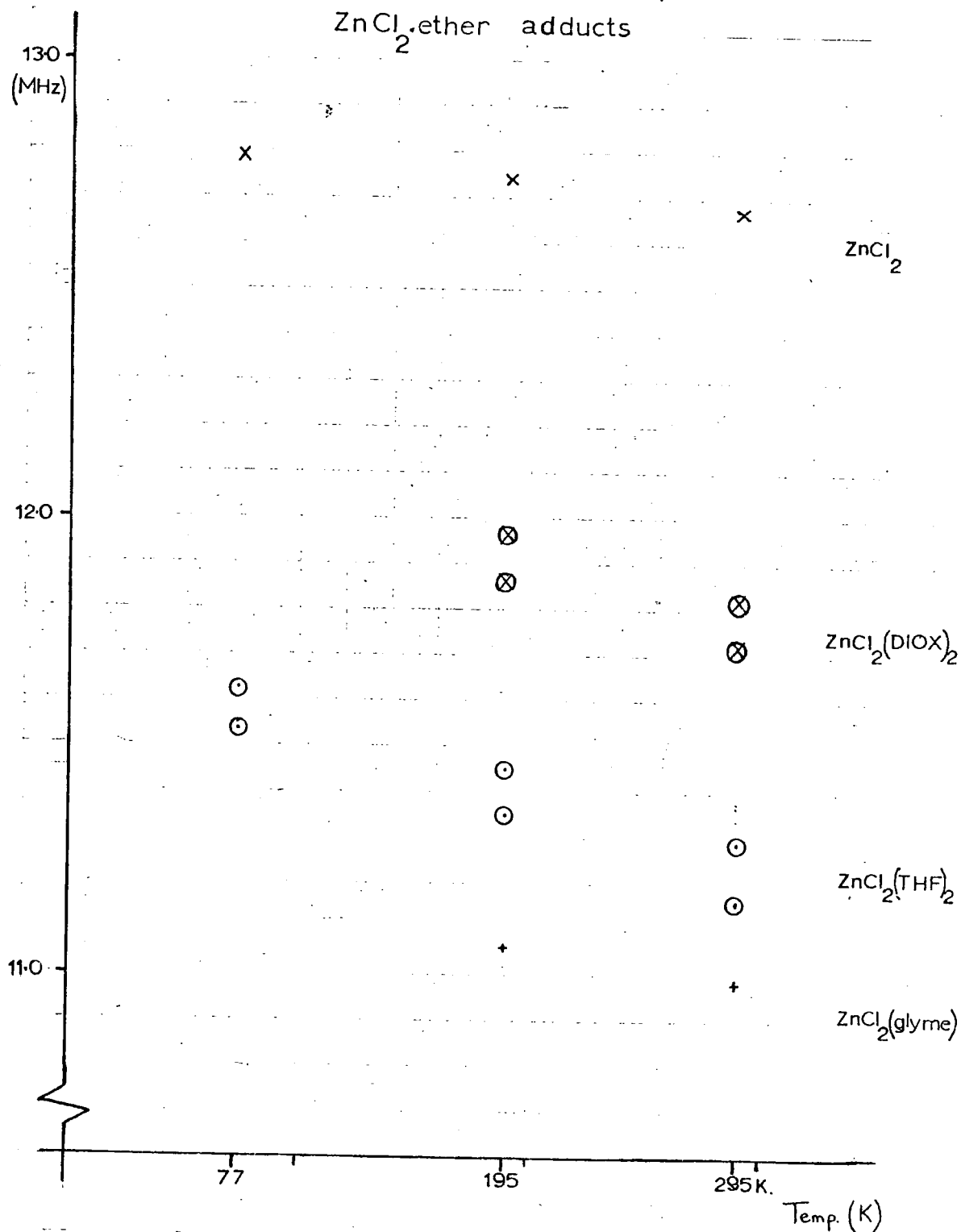
Fig. 2
Averaged ^{35}Cl nqr spectrum
 ZnCl_2 at 291K (~~$\text{N} \approx 35$~~)

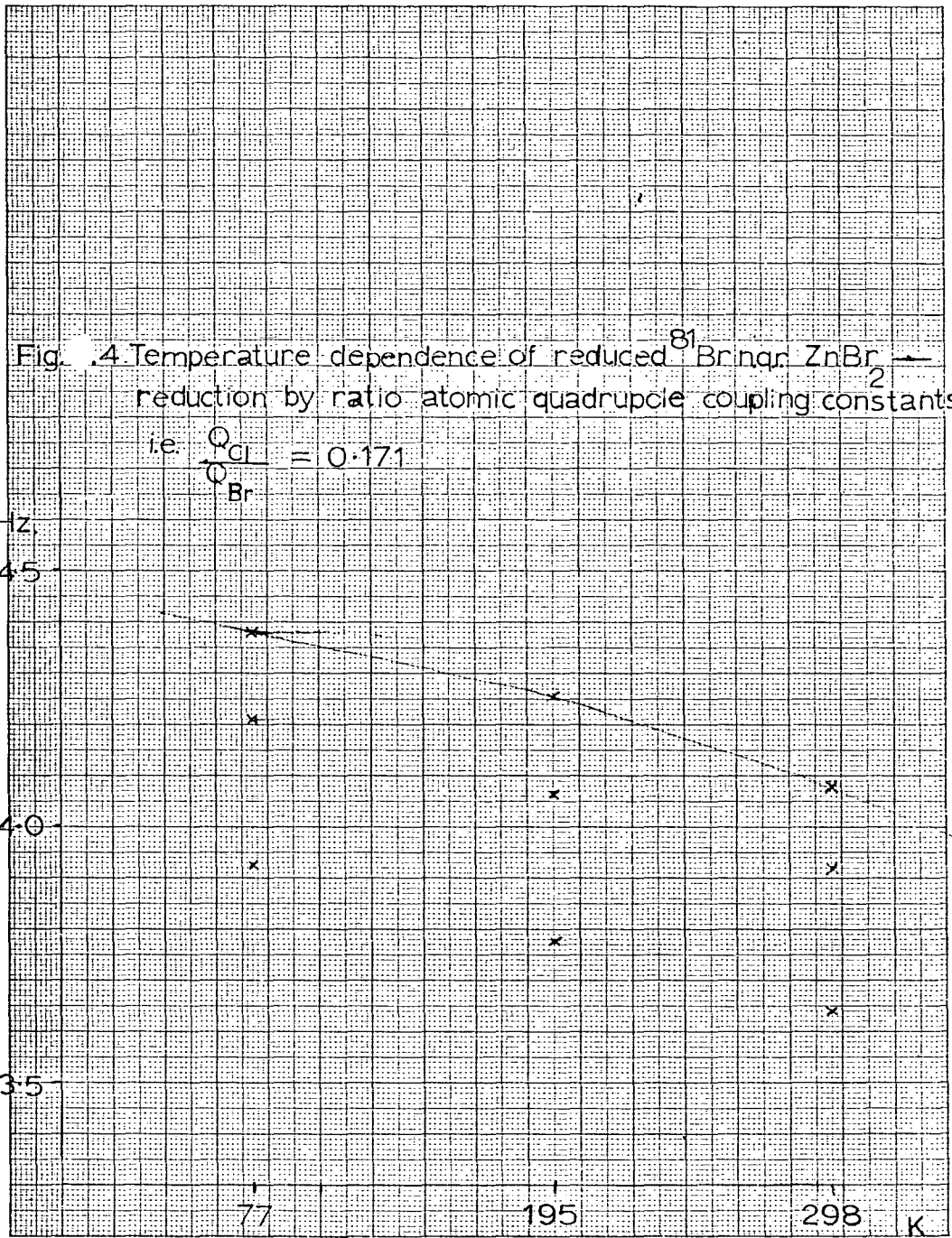


12.740MHZ.

12.588

Fig. 3 Temperature dependence of ^{35}Cl nqr lines of ZnCl_2 ether adducts





Source	Commercial stick	Melt	Sublimation	Commercial granulated
n.q.r. frequency (MHz)	12.67	12.57	12.53	12.67

The frequency reported in Table 1 is that of the stick and the granulated samples. The n.q.r. signals from these samples were a little stronger than those from the other two, reflecting possible better crystallinity. The anhydrous zinc chloride was handled in a nitrogen dry box and was kept in sealed vials to avoid hydration. The same handling techniques were used with the ether adducts.

Zinc is usually found tetrahedrally coordinated, as it is in the chloride. Tetrahedral monomeric complexes of ammonia (6), ethylamines (7) and pyridines (8) are reported. These strong nitrogen Lewis bases are able to completely break down the halogen bridging in zinc chloride. A tetrahedral complex of zinc chloride with tetrahydrofuran (T.H.F.) is reported also (9). In a study of the 1:1 adducts of cadmium halides with polyethers the inability of these oxygen Lewis bases to completely break down halogen bridging has led to the postulation of interesting chelating structures (10). The tetrahydrofuran adduct of zinc chloride was prepared, as were adducts with 1,4 dioxan (DIOX) and monoglyme (GLYME). Their possible structures were investigated using ^{35}Cl n.q.r. spectroscopy and infra-red vibrational spectroscopy. Results are given in Tables 1 and 2 respectively.

Preparation of the ether adducts was common to the three.

Anhydrous zinc chloride, obtained commercially (sticks - B.D.H. and granulated - Hopkins and Williams), was purified by sublimation at 350 - 400°C and 0.01 mm Hg pressure. Quantities of the chloride were stirred, with heating, in the dry solvent ethers under nitrogen. Filtered hot after about two hours, the liquor was allowed to crystallise slowly under nitrogen in a refrigerator. The crystals were filtered off and were sealed in 13mm n.q.r. sample tubes with a slight excess of the ether to minimise decomposition. All subsequent operations, including mulling with Nujol for infra-red spectra and the sealing of analysis capsules were performed in a dry, nitrogen-filled glove box. The n.q.r. spectra were recorded on a Decca Radar n.q.r. spectrometer and the infra-red spectra on a Perkin Elmer 457. Analysis of chlorine was by the Volhard method, carbon and hydrogen by a combustion analyser while zinc was estimated by atomic absorption. The analysis results for the crystalline products are shown later in Table 3. The poor correlation of carbon analysis in $ZnCl_2(THF)_2$ must be attributed to accidental interference but may be compared with that apparent in a similar analysis of $CdCl_2(THF)$ (11).

Many metal halides form complexes with ethers. Complexes of 1, 4-dioxan (DIOX) with dihalides of calcium, manganese, iron, cobalt, nickel and copper have been investigated by Fowles et al (12) and were found to be of 1:1 stoichiometry save for $(\text{CuCl}_2)_3 \cdot 2 \text{DIOX}$. Bridging dioxan with six-coordinate metal atoms is proposed for all the 1:1 complexes, which are isostructural with one another. Unidentate 1,4-dioxan has been suggested for the copper complex (13) but Fowles maintains that the evidence is only tenable if the bonding of the dioxan is very weak. Complexes with 1,4-dioxan of 1:2 stoichiometry have been reported for nickel and manganese dibromides in a later paper (14). Similarity of their infra-red (ir) spectra with that of $\text{HgCl}_2 \cdot \text{DIOX}$ prompted the suggestion of octahedral coordination for these complexes. Bridging by the dioxan is again suggested but without that by the halogen atoms (12). The proposed structures for 1:1 and 1:2 complexes are shown in Figs. 5 and 6. As discussed below, the authors demonstrate that in all cases 1,4-dioxan is present in its chair conformation.

From related work upon metal dichloride complexes with 1,4-dioxan Barnes et al (15) have suggested that the ligand field strength of 1,4-dioxan is slightly less than that of chloride ion. The (d-d) bands in 1:1 $\text{MCl}_2 \cdot \text{DIOX}$ (M=Mn, Fe, Ni and Co) are $\leq 0.3\text{kK}$ (300 cm^{-1}) to lower energy compared with the isostructural metal chloride. Nuclear quadrupole resonance (n.q.r.) spectroscopy could be employed to resolve a choice of octahedral structures proposed for the hydrated complexes $\text{MX}_2 \cdot \text{DIOX} \cdot 2\text{H}_2\text{O}$. Although both Figs. 7 and 8 would generate similar (d-d) spectra to that of $\text{MCl}_2 \cdot 2\text{H}_2\text{O}$ due to the trans $-\text{M}(\text{Cl}_2\text{OH}_2)$ chromophore, ^{35}Cl n.q.r. might distinguish between the terminal and bridging chlorides.

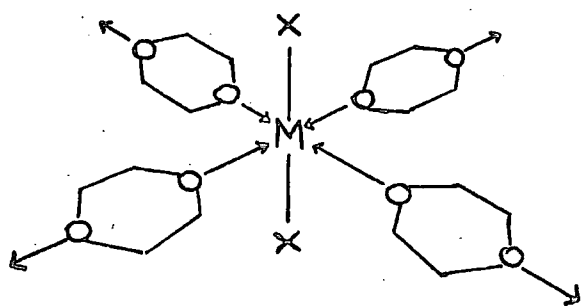


Fig. 5

eg. $MnBr_2 \cdot 2DIOX$

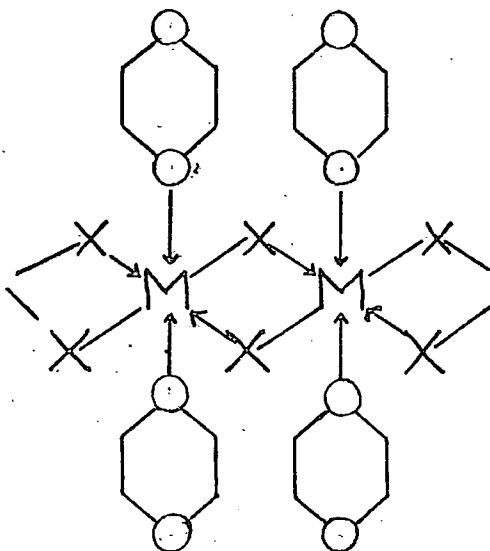


Fig. 6

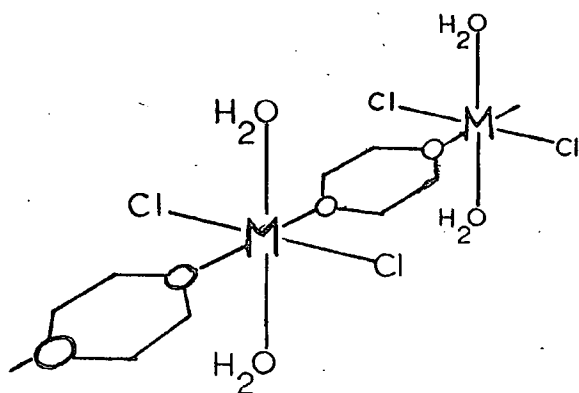


Fig. 7

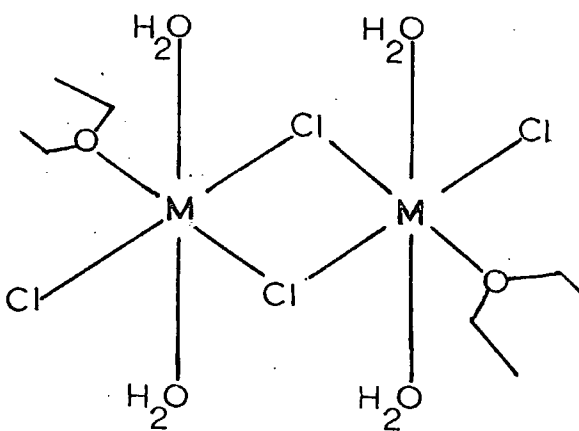


Fig. 3

Chains resembling those (longer) existing in copper II chloride and bromide, were found in copper II complexes including those with 1,4-dioxan and tetrahydrofuran (THF) (13) . The ether ligands assume terminal positions on the chains which are also inter-linked by weaker Cu---Cl bonding, giving copper a coordination number of six.

More successful cleaving of halide bridging is achieved in complexes of cadmium halides with ethers including 1,4-dioxan and THF (11) . Barnes and Duncan find that for a given halide the 1,4-dioxan complex is the stablest and that with THF the weakest. Chain structures of $(\text{CdX}_2)_n \cdot 2L$ units are suggested for the predominantly 1:1 complexes. Unlike those between 1,4-dioxan and the metal chlorides of the first transition series, these complexes are not isostructural with the cadmium halides. 1,3-dioxan is reported to produce related 1:1 complexes and in addition produces $(\text{MX}_2)_3 \cdot 2(1,3\text{-dioxan})$ for M=cadmium and copper (11), (16) . Structures similar to those of 1,4-dioxan complexes are proposed (i.e. polymeric pseudo-octahedral with bridging (Mn, Co, Ni) or terminal (Cu) 1,3-dioxan. Some differences are observed, such as the absence of mixed hydrate complexes $(\text{MX}_2 \cdot (1,3\text{-dioxan}) \cdot \text{H}_2\text{O})$ although they are found for 1,4-dioxan. The involvement of internal interactions has been suggested. The oxygen atoms of 1,4-dioxan may link hydrated metal ions through hydrogen-bonding (16) .

1,4-dioxan can assume two conformations - the chair or boat conformations which may be distinguished by vibrational spectroscopy. Ramsey (17) showed that for the boat and chair conformations seventeen and eleven ir-active fundamentals respectively are

permitted. The free ligand in the liquid and solid states has been shown to exist in the chair form (18). In non-chelate complexes this form is more likely but if chelated, the boat form would be assumed. Hendra and Powell (19) investigated the ir spectra of a series of 1:1 metal halide complexes with 1,4-dioxan. The spectra closely resembled each other and that of the free ligand. The chair conformation was therefore proposed, the dioxan assuming a bridging position in a polymeric structure. Confirmation of the presence of 1,4-dioxan in the chair form has been provided by Fowles et al (14) using Raman and ir spectra. The mutual exclusion principle allowed the centrosymmetric chair form to be distinguished from the non-centrosymmetric boat form.

Tetrahydrofuran (THF) as an ether ligand to metal dihalides has been shown to produce complexes of 1:1 and, apparently, 1:1.5 stoichiometry (20). The structure proposed for 1:1 $\text{CoX}_2 \cdot \text{THF}$ ($\text{X}=\text{Br}$ and I) is pseudo-octahedral polymeric chains interlinked by weaker $\text{Co} \cdots \text{X}$ interactions (Fig. 9). The 1:1.5 complexes $[(\text{MX}_2)_2 \cdot 3\text{THF}]$ for $\text{M}=\text{Mn}$, Fe and Co are believed to be a mixture of 1:1 and 1:2 complexes viz. $\text{CoCl}_2 \cdot \text{THF}$ and $\text{CoCl}_2 \cdot 2\text{THF}$. Similarity in the thermal decomposition of $\text{CdX}_2 \cdot \text{THF}$ and $\text{CdX}_2 \cdot \text{DIOX}$ has prompted Barnes to suggest that the compounds are structurally similar (11). Other complexes are reported (21) of which that with zinc chloride is further investigated and discussed below.

1,2-dimethoxyethane, and other glymes have also been investigated as ether ligands to metal dihalides. 1:1 complexes of monoglyme with manganese, iron II, nickel and copper dihalides are reported by Fowles (20) for which polymeric structures are proposed

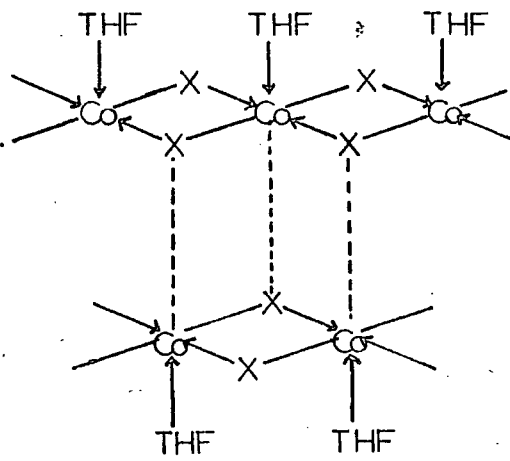


Fig. 9 $\text{CoX}_2 \cdot \text{THF}$

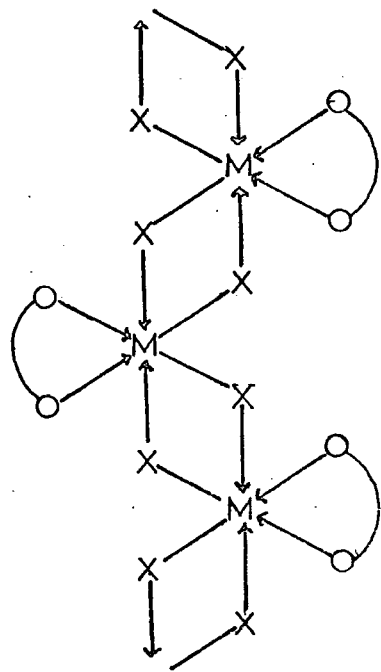



Fig. 10 $\text{X} = \text{Cl}$

For Fig. 12, $\text{X} = \text{Br}$ and
 = $\text{HCOCH}_2\text{CH}_2\text{OCH}_3$

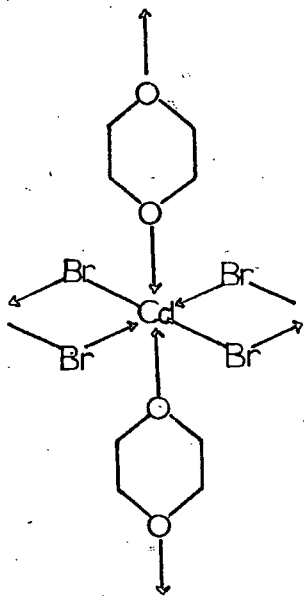


Fig. 11 $\text{CdBr}_2 \cdot \text{DIOX}$

(Fig. 10). Wulfsberg and Weiss (10), studying bridging effects in mercury II and cadmium II halide complexes with polyethers, show that the low-frequency Raman spectra of the 1:1 cadmium halide complexes are closely similar to those (1:1) of the mercury halides. Following the structural analysis of HgCl_2 . tetraglyme in which Iwamoto (22) showed that the polyether was fully chelating, Wulfsberg et al. propose that the 1:1 cadmium halide complexes with polyethers are also completely chelating. Complexes of other than 1:1 stoichiometry appear to contain ether ligands not fully chelating to the cadmium (atom). The vibrational spectra of the complexes usually show a shift to lower frequencies for C-O stretching and C-O-C bending modes in comparison with the bands in the free ligand. The authors propose that the magnitude of this shift follows the sequence free ligand $\rangle \text{HgX}_2$ adduct $\rangle \text{CdX}_2$ adduct, suggesting this as evidence of the higher Lewis acidity of cadmium over mercury halides.

In order to study the electronic environments and bonding of the halogen atoms in the complexes, Wulfsberg and Weiss made use of ^{35}Cl , ^{81}Br and ^{127}I n.q.r. techniques. Using a Decca spectrometer they observed the halogen quadrupole resonances which when plotted against the number of chelating oxygen atoms revealed a sequence of frequency steps or "jumps". These "jumps" to higher n.q.r. frequency (ν_Q) correspond to the reducing coordination of the halogens i.e.

CdI_2	\longrightarrow	Bridging halogen	\longrightarrow	terminal halogen
coord. no. = 3		coord. no. = 2		coord. no. = 1
(lowest ν_Q)				(highest ν_Q)

After each upward step there follows a gradual decrease in n.q.r. frequency before the next step. This decrease is accounted for by the rising coordination number of the cadmium increasing the ionicity of the halogen atoms bonded to it.

From the n.q.r. results the following halogen bridging is proposed:

bridging halogens

terminal halogens

$\text{CdI}_2 \cdot \text{glyme}$

Other 1:1 complexes

$\text{CdBr}_2 \cdot \text{glyme}$

i.e. $\text{CdI}_2 \cdot \text{diglyme}$

$\text{CdI}_2 \cdot \text{triglyme}$

$\text{CdBr}_2 \cdot \text{dioxan}$

$\text{CdBr}_2 \cdot \text{tetraglyme}$

$\text{CdX}_2 \cdot 18\text{-crown-5} (\text{X}=\text{Br}, \text{I})$

The glyme polyethers in general appear too weak as bases to break up completely the halogen bridging found in cadmium II chloride and bromide. However, tetraglyme in $\text{CdBr}_2 \cdot \text{tetraglyme}$ appears to completely remove the bridging, possibly because in doing so the coordination number of the cadmium atom may be increased (10). For 2:1 and 3:2 adducts of cadmium bromide the ^{81}Br n.q.r. frequencies are very similar to each other and to those of its complexes with 1,4-dioxan and monoglyme. From this it is concluded that the 2:1 and 3:2 adducts contain bridging bromide atoms. The structure of $\text{CdBr}_2 \cdot \text{DIOX}$ has been confirmed by Barnes (23) as represented by Fig. 11 in which bridging through the bromine atoms resembles that found in $\text{HgCl}_2 \cdot \text{DIOX}$ (24). This may be contrasted with the structure proposed by Wulfsberg and Weiss (10) for $\text{CdBr}_2 \cdot \text{glyme}$ (Fig. 12). The difference in ether ligand bonding is not, however, reflected simply in the ^{81}Br n.q.r. frequencies of the compounds which are 54.000MHz and 54.646MHz for the glyme and 1,4-dioxan complexes respectively. Barnes (13) has suggested the presence of additional weaker bonding in metal halide - ether complexes. In a study of Cu^{II} complexes higher heats of dissociation were noted for the complexes

with 1,4-dioxan compared to those found for comparable tetrahydrofuran, water and acetonitrile complexes. In addition to the proposal that additional out-of-plane bonding between the second oxygen of 1,4-dioxan and the copper atoms may occur, he suggests that the dioxan molecule may pack particularly compactly into the crystal lattice thereby giving greater stabilisation than the other ligands. Chain length in these complexes may be determined by such forces. Daasch (25) has also commented upon the possible influence of crystal packing. He has suggested that small shifts and splittings in vibrational spectra (i.e. in addition to a general shift) varying from complex to complex may result from packing in the crystal lattice rather than from the interaction between 1,4-dioxan and the metal ion.

The bridging by halogen atoms within the 1:1 cadmium halide-glyme complexes was observed by Wulfsberg and Weiss to reduce the Raman metal-halogen stretching frequency below that estimated for the monomeric metal-halogen bond (10). Fowles et al. (14) have observed high metal-halogen vibrational frequencies in i.r. spectra of zinc chloride-ether complexes supporting their suggestion that halogen bridging is broken down in them and that monomeric units exist. A recent n.q.r. study of the diethyl ether complex of magnesium dibromide has revealed a phase transition between 233K and 213K (42). The transition appears to be related to a conformational change in the ether.

A study of zinc chloride and some of its complexes with ethers appeared a useful extension of the previous studies. The possibility that ^{35}Cl n.q.r. could distinguish between chlorine in terminal and bridging positions offered scope for the proposal of structures.

Juhász and Yntema (26) prepared several complexes of 1,4-dioxan with the zinc halides by their dissolution in the ether and subsequent removal of the excess ether by evaporation in a desiccator. The chloride, bromide and iodide all produced 1:2 complexes $ZnX_2 \cdot 2DIOX$ but, in addition, the chloride produced a 1:1 complex if crystallisation took place under different conditions. In each case a white hygroscopic crystalline complex was obtained. In a similar manner, but using heated dioxan ($90^\circ C$); yellow crystals which analysed as 1:1 $ZnCl_2 \cdot DIOX$ were prepared by Hatch and Everett (21). These were found to be very hygroscopic and had an ir spectrum which showed more bands than expected for 1,4-dioxan in the chair conformation. The authors, investigating a stereospecific chlorination of 1,4-dioxan, proposed a chelated structure for the adduct. Chelation of the two oxygen atoms to zinc was suggested, requiring the 1,4-dioxan to adopt the boat conformation (Fig. 13). This structure is closely similar to that of $CdI_2 \cdot DIOX$ elucidated by X-ray crystallography (27) which caused Wulfsberg and Weiss to propose a chelated structure for $CdI_2 \cdot diglyme$. Each of these structures is monomeric with zinc having its usual tetrahedral coordination.

Fowles et al. (14) prepared a white 1:1 complex $ZnCl_2 \cdot DIOX$ which ir investigation showed to contain dioxan in the chair conformation. It is proposed that the dioxan molecules provide bridging between the tetrahedral units (Fig. 14). He found the suggested structure of Hatch and Everett for the 1:1 complex unlikely unless a different form had been isolated. This seems possible since the colours reported for the crystals differ. Although generally reported as bridging or bidentate, 1,4-dioxan has been reported to yield 1:1 complexes with strong Lewis acids such as aluminium trichloride in which it appears to be attached by only one

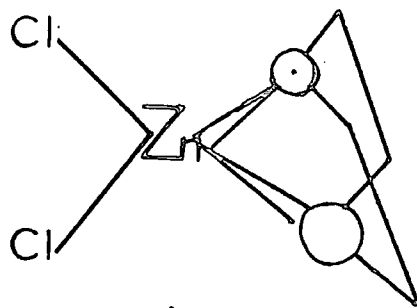


Fig. 13 $\text{ZnCl}_2 \cdot \text{DIOX}$

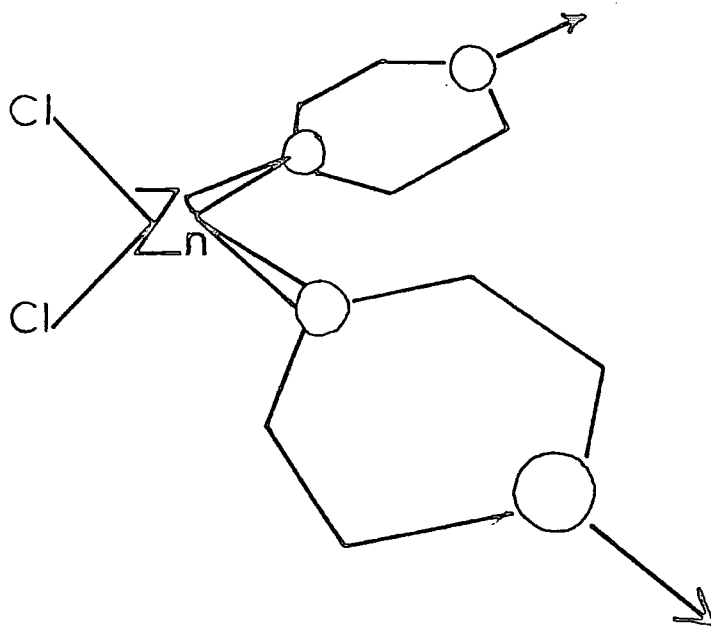


Fig. 14 $\text{ZnCl}_2 \cdot \text{DIOX}$

oxygen, i.e. monodentate (25). The ir spectra of these dioxan complexes differ little from those in which dioxan is bonded through both oxygen atoms. Hendra and Powell (19) have prepared 1:2 complexes $MCl_2 \cdot 2L$ ($L = C_4H_8OS$, thioxan) which have monodentate thioxan in the chair conformation. These complexes are likely to be monomeric within the lattice.

The Structures of the $ZnCl_2$. ether complexes

The usual tetrahedral coordination of zinc is almost certainly retained. The movements in ^{35}Cl n.q.r. frequencies and in the i.r. stretching bands of Zn-Cl are not large enough to suggest a complete change of structure from the anhydrous zinc chloride. Some of the chlorine bridging is probably retained to bind the tetrahedral species together.

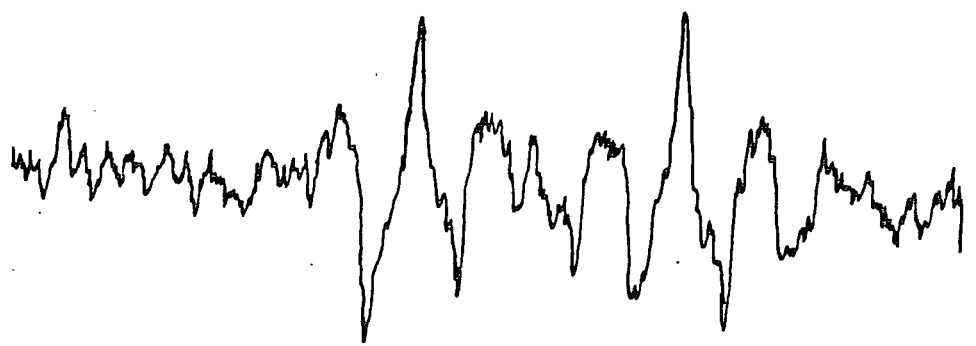
It is proposed that the variation in n.q.r. frequency (ν_Q) about that of zinc chloride results from a competition between two factors. They are i) the weakening of the intermolecular chloride bridging (tending to raise ν_Q) and ii) the increased ionicity of the Zn-Cl bond caused by the oxygen bases (tending to lower ν_Q).

Zinc chloride.tetrahydrofuran adduct

The quadrupole resonances for this complex lie at lower frequencies than that of zinc chloride (Table 1). There are two lines but their small separation suggests that they are chemically similar (Fig.15). It is more probable that the chlorine atoms bonded to zinc are crystallographically inequivalent or that there is more than one molecule in the unit cell. Analysis results on the fine, colourless needle crystals of the complex are given in Table 3, and support the formula of Kern (9). The result for carbon was repeatedly low probably due to interference in the automatic analysis. The analysis supports a 1:2 stoichiometry of $ZnCl_2 \cdot 2T.H.F.$

Shifts to lower frequency in the i.r. spectrum of the coordinated T.H.F. molecule, especially in the asymmetric C-O-C stretching mode, clearly indicate that the bonding to zinc is through its

Fig. 15 ^{35}Cl n.q.r. $\text{ZnCl}_2(\text{THF})_2$ at 295K.



MHZ. 11.3 11.2 11.1

TABLE 1 ^{35}Cl n.q.r. results for zinc chloride and some ether adducts at R.T.

COMPOUND	^{35}Cl N.Q.R. (MHz) AT 295K	S/N
ZnCl_2 (ANHYDROUS)	12.670	5/1
ZnCl_2 (T.H.F.) ₂	11.159	10/1
	11.289	10/1
ZnCl_2 (1.4 DIOXAN) ₂	11.711	2/1
	11.822	2/1
ZnCl_2 (MONOGLYME)	10.985	2/1

oxygen atom. (Table 2). Though inconclusive, the similarity of i.r. frequencies for Zn-Cl stretching modes in zinc chloride and the ether complexes suggests that the general character of the bond remains unchanged. The frequencies are observed to fall as the base strength increases i.e. monoglyme to 1,4-dioxan to tetrahydrofuran (Table 2). It is proposed that this trend is evidence of the increased ionicity in the Zn-Cl bond of the complexes over the complexes. However, chlorine-chlorine intermolecular interactions, present in zinc chloride, appear to be retained in the complexes, although they are weakened.

The temperature dependence of the higher frequency n.q.r. line is -1.50 kHz K^{-1} at 195K which is much greater than that observed for zinc chloride itself, -0.57 kHz K^{-1} at 195K. The greater size of the T.H.F. molecule, compared to chloride, probably causes an expansion of the lattice which may explain the greater temperature dependence. This opening up of the lattice may weaken intermolecular chlorine bridging compared to that in zinc chloride and any reduction in bridging would then tend to raise the n.q.r. frequency above that of zinc chloride.

Acting to reduce the ^{35}Cl n.q.r. frequency below that of zinc chloride is the donation of electronic charge by the oxygen atom of the ether to the zinc. The increase in the ionicity of the Zn-Cl bond is related to the strength of the base. Of the three bases used in this work, tetrahydrofuran may be expected to be the strongest and therefore to produce the greatest lowering of the quadrupole resonance.

The observed n.q.r. frequencies for $\text{ZnCl}_2 \cdot 2\text{THF}$ lie approximately 1.45 MHz below that of ZnCl_2 - a 11.4% reduction in ν_Q . This is

TABLE 2. COMPARATIVE I.R. DATA FOR ZINC CHLORIDE COMPLEXES.

	ZnCl ₂ .2T.H.F.		ZnCl ₂ .2DIOX		ZnCl ₂ .GLYME		ZnCl ₂
ASYMMETRIC C-O-C STRETCH (cm ⁻¹)	1023	*Shift -46	1110	Shift -9	1096	Shift -41	-
SYMMETRIC C-O-C STRETCH (cm ⁻¹)	874	Shift -35	900 877	Shift +9 avg	864 821	Shift +11	-
Zn-Cl STRETCH (cm ⁻¹)	728 587 358 300		727 - 388 -321		728 - 403 345		728 557 - -

* SHIFT is frequency difference from corresponding band in free liquid ether.

similar to reductions observed for complexes of mercury II chloride with ethers (45) where a 15.1% reduction was observed for one line in $\text{HgCl}_2 \cdot \text{T.H.F.}$ The frequency of the adduct may be seen as the result of a balance between the increased ionicity of Zn-Cl bond and the decreased chlorine bridging. If the three complexes are structurally similar then, relative to zinc chloride, T.H.F. may be expected to produce the largest reduction in frequency and, as the smallest base, the smallest subsequent increase in frequency.

Zinc chloride. 1,4-dioxan adduct

The n.q.r. frequency of this complex indeed lies above that of the adduct with T.H.F. Analysis of the needle-like crystals of the complex shows it to be of 1:2 stoichiometry with two molecules of 1,4-dioxan to each ZnCl_2 unit (Table 3). Complexes of cadmium halides with 1,4-dioxan have been shown to be more stable than those with T.H.F. (11). This may point to the existence of stabilising intermolecular interactions making use of the additional oxygen atom. Such interactions in the form of dioxan bridges between HgCl_2 chains exist in the $\text{HgCl}_2 \cdot \text{Dioxan}$ complex (45). Monodentate 1,4-dioxan has been reported in complexes with strong Lewis acids (25). It may be present in the 1:2 complex to complete the tetrahedral coordination of zinc, although use of its second oxygen should not be ruled out. The similarity in the structures of cadmium halide complexes with T.H.F. and 1,4-dioxan (11) may be taken to support this proposal.

1,4-dioxan is expected to be a weaker donor than T.H.F. due to competing inductive effects of the two oxygen atoms. Due to the weaker interaction, the reduction in the mean ^{35}Cl n.q.r. frequency

TABLE 3

	$ZnCl_2(T.H.F.)_2$		$ZnCl_2(DIOX)_2$		$ZnCl_2(GLYME)$	
ANALYSIS	Formula wt=280.33		Formula wt=312.33		Formula wt=226.33	
%	Found	calc.	Found	calc.	Found	calc.
C	26.31	34.25	29.36	30.74	21.50	21.21
H	5.90	5.71	5.25	5.12	4.92	4.42
Zn	24.08	23.32	20.47	20.93	27.85	28.89
Cl	25.39	25.31	23.60	22.72	30.48	31.35

from that of zinc chloride is less than that of the adduct with T.H.F. As with the tetrahydrofuran adduct, the two n.q.r. lines may indicate crystallographic inequivalence of the chlorine atoms or more than one molecule in the unit cell.

The weaker and longer Zn-O bonds together with the increased size of 1,4-dioxan molecules probably open up the crystal lattice rather more than T.H.F. A similar temperature dependence of the n.q.r. lines is found, -1.38 kHz K^{-1} , which is markedly greater than that of zinc chloride (Fig.3). The expansion may be expected to produce a weakening of the intermolecular chloride bridging present in zinc chloride. The resulting tendency to increase the n.q.r. frequency is expected to be greater than that with T.H.F.

Taken together, the increased ionicity of Zn-Cl and the reduced chlorine bridging predict that the n.q.r. frequencies for $\text{ZnCl}_2 \cdot 2$ (1,4-dioxan) will be above those of the corresponding T.H.F. adduct. This is confirmed (Table 1). The 7.8% shift in n.q.r. frequency from that of zinc chloride suggests only a small amount of charge transfer which the small shift to lower frequencies in the i.r. spectrum of the adduct confirm (Table 2).

Zinc chloride.monoglyme adduct

Monoglyme, $\text{CH}_3\text{OCH}_2\text{CH}_2\text{OCH}_3$, is an open chain ether with two oxygen atoms available to complex with the zinc atom. The possibility arises of a structural change from those of the two previous complexes. As a base, monoglyme should be slightly stronger than 1,4-dioxan due to the terminal methyl groups but Wulfsberg (28) has observed monoglyme to be the weaker in the polymeric complexes

with mercury (II) chloride. If a structure similar to those of the complexes with T.H.F. and dioxan were retained, it might be predicted that two quadrupole resonances from the likely two chlorine sites would be, perhaps, about 11.6 MHz at room temperature. However, what is in fact found is a single resonance at 10.960 MHz.

That the monoglyme is bonded to the zinc through oxygen is indicated by the shift in the asymmetric C-O-C stretch of monoglyme at about 1100 cm^{-1} (Table 2). The fact that this complex has cubic crystals, while the other two have needles, suggests that a change in structure may have occurred. Analysis showed the complex to be of 1:1 stoichiometry i.e. $\text{ZnCl}_2 \cdot \text{monoglyme}$ (Table 3). If both oxygen atoms of the ether are used in coordination to zinc, there arises the possibility that the monoglyme has assumed a bidentate position. Such a position has been proposed for monoglyme in cadmium (II) chloride.monoglyme (Fig. 10) (20).

The temperature dependence for the monoglyme adduct of zinc chloride is -0.69 kHz K^{-1} at 195K which is much closer to that of zinc chloride than those of the previous complexes. This fact and the stronger Zn-Cl bonds suggested by the higher i.r. frequencies (Table 2), make it plausible to propose that in this complex the bonding retains much of the character of that of zinc chloride. Under these circumstances, the major influence upon the n.q.r. response of the complex will be the increased ionicity of the Zn-Cl bond caused by the base. Compared to the previous complexes, the resulting reduction in n.q.r. frequency relative to that of zinc chloride will be similar to that of $\text{ZnCl}_2 \cdot (\text{DIOX})_2$ but, as the chlorine bridging is retained to a greater extent, there will be little compensation for the initial lowering in n.q.r. frequency. Qualitatively, this explains the frequency of 10.960 MHz, although a 13.5% decrease from the frequency of zinc chloride seems rather

large if it is due solely to an increase in ionicity. Without results on other 1:1 adducts, it is not possible to speculate on the effect of complexing upon the intermolecular interactions found in zinc chloride. It may be that the resulting charges cause a decrease in ^{35}Cl n.q.r. frequency in addition to that caused by increased ionicity.

Structures of ZnCl_2 .ether complexes

The generally small shifts in ^{35}Cl n.q.r. and i.r. frequencies from those of zinc chloride suggest that much of the bonding character of the parent is retained in these complexes. It seems unlikely that the ether bases used are strong enough to break down completely the chlorine bridging held to exist in all forms of zinc chloride. It is with stronger nitrogen bases such as 4-toluidine that full monomeric species are found. A 32.4% decrease in n.q.r. frequency from that of zinc chloride is observed, (8.572 MHz at 77K). Although likely to exist in a polymeric lattice involving bridging chlorines, the structures of "the monomeric blocks" of the three adducts reported here may be proposed. They are shown in Figs. 16-18.

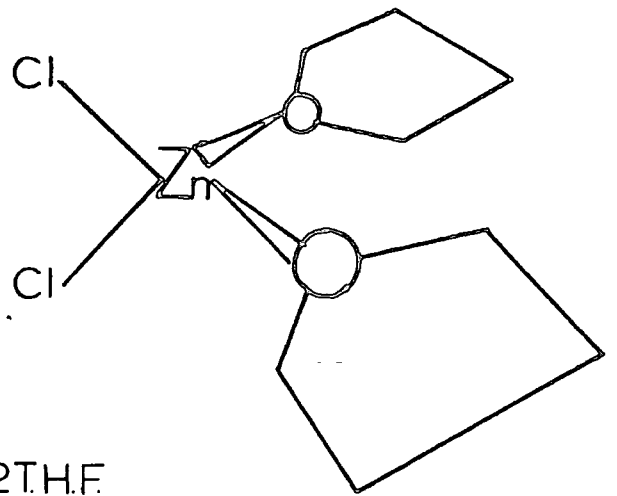


Fig. 16 $\text{ZnCl}_2 \cdot 2\text{T.H.F.}$

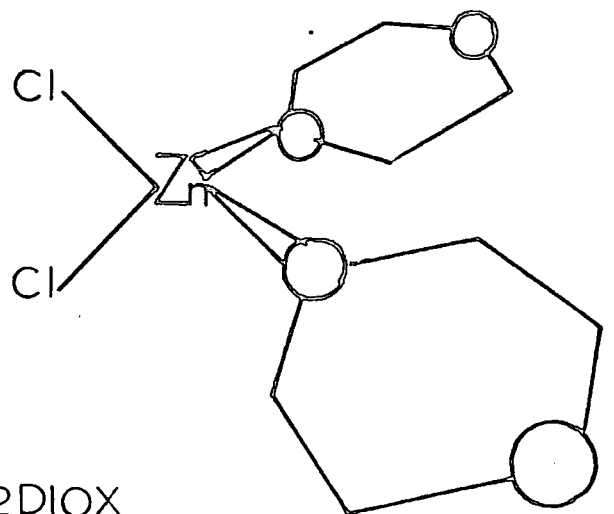


Fig. 17 $\text{ZnCl}_2 \cdot 2\text{DIOX}$

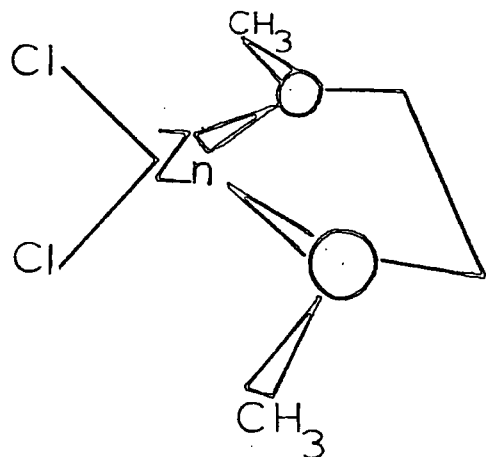


Fig. 18 $\text{ZnCl}_2 \cdot \text{GLYME}$

Zinc Chloride Amine complexes

Zinc is normally found tetrahedrally coordinated and monomeric complexes of the form $ZnCl_2 \cdot L_2$ are well known for amine ligands (6,7,8). Other coordination is however known. Five coordination of zinc occurs in the 1:1 complex of zinc chloride and 2,2',2'' terpyridyl (29-32). Chain bridged structures occur in hydrazine (33,34) and ethylenediamine (en) (35,36) complexes with zinc chloride.

Scaife (2) reported that with $ZnCl_2 \cdot L_2$ complexes of $L =$ pyridine and ammonia ^{35}Cl n.q.r. signals were not observed. Basu (44) has reported the ^{35}Cl n.q.r. frequencies for several amine complexes of mercury II and cadmium II chlorides including $CdCl_2(pyridine)_2$ (19.60 MHz at 295K). Other tetrahedral monomeric complexes were prepared therefore in this work, namely, $(4\text{-toluidine})_2ZnCl_2$ and $(quinoline)_2ZnCl_2$ (37). To investigate different coordination of zinc the complex $(Zn(en)Cl_2)_\infty$ was prepared which has an infinite polymeric chain structure bridged through the nitrogen atoms.

Only $(4\text{-toluidine})_2ZnCl_2$ yielded a ^{35}Cl n.q.r. signal although wide searching at 77K and room temperature was carried out for all the complexes (6MHz - 25 MHz).

	Temp	^{35}Cl NQR (KHz)	S/N
$(4\text{-toluidine})_2ZnCl_2$	77°K	8.572	2/1

Signal averaging was not thought worthwhile because of the narrow sweep width of the existing c.a.t. The investigation of $ZnBr_2$ analogues was not undertaken due to lack of time.

Scaife (2) reported that in amine complexes of zinc bromide and zinc iodide the n.q.r. frequencies observed were close to the mean of that of the corresponding tetrahalozincate. The value for $(ZnCl_4)^{2-}$ in Cs_2ZnCl_4 is 9.20 MHz (mean) at 77K and so this

relationship for the replacement of two chloride ions by two neutral amine groups appears to hold for all zinc halides.

Using a super-regenerative oscillator detector, Farlee has observed the ^{35}Cl quadrupole resonances for $\text{Zn}(\text{py})_2\text{Cl}_2$ (38). At 298K they occur at 10.14 and 10.29MHz. Hsieh et al have estimated the charge distribution in the complex, apportioning charges to chlorine and zinc atoms as - 0.81 and +1.2 electron charges respectively. Comparable figures for $\text{Zn}(4\text{-toluidine})_2\text{Cl}_2$ are -0.34 and +1.3 if a similar donor orbital occupancy is assumed for the nitrogen of 4-toluidine. It is likely, however, that the charge on the zinc is lower due to the greater basicity of 4-toluidine over pyridine.

The preparative details for the zinc chloride amine complexes are given below. Table 4 carries the infra red spectra and analysis results for the complexes. Carbon and hydrogen analyses were made with a Perkin Elmer (PE) analyser. Nitrogen analysis was by the Kjeldahl method while chlorine was estimated potentiometrically as chloride using silver nitrate. Atomic absorption on a PE403 was used for zinc.

For the 4-toluidine and quinoline complexes solutions of the amines in ethanol were added to solutions of zinc chloride in ethanol in the molar ratio 2:1. The deposited crystals were recrystallised from ethanol, washed with dry ether and dried in vacuo (39,40). The complex with 4-toluidine crystallised as white platelets while that with quinoline was deposited as a pale brown powder (even after repeated recrystallisation).

Into 9.1 ml of 98% ethylenediamine in 4ml conc. hydrochloric acid,

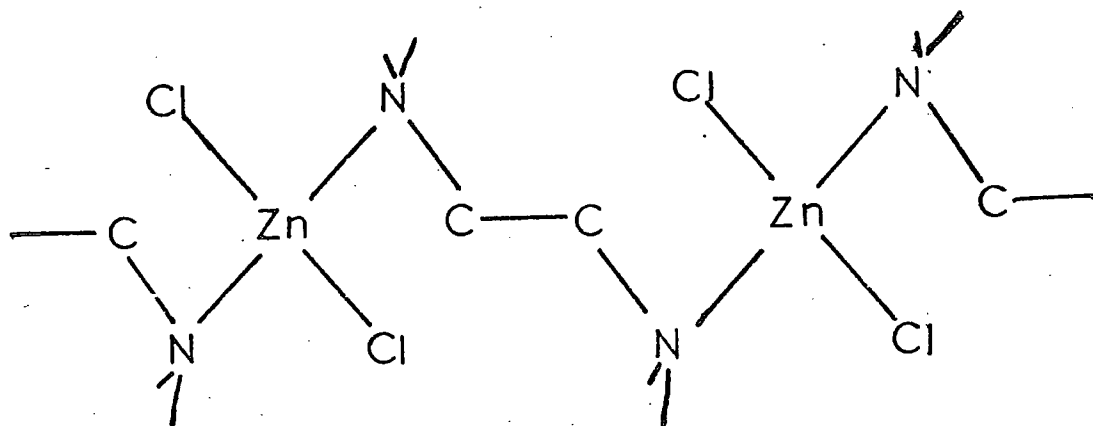
TABLE 4	bis(4-toluidine) zinc dichloride (p-tol) ₂ ZnCl ₂	bis(quinoline) zinc dichloride (quin) ₂ ZnCl ₂	Ethylene-diamine zinc dichloride (Zn(en)Cl ₂) _∞
I.R. (cm ⁻¹)	3286	3060	3420
	3240	1598	3275
	3088	1590	3215
	2927	1513	3105
	1584	1406	2940
	1513	1381	2915
	1095(sh)	1322	1580
	1076	1315	1460
	829	1147	1353
	814	1137	1182
	742	1064	1142
	708	1060	1060
	669	817	1006
	640	787	988
	532	747	660
	424	641	636
	405	630	624
	318	538	612
		530	405
		496	315
		476	285
		404	
		324	
		305	

TABLE .4 cont.

<u>ANALYSIS</u>	Formula wt=350.27		Formula wt=394.60		Formula wt=196.27	
	Found	calc.	Found	calc.	Found	calc.
%						
C	46.33	47.96	53.78	54.78	12.35	12.23
N	6.97	8.00	8.04	7.10	14.62	14.27
H	4.59	5.14	4.07	3.55	4.08	4.08
Zn	17.86	18.66	16.29	16.57	33.25	33.31
Cl	21.13	20.24	18.30	17.97	35.98	36.12

was dissolved 10gm. zinc chloride. After making up to 65ml. with distilled water, the solution was left to stand. Colourless, well-formed crystals were deposited over about an hour which were filtered off, washed and dried in vacuo.

Krishnan and Plane (35) have reported the structure as consisting of infinite chains bridged through the nitrogen atoms thus:



Introduction

A reinvestigation of the Zeeman n.q.r. lineshapes of polycrystalline samples of group IV tetrahalides has been made in an attempt to clarify the values of their asymmetry parameters (η). Conventional determination by the method of Morino and Toyama has been prevented by the uncharacteristic Zeeman lineshapes. Comparison with simulated lineshapes has yielded estimates for η of about 0.45 for GeCl_4 and about 0.60 for SiCl_4 .

Properties of the higher members of the group IV tetrahalides such as bond length, for example, prompted the proposal of double-bond character in the $M^{IV}-Cl$ bond. (1,2,3). A theoretical study showed that for a sufficiently large difference in electronegativity between the central group IV atom (M^{IV}) and a halogen atom, d-orbitals of M^{IV} could be involved in $d_{\pi}-p_{\pi}$ bonding with the chlorine halogen (4). Such d-orbitals appear in the ground state of the third period elements i.e. silicon in group IV. The bond energies of Si-Hal and Ge-Hal bonds (Hal = F, Cl, Br) are greater than that of C-Hal but, due to their increased polarity, they are usually more reactive. This is indicated by the electronegativities of the elements which are given below. The electronegativity sequence has been observed in several determinations and is probably significant. It is likely to be due to decreased screening of the valence electrons when 3d orbitals are filled in the period containing germanium.

	Electronegativities ref. 6a)	ref. 6b)
carbon	2.5	2.50
silicon	1.8	1.74
germanium	1.8	2.02
tin	1.7	1.72

On the grounds of electronegativity alone the ^{35}Cl n.q.r. frequencies of the group IV tetrachlorides might be expected to follow the sequence : $CCl_4 > GeCl_4 > SiCl_4 > SnCl_4$. Generally this is observed (below) but the large separation in frequencies between carbon tetrachloride and the other members caused Livingston to suggest that the latter were abnormally low (5).

³⁵Cl N.q.r. frequencies

CCl ₄	avg.	40.629	MHz	(7)
SiCl ₄	"	20.390	"	"
GeCl ₄	"	25.661	"	"
SnCl ₄	"	24.096	"	"

Amongst chemical evidence that the electronegativity of germanium is greater than that of silicon is the increased reactivity of M^{IV}Hal₄. Tetrahalides of silicon (except SiF₄) are immediately and completely hydrolysed in water whereas germanium tetrahalides are hydrolysed only slowly and reversibly. The energy to reach the transition state in substitution reactions involving a five-coordinate intermediate appears to be lower than would be expected without the use of the d-orbitals of silicon.

The difference in ³⁵Cl n.q.r. frequencies of silicon and germanium tetrachlorides prompts the proposal that substantial p π -d π bonding in the Si-Cl bond has lowered the quadrupole resonance. That some p π -d π bond character exists in certain bonds to silicon may be inferred from molecular structures. The rather large bond angles in siloxanes (150° approx.) (8) suggest such bonding in Si-O-Si when compared to the highly bent germanium analogues (9). There is some direct evidence for bond shortening due to π -bonding in, for example, H₃SiNCS (10). It seems that Ge-X bonds are less shortened relative to the sum of covalent radii than are Si-X bonds (11). The tendency towards use of d-orbitals for π -bonding, therefore, seems to decrease from silicon to germanium.

In an attempt to interpret the character of silicon-halogen bonds, correlations of the halogen n.q.r. frequencies for series of tetrahedral derivatives of group IV (A) were sought firstly with Taft polarity parameters (12,13) and later with

with Taft-Hammett parameters (14). The latter allowed separation of inductive and conjugative characteristics. Taft originally defined a substituent constant (σ_x) describing the electron-donating or -withdrawing properties of the substituent X and a reaction constant (ρ) which was a measure of the sensitivity of the rate of reaction of B-X to changes in the polar properties of X (15). A series of values of σ_x was then established for a wide range of substituents. The earlier work (12,13) showed the generally lower sensitivity of silicon than of the chloroalkanes to the nature of substituents. This was in agreement with the early observation by Hooper and Bray (16) that the chlorosilanes have ^{35}Cl n.q.r. frequencies lower than those in corresponding chloroalkanes, by a factor of about 2.

Semin and Bryuchova (14) produced correlations of n.q.r. frequencies (ν_q) with the Taft-Hammett parameters (σ_I and σ_C) for a series of tetrahedral molecules of group IV (A), $(\text{R}_1\text{R}_2\text{R}_3\text{M}-\text{X})$. They used an equation of the form

$$\frac{\nu_q - \nu_0}{\nu_0} = \alpha \sum \sigma_I + \beta \sum \sigma_C$$

where ν_0 , α and β are constants characteristic of the $\text{M}^{\text{IV}}-\text{X}$ bond. The ratio of α to β provides a measure of the relative importance of inductive and conjugative substituent effects on $\text{M}^{\text{IV}}-\text{X}$. In the chlorine derivatives of silicon and germanium, values of the ratio $\frac{\alpha}{\beta}$ are -12.10 and -7.29 respectively, indicating that the transmission of conjugation through those atoms is not substantial.

Recent application of pulse techniques to the Stark effect in nuclear quadrupole resonance has yielded direct evidence that intermolecular forces, and perhaps π -bonding, are of minor importance in the tetrahedral derivatives of group IV (A). (17,18).

That external electrostatic fields should influence n.q.r. spectra was first predicted by Bloembergen (19). It was he who later elucidated the theory of the Stark effect in n.q.r. and developed a means of interpretation (20). The shift of the n.q.r. frequency under the influence of an external electrostatic field is written as $\frac{\partial \nu}{\partial E_z}$ where ν is the n.q.r. frequency and E_z the field. If the n.q.r. frequency is given by

$$\nu_{ij} = \frac{e^2 Q}{a_I} q_{zz} \Delta E_{ij} (\zeta) \quad (1)$$

then
$$\frac{\partial \nu_{ij}}{\partial E_z} = \frac{e^2 Q}{a_I} R_{zzz} \left\{ \Delta E_{ij}(\zeta) + \frac{\partial \Delta E_{ij}(\zeta)}{\partial \zeta} \left(\frac{R_{zxx} - R_{zyy}}{R_{zzz}} - \zeta \right) \right\} \quad (2)$$

For $I = 3/2$ and $\zeta \neq 0$, the field constant $\frac{\partial \nu_{ij}}{\partial E_z}$ is given by

$$\frac{\partial \nu_{ij}}{\partial E_z} = \frac{e^2 Q R_{zzz}}{2} \left(1 + \frac{\zeta^2}{3} \right)^{-\frac{1}{2}} \left\{ 1 + \frac{\zeta}{3} \left(\frac{R_{zxx} - R_{zyy}}{R_{zzz}} \right) \right\} \quad (3)$$

R_{ijk} are the components of the tensor $\frac{\partial q_{ij}}{\partial E_k}$. In order to relate

the shift $\left(\frac{\partial \nu}{\partial E_z} \right)$ to bond characteristics, equation 33, chapter 2 may be used in the form

$$\frac{\nu}{\nu_{\text{atomic}}} = U_p$$

where U_p is the number of unbalanced electrons in the p orbitals of the halogen. Thus defining a new parameter, reduced field

constant,
$$\frac{\partial \nu}{\partial E_z} \cdot \frac{1}{\nu_{\text{at}}} = \frac{\partial U_p}{\partial E_z} \quad (4)$$

The parameter $\frac{\partial U_p}{\partial E_z}$ is equal to the reduced field constant and

has been related to the characteristics of a halogen bond thus (20)

$$\frac{\partial U_p}{\partial E_z} = \frac{eR}{\sqrt{2}} \left\{ \frac{1}{(1-S_\sigma^2)^{\frac{1}{2}}} \Delta_\sigma - \sum \frac{1}{(1-S_\pi^2)^{\frac{1}{2}}} \Delta_\pi \right\} \quad (5)$$

R is the length of the chemical bond, S_σ and S_π are the overlap integrals of the σ and π bonds, and Δ_σ and Δ_π the differences between the ground and excited states of the electrons participating

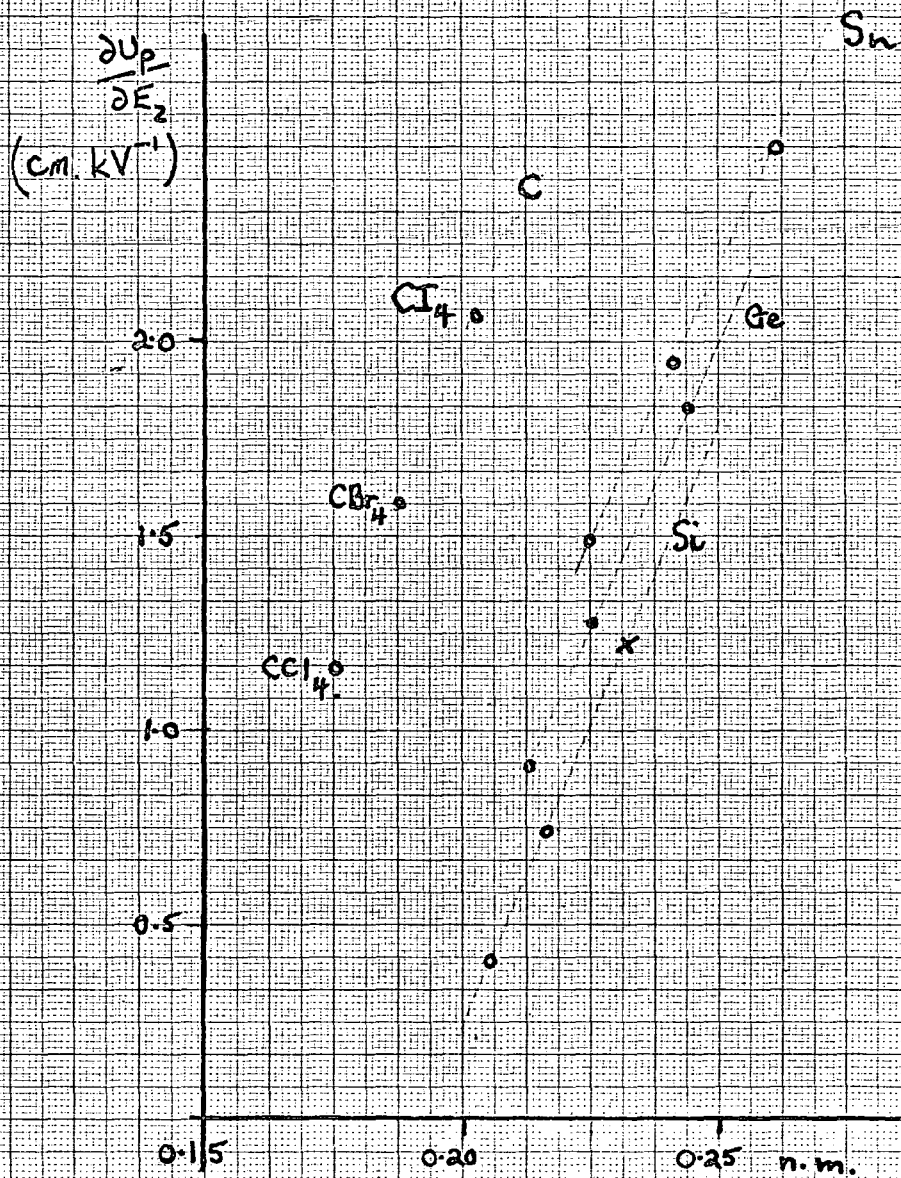
in the σ and π bonds. From this expression, it is clear that as the bond length increases so the quantity $\frac{\partial U_p}{\partial E_z}$ should increase and also that π -bonding will reduce the overall^z value of the reduced field constant.

Semin et al. (17) have shown that polycrystalline samples of organic compounds containing chlorine produce distinctive field constants depending upon the hybridisation of the carbon to which chlorine is attached, viz.

<u>Carbon</u> <u>hybridisation</u>	$\frac{\partial \nu}{\partial E_z}$ (Hz. cm kV ⁻¹)
sp ³	57.5
sp ²	45.5
sp ² _{aryl}	38.5
sp	24.5

As equation (5) predicts, this variation of field constant mirrors the variation in bond length. The value of $\frac{\partial \nu}{\partial E_z}$ is constant (within experimental error of ± 1.5 Hz.cm kV⁻¹) for a given type of bond between the element of group IV and the halogen. With additional coordination interactions absent, $\frac{\partial \nu}{\partial E_z}$ is independent of the number and nature of substituents^z to the group IV element. i.e. it is the field constant for the n.q.r. frequency. The general absence of intermolecular interactions in polycrystalline samples (at 77K) of tetrahedral halogen derivatives of Si, Ge and Sn is suggested by their linear relationship to bond length which parallels that for the carbon tetrahalides. (Fig. 1). With practical limitations upon the strength of electrical fields that may be used, the Stark effect is likely to be small (shifts of order 1 - 3 kHz) and the accuracy of the results for $\frac{\partial \nu}{\partial E_z}$ is open to question.

Fig. 1. Reduced field constants of h.g.r. frequencies, $\frac{\partial \nu_p}{\partial E_2}$, versus bond length r_{C-C} in tetrahalides of group IV elements (from Ref. 11)



More specific evidence that there is little reorganisation of the electronic charge distribution at the halogen in group IV tetrahalides has been provided by Semin, Kazakov and Bryuchova (18). They use the existing correlations of Taft substituent constants (σ^*) with halogen n.q.r. frequencies (7) in tetrahedral compounds of group IV elements, $R_1R_2R_3M^{IV}$, i.e.

$$\nu = \nu_0 + \alpha \sum \sigma^* \quad (6)$$

Division of equation (6) by ν_{at} yields

$$U_p = U_{po} + \frac{\alpha}{\nu_{at}} \sum \sigma^* \quad (7)$$

If U_p , the number of unbalanced p electrons in the halogen atoms, depends primarily upon the changes in intramolecular fields,

a relation such as

$$\frac{\partial U_p}{\partial E_z} = \frac{\alpha}{\nu_{at}} \cdot \frac{\partial \sigma^*}{\partial E_z} \quad (8)$$

should exist.

Using $\frac{\partial U_p}{\partial E_z}$ (equivalent to the reduced field constant) and the known values of α , the authors showed that a straight line closely described the relationship between $\frac{\partial U_p}{\partial E_z}$ and $\frac{\alpha}{\nu_{at}}$. They concluded that changes in the intramolecular electric fields were chiefly responsible for n.q.r. frequency variations in the M^{IV} - halogen bond. The quality of the fit to a straight line for a wide range of group IV halogen derivatives overcomes misgivings as to the reliability of the Taft σ^* correlations. Other authors have suggested that intermolecular forces in molecular crystals make only small contributions to the e.f.g. experienced by a halogen in the molecule. In an n.q.r. study of $(CH_3)_2SnCl_2$, De Bertha calculated the maximum contribution from intermolecular interaction of near neighbours to be 20% (21). A more general estimate that no more than 2% of the n.q.r.

frequency for molecular compounds is attributable to crystal lattice effects has been made (22). Gutowsky and McCall suggest that intermolecular forces in chloromethanes may account for 5 - 10% of the e.f.g. (23). A recent estimation of the relative contributions to the crystal field effect in the n.q.c.c. values of organochlorine compounds (24) has yielded the following: long range order effects, 4%; short range order effects 1-2%; polarisability of chlorine 11%.

As intermolecular interactions play such a secondary role in the strength and character of the halogen e.f.g. in molecular crystals, Graybeal and Green have proposed that measurement of the asymmetry parameter (η) of the ^{35}Cl e.f.g. in the tetra-chlorides of group IV would provide information on the nature of the $\text{M}^{\text{IV}}-\text{Cl}$ bond. (25). They postulated that values of the asymmetry parameter could furnish direct evidence for the existence of $p\pi - d\pi$ bonding. Measurement of η by Zeeman n.q.r. only reflects a difference in the π -bonding in two planes at right angles. Contending that the available d orbitals on Si, Ge, and Sn provided for 1.25 π -bonds per chlorine, they suggested that if π -bonding were present it could be asymmetric with respect to the e.f.g. (presumed to lie along the $\text{M}-\text{Cl}$ axis). Measurements by the method of Morino and Toyama (26) yielded the following results for polycrystalline samples at 77K.

CCl_4	$\eta < 0.1$
SiCl_4	$\eta = 0.45 \pm 0.10$
GeCl_4	$\eta = 0.35 \pm 0.08$
SnCl_4	$\eta = 0.25 \pm 0.07$

The conclusion of Graybeal and Green is that these values indicate a π -bonding character of the $\text{M}^{\text{IV}}-\text{Cl}$ bond of between

20 and 40% for Si, Ge and Sn. This compares with the estimates for MH_3Cl of an earlier paper based upon the Townes - Dailey approximation where the asymmetry parameter is assumed to be zero (27).

Asymmetry about an axis is precluded if there exists threefold or greater symmetry. For a purely tetrahedral molecule MCl_4 , therefore, the asymmetry parameter should be zero. In a single crystal n.q.r. investigation upon SnBr_4 , Shimamura found a value for η of ≤ 0.025 (28). Limited molecular distortion has however been found to exist in the solid form of SnBr_4 (29). A single crystal X-ray determination of the structure of carbon tetrachloride at 195K has, by contrast, revealed that the molecules are all regular tetrahedra (within experimental error) (30). The unit cell contains four molecules in which there are sixteen crystallographically unique C-Cl distances, the average of which is 17.73nm. This is in agreement with the sixteen-line n.q.r. spectrum observed for polycrystalline carbon tetrachloride at 77K. However, it is possible that some distortions take place in the higher group IV tetrachlorides. Their tetrahedral symmetry (T_d) prevents the observation of their microwave spectra and therefore the measurement of their gas phase nuclear quadrupole coupling constant. A comparison of the gas (microwave) and solid phase (n.q.r.) values of e^2qQ would have helped quantify the contribution due to distortion.

N.q.r. results show a lower sensitivity of chlorosilanes to substituent effects in comparison with those of chloroalkanes and chlorogermans. Lucken (31) has suggested that this insensitivity may be due to the effects of π -bonding between the outer

3d orbitals of silicon and the lone pairs of the halogen atoms. Such double-bonding has often been ascribed to elements of the second short period which possess empty, low-energy d-orbitals (3d). Lower sensitivity to substituents for chlorosilanes may be explained in this way: consider the chlorosilane, $R-SiCl_3$, in which R is an electron-withdrawing substituent. R removes electronic charge from both σ - and π -orbitals leaving the difference between them little changed and hence the n.q.c.c. little altered. The n.q.r. frequency does not therefore change much. However, in the cases of substituted chloroalkanes ($R-CCl_3$) and chlorogermanes ($R-GeCl_3$), where the π population on chlorine is fixed at 2, removal of electronic charge from σ -orbital does change the coupling constant and therefore the n.q.r. frequency. Lucken states that in the highly symmetrical compounds $R-M^{IV}Cl_3$ and $M^{IV}Cl_4$ this partial double bonding would not be revealed by measurement of the asymmetry parameter (η) which, crystal field effects apart, should be zero. Indeed, for the tetraiodides of group IV, where η can be determined from the iodine n.q.r. frequencies, the asymmetry parameters are found to be zero.

The weight of evidence against the results of Graybeal and Green suggested to the author that a reinvestigation of the Zeeman lineshapes for $SiCl_4$ and $GeCl_4$ might be of value.

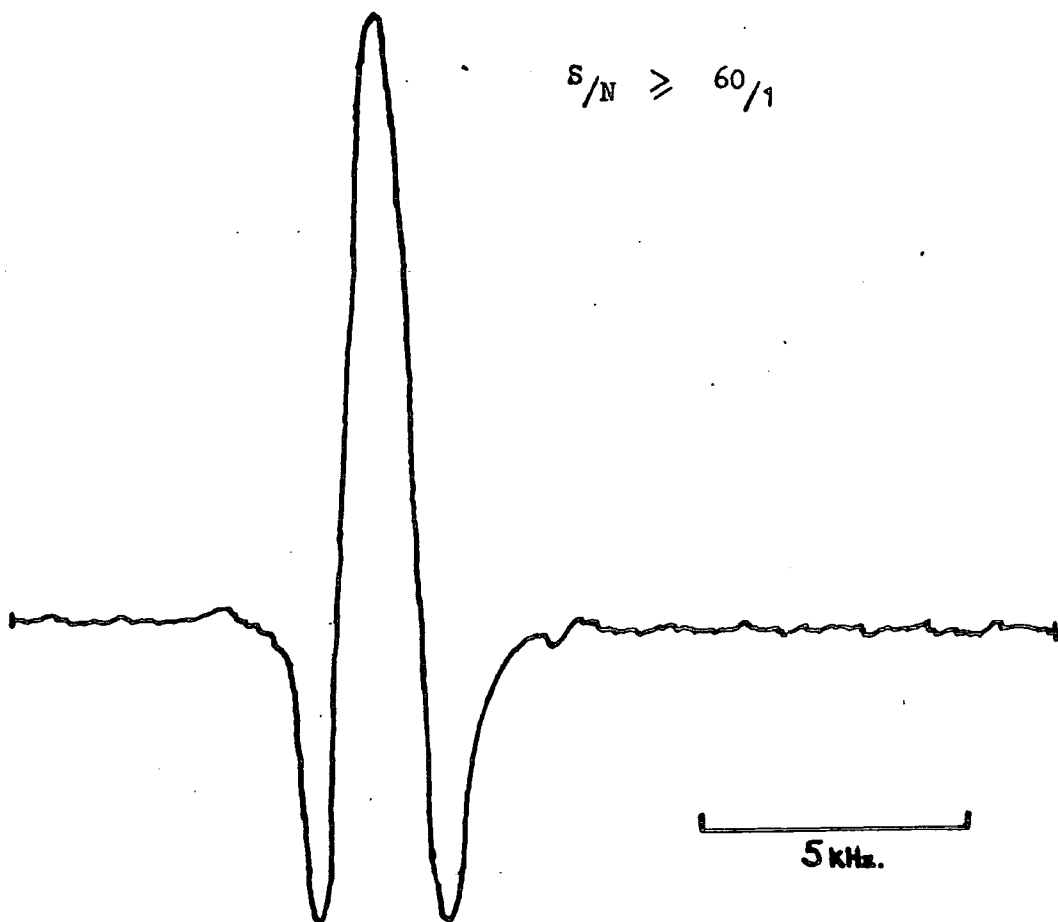
Graybeal and Green measured the asymmetry parameters in polycrystalline samples of group IV tetrachlorides using a self-quenched super-regenerative oscillator (S.R.O.) spectrometer (25). In the present study, a Robinson type spectrometer as described in Chapter 3 was used. This spectrometer gave high signal strengths without possible interference from side bands when operated in the frequency-modulated mode. Sinusoidal Zeeman modulation did not produce such high strengths and was not needed because no spurious resonances occurred near to the resonance frequencies. The magnetic field applied to the samples was generated by the Helmholtz coils also described in Chapter 3.

The investigation of Zeeman lineshapes was concentrated on silicon tetrachloride and germanium tetrachloride because much lesser fields had been used by Graybeal and Green with these than with tin tetrachloride (25). Figures 2 and 9 show zero field lineshapes for silicon- and germanium-tetrachloride respectively. The purity of lineshape produced by the present spectrometer is demonstrated with linewidths of 2.5 - 3.5 kHz obtained.

A method of determining the asymmetry parameter of chlorine in polycrystalline compounds has been developed by Morino and Toyama (26). The method is described above (Chapter 3) and makes use of certain measurements (δ_2) taken from the broadened lineshapes obtained at varying magnetic field strengths. These measurements (δ_2) have been related to the asymmetry parameter but extrapolation to infinite field strength is required. A minimum field strength should be exceeded for results to be significant (25) i.e.

$$H > \frac{2\pi \cdot \Delta\nu}{\gamma \cdot \delta}$$

Fig. 2 ^{35}Cl n.o.r. SiCl_4 at 77K, $I = 0$



or, in the case of ^{35}Cl , $H > \frac{\Delta\nu}{\eta \cdot (0.41)} \times 10^{-4}$ Tesla.

The minimum fields required for silicon tetrachloride

($\Delta\nu \sim 2.5$ kHz) and germanium tetrachloride ($\Delta\nu \sim 3.5$ kHz)

are given below:

$$\text{for SiCl}_4, \quad H > (6.1) \cdot \frac{1}{2} \times 10^{-4} \text{T}$$

$$\text{for GeCl}_4, \quad H > (8.5) \cdot \frac{1}{2} \times 10^{-4} \text{T}.$$

Darville (32) has, however, shown that accurate measurements of η are possible at fields below this 'minimum' if features are sufficiently well resolved. Values of δ_i have, therefore, been recorded for such spectra, there being no discernible difference within the experimental errors.

A further restriction on the method is that, due to approximations, Morino and Toyama placed a limit on the range of asymmetry parameter values which could be accommodated. A value of $\eta = 50\%$ is taken as the ceiling, after which serious errors are introduced. Partly for this reason, methods of lineshape simulation have been developed with field strength and η among the variables. The method should allow determination of large values of the asymmetry parameter by the comparison of experimental and simulated lineshapes. Brooker and Creel (33) have reported such a simulation system which calculates the powder lineshape for any value of η and presents frequency expressions exact in η and magnetic field (H) for the main features of the pattern. Any value of η or H may be taken without the introduction of serious error into the resultant lineshape. Initial (zero field) linewidth characteristics are matched to an experimental $I = 3/2$ n.q.r. line. It is then possible to vary the values of η and the magnetic field. After fixing the magnetic field (in Gauss), a value of η may be determined for the n.q.r. signal by comparing simulations of varying η with an experimental Zeeman lineshape.

Whichever simulation most closely matches the experimental lineshape in the frequencies of features yields the value of λ . Brooker and Creel have applied this technique to the lineshapes obtained by Graybeal and Green. Use has been made of the Brooker and Creel method and reference to the predicted lineshapes is made later. The results obtained by the author are now reported.

Silicon Tetrachloride

Following the suggestion of Graybeal and Green, the lowest n.q.r. frequency (20.273 MHz @ 77K) was used in order to avoid interference between the four quadrupole resonances of silicon tetrachloride. This line does not overlap with the others when broadened by the magnetic field because it lies at least 135 kHz to low frequency of them. A value of 0.45 ± 0.10 was reported for the asymmetry parameter by Graybeal and Green who used a maximum field of 1.6 mT.

Table 1 and Fig. 4 include data on various δ measurements. δ_1 , δ_2 and δ_3 are defined in Fig. 6b) (Chapter 1). Measurements of $\frac{\delta_i}{2\nu_H}$ are summarised in Table 1 and are plotted against the inverse of field strength (measured as current through the coils) in Fig. 4. The measurement of δ_i uses accurate frequencies but an element of estimation is needed to fix the limits of the measurements. For this reason, the error in $\frac{\delta_i}{2\nu_H}$ is estimated as equivalent to the scatter of points. Extrapolation to $\frac{1}{H} = 0$ also involves estimation; for example, the slight upward turn of $\frac{\delta_1^+}{2\nu_H}$ at high fields makes plausible an estimate for η of about 0.6. Certainly a minimum value of 0.35 - 0.40 is indicated for $\frac{\delta_1^+}{2\nu_H}$, which Darville (32) has suggested to be closely related to a minimum value for η . The values of $\frac{\delta_i}{2\nu_H}$, and therefore the value of η , are dependent on the value of the Larmor frequency, ν_H . The values of $2\nu_H$ calculated from the applied current and the calibration of the coils ($23.090 \times 10^{-4} \text{ T.A.}^{-1}$) were found to be in good agreement with those measured on the spectra (See Fig. 3).

Brooker and Creel have developed a computer simulation for the

Fig. 3a) - INVERTED spectrum

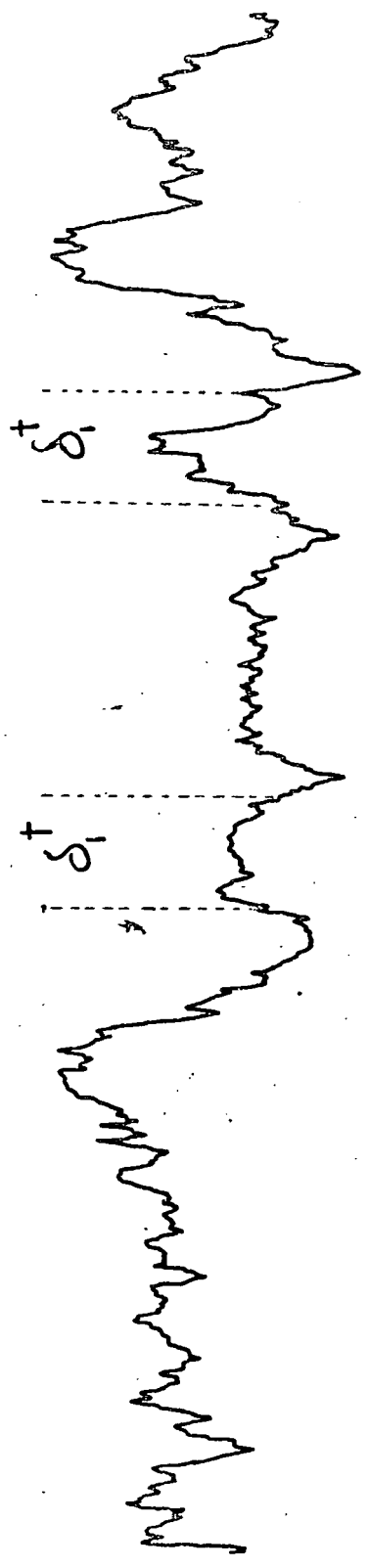
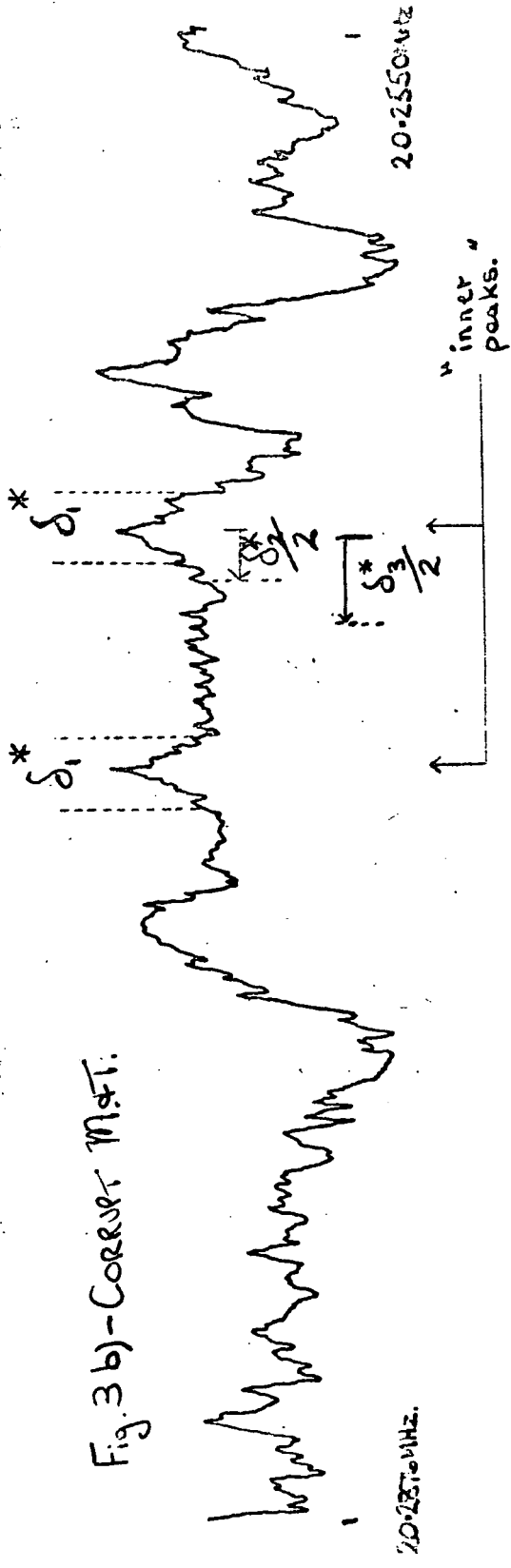


Fig. 3 b) - CORRECT M.F.T.



← $2\nu_H$ →

"inner peaks"

20.2550 MHz.

20.2550 MHz

^{35}Cl n.g.r. SiCl₄ at 77K $I = 0.45$ amps.
 $\equiv H = 10.39 \times 10^{-4}$ Tesla.

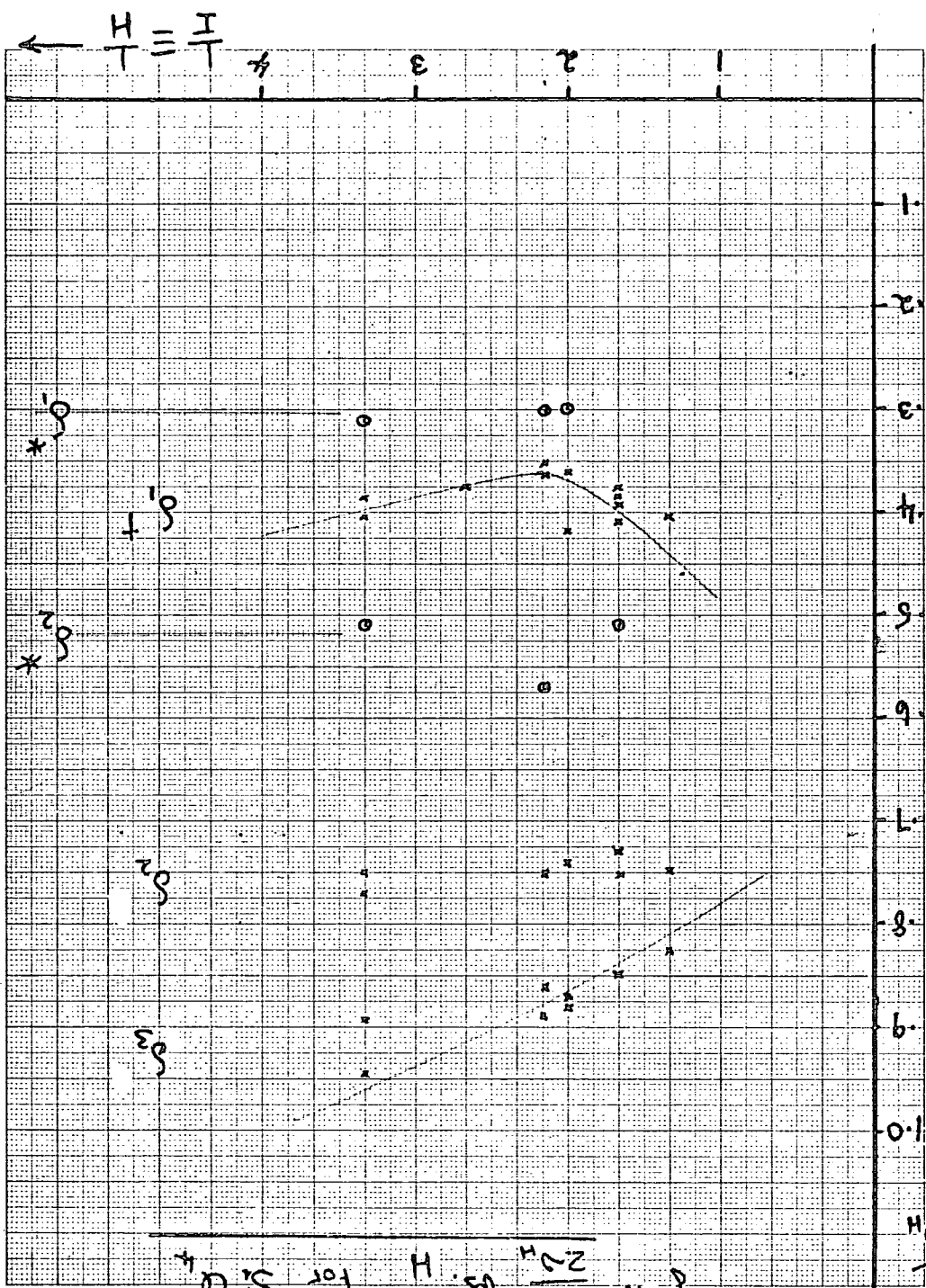


Fig. 4 $\frac{H}{2I}$ vs. $\frac{H}{I}$ for $S_i C_i$

$\frac{H}{2I}$

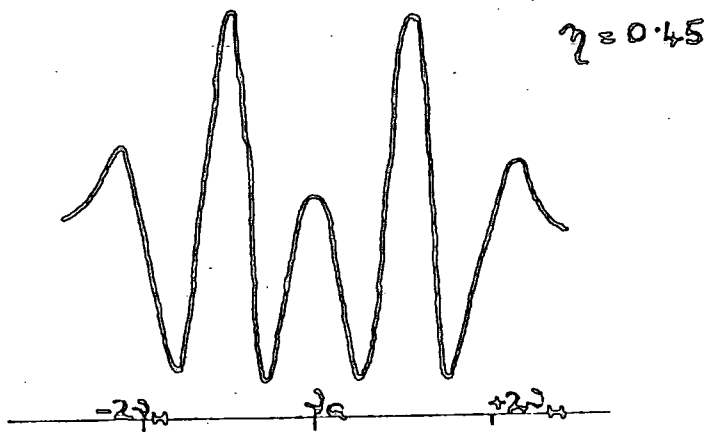
TABLE 1

	SiCl ₄						
I (amps.)	.3	.375	.45	.5	.6	.7	.75
H (mT.)	.693	.866	1.039	1.155	1.385	1.616	1.732
$\frac{\delta_1}{2\nu_H}$.405	.375	.364	.42	.392	-	.404
	.385 (.31)		.350 (.30)	.360	.385 .376		
$\frac{\delta_2}{2\nu_H}$.769	-	.750	.738	.750	-	.747
	.750	-			.729		
$\frac{\delta_3}{2\nu_H}$.946	-	.880	.880	.849	-	.820
	.896		.860	.870			

n.q.r. powder lineshapes, split by a magnetic field parallel to the n.q.r. spectrometer sample coil, (31). Their paper makes reference and comparison to that of Graybeal and Green. Using the zero field lineshape characteristics and the field strength (8×10^{-4} Tesla), as reported by Graybeal and Green, they have presented simulated lineshapes for various values of η . The simulated lineshape for $\eta = 0.45$ (the value determined by Graybeal and Green)(Fig. 5) is, they suggest, quite unlike the observed lineshape (25)(Fig. 6). They report that much closer similarity between the observed and simulated lineshape is achieved when using an asymmetry parameter of 0.8 (Fig. 7). The significance of this conclusion was not developed except for suggesting that the spectra of Graybeal and Green failed to resolve all the features of the lineshape at this field strength. Under comparable conditions of linewidth and field strength, the lineshape observed by the author differs from that of Graybeal and Green and from that of Brooker et al. (Fig. 3). However, similarity between the simulated lineshape of Brooker for $\eta = 0.45$ (Fig. 5) and Fig. 3 can be seen if one is inverted (3a). Careful checks upon experimental lineshape development leads the author to conclude that an error in sign in the development by Brooker and Creel has caused the need for inversion. Subsequent conclusions based on comparisons with simulated lineshapes assume this inversion of the simulated one.

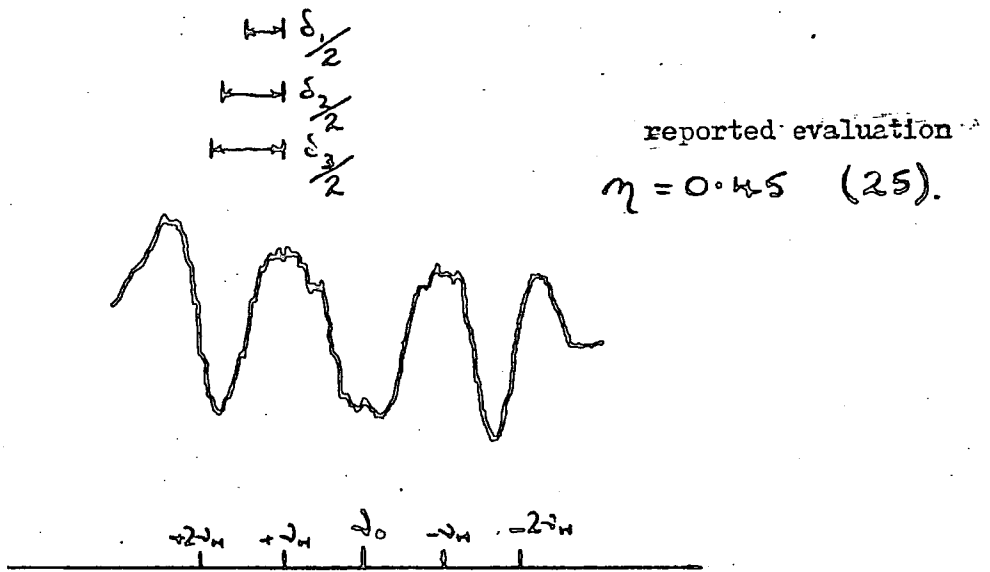
Closer examination of the relationship between Zeeman n.q.r. lineshapes produced by Graybeal and Green and those recorded in this work has prompted the author to propose that the earlier workers inverted their spectra also before carrying out the Morino and Toyama analysis. The spectra may have been inverted in order that measurements might be made upon the better defined features.

Fig. 5



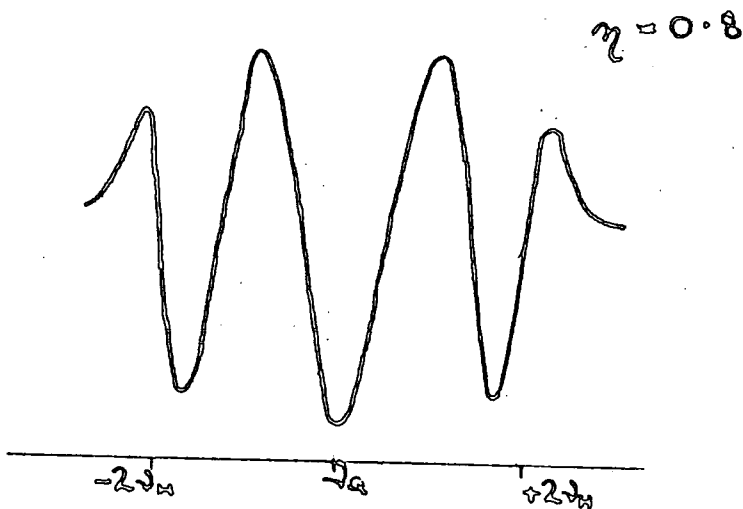
Computer simulated second derivative trace with parameters adjusted to fit experimental conditions under which SiCl_4 (ref. 19) was generated.

Fig. 6



Observed envelope shape of the ν_1 ^{35}Cl quadrupole resonance of SiCl_4 at 77K for a static magnetic field of 0.8 mT - from ref. 25.

Fig. 7



Computer simulated second derivative trace with parameters adjusted to obtain qualitative agreement with the trace of Fig. 6. Note required ζ value.

Compare Fig. 6 with Fig. 3 (Fig. 3b - spectrum as recorded; Fig. 3a - the same inverted). The magnetic fields are both approximately 0.8 mT and an approximate fit of lineshapes is found. The proposal that Zeeman spectra were inverted by Graybeal and Green was further investigated by measurement of δ_1^+ as illustrated in Fig. 3a. The corresponding plot in Fig. 4 follows the characteristic shape for such "Morino and Toyama" plots and yields a value for η of between 0.4 and 0.6. It is believed that this relates to the value of 0.45 ± 0.10 reported by Graybeal and Green.

The variation in δ_1 about the "inner peaks" (shown in Fig. 3b) seen in the majority of Zeeman lineshapes is plotted in Fig. 4. The points are distinguished as δ_1^* . As is shown below, these inner singularities do not lie centred on $\nu_Q \pm \nu_H$ as do those normally monitored by the Morino and Toyama method. (They are included on account of the compatibility of the results i.e. $\eta \approx 0.45$, with that yielded by the simulation method). The results are therefore designated as of "corrupt Morino and Toyama" origin. In general, spectra similar to that in Fig. 3b yielded the plots of Fig. 4, from which we determine that $\eta = 0.4 - 0.6$. An idealised lineshape intermediate between those of Figs. 5 ($\eta = 0.45$) and 7 ($\eta = 0.80$) may be expected from the Brooker and Creel simulation. Numerous simulations reveal that as η approaches a value of one, the inner singularities, previously centred on $\nu_Q \pm \nu_H$, start to approach one another, until at $\eta = 1$ they coalesce at the n.q.r. frequency, ν_Q . Inner peaks are identified in Fig. 3b. That some movement of these has occurred (indicating η approaching 0.8) is supported by the generally high values of $\frac{\delta_2}{2\nu_H}$ and $\frac{\delta_3}{2\nu_H}$ seen in Fig. 4. The values of δ_2 and δ_3 are more susceptible to the position of the trough or minimum beyond $\nu_Q \pm \nu_H$ than is δ_1 .

If the peaks had shifted closer together, values of δ_2 and δ_3 would then tend to be raised. The observed values of $\frac{\delta_2}{2\nu_H}$ and $\frac{\delta_3}{2\nu_H}$ reflect such an increase. On the grounds of this development from simulation lineshapes (Figs. 5 and 7) and general compatibility with the results from the Morino and Toyama extrapolations, a value of 0.6 is reported for ξ in SiCl_4 .

Germanium Tetrachloride

In an manner similar to that used for silicon tetrachloride, a determination of the ^{35}Cl asymmetry parameter has been made for the lowest frequency quadrupole resonance of germanium tetrachloride. The results are displayed in Table 2. A plot of $\frac{\delta_i}{2\nu_H}$ against the inverse of field strength (H) is shown in Fig. 8. This plot was obtained from measurements made upon spectra similar to those of Figs. 9, 10 and 11 in which the magnetic fields are zero, 0.693 and 1.039 mT. (10^{-3} Tesla) respectively.

The Zeeman lineshapes obtained at fields of 0.693 - 2.078 mT are again at variance with those reported by Graybeal and Green and with the $\eta = 0.45$ (0.80 mT) simulation of Brooker and Creel. Inner peaks are clearly evident which, as in the case of SiCl_4 , are no longer centred on $\nu_Q \pm \nu_H$ but have shifted towards ν . Fig. 8 includes plots for δ , taken about these inner peaks (δ_i^*) and for δ , taken about the "troughs" on either side (δ_i^+). The measurements about the troughs are, the author suggests, analogous to those measurements made by Graybeal and Green who, he believes, inverted their spectra to furnish measurements about better defined features. Compare Fig. 11 (H = 1.039 mT) with Figs. 12, taken from the article by Graybeal and Green. The differences between the slope of the base-line in the zero-field lineshape and those in the lineshapes of 0.6 and 1.0 mT should be noted. The author suggests that a pair of inner peaks can be discerned in Figs. 12c and 12d. If inverted, Fig. 12c compares closely with Fig. 11.

The author believes that the measurements recorded in Fig. 8 as δ_i^* are inappropriate for the determination of η by the method of Morino and Toyama (N and T). As before, they have

Fig. 8 $\frac{\delta_i}{2\psi_H}$ vs. $\frac{1}{H}$ For GeCl_4

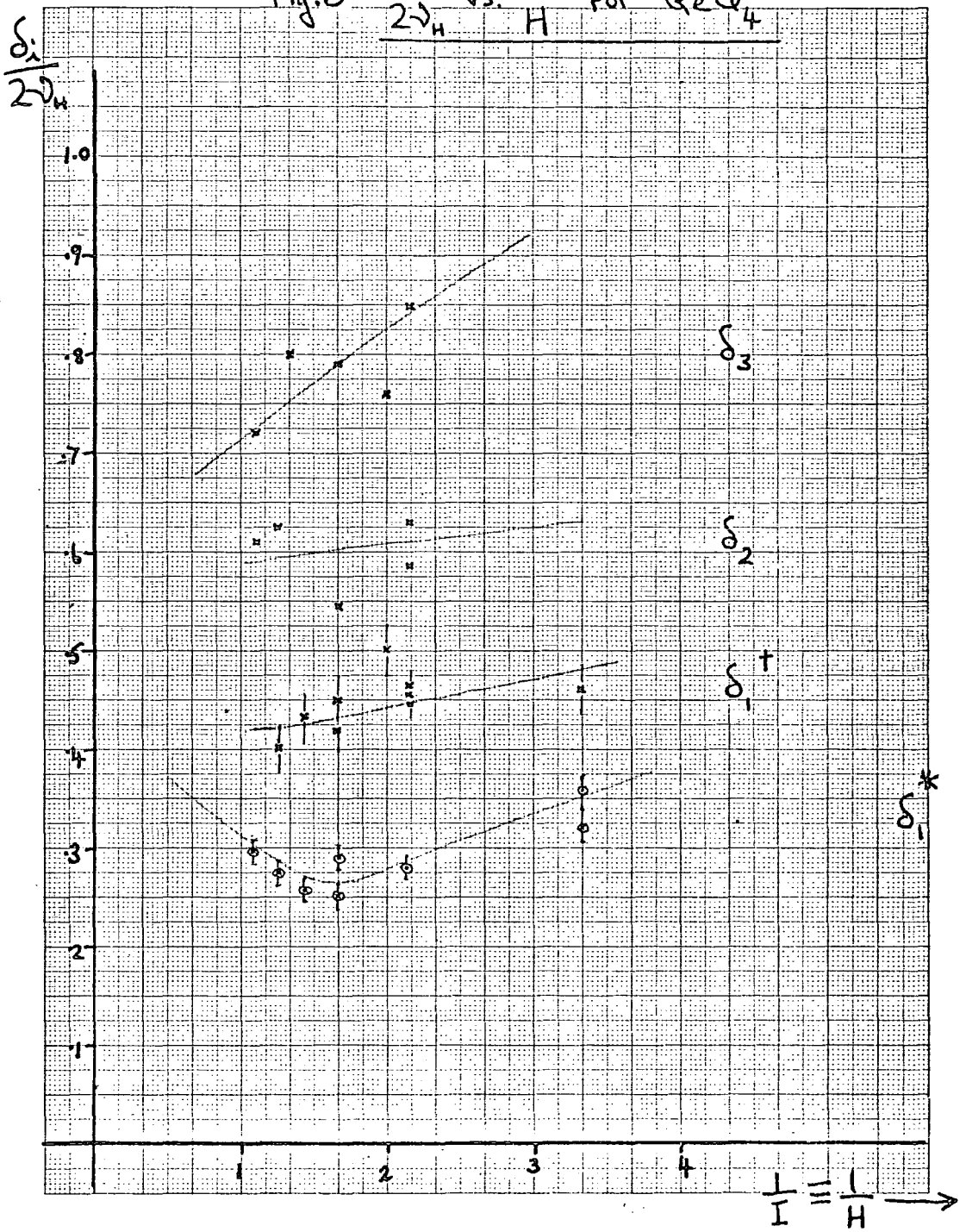


Fig. 9 ³⁵Cl n.q.r.

GeCl₄ at 77K, I = 0 amp.

$\nu_Q = 25.451$ MHz, S/N $\geq 90/1$

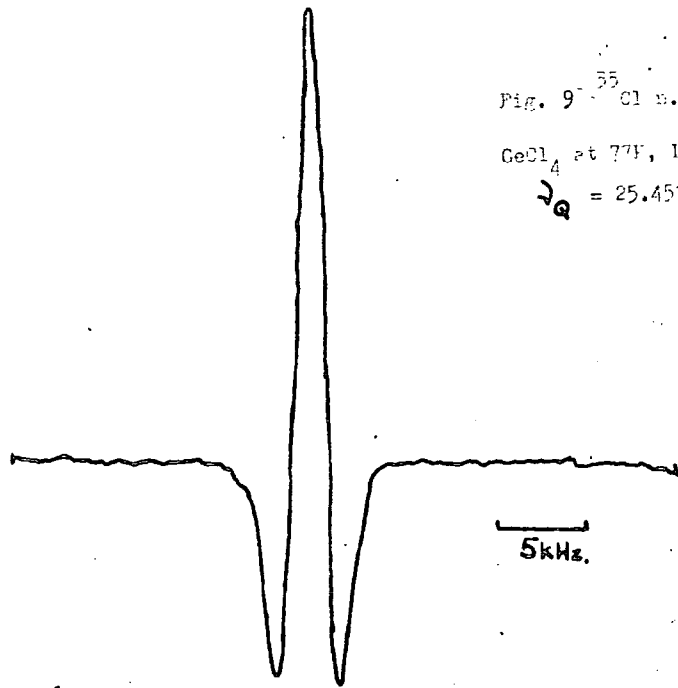
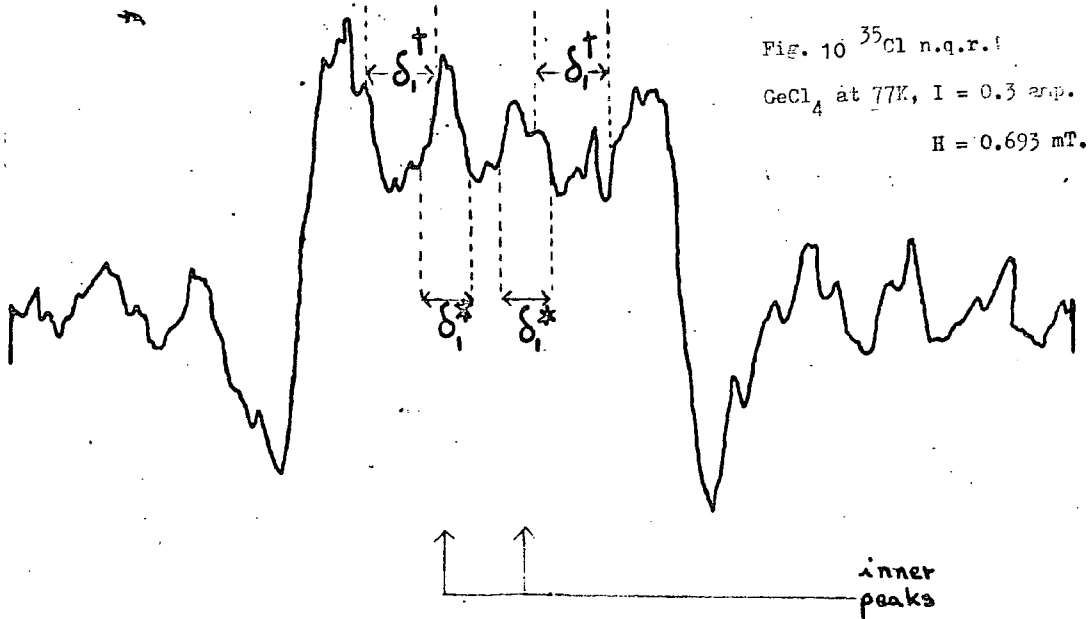


Fig. 10 ³⁵Cl n.q.r.

GeCl₄ at 77K, I = 0.3 amp.

H = 0.693 mT.

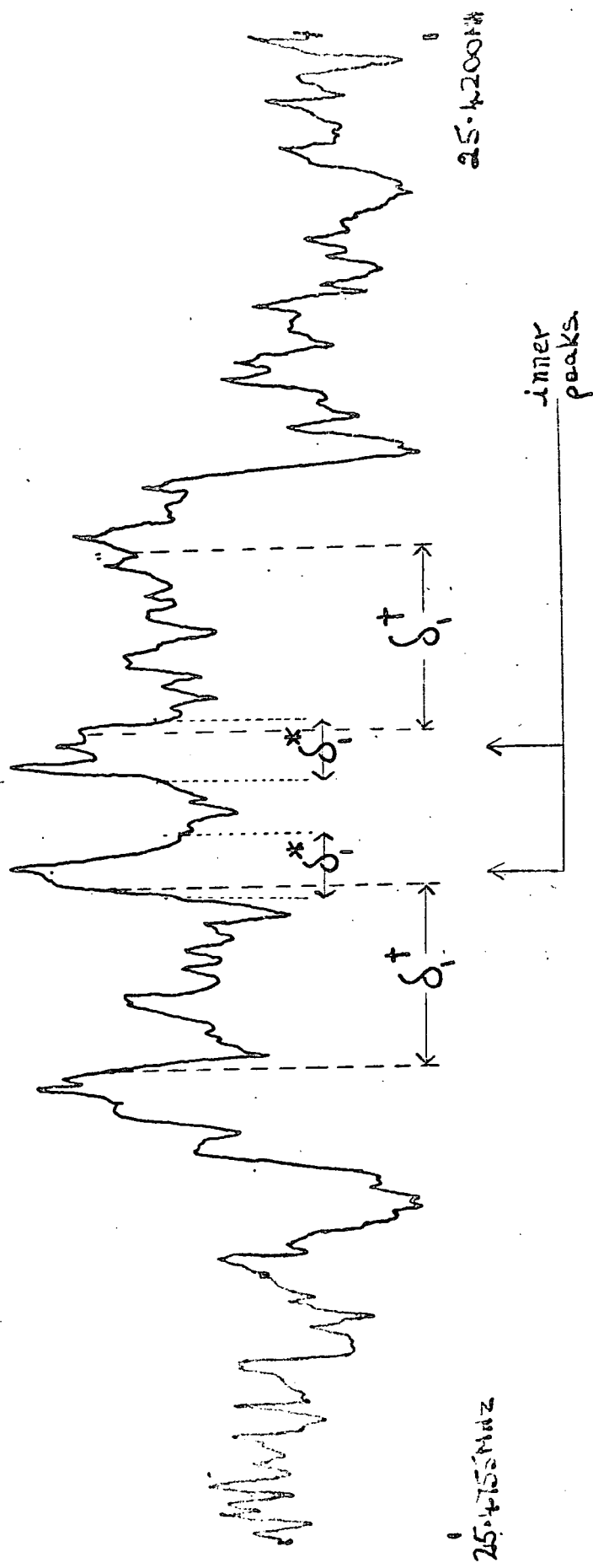


25.463 MHz.

2.5 MHz

25.430

Fig. 11. ^{35}Cl n.g.r. GeCl_4 at 77K, $I = 0.45 \text{ amp.}$, $H = 1.039 \text{ mT.}$



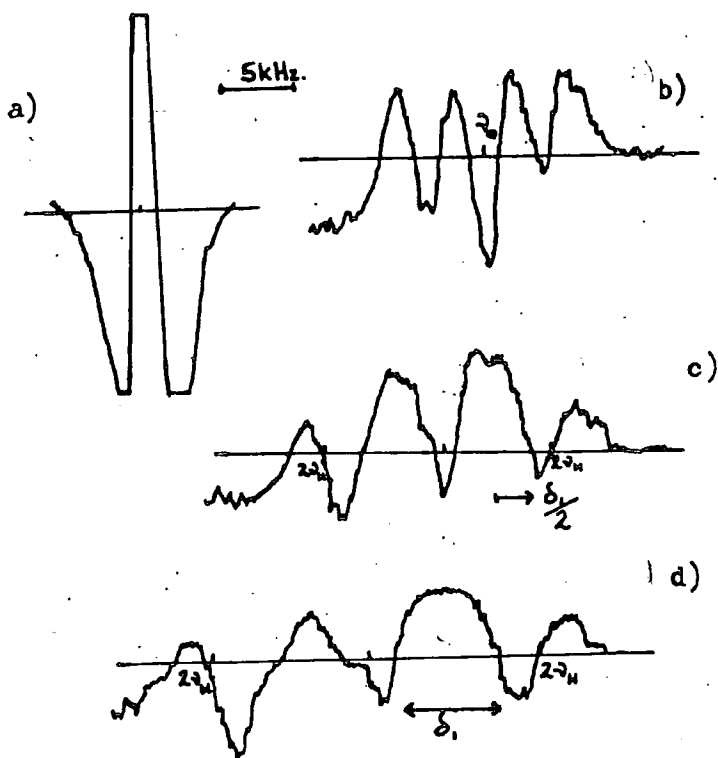


Fig. 12. ^{35}Cl Zeeman n.q.r. lineshapes GeCl_4 at 77K

Magnetic fields a) 0 mT., b) 0.6 mT.,

c) 1.0 mT., d) 1.5 mT.

Taken from ref. 25, p. 2952

been denoted "corrupt M and T" measurements. Those measurements shown as δ_1 would yield an estimate for η of between 0.35 and 0.45 which agrees closely with those reported by Graybeal and Green (0.35 ± 0.08). This lends weight to the suggestion that they are the measurements used by Graybeal and Green and to the suggestion that spectra were inverted. The measurements shown in Fig. 8 as δ_2 and δ_3 are taken about the inner peaks and so, with δ_1^* , suggest for the "corrupt" Morino and Toyama method a value for η of between 0.4 and 0.6.

As was suggested in the case of silicon tetrachloride, the inner peaks may be compared with those features observed in the simulated Zeeman lineshape of Fig. 5, if this figure is inverted. It has been suggested that a possible error in sign during the development by Brooker and Creel may have caused a need for inversion.

Assuming this requirement, comparison of inverted Fig. 5 and the Zeeman lineshapes obtained for GeCl_4 leads the author to propose that η lies between 0.4 and 0.6.

Discussion

The results obtained from the investigations on silicon and germanium tetrachlorides yield values of the asymmetry parameter (η) substantially in agreement with those of Graybeal and Green. It is, however, from comparisons with lineshape simulations and not with the Morino and Toyama method that the present values result. The δ_i measurements used by Graybeal and Green were illustrated in their article and are shown in Figs. 6 (SiCl_4) and 12 (GeCl_4). It is proposed that they inverted the Zeeman n.q.r. lineshapes before their analysis. Measurements (δ_i) seem to have been made upon features of the lineshapes which are apparent as peaks only because the lineshapes have been inverted. Such measurements have been illustrated in Figs. 3a) and 11 and are marked δ_i^\dagger . Resulting values of $\frac{\delta_i}{2\nu_n}$ are shown by the author in Figs. 4 (SiCl_4) and 8 (GeCl_4). It is the belief of the author that the lineshapes obtained by Graybeal and Green did not possess sufficient detail to display clearly the inner peaks shown to be present in this work. If such peaks had been observed, it is unlikely that such an inversion would have been made. The failure to observe these peaks, clearly visible in Figs. 10 and 11, may be due to Graybeal and Green using an s.r.o.-type spectrometer, which probably did not have the lineshape fidelity found in the present Robinson spectrometer.

There is sufficient disparity between the lineshapes reported in this thesis and the idealised lineshapes of Morino and Toyama to suggest that their method is inappropriate. It is surprising, therefore, that measurements of δ_i^* about the inner peaks do give the characteristic variation with field strength, yielding a value of η which is in reasonable agreement with that of the

simulation or, at least, is in agreement if the lineshape simulations are themselves inverted. The change in lineshape as η rises above, say, 0.5 strongly suggests that determination of large values of η should make use of such simulations. Further investigation of lineshape changes for high values of η should be made to determine the appropriateness and accuracy of the Morino and Toyama method in such instances.

Using the Townes Bailey approximation - equation 44, chapter 2 - an estimate of 20-30% is found for the π -contribution to the $M^{IV}-Cl$ bond in the group IV tetrachlorides, $M^{IV}Cl_4$. Whitehead and Jaffé (34) attempted to make allowance for the involvement of p_π electrons on chlorine in the bonding and from orbital electronegativities calculated a π -character of approximately 30-40% for the higher members ($M^{IV} = Si, Ge, Sn$). A formula originally developed for the estimation of π -character in the C-Cl bond of substituted chlorobenzenes makes use of measured η values (35). The difference in occupancy of p_x and p_y orbitals of chlorine can be calculated thus:

$$\pi_x - \pi_y = \frac{2}{3} \eta \left(\frac{e^2 q Q}{e^2 q_0 Q} \right)$$

For $\eta = 0.45$, the value of $\pi_x - \pi_y$ is 0.138 while for $\eta = 0.6$, the value is 0.144. These values are however greater than those determined in the more favourable case of benzyl chloride. Although the difference in contributions ($\pi_x - \pi_y$) could be accommodated in the total estimates of π -character for the $M^{IV}-Cl$ bonds, it does not seem very plausible. In developing the case for such π -contributions, Graybeal and Green suggest that the central silicon or germanium atom may make use of the empty d^5 orbitals to accept π -backbonding from the chlorine atoms. They argue that such a set can only supply 1.25 π -bonds per chlorine thereby

providing the opportunity of unequal contributions of p_x and p_y orbitals. Some credence for this proposal is furnished by the low asymmetry parameter reported by Graybeal and Green for carbon tetrachloride where on C no such vacant d-orbitals are available. Countering this, however, is the observation that straight lines can relate ^{35}Cl n.q.r. frequencies to the number of methyl groups in the group IV tetrachlorides (Fig. 13). The replacement of chlorine by methyl groups might have been expected to reduce the π -contributions. This, coupled with the known inductive effects of methyl groups, should have yielded a less regular correlation. The measurement of η in SnMe_2Cl_2 as 0.36 may however indicate that the consequences upon π in the $\text{M}^{\text{IV}}-\text{Cl}$ bond are minor (21). Nonetheless, the values found for the asymmetry parameter in silicon- and germanium- tetrachloride (viz. $\eta = 0.4 - 0.6$) are incompatible with any asymmetry expected from intramolecular effects alone.

The structures of solid- and liquid- phase carbon tetrachloride have recently been reported (30, 36). Granada et al. have compared the bond lengths $\text{M}^{\text{IV}}-\text{Cl}$ for the group IV tetrachlorides as determined in gas-, liquid- and solid-phases. Close agreement between liquid and gas determinations was found but, with the exception of carbon tetrachloride, the other tetrachlorides showed marked increases in $\text{M}^{\text{IV}}-\text{Cl}$ bond length in the solid phase. The greatest increase was in silicon tetrachloride. This may partially explain why the ^{35}Cl n.q.r. frequency of SiCl_4 is lower than that of GeCl_4 .

The bond orders of group IV tetrahalides have been determined

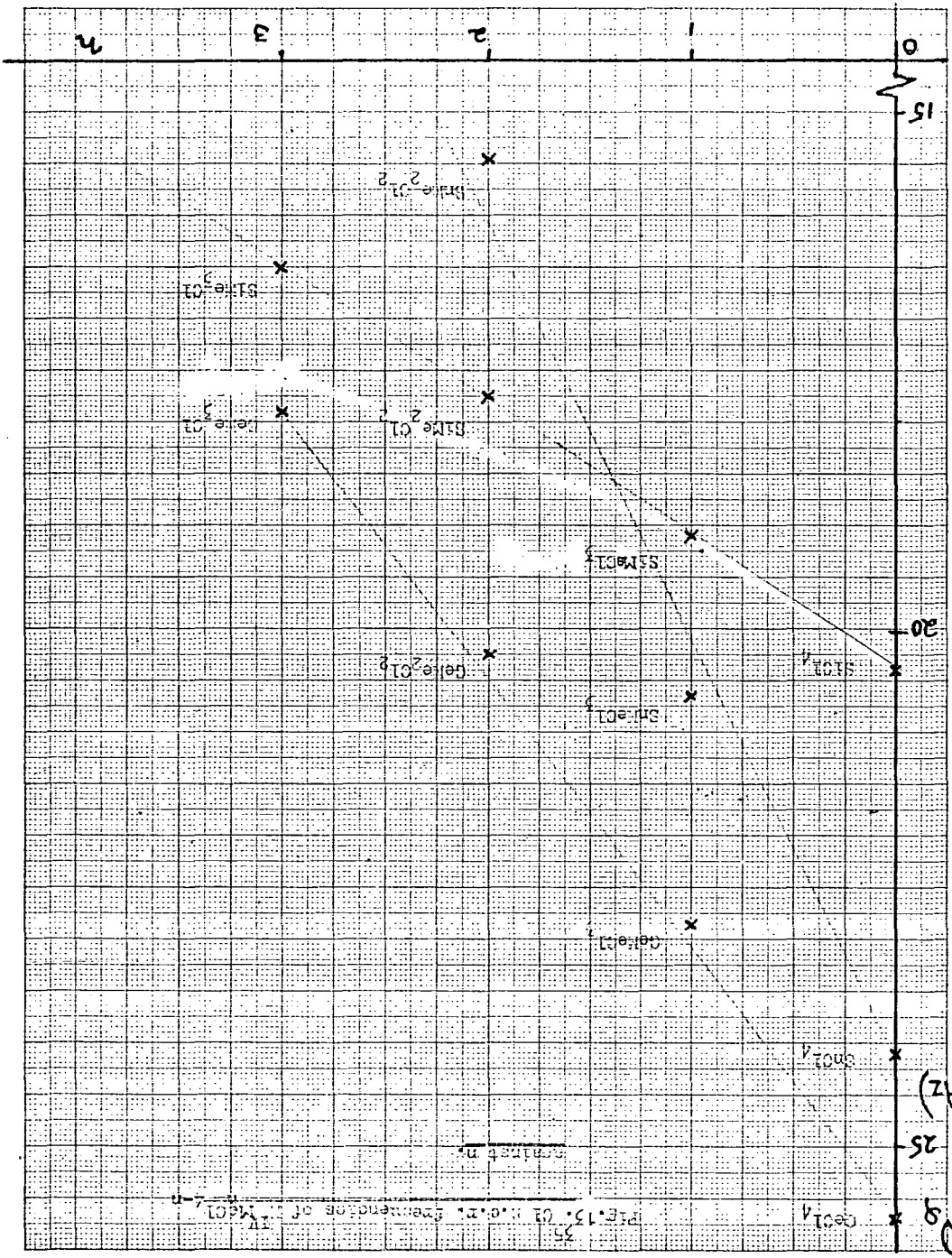


FIG. 15.01. Dependence of μ on ω

(MHz)

25

30

from absolute intensity measurements of Raman and infra-red absorptions of their solutions (37). A comparison of results obtained from a variety of techniques suggests that no one method may be regarded as definitive. It would appear from the solution measurements that the M^{IV} - Hal bond orders increase $Si \rightarrow Ge \rightarrow Sn$ within any tetrahalide. Using solid state n.q.r. results with the orbital electronegativity procedure (38), calculation suggests a minimum bond order for silicon tetrahalides.

Taken together the above results point to a weakening of the M^{IV} - Cl bond (especially Si-Cl) in the solid state which may be the result of significant intermolecular interactions. These may lead to changes in orbital occupancy of the chlorine atoms causing asymmetry in their electric field gradient. A possible source of this interaction is now explored.

Tin tetrabromide has an n.q.r. spectrum consisting of three lines grouped together with a fourth line at noticeably lower frequency. Shimomura has suggested that the group IV tetrachlorides (SiCl_4 , GeCl_4 and SnCl_4) which have similar spectra are isomorphous with SnBr_4 (28). Although a considerable amount of double bonding was expected for the Sn-Br bond, he has determined the asymmetry parameter (η) as less than 0.025. The small value of η is ascribed to the 3-fold symmetry character of the SnBr_4 molecule about the Sn-Br bonds. In an earlier paper, Shimomura investigated the ^{127}I n.q.r. of silicon-, germanium- and tin- tetraiodides (39). Values of near zero were also found for the asymmetry parameters of the tetraiodides but their spectral pattern differed from that of tin tetrabromide. The doublet of 3:1 intensity ratio and about 1 MHz separation may be explained in terms of their crystal structure. In the tetraiodides, the unit cell consists of two $\text{M}^{\text{IV}}\text{I}_4$ tetrahedra with two planes facing each other. The six iodine atoms of the planes yield the stronger lower frequency n.q.r. line whilst the iodine atoms at the opposing extremes produce the weaker line.

From the results of his single crystal study on tin tetrabromide, Shimomura deduces the existence of a pair of SnBr_4 tetrahedra, whose interactions with each other are more pronounced than those with the other neighbouring molecules. The spectral pattern helps determine that in this case the two tetrahedra approach one another through apical bromine atoms. In the absence of any intermolecular interactions, this arrangement would yield a doublet with the stronger resonance to higher frequency. However, weak interactions produce crystal splittings on the higher frequency resonances. The weaker line appears about 2.5 MHz to low frequency which may

indicate that the apical intermolecular interactions are quite substantial.

In the present polycrystalline Zeeman n.q.r. examination of silicon tetrachloride and germanium tetrachloride, it is tempting to draw a comparison with the tin tetrabromide investigation. If the compounds in the crystalline state are isomorphous, the presence of intermolecular interactions seems likely. That they are concentrated on the atoms with the lowest n.q.r. frequencies is very interesting. These are the lines upon which the present studies have been made. The author does not find the values of 0.4 - 0.6 for ζ acceptable on chemical grounds. It seems more likely that some aspect of the Zeeman n.q.r. investigation is at fault. He proposes, therefore, that intermolecular interaction takes place and that this may disturb the e.f.g. at the chlorine atoms generating the lowest ^{35}Cl quadrupole resonance. Various influences have been cited as the possible cause of the inconclusive Zeeman n.q.r. results upon mercury II chloride (40,41). The author believes that here too interference has yielded perverse results.

1) THE ASYMMETRY PARAMETER IN THE P-Cl BOND

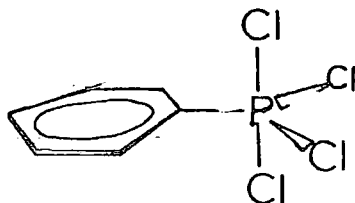
The π -character of the P-Cl bonds in tetrachlorophenylphosphorane has been estimated. A determination of the e.f.g. asymmetry parameter at the equatorial chlorine atoms of this trigonal bipyramidal molecule is reported.

Introduction

The P-Cl bond has been investigated by ^{35}Cl n.q.r. in a variety of compounds including PCl_5 (1,2), $(\text{PnCl}_2)_n$ ($n = 3,4$) (3), alkyl- and aryl-chlorophosphoranes and their addition compounds with Lewis acids (4,5). The quadrupole frequencies have been found especially useful in establishing the ionic or molecular nature of the species present and their geometrical configurations (5).

Following the determinations of asymmetry parameters (3) in group IV tetrachlorides, an attempt was made to determine η in the isoelectronic ion $(\text{PCl}_4)^{\oplus}$. Lucken has shown π -bonding to be present in this species (6). Although reported as producing a very strong single ^{35}Cl quadrupole resonance (7), repeated preparation failed to yield a sample of $(\text{PCl}_4)^{\oplus}(\text{ICl}_2)^{\ominus}$ giving a sufficiently strong signal for Zeeman investigation on either the Decca or "AEI" spectrometers. Other derivatives of $(\text{PCl}_4)^{\oplus}$ were not considered suitable for Zeeman experiments either because the multiplicity of lines would cause interference or because the zero magnetic field signal strength was insufficient.

Turning to chlorophosphoranes, tetrachlorophenylphosphorane was recognised as a practical and worthwhile subject for the determination of its asymmetry parameters. This covalent molecule exists as a trigonal bipyramid with the structure:



The chlorine atoms in the horizontal plane of the phenyl ring are termed "equatorial" and those in the vertical plane "axial". That these pairs of chlorine atoms have differing P-Cl bond characteristics is confirmed by the n.q.r. spectrum of the compound. This consists of two pairs of lines widely separated, viz.

25.51 MHz
24.61 "

33.74 "
33.59 "

at 77K (4).

The equatorial and axial chlorine atoms in the molecule are known to possess different P-Cl bond lengths, causing a separation in their n.q.r. frequencies. The small separation in each pair is probably due to solid-state effects in the lattice. The higher frequency pair of n.q.r. lines are assigned to the equatorial chlorine atoms and the lower pair to the axial chlorines. This reflects the greater length, and presumed greater ionicity, of the axial chlorines.

The presence of empty d-orbitals on the central phosphorus atom makes possible $p_{\pi}-d_{\pi}$ bonding (chlorine to phosphorus) of the type discussed in Chapter 6 for group IV tetrahalides. An irregular decrease in n.q.r. frequency has been observed by Lynch and Waddington for the series $(\text{Ph}_n\text{PCl}_{4-n})^{\oplus}$ which has been interpreted in terms of conjugation through π -bonding (9). Similar conjugation may be predicted between the chlorines and

phenyl group in tetrachlorophosphorane. Zeeman investigation of the n.q.r. lines of the equatorial chlorines was first made because they were the stronger resonances and should provide higher conjugation. The Decca spectrometer was used with frequency modulation and adjustment of the lineshape to first derivative (Fig. 1). The spectrometer Zeeman modulation coils were used to provide the static magnetic field. Lineshapes at varying field strengths up to approximately 45×10^{-4} Tesla were characterised by the method of Morino and Toyama. The parameter δ_1 was found to be the best characterised and it is therefore measurements of $\frac{\delta_1}{2\nu_M}$ which are plotted against the inverse of field strength in Fig. 2. Examples of the lineshapes used are given in Figs. 3a) - c) which illustrate δ_1 measurements observed at varying field strengths. Details of the measurements are given in Table 1. Measurements on both n.q.r. lines were made and are distinguished in Fig. 2 by the symbols \otimes (33.74 MHz) and \odot (33.59 MHz). The magnetic field strengths used exceeded the minimum value as determined by the Morino and Toyama formula (Chapter 1, equation 43). This minimum value is marked on Fig. 2 as "M - T min^m field". The plot indicates a minimum value for the asymmetry parameter of approximately 0.17 in both the equatorial P-Cl bonds.

Upon attempting the similar investigation of the axial chlorines, it was found that the zero field intensities of the signals were too low to support any Zeeman lineshapes capable of characterisation. Use of the computer of average transients (c.a.t.) failed to enhance the strengths of these lineshapes due to a slow drift in frequency at 77K.

Fig. 1 ^{35}Cl n.g.r. of AlPO_4 at 77K (zero magnetic field).

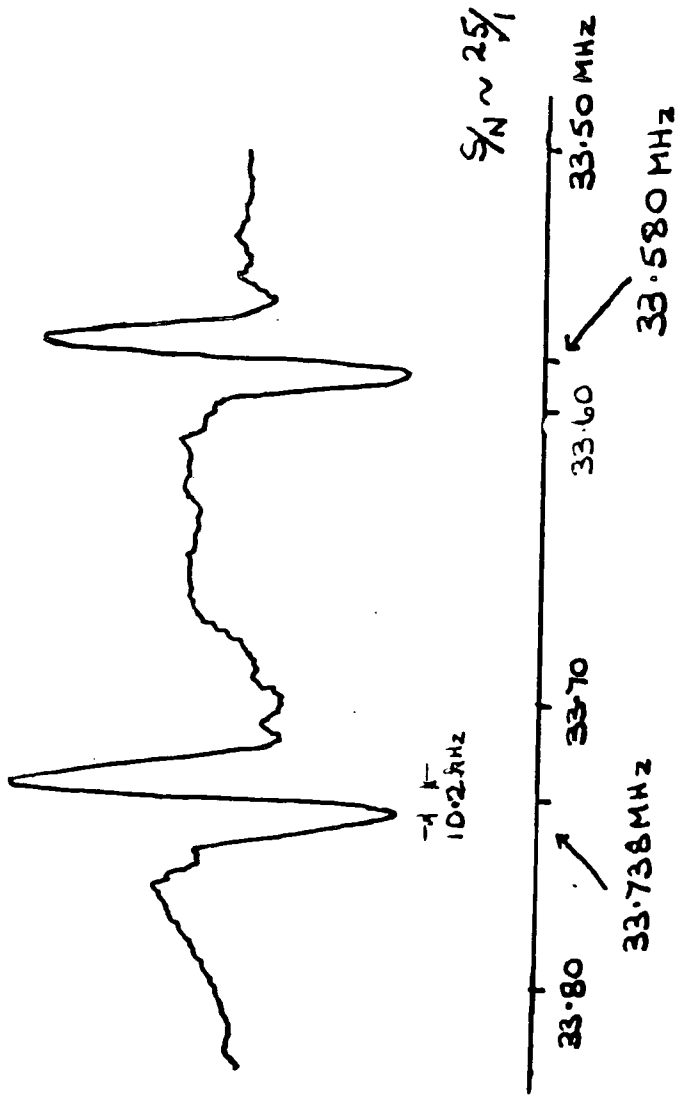


Fig. 2 Plot to determine γ in equatorial chlorines PRPCl_2

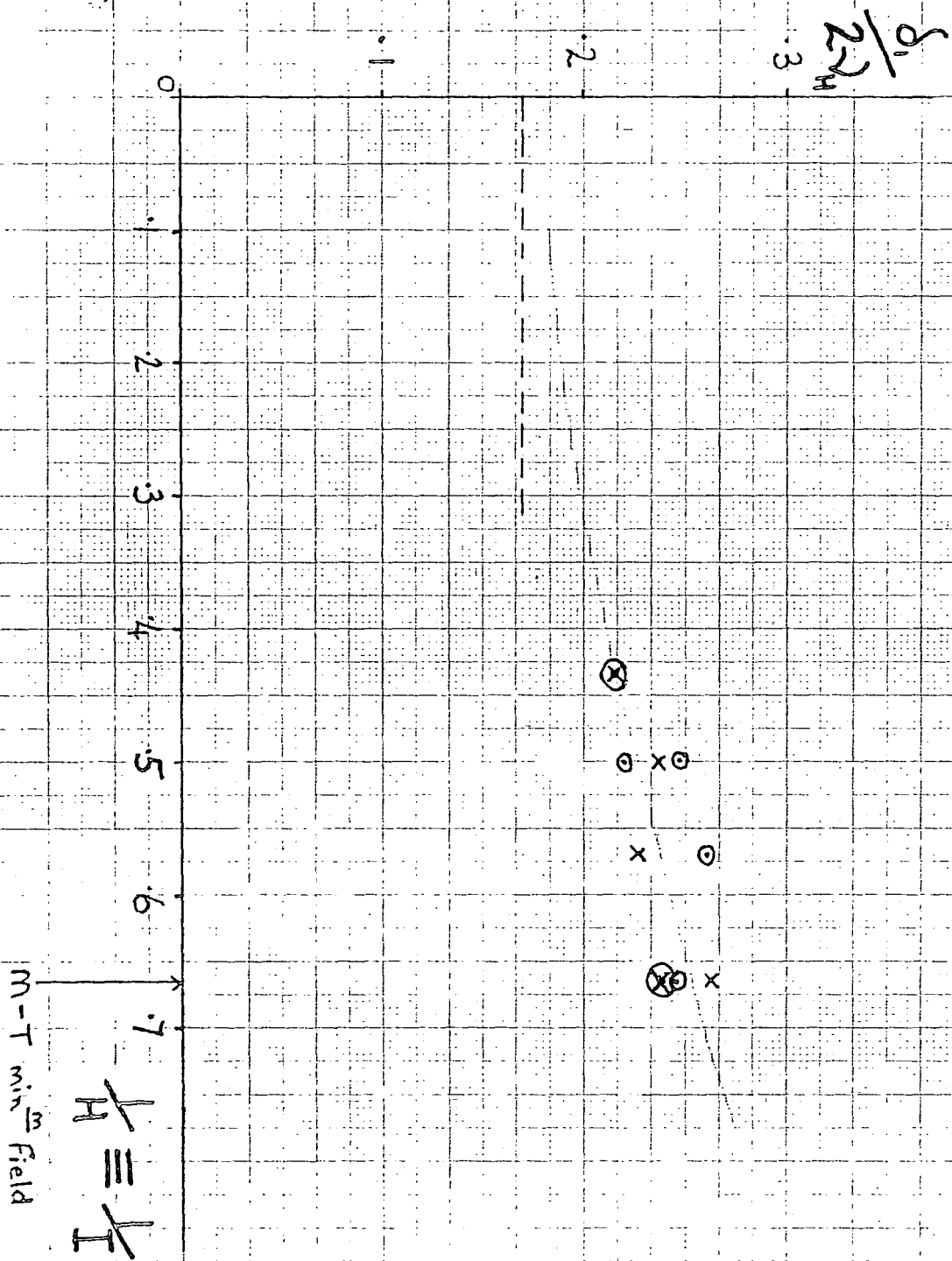


Fig.3a) Zeeman n.q.r. spectrum PbPO_4 at 77K. Magnetic field = $4.7 \times 10^{-4} \text{ T}$.

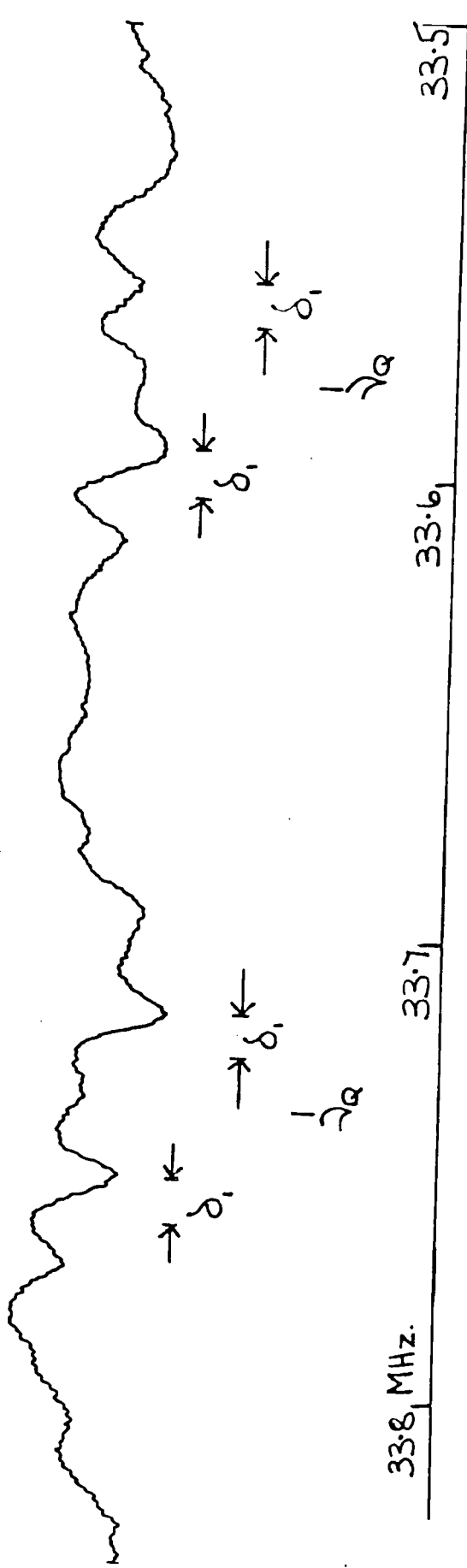


Fig. 3b)

Magnetic field = 73×10^{-4} T.

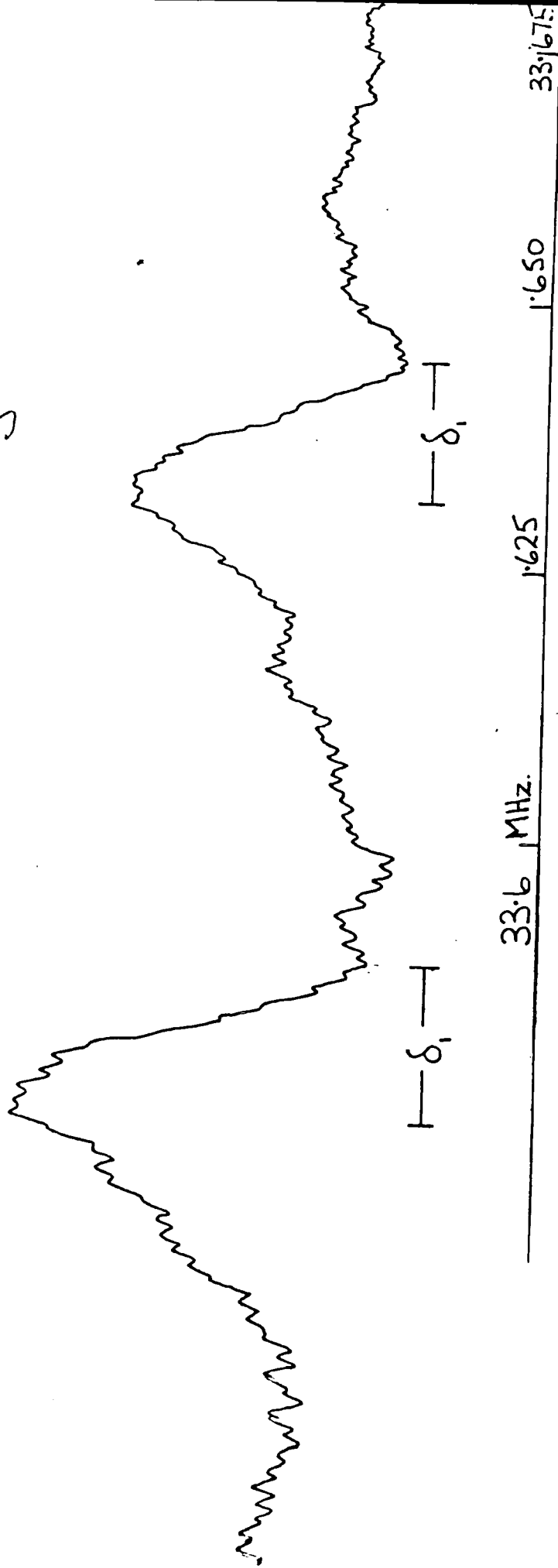


Fig. 3c)

Magnetic Field = 73×10^{-4} T.

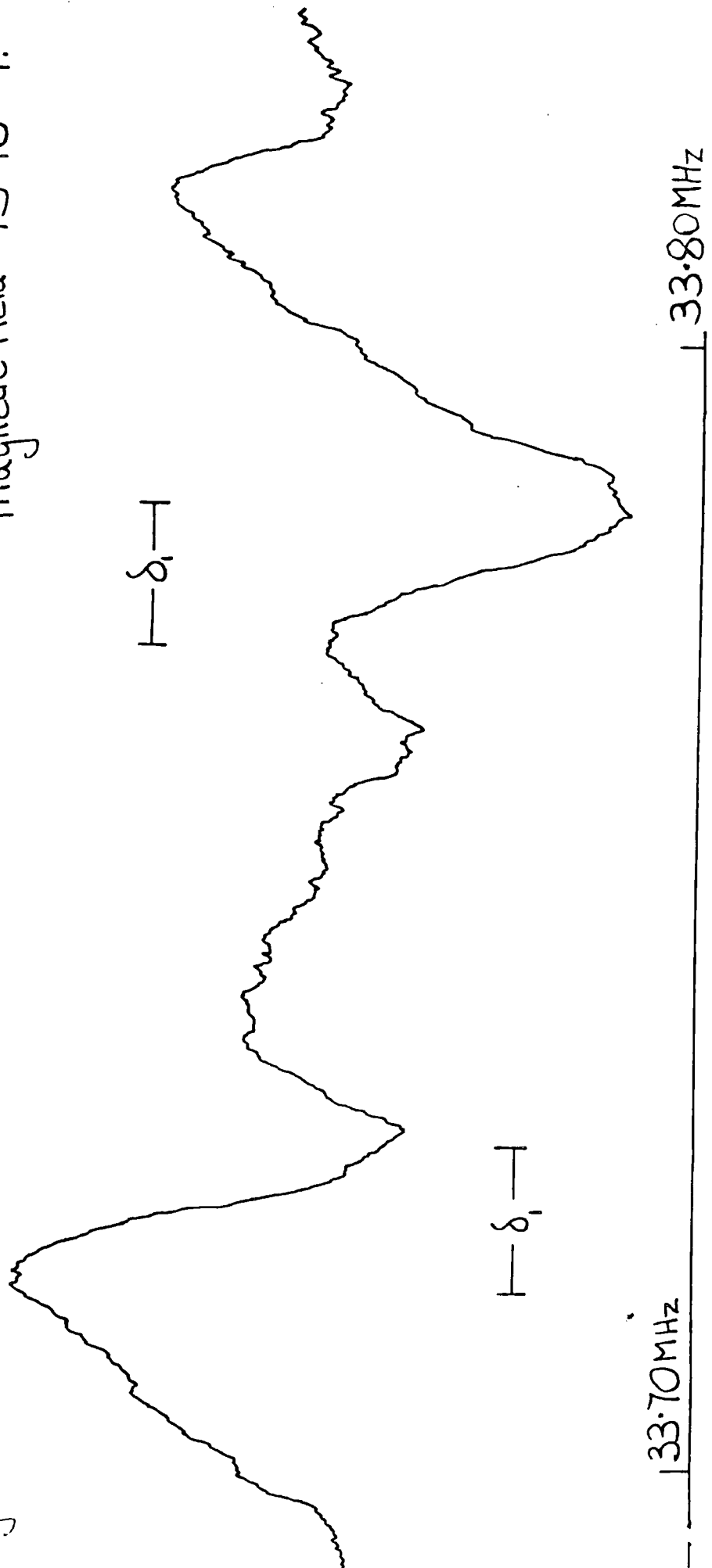


TABLE 1. Zeeman n.q.r. analysis for equatorial chlorines PhPCl_4

Current I (amp)	Mag ^c field H (mT.)	δ_1 (kHz)	γ_H kHz	$\frac{\delta_1}{2\gamma_H}$
1.5	4.76	x 9.39 ⊙ 9.39 x 10.31 ⊙ 9.55	19.52	0.240 .240 .264 .245
1.75	5.55	x 10.38 ⊙ 11.77	22.76	0.228 0.259
2.0	6.34	x 12.27 ⊙ 12.70 ⊙ 11.37 (avg)	25.99	0.236 0.244 (avg) 0.219
2.3	7.29	x 12.88 ⊙ 12.88	29.89	0.215 0.215

Extrapolation of $\frac{\delta_1}{2\gamma_H}$ to $\frac{1}{H} = 0 \rightarrow \gamma = 0.17 \pm 0.02^*$

*Error on $\delta_1 \leq \pm 10\%$

x \equiv 33.738 MHz line

⊙ \equiv 33.580 MHz line

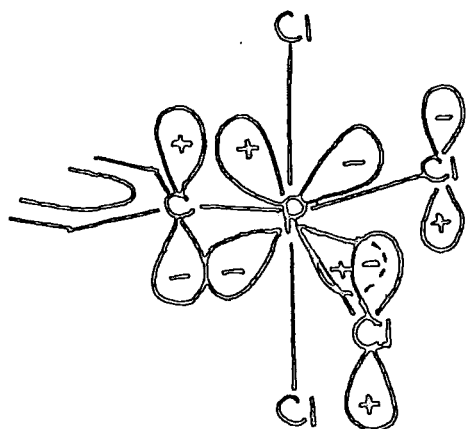
Discussion

A comparison of the P-Cl bond characteristics in tetrachlorophosphorane and phosphorus pentachloride is possible through the n.q.r. study of a metastable molecular modification of PCl_5 by Chihara et al. (2). Both the molecules exist as trigonal bipyramids in the solid and yield n.q.r. spectra reflecting the presence of chlorine in equatorial and axial positions. The P-Cl bond lengths in gaseous PCl_5 have been measured as 0.201 and 0.207 nm. for the equatorial and axial bonds respectively (8). Although the lengths may be different in the solid, Chihara et al. estimated the π -character of the P-Cl bonds as 0.08 and 0.0 for equatorial and axial chlorines respectively, in molecular PCl_5 . They also estimated π for $(\text{PCl}_4)^{\oplus}$ as 0.18. Although the values for π are not very accurate, they may be compared with a value of 0.07 estimated from $\eta = 0.17$ for equatorial chlorines of tetrachlorophosphorane using equation 2.44. In comparison with that of PCl_5 , this value seems reasonable since the $p_{\pi}-d_{\pi}$ overlap between each equatorial chlorine and phosphorus is likely to be reduced by the substitution of a chlorine atom with a phenyl group in PhPCl_4 . The phenyl group is expected to conjugate with phosphorus better than chlorine (9).

In ^{35}Cl n.q.r. studies of organo-phosphorus (V) (9) and organo-arsenic (V) compounds (10), the case for the existence of $p_{\pi}-d_{\pi}$ bonding in substituted phosphonium- and arsonium ions has been persuasively presented. The positive charge on the central atom is likely to contract the d-orbitals and increase their availability for π -bonding. In phenyl-substituted group V cations $(\text{Ph}_n\text{MCl}_{4-n})^{\oplus}$,

it is argued that conjugation between the chlorine atoms and the phenyl group will be diminished in the cases of $n=1$ and 3 . This probably promotes the degree of $p_{\pi}-d_{\pi}$ bonding between the central atom and chlorine in these cases. From a comparison of ^{35}Cl n.q.r. data on methyl- and phenyl-substituted phosphonium ions, K.B. Dillon et al. deduce that the π -character of the P-Cl bond probably decreases in the series $\text{PCl}_4^{\oplus} > \text{PhPCl}_3^{\oplus} > \text{Ph}_2\text{PCl}_2^{\oplus} > \text{Ph}_3\text{PCl}^{\oplus}$.

The ^{35}Cl n.q.r. frequencies for PCl_4^{\oplus} in $(\text{PCl}_4)^{\oplus}(\text{PCl}_6)^{\ominus}$ average 32.43 MHz at 77K (9). This may be compared with the frequencies for equatorial chlorine in Ph_2PCl_3 (33.45 MHz)(4), PhPCl_4 (33.59, 33.74 MHz)(4) and in molecular PCl_5 (33.75 MHz)(2), all at 77K. The bonding in the chloro(phenyl)phosphoranes probably resembles that in the phosphonium ions. It may be expected that, in the absence of a positive charge, the overlap between $3d$ -orbitals of phosphorus and $3p$ -orbitals on the chlorine atoms is reduced. However, in the case of tetrachlorophenyl phosphorane conjugation between the equatorial chlorine atoms (Cl_{eq}) and the phenyl group should promote π -bonding in the $\text{M}-\text{Cl}_{\text{eq}}$ bonds through a d -orbital on phosphorus of d_{xz} symmetry, i.e. to fulfil C_v symmetry.



2) THE ^{59}Co N.Q.R. OF π -CYCLOPENTADIENYL-COBALT-DICARBONYL

The ^{59}Co n.q.r. spectrum of π -cyclopentadienyl-cobalt-dicarbonyl has been obtained and its temperature dependence determined. The far-i.r. (at liquid nitrogen temperature) and Raman (at liquid air temperature) spectra have been recorded. The 60cm^{-1} Raman line (presumed to be ring rotation) has been identified as the major cause of the n.q.r. temperature dependence.

Introduction

Following the observation of ^{59}Co n.q.r. signals from several cobalticinium compounds, the Decca spectrometer was applied to the study of ^{59}Co resonances as yet unreported. Cobalticinium hexafluorophosphate yields triplet quadrupole resonances of average frequencies 36.683, 24.422 and 12.254 MHz which clearly indicate a zero asymmetry parameter. An average value of 170 MHz ($\eta = 0$) is produced for the nuclear quadrupole coupling constant of ^{59}Co in a variety of cobalticinium complexes. Anticipating similar frequency and coupling constant values for π -cyclopentadienyl-cobalt-dicarbonyl, the Decca n.q.r. spectrometer was swept over the frequency range 10-40 MHz.

Discussion

Cyclopentadienyl-cobalt-dicarbonyl was obtained commercially

(Alpha Organics) and is a dark-red oily liquid which decomposes in air. It was therefore handled in a nitrogen-filled dry box before being sealed in ampoules. The liquid freezes at -22°C and so ampoules were shaken in liquid nitrogen to ensure polycrystallinity before use in the n.q.r. spectrometer. The n.q.r. spectrum observed at 77K was of three lines, corresponding to transitions between the four energy levels of the ^{59}Co nucleus. Frequencies observed at 77K, 20K and the melting point of the sample, 251K, are reported in Table 1. From $I = 7/2$ tables (1), a value of 0.30 ± 0.01 is determined for the asymmetry parameter. This value appears to be constant over the range 77K to 251K. This has been checked by numerous comparisons of the ratios of the n.q.r. frequencies with those given for $\eta = 0.30$ in the tables of G.K. Semin et al.(1).

Figs. 1 to 3 illustrate the temperature dependences of the three quadrupole resonances. There are no discontinuities which indicates that phase changes are unlikely between 77K and 251K (the melting point). These lines were fitted by regression to quadratics in temperature.

Table 2 contains the vibrational spectra obtained on a Beckmann Fs 720 far- i.r. spectrometer and a Cary 81 Raman-spectrometer. An i.r. spectrum obtained to 180 cm^{-1} on a Perkin-Elmer 557 spectrometer agreed with that of Fischer (2). The low frequency Raman spectrum is comparable with that observed earlier (3) but has revealed a new peak at 60 cm^{-1} . Rocquet et al., investigating ferrocene, have observed an infra-red line at 44 cm^{-1} which they attributed to rotation of the rings

TABLE 1 ⁵⁹Co n.q.r. frequencies of π -cyclopentadienylcobalt-dicarbonyl at various temperatures.

TEMP. FREQ. (MHz)	251K	200K	77K
$\nu_{\pm 1/2 \leftrightarrow \pm 3/2}$	14.143	14.168	14.158
$\nu_{\pm 3/2 \leftrightarrow \pm 5/2}$	21.128	21.318	21.560
$\nu_{\pm 5/2 \leftrightarrow \pm 7/2}$	32.684	32.942	33.312

Values of n.q.r. frequencies \rightarrow

asymmetry parameter, $\eta = 0.30 \pm 0.01$

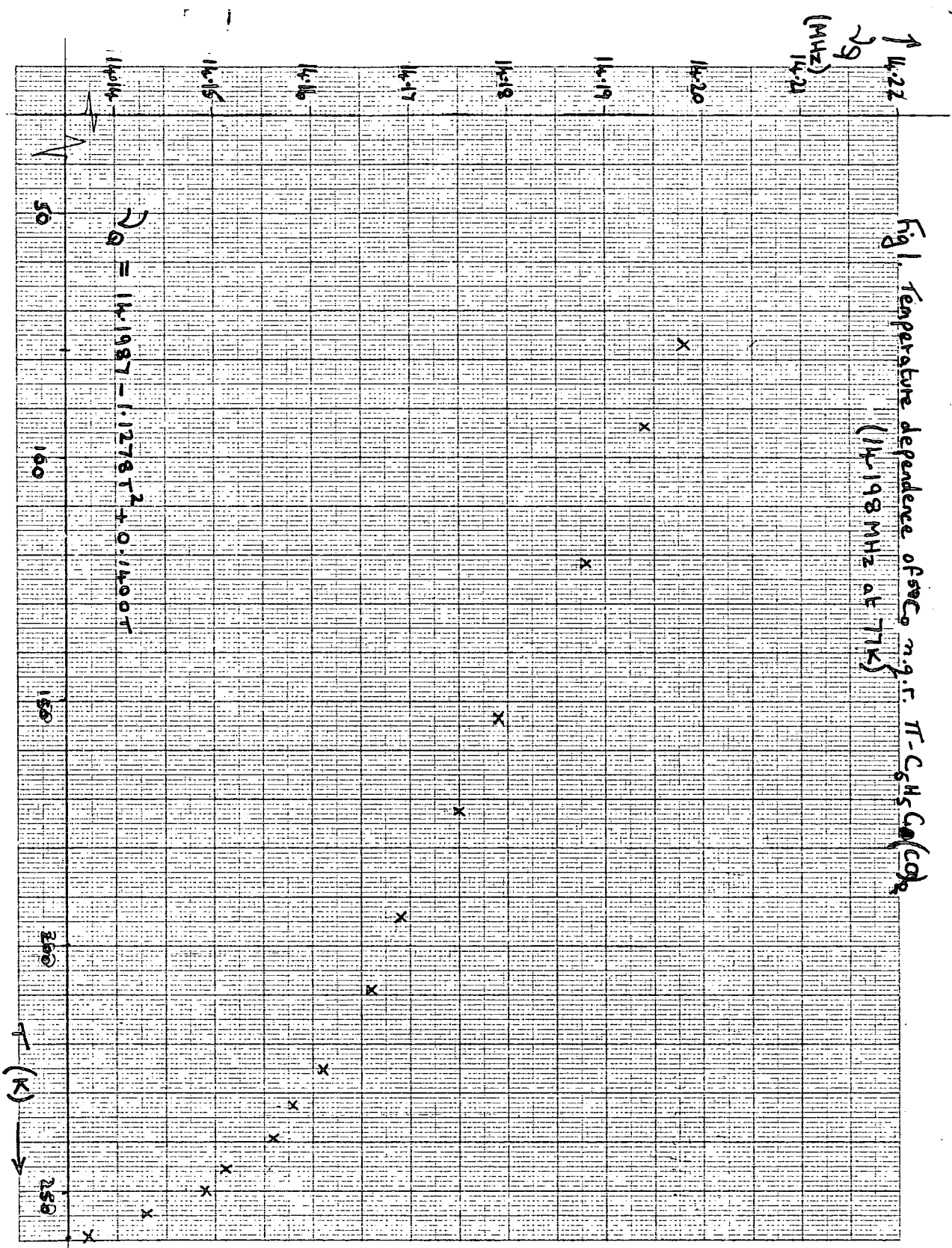
Hence, from equation 7 (Chapter 1)

$$\left| \frac{e^2 q Q}{2} \right| = 156.81 \pm 0.1 \text{ MHz at 77K. } \eta = 0.30$$

$$\left| \frac{e^2 q Q}{2} \right| = 156.40 \pm 0.1 \text{ " " 200K. " "}$$

$$\left| \frac{e^2 q Q}{2} \right| = 156.13 \pm 0.1 \text{ " " 251K. " "}$$

Fig. 1 Temperature dependence of ν_{CO} m.g.r. π - $C_6H_5CO(CO)_2$
 (14.198 MHz at 77K)



ν
(MHz)

21.1

21.2

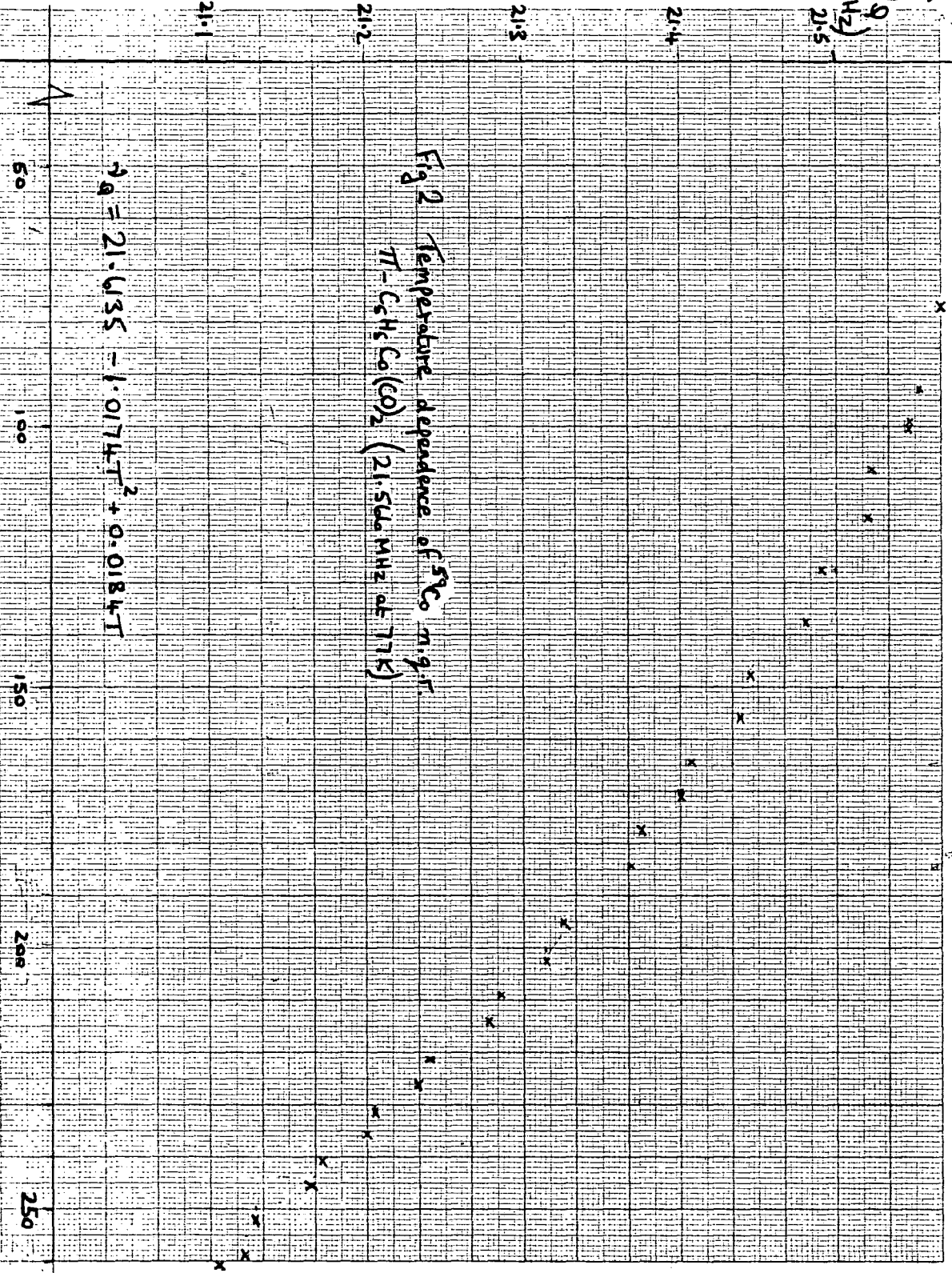
21.3

21.4

21.5

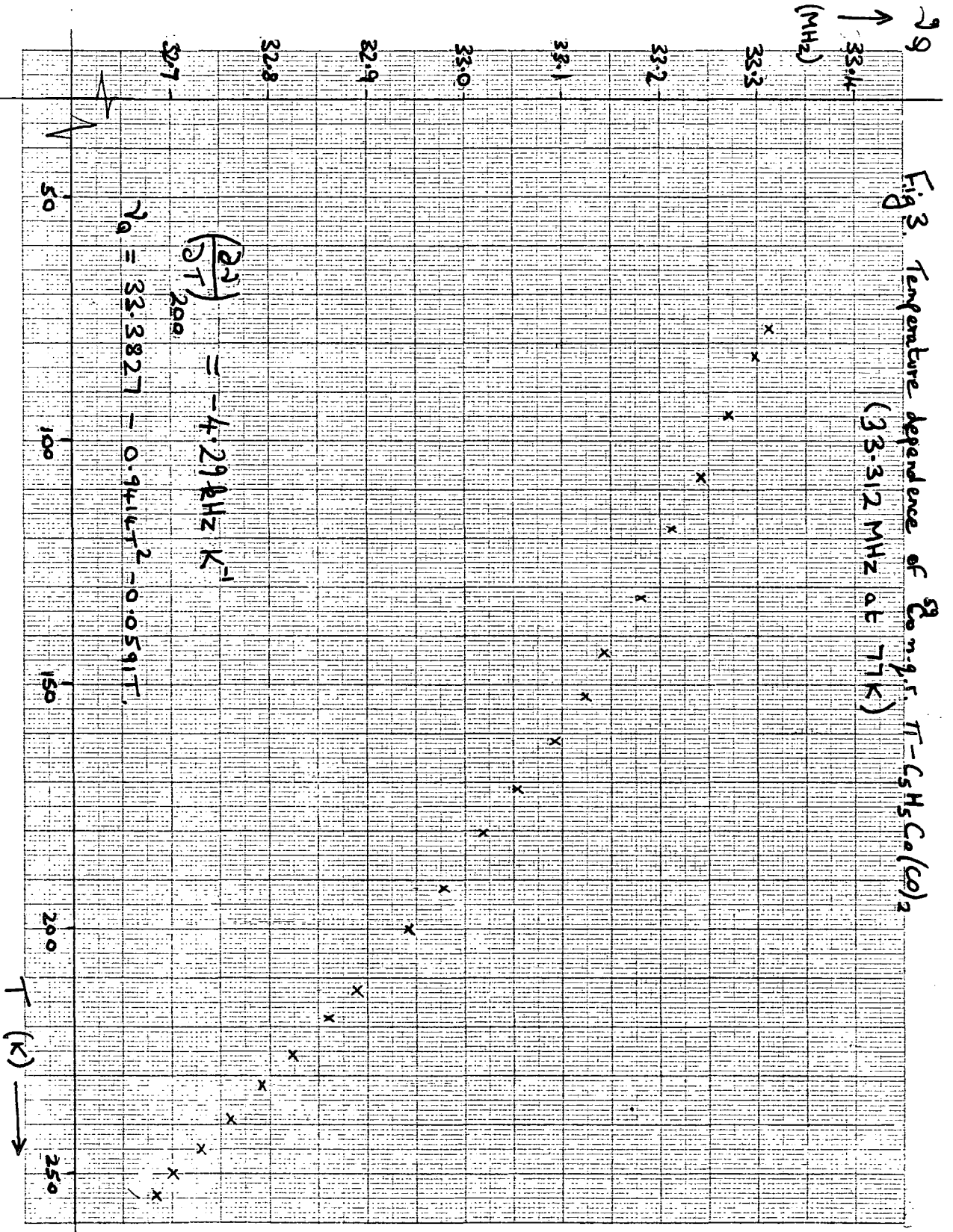
Fig 2 Temperature dependence of ^{59}Co n.g.f.
 $\text{T-C}_6\text{H}_5\text{Co}(\text{CO})_2$ (21.566 MHz at 77K)

$$\nu = 21.635 - 1.0174T^2 + 0.0184T$$



T (K) →

Fig. 3. Temperature dependence of ν_9 of $\text{C}_5\text{H}_5\text{Co}(\text{CO})_2$
 (33.312 MHz at 77K)



$$\left(\frac{d\nu_9}{dT}\right)_{298} = -4.29 \text{ kHz K}^{-1}$$

$$\nu_9 = 33.3827 - 0.9416T^2 - 0.0591T$$

TABLE 2

Vibrational Spectra of π -cyclopentadienyl-cobalt-dicarbonyl

<u>RAMAN (80K)</u> (20-1000 cm^{-1})	<u>FAR-InfRA-RED (77K)</u> (48-400 cm^{-1})
60 \pm 3	122.5 \pm 0.5
112 " (v.w.)	347.0 "
350 "	
378 " (v.w.)	368.5 "
517 "	

about the C_{5n} axis. It is possible that the peak at 60 cm^{-1} is the result of similar rotation of the cyclopentadienyl ring in $\pi\text{-C}_5\text{H}_5\text{Co}(\text{CO})_2$.

Although an X-ray crystallographic study of π -cyclopentadienyl-cobalt-dicarbonyl is not reported, a complete structural determination has been made upon its complexes with mercury (II) chloride (5). The covalent 1:1 complex $\pi\text{-C}_5\text{H}_5\text{Co}(\text{CO})_2\cdot\text{HgCl}_2$ contains units which probably closely resemble free molecules of π -cyclopentadienyl-cobalt-dicarbonyl. In the 1:1 complex the distance between the cobalt atom and the plane through the C_5H_5 ring has been determined as 0.170 ± 0.005 n.m.

The e.f.g. at ^{59}Co in cobalticinium complexes is presumed to lie along the axis joining the centres of the cyclopentadienyl rings and passing through cobalt. This seems most likely in view of the zero asymmetry parameters. In $\pi\text{-C}_5\text{H}_5\text{Co}(\text{CO})_2$ the principal axis of the e.f.g. probably follows a similar axis joining cobalt and the centre of the C_5H_5 ring. This appears plausible from the similarity of coupling constants in $(\text{Cp})_2\text{Co}^{\oplus}$ compounds and in $\pi\text{-CpCo}(\text{CO})_2$. It has been assumed that the temperature dependences of the ^{59}Co n.q.r. lines of cyclopentadienyl cobalt dicarbonyl originate in the averaging of the e.f.g. by motion about the axis i.e. in two planes at right angles to the axis. Application of the Bayer theory using equation 56 (Chapter 1) then yields a librational frequency of 37 cm^{-1} . The theory makes several approximations and it is possible to suggest that this calculated value represents the observed Raman line at 60 cm^{-1} . A revision of its assignment to ring rotation may therefore be suggested.

3) ^{35}Cl N.G.R. DETERMINATION OF ASYMMETRY IN THE C-CL BOND OF

CHLOROMETHANES

Introduction

Dinesh and Narasimhan reported values for the asymmetry parameter (η) of the C-Cl bonds in several organic chlorides. (1,2). They used an s.r.o.-type spectrometer and the method of Morino and Toyama (3) on polycrystalline samples frozen in liquid nitrogen. The reported values for η in chloromethanes seem high when compared with $\eta \leq 0.10$ reported for carbon tetrachloride by Graybeal and Green (4) - Table 1. Although only a slight increase in ^{35}Cl n.q.r. frequencies was observed upon deuteration of chloroform, a discernible difference in the values of η is reported (1), Table 1.

In addition to re-measuring the asymmetry parameters reported for methylene chloride, methyl chloride and chloroform, an attempt has been made at a systematic investigation of the effects of deuteration upon η .

Methylene chloride

Narasimhan reported a value for η of 0.43 (1) in methylene chloride which appears very high in comparison with $\eta \leq 0.10$ reported for carbon tetrachloride (4). No experimental details are provided by Narasimhan for such as linewidths, δ - measurements nor magnetic field strengths. Before drawing

TABLE 1

³⁵Cl n.o.r. frequencies and asymmetry parameters for some simple
chloroalkanes

<u>Compounds</u>	<u>N.o.r. frequencies (77K)</u> (MHz)	<u>Asymmetry parameter</u>	<u>3</u>
CCl ₄	40.6291 (avg.)	≤ 0.10	(4)
CHCl ₃	38.2553 38.3085	0.29 ± 0.01 0.21 ± 0.02	(1)
CDCl ₃	38.2626 38.3125	0.31 ± 0.01 0.19 ± 0.02	(1)
CH ₂ Cl ₂	35.9912	0.43 ± 0.01	(1)
CD ₂ Cl ₂	35.9708	-	(9)
CH ₃ Cl	34.029	-	(9)
CD ₃ Cl	37.20 ± 3 (est. microwave)	-	(11)
H ₃ C-CCl ₃	37.8352 38.0461	0.29 ± 0.01 0.19 ± 0.01	(1)
C ₆ H ₅ Cl	34.6224	0.10 ± 0.01	(2)

conclusions from the large difference in values of η , the asymmetry parameter for methylene chloride was remeasured by the author. The method of Morino and Toyama was applied to a polycrystalline sample, frozen in liquid nitrogen.

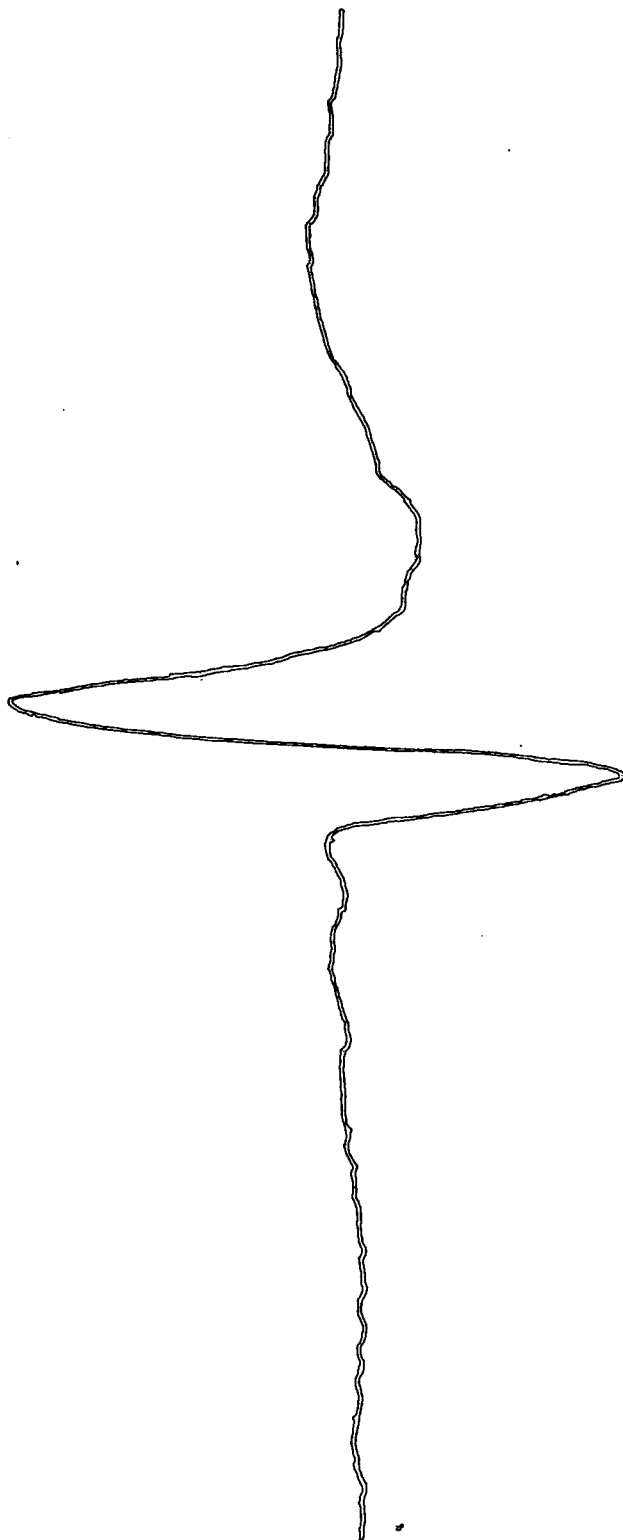
Due to the reduced sensitivity of the Robinson-type spectrometer above 33 MHz and to ensure sufficiently high signal strength, the s.r.o. - type Decca spectrometer was used. Adjustments to the CSC and frequency modulation produced a closely first - derivative response (Fig. 1). Magnetic fields of up to 15 mT were applied through the Zeeman coils of the spectrometer.

Examples of the lineshapes produced are given in Figs. 2a) - c), where fields of 9.20, 10.14 and 12.68 mT are applied. From measurements of δ , an estimate for η has been made by extrapolation of the $\frac{\delta_1}{2\nu_H}$ vs $\frac{1}{H}$ plot to infinite field strength (Fig. 3). The result is an estimated value of $\eta \approx 0.45$ which is in close agreement with Narasimhan, who used similar equipment and the same method of evaluation.

The temperature dependence of methylene chloride between 77K and its melting point has been recorded (Fig. 4 - graph and table) and is discussed below.

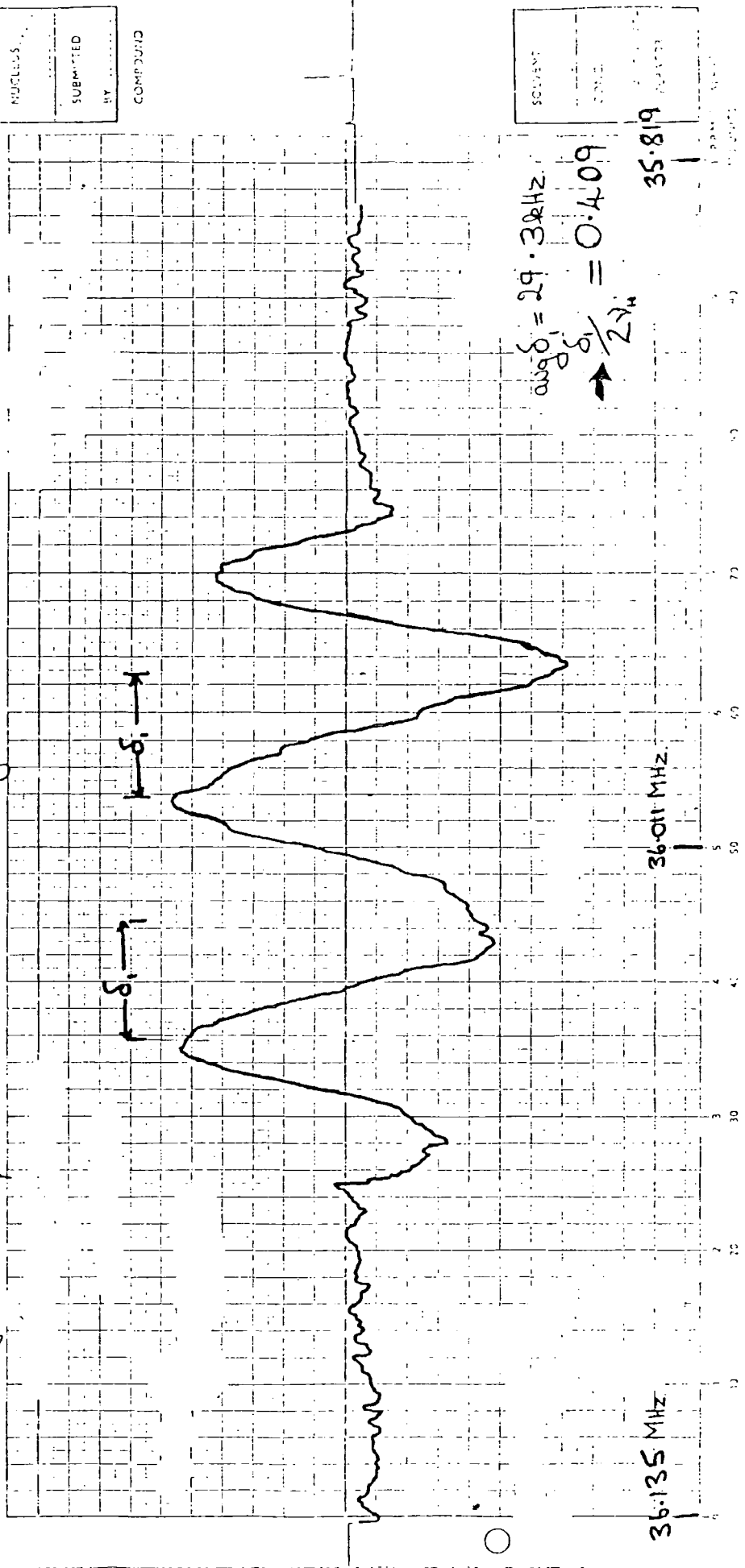
lit. $\nu_9 = 35.991 \text{ MHz.}$
obs. $\frac{5}{10} \frac{35}{1}$

Fig. ^{35}Cl n.g.r. CH_2Cl_2 at 77K - zero magnetic field.



→ Δ 2 K
14-25 Hz.

Fig 20) ^{35}Cl n.g.f. CH_2Cl_2 at 77K. Magnetic field = 9.20 m.t.



EXPERIMENT	NO.
NUCLEUS	
SUBMITTED	
BY	
COMPOUND	

SOLVENT	
CONC.	
TEMP.	

Fig 2b) ^{35}Cl n.p.r. CH_2Cl_2 at 77K Magnetic Field = 10.14 m.T.

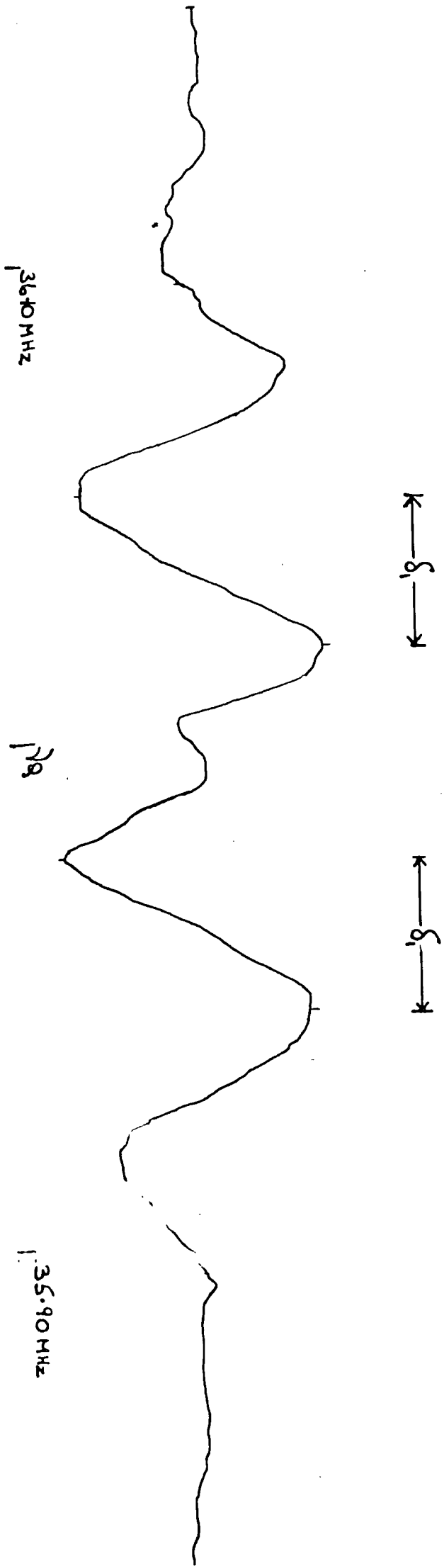
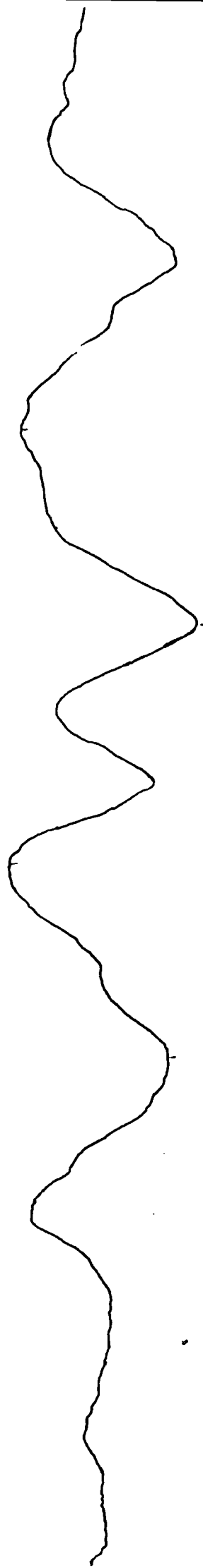


Fig. 2c) ^{35}Cl n.g.r. CH_2Cl_2 at 77K. Magnetic field = 12.68 m.T.

$\longleftrightarrow \delta_1 \longleftrightarrow$

$\longleftrightarrow \delta_1 \longleftrightarrow$



36.10MHz.

129

35.90MHz

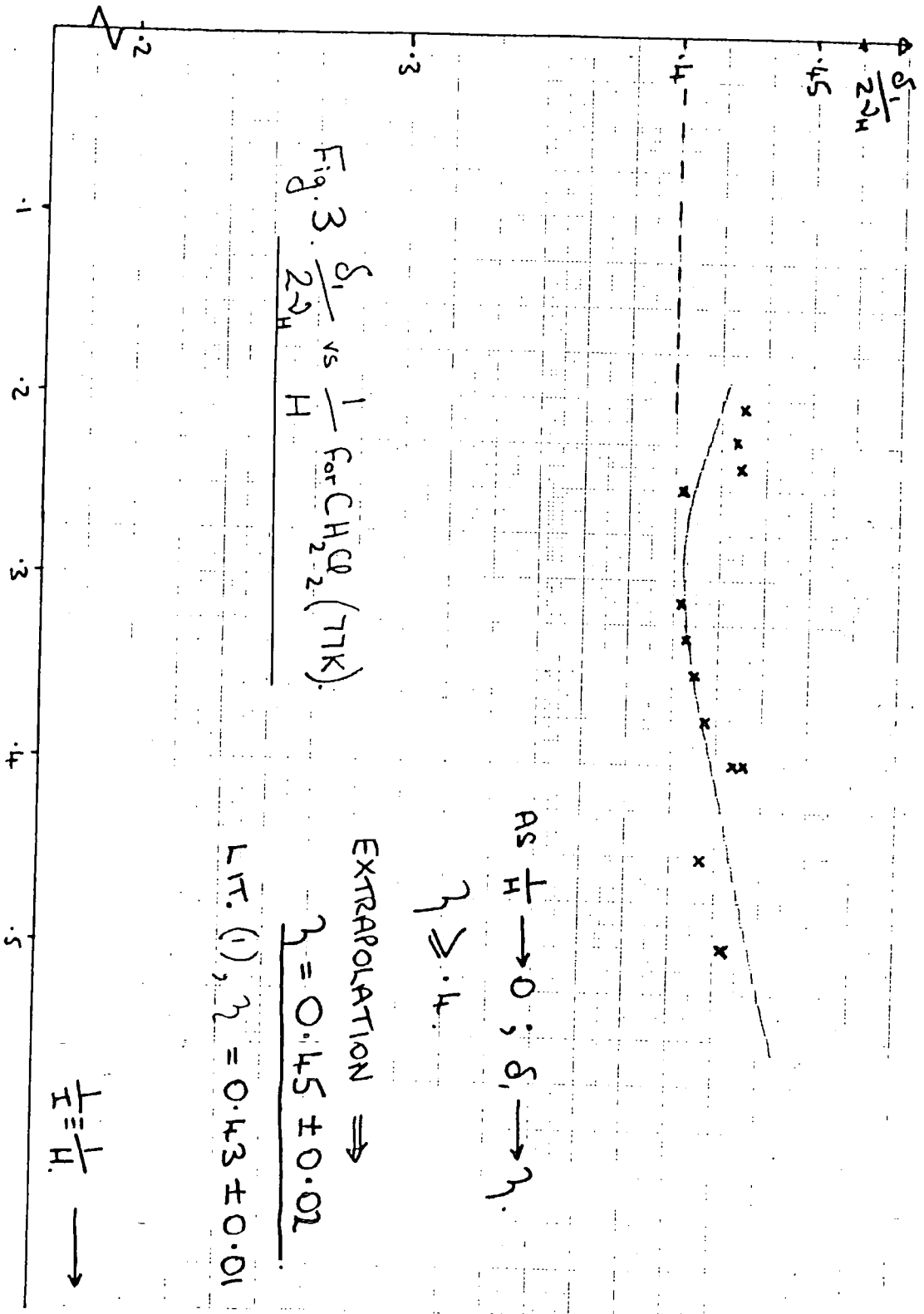


Fig 1b Temperature dependence
 ^{35}Cl n.m.r. of CH_2Cl_2

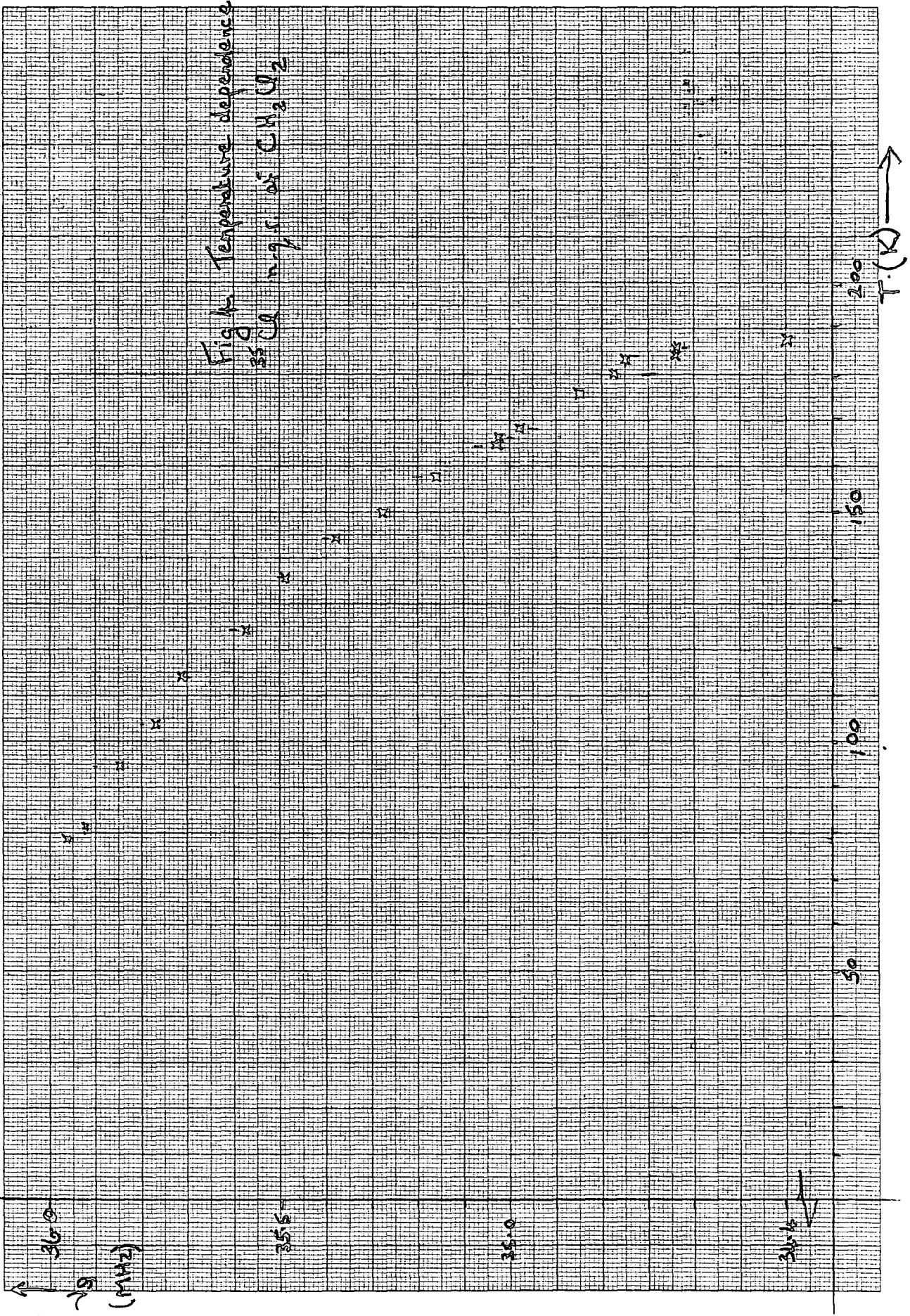


Fig. 4 (contd.)

Temperature dependence ^{35}Cl n.q.r. CH_2Cl_2

Frequency (MHz)

Temperature ($^{\circ}\text{K}$)

35.952	78.7
35.922	81.2
35.848	94.5
35.771	103.7
35.712	114.0
35.575	124.1
35.486	135.8
35.380	144.0
35.275	149.6
35.158	157.5
35.029	164.3
35.026	166.2
34.979	168.0
34.850	175.8
34.775	180.0
34.750	183.0
34.640	183.9
34.642	185.8
34.400	187.2

Discussion

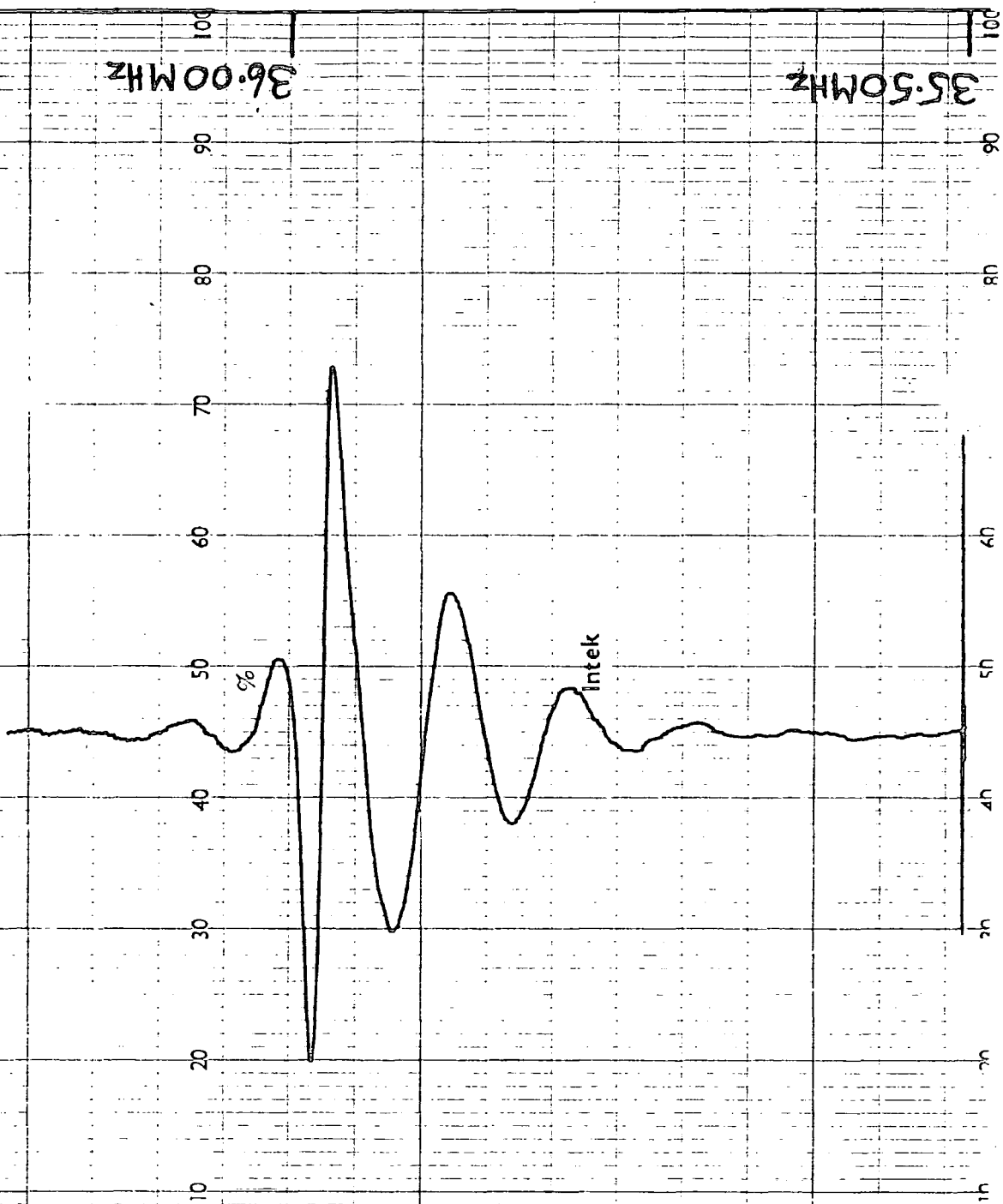
The existence of threefold (or greater) symmetry about a bond axis prevents asymmetry in that bond. Although possible in CH_2Cl_2 , asymmetry can be expected to be slight. The disturbance in the axial symmetry of the C-Cl bond in organic chlorides may be caused by intramolecular and/or intermolecular interactions. The involvement of such effects can be probed by pulse n.q.r. techniques measuring such parameters as spin-lattice relaxation times (T). Gutowsky and McCall followed the temperature dependence of the ^{35}Cl quadrupole resonances of methylene chloride and chloroform. They observed no discontinuities up to the melting points of the compounds and concluded that, in addition to the absence of phase changes, no significant re-orientation modes (with a frequency $> 10^4 \text{ sec}^{-1}$) are present prior to melting (5). However, a similar study on methylene chloride reported that, upon warming a sample from 85K, three phases are indicated by two discontinuities in the frequency-temperature plot (6). A further study by Minott and Ragle (7) found only one phase between 77K and the melting point. The author is in agreement with the reports of one phase only. Fig. 4 shows the temperature dependence of CH_2Cl_2 . Minott and Ragle also confirmed the finding of Woessner and Gutowsky (8) that the ^{35}Cl spin-lattice relaxation times are highly temperature dependent for the 25K degrees below melting point.

Differences in behaviour between members of the chloromethanes were noted by Gutowsky and McCall. The ^{35}Cl quadrupole resonances of CH_2Cl_2 and CHCl_3 did not fade out at temperatures below the melting point, whereas those of CCl_4 did. This, they

proposed, was evidence of reorientation motions at the transition or phase change of CCl_4 . Minott and Magle, investigating the deuteron coupling and chlorine relaxation in frozen methylene chloride and methylene chloride- d_2 , found strong evidence for the activation of a slow rotational motion in the 25K degrees below their freezing points. CH_2Cl_2 and CD_2Cl_2 were found to be indistinguishable in their T_1 behaviour. There is no phase change associated with the rotation which they suggest is about the molecular twofold axis. The possible cause of this rotation is that greater freedom is allowed due to either thermal expansion of the lattice or increasing lattice defects (7). The fact that the behaviour of CH_2Cl_2 and CD_2Cl_2 were found to be so similar does suggest that the influence of hydrogen-bonding is unlikely. The very close similarity of their ^{35}Cl n.q.r. frequencies supports this theory (Table 1).

Extension of the work by Dinesh and Narasimhan to determine [?] in all the chloromethanes and their deuterated analogues has unfortunately not been possible. The method of Morino and Toyama was to have been used. Due to the insensitivity of the "AEI" spectrometer above 33 MHz, only the Decca s.r.o. spectrometer could be used. As in the cases of thionyl chloride and tetrachlorophenylphosphorane, adjustments to the lineshape output were made in order to achieve the best possible zero-field lineshape. The zero-field lineshape for CH_2Cl_2 is given in Fig. 1. That obtained for CD_2Cl_2 is given in Fig. 5. The "ringing" characteristic to low frequency of the n.q.r. line of CD_2Cl_2 may be due to coupling of the quadrupoles on the chlorine nuclei with those of the deuterium nuclei. It was, however, observed for all the chloromethanes and deuterio-chloromethanes except

Fig. 5 ^{35}Cl n.g.f. kinescope of CD_2Cl_2 at 77K. (Zero magnetic field) $\nu_g = 35.971\text{MHz}$



CH_2Cl_2 . Neither adjustment of the C.S.C. and frequency modulation of the Decca spectrometer nor annealing of the sample would remove the unusual distortion of the lineshape. An attempt was made to apply the Morino and Toyama method to such lineshapes under the influence of small magnetic fields. However, these attempts to generate δ measurements resulted in plots of $\frac{\delta}{2\nu_H}$ vs $\frac{1}{H}$ with negative gradients (with respect to H). The constantly rising δ values are not related to $2\nu_H$ but probably originate in line-broadening by the magnetic field. Such a plot (for CH_2Cl_2) is shown in Fig. 6 and sample spectra in Figs. 7a) - c). Any extension of values of δ in $\text{CH}_n\text{Cl}_{4-n}$ and their deuterated analogues was therefore not possible. In the absence of such information, it is not possible to identify the causes of high asymmetry parameters in methylene chloride and chloroform. It may be suggested that hydrogen-bonding is unlikely and that intramolecular effects are too weak to generate large asymmetry. The unit cell of methylene chloride appears to contain four molecules (10) but no crystallographic determination appears to have been made. Perhaps close approaches in the lattice influence the e.f.g. and render the present polycrystalline determination of δ inappropriate.

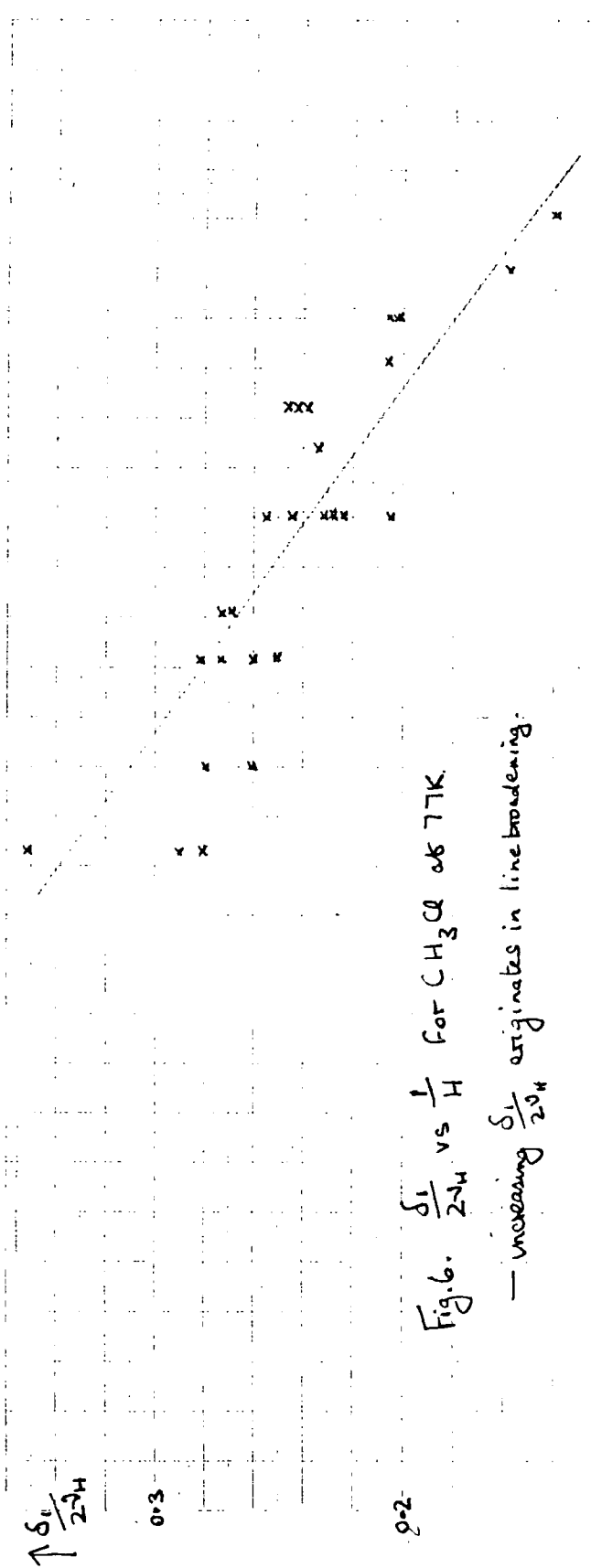


Fig. 6. $\frac{\delta_1}{2\nu_H}$ vs $\frac{1}{H}$ for CH_3Cl at 77K

— increasing $\frac{\delta_1}{2\nu_H}$ originates in line broadening.

0.1

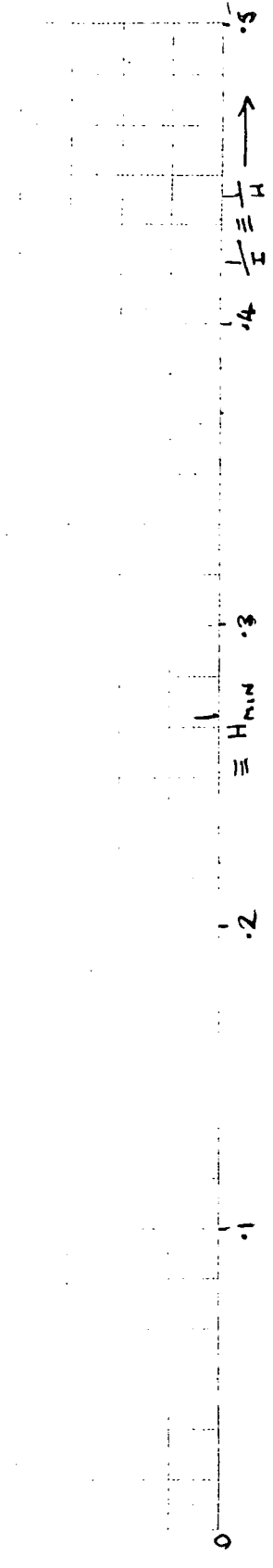


Fig. 6 (cont.)

Zeeman n.o.r. data on CH_2Cl at 77K.

Coil current (amp)	$\frac{1}{I} \equiv \frac{1}{H}$	$\frac{\delta_1}{2\nu_H}$
2.3	.435	.140
2.4	.417	.149
2.5	.400	.202 .204 .211 .224
2.6	.385	.205
2.7	.370	.239 .243 .246 .247
2.8	.357	.234
2.82	.355	.240
3.0	.333	.222 .230 .232 .247 .255
3.3	.303	.269 .273
3.5	.286	.275 .282
4.0	.250	.268 .280
4.5	.222	.280 .290 .350

Fig. 7.9 ^{35}Cl n.m.r. CH_3Cl at 77K. Magnetic Field = 7.3 mT.

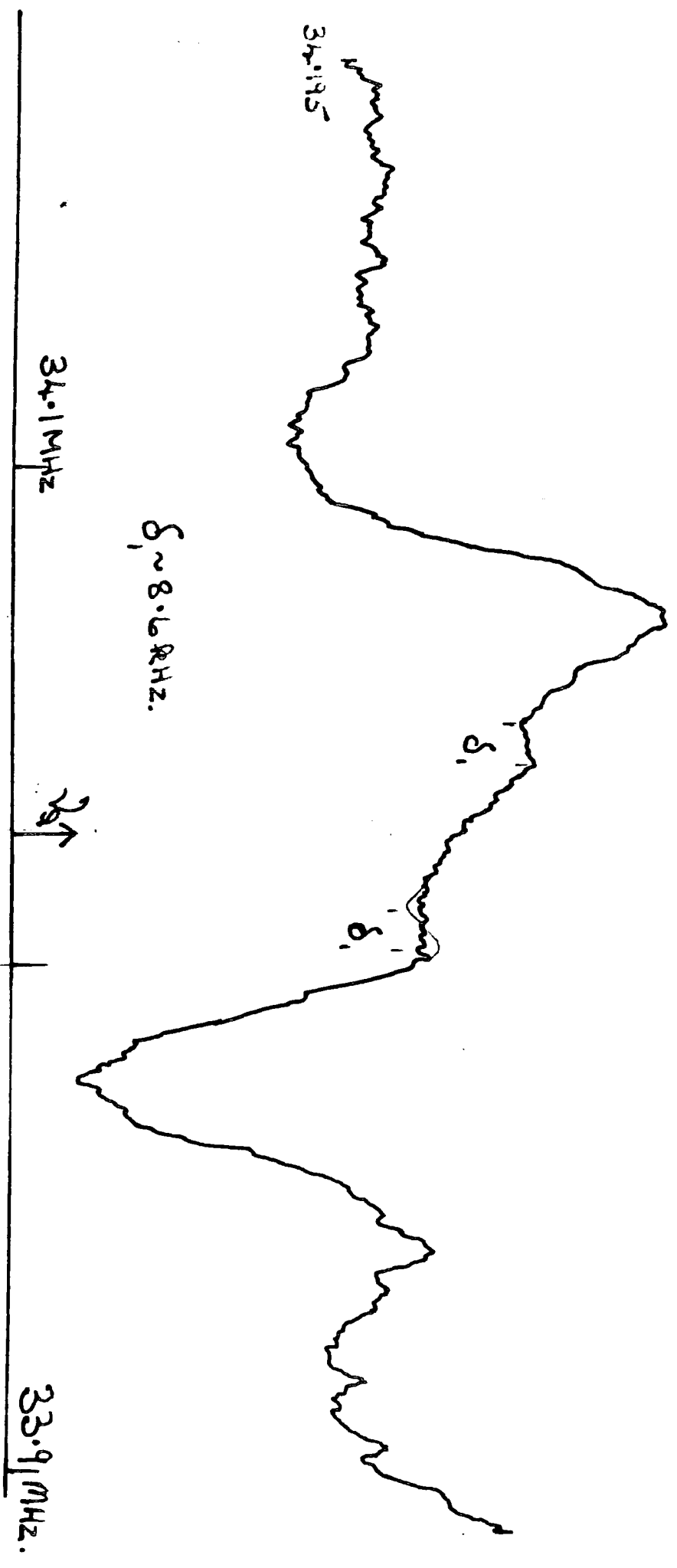


Fig. 7b) ^{35}Cl n.p.r. CH_3Cl at 77K. Magnetic field = 9.5 mT.

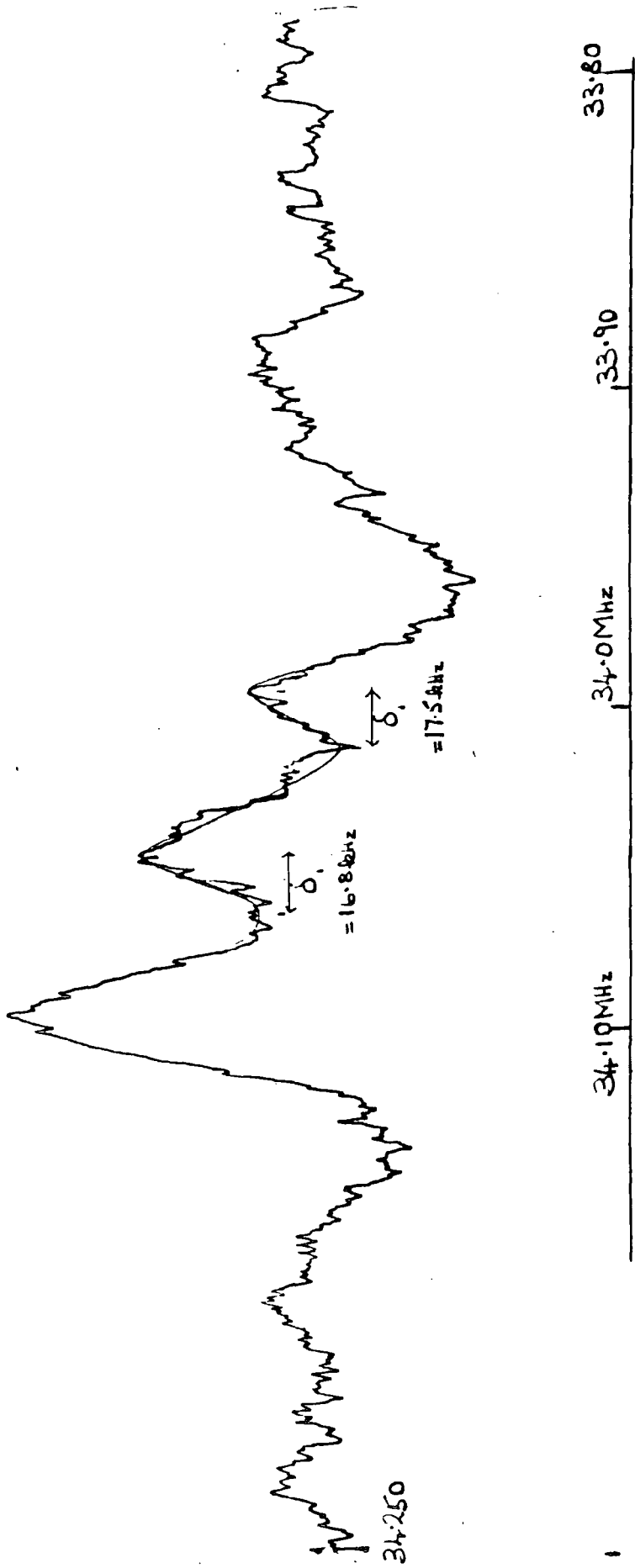
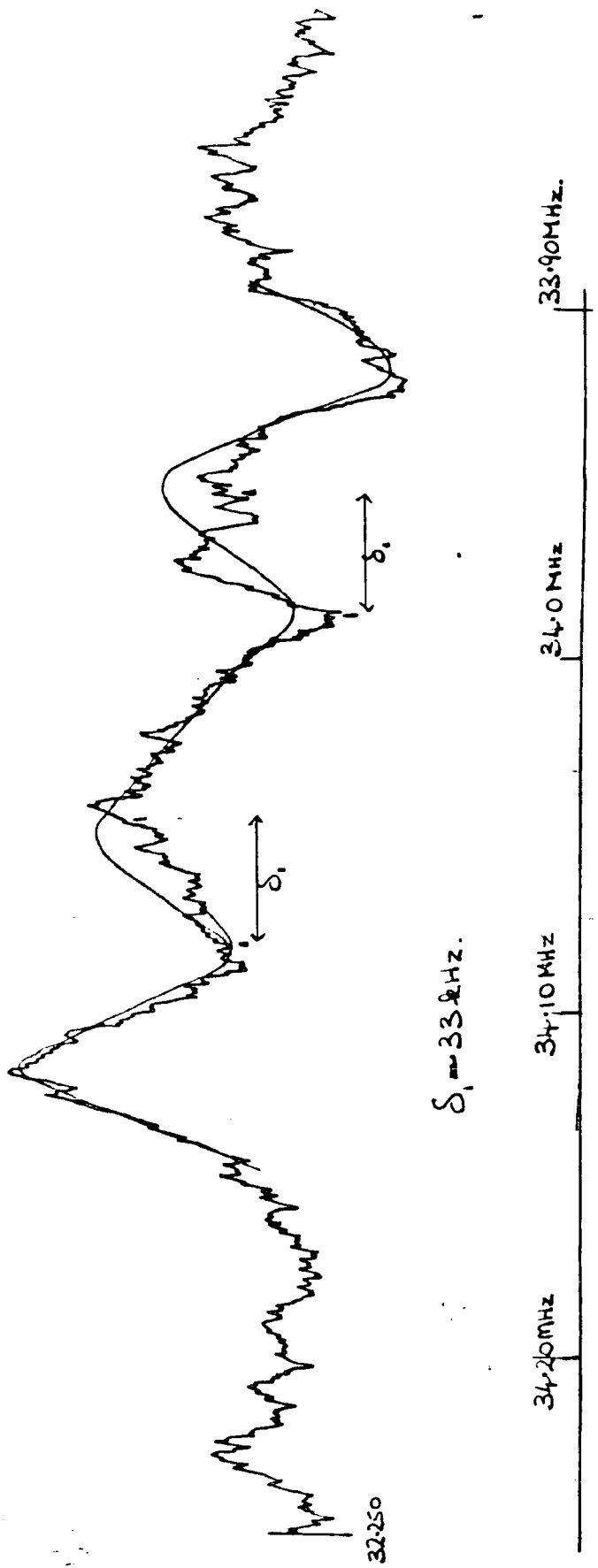


Fig 7c) ^{35}Cl n.p.r. CH_3Cl at 77K. Magnetic field = 1423 mT.



CHAPTER 1 - THEORY OF THE NUCLEAR QUADRUPOLE INTERACTION - REFERENCES

- 1) M.H. Cohen ; Phys.Rev., 96, 1278, (1954)
- 2) A.Abragam ; "The Principles of Nuclear Magnetism", Oxford, (1961)
- 3) C.P. Slichter ; "Principles of Magnetic Resonances", Harper & Row, New York, (1963)
- 4) N.F. Ramsey ; "Nuclear Moments", Wiley, New York, (1953)
- 5) T.C. Wang ; Phys.Rev., 99, 566, (1955)
- 6) Dinesh and J.A.S. Smith ; Adv.Nucl.Quad.Reson., 7, 31 (1974) Heydon, London.
- 7) M.E. Rose ; "Elementary Theory of Angular Momentum", Wiley & Sons, New York, 28, (1957)
- 8)a. J.A.S. Smith ; J.Chem Education, 48, 39, (1971)
b. G.K. Semin, T.A. Babushkina, G.G. Jacobsen ; "Applications of N.Q.R.in Chemistry", (1972)
c. S.L. Segel, R.G. Barnes ; Catalogue Nuc. Quad. Inter. and Resonance Frequencies in Solids, USAEA Report IS-520 I & II
- 9) T. Kushida, Y. Koi, Y. Imada ; J.Phys.Soc., Japan, 9, 809, (1954)
- 10) S. Kojima, T. Tsukada, Y. Hinaga ; J.Phys.Soc., Japan, 10, 498 (1955)
- 11) Y. Morino, T. Chiba, T. Shimozawa ; ibid., 13, 864, (1958)
M. Toyama
- 12) V. Rehn ; J.Chem.Phys., 38, 749, (1963)
- 13) P. Bucci, P. Cecclin, E. Scrocco ; Ric. Scient., 34(IIA), 129 (1964)
- 14) C. Dean ; Phys. Rev., 86, 607, (1952)
- 15) C. Dean, R.V. Pound ; J.Chem.Phys., 20, 195, (1952)
- 16) S. Kojima, K. Tsukada, A. Shimauchi ; J.Phys.Soc.Japan, 9, 795, (1954)
Y. Hinaga
- 17) Y. Morino, M. Toyama ; J.Chem.Phys., 35, 1289, (1961)

- 18) J.D. Graybeal, P.J. Green ; J.Phys.Chem., 73, 2948, (1969)
- 19) Dinesh, P.T. Narasimhan ; J.Chem.Phys., 45, 2170, (1966)
- 20) J.A.S. Smith, D.A. Tong ; J.Chem.Soc.(A), 173, (1971)
- 21) F.J. Adrian ; J.Chem.Phys., 29, 1381, (1958)
- 22) K.V. Raman, P.T. Narasimhan ; Proc.Nuc.Phys. and Solid State
Phys.Symp. 13th, (1968)
- 23) K.V. Raman, J. Jagannathan, ; J.Chem.Phys., 59, 792, (1972)
P.T. Narasimhan
- 24) Dinesh, P.T. Narasimhan ; Proc.Nuc.Phys. and Solid State
Phys.Symp. 11th, 244, (1967)
- 25) C. Dean ; Phys.Rev., 96, 1053, (1954)
- 26) M. Toyama ; J.Phys.Soc.Japan, 14, 1727, (1959)
- 27) R.B. Creel, S.L. Segel, ; J.Chem.Phys., 50, 4908, (1969)
L.A. Anderson
- 28) R.B. Creel, E.D. Von Meerwall ; Mag.Res., 20, 1, (1975)
H.R. Brooker
- 29) Y. Ting, E. Manning, D. Williams ; Phys.Rev., 96, 408, (1954)
- 30) H. Negita ; Inorg. Chem., 5, 2126, (1966)
- 31) J. Ramakrishna ; Phil.Mag., 14, 589, (1966)
- 32) T.P. Das, E.L. Hahn ; Solid State Phys.(Suppl. 1),
"Nuclear Quadrupole Resonance
Spectroscopy," (1958)
- 33) J.F. Baugher, T. Oja, ; J.Chem.Phys., 50, 4914, (1969)
P.C. Taylor, P.T. Bray
- 34) H.R. Brooker, R.B. Creel ; J.Chem.Phys., 61, 3658, (1974)
- 35) H. Bayer ; Z. Physik, 130, 227, (1951)
- 36) M.M. McEnnan, E. Schempp ; "Adv.Nuclear Quad. Resonance",
J.A.S. Smith ed., Vol. 1, p263
Heydon, London, (1974)
- 37) " " ; J.Mag.Res., 11, 28, (1973)

- 38) T. Kushida ; J.Sci. Hiroshima Univ., Ser A19
327, (1955)
- 39) R.N. Hastings, T. Oja ; J.Chem.Phys., 57, 2139, (1972)
- 40) H.D. Stidham ; J.Chem.Phys., 49, 2041, (1968)
- 41) P.N. Yi, A.T. Gavrielides ; J.Chem.Phys., 54, 3777, (1971)
- 42) E. Schempp, P.R.P. Silva ; Phys.Rev., B7, 2983, (1973)
- 43) " " ; J.Chem.Phys., 58, 5116, (1973)
- 44) M.M. McEnnan, E. Schempp ; Bull.Amer.Phys.Soc., 18, 87(1973)
- 45) T. Kushida, G.B. Benedek, ; Phys.Rev., 104, 1364, (1956)
N. Bloembergen
- 46)a. D.B. Utton ; J.Chem.Phys., 47, 371, (1967)
b. M. Kaplansky, M.A. Whitehead ; Canadian J.Chem., 45, 1669, (1967)
- 47) R.J.C. Brown ; J.Chem.Phys., 32, 116, (1960)
- 48) I. Ichishima ; J.Chem.Soc.Japan, 71, 607, (1950)
- 49) J.R. Brookeman, M.M. McEnnan ; Phys.Rev., B4, 3661, (1971)
T.A. Scott
- 50) J.Duchesne ; J.Chem.Phys., 20, 1804, (1952)
- 51) E. Schempp, P.T. Bray ; "Physical Chemistry - an Advanced
Treatise" Vol.IV --Molecular
Properties, Academic Press,(1970)
(H. Eyring, D. Henderson, W.Yost.ed.)
- 52) D. Millen, J. Pannell ; J.Chem.Soc., 1322, (1961)

CHAPTER 2 - INTERPRETATION OF N.Q.R. SPECTROSCOPY - REFERENCES

- 1) T.P. Das, E.L. Hahn ; "Nuclear Quadrupole Resonance Spectroscopy", Academic Press, New York and London, (1958)
- 2) R. Van Wachem, A. Dymanus ; J.Chem. Phys., 46, 3749, (1967)
- 3) J. Kraitchman, B.P. Dailey ; J.Chem. Phys., 22, 1477, (1954)
- 4) R. Bonnacorsi, E. Scrocco, J. Tomasi ; J.Chem. Phys., 50, 2940, (1969)
- 5) A. McLean, M. Yoshimine ; J.Chem. Phys., 47, 3256, (1967)
- 6) R. Sternheimer ; Phys. Rev., 164, 10, (1967)
- 7) E. Scrocco, J. Tomasi ; J.Theoret. Chem. Acta, 2, 386, (1964)
- 8) R. Sternheimer ; Phys. Rev., 105, 158, (1957)
- 9) N.F. Ramsey ; "Molecular Beams", Oxford Univ. Press, London, (1956)
- 10) H. Kopferman ; "Nuclear Moments", Academic Press, New York and London, (1953)
- 11) F.W. Langhoff, R.P. Hurst ; Phys. Rev., 139A, 1415, (1965)
- 12) C.H. Townes, B.P. Dailey ; J.Chem. Phys., 17, 782, (1949)
- 13) F.A. Cotton, C.B. Harris ; Proc. Nat. Acad. Sci., 56 12, (1966)
- 14) R.S. Mulliken ; J.Chem. Phys., 23, 1833, (1955)
- 15) F.A. Cotton, C.B. Harris ; Inorg. Chem., 6, 369/376, (1967)
- 16) C.H. Townes, B.P. Dailey ; J.Chem. Phys., 23, 118, (1955)
- 17) E. Schempp, P.J. Bray ; "Physical Chemistry", Academic Press (1970)
- 18) L. Guibé ; Ann. Phys. (Paris), 7, 177, (1961)
- 19) W. Gordy ; Disc. Faraday Soc., 19, 14, (1955)
- 20) M.A. Whitehead, H.H. Jaffe a) ; J.Chem. Phys., 34, 2204, (1961)
b) ; Theor.Chim.Acta., 1, 209, (1963)

- 21) E.A.C. Lucken ;Zeitschrift Chemie Forschung, 30,
156, (1972)
- 22) J. Ragle, A. Carron ;J.Chem.Phys., 40, 3497, (1964)
J. Ragle, H.W. Dodgen ;J.Chem.Phys., 25, 376, (1956)
J. Ragle ;J.Phys.Chem., 63, 1395, (1959)
- 23) D.E. Woessner, H.S. Gutowsky ;J.Chem.Phys., 39, 440, (1963)
- 24) M. Rouault ;Ann. Physique, 14, 78, (1940)
- 25) D. Clark, H.M. Powell, ;J.Chem.Soc., 642, (1942)
A.F. Wells
- 26) H. Chihara, N. Nakamura ;Bull. Chem. Soc. Japan, 46, 94 (1973)
- 27) H. Chihara, N. Nakamura, ;ibid., 40, 50, (1967)
S. Seki
- 28) R.R. Holmes, R.P. Carter ;Inorg. Chem., 3, 1748, (1964)
G.E. Peterson
- 29) R.R. Holmes ;J.Chem.Phys., 46, 3718, (1967)
- 30) K.B. Dillon, R.J. Lynch ;J.C.S. (Dalton), 1243, (1976)
- 31) P. Thaddeus, L.C. Krisher ;J.Chem.Phys., 40, 257, (1964)
- 32) S. Rottenburg, R.H. Young ;J.Amer.Chem.Soc., 92, 3243, (1970)
H.F. Schaefer
- 33) C.F. O'Konski, Tae-Kyu Ha ;J.Chem.Phys., 49, 5354, (1968)
- 34) P.E. Cade, K.D. Sales ;J.Chem.Phys., 44, 1973, (1966)
A.C. Wahl
- 35) E. Kochanski, J.M. Lehn ;Chem.Phys.Lett., 4, 75, (1969)
B. Levy ;Theoret.Chim.Acta, 22, 11, (1971)
- 36) M. Mackowiak, J. Stanowski ;J.Magn.Res., 33, 41, (1979)
M. Zdanowska
- 37) M. Kaplansky, M.A. Whitehead;Trans. Fara. Soc., 65, 641, (1969)

CHAPTER 3 - EXPERIMENTAL DETECTION OF n.q.r. - REFERENCES

- 1) H.G. Dehmelt, H. Krüger ; Naturwiss., 37, 111, (1950)
- 2) W.G. Clarke ; Rev.Sci.Inst., 35, 316,(1964)
- 3) B. Hertzog, E.L. Hahn ; Phys.Rev., 103, 148, (1956)
- 4) R.V. Pound, W.D. Knight ; Rev.Sci.Inst., 21, 219,(1950)
- 5) B.V. Rollin ; Nature, 158, 669, (1946)
- 6) F.N.H. Robinson ; J. Sci.Inst., 36, 481, (1959)
- 7) D.T. Edmonds, F.N.H.
Robinson ; J.Sci.Inst., 44, 475, (1967)
- 8) K.V. Raman, S. Aravamundham ; Proc. 2nd Int. Symp. on n.q.r.,
P.T. Narasimham ; Viareggio, Ed. A Colligiani,
A. Vallarissi, Pisa,(1973)
- 9) D.A. Tong ; J.Sci.Inst., 1, 1153, (1968)
- 10) M. Read ; "Advances in n.q.r." Ed.J.A.S.
Smith, Heyden & Son, London
(1974) Vol. 1, p203
- 11) H.R. Brooker, W.W. Startup ; Rev.Sci.Inst., 42, 83, (1971)
- 12) R.R. Ernst ; Rev.Sci.Inst., 36, 1689, (1965)
- 13) M.A. Whitehead, R.M. Hart ; Trans.Fara.Soc., 67, 3451,(1971)
- 14) G.M. Muha ; Rev.Sci.Inst., 41, 1238, (1970)
- 15) Y. Morino, M. Toyama ; J.Chem.Phys., 35, 1289, (1961)
- 16) J.A.S. Smith, D.A. Tong ; J. Phys.Ser.E., 1, 8, (1968)
- 17) E.A.C. Lucken ; "Nuclear Quadrupole Coupling
Constants", Academic press,
London, 1969
- 18) E. Schempp, P.J. Bray ; Nuclear quadrupole resonance
Spectroscopy in "Physical
Chemistry, An Advanced Treatise"
- Academic press, (1970)

- 19) H.Y. Carr, E.M. Purcell ; Phys.Rev., 94, 630, (1954)
- 20) A. Abragam ; "The Principles of Nuclear
Magnetism" O.U.P. (1961) p44
- 21) R.E. Slusher, E.L. Hahn ; Phys.Rev., 166, 332, (1968)
- 22) D.T.E. Edmonds, P.A. Speight ; Phys.Letters, A34, 325, (1971)
D.T.E. Edmonds ; Pure & Appl. Chem., 40, 193, (1974)
- 23) E.T. Jones, S.R. Hartmann ; Phys.Rev.(B), 6, 757, (1972)
- 24) D.T.E. Edmonds, A.L. Mackay ; Jour.Mag.Reson., 20, 515, (1975)
D.T.E. Edmonds, S.D. Goren ; *ibid.* 23, 505, (1976)
A.L. Mackay, A.K.L. White
W.F. Sherman

-CHAPTER 4

REFERENCES

- 1) M.A. Whitehead and R.M. Hart ; Trans.Fara.Soc., 67, 3451, (1971)
- 2) T.A. Babushkina, V.S. Levin ; Izv.Akad.Nauk.SSSR., Ser. Khim.,
M.I. Kalinkin, G.K. Semin 2199, (1969) (Eng)
- 3) R.M. Hart, M.A. Whitehead ; Mol.Phys., 19, 383, (1970)
- 4) T.A. Babushkina, M.I. Kalinkin ; Izv.Akad.Nauk.SSSR., Ser.Khim.,
157, (1969)
- 5) E.A. Lucken ; "Nuclear Quadrupole Coupling
Constants", Academic Press,
New York, (1970)
- 6) E. Scrocco ; Adv.Chem.Phys., 5, 319, (1963)
- 7) N.C. Baird, M.A. Whitehead ; Theor.Chim.Acta., 6, 167, (1966)
- 8) B.R. Hollebone ; J.Chem.Soc.(A)., 3008-21, (1971)
- 9) S.N. Nabi, M.A. Khaleque ; J.Chem.Soc., 3626, (1965)
- 10) S.N. Nabi, M.S. Amin ; J.Chem.Soc.(A)., 1018, (1966)
- 11) H.G. Heal, J. Kane ; J.Inorg.Nucl.Chem., 29, 1539,
(1967)
- 12) C. Friedel, J.M. Crafts ; Annales de Chemie et de Physique,
6, 1-530, (1884)
- 13) I.R. Beattie, H. Chudzynska ; J.Chem.Soc(A)., 984, (1967)
- 14) R.M. Hart, L. Krause ; J.Chem.Phys., 56, 3038, (1972)
M.A. Whitehead
- 15) J.R. Partington ; J., 2573, (1929)
- 16) H.E. Doorenbos, J.C. Evans ; J.Phys.Chem., 74, 3385, (1970)
R.O. Kagel
- 17) O. Ruff, H. Golla ; Z.Anorg.Allgem.Chem., 138, 17,
(1924)
- 18) R. Barnes, R. Engardt ; J.Chem.Phys., 21, 248, (1958)
R. Hamlen, W.S. Koski ; ibid., 25, 360, (1956)

- 19) J.A. Creighton, J.R.S. Green ; J.Chem.Soc.(A.), 808, (1968)
- 20) M.P. Jaillard ; Annales de Chimie et Physique,
Ser.3, 59, 454, (1860)
- " ; Comptes Rendus, T50, 149
- 21) T. Chiba ; J.Phys.Soc.Japan, 13, 860 (1958)
- 22) D. Biedenkapp, A. Weiss ; Z.Naturforsch., 19a, 1518, (1964)
- 23) R.J. Lynch ; Ph.D.Thesis, University of
Warwick, 1972.
- 24) T. Okuda, K. Yamada ; Bull.Chem.Soc.Japan, 48,
Y. Furukawa, H. Negita 392, (1975)
- 25) B. Krebs, E. Huss, D. Altena ; Z.Anorg.Allg.Chem., 386, 257,
(1971)
- 26) V.V. Saatsazov, T.L. Khotsyanova ; Izv.Akad.Nauk.SSSR, 23, 2754
K.N. Magdesieva, S.I. Kuznetsov (1974) (Eng.)
I.M. Alymov, A.A. Ryandziketsian,
E.V. Bryukhova
- 27) A.E. Burg, R.L. Ross ; J.Amer.Chem.Soc., 65, 1637(1943)
- 28) R. Newley, R.S.R. Kurty, L... Sunden ; Trans.Fara.Soc., 56, 1732, (1960)
- 29) E.M. Neumar, A.W. Jaché ; J.Chem.Phys., 32, 596, (1963)
- 30) Y. Morino, K. Toyama ; J.Chem.Phys., 35, 1289, (1961)
- 31) A. Finch, F.N. Gates, P.H. Pate ; Inorganica Chimica Acta.,
25, 149, (1977)
- 32) R. Livingston ; J.Phys.Chem. 57, 496, (1953)
- 33) Z.A. Fokina, S.E. Kuznetsov ; Coord.Chim., 2, 1235, (1977)
E.V. Erukova, E.E. Timochenko
- 34) A.C. Edwards ; J.C.S. (Dalton), 1723, (1978)
- 35) R.J. Gillespie, L... Robinson ; Can.J.Chem., 38, 2171, (1961)
- 36) H. Gerdine, P.Hautgraaf ; Rec.Trav.Chem., 72, 21, (1953)

- 37) K.B. Dillon, T.C. Waddington; *Inorg.Nucl.Chem.Lett.*, 14, 415 (1978)
- 38) Y. Kurita, D. Nakamura ; *J.Chem.Soc.Japan, Pure Chem.Soc.*,
N. Nayakawa 79, 1093, (1953)
- 39) H.J. Elema, J.L. de Boer, A. Vos; *Acta. Cryst.*, 16, 243, (1963)
- 40) B.O. Cozzini ; *Diss.Abs.B.*, 27, 1850, (1966)
- 41) M. Feuerhahn, R. Minkwitz ; *Z.anorg.Allgem.Chem.*, 426, 247 (1976)
- 42) A. Finch, P.N. Gates, T.H. Page; *J.C.S.(Dalton)* as yet unpublished
K.B. Dillon, T.C. Waddington
- 43) G. Mamantov, R. Marassi ; *J.Inorg.Nucl.Chem.*, 41, 260 (1979)
F. Poulsen, S.E. Springs, J.P.
Wiaux, R. Haglen, N.R. Smyrl
- 44) W.S. Sawodny, K. Dehnicke ; *Z.anorg.Allgem.Chem.*, 349, 169 (1967)
- 45) V. Gutmann, A. Maschka, R. Sponer; *Mh.Chem.*, 86, 52, (1955)
- 46) H. Gerding ; *Chem.Weekbl.*, 92, 204, (1956)
- 47) J.A. Creighton, J.H.S. Green ; *J.Chem.Soc.(A)*, 808, (1968)
- 48) H. Stammreich, R. Fornieris ; *Spectrochim.Acta*, 16, 363, (1960)
- 49) D.J. Millen, D. Watson ; *J.Chem.Soc.*, 1369, (1957)
- 50) T.A. Zavaritskaya ; *Titani Ego.Splavy Akad.Nauk*,
Inst.Met., 5, 195, (1961)

CHAPTER 5 - N.S.R. INVESTIGATION OF ZINC CHLORIDE AND SOME

COMPLEXES - REFERENCES

- 1) D. E. Scaife ; Aust. J.Chem., 24, 1315, (1971)
- 2) W.J. Asker, D.E. Scaife,
J.A. Watts ; Aust. J.Chem., 25, 2301, (1972)
- 3) M. Farnworth, C.H. Kline ; "Zinc Compounds", Zinc Develop-
ment Association, London, (1973)
- 4) H.R. Oswald, H. Jaggi ; Helv. Chim.Acta., 43, 72, (1960)
- 5) T.J. Bastow, H.J. Whitfield ; Aust. J.Chem., 27, 1397 (1974)
- 6) C.H. McGillavry, J.M. Bijvoet ; Z.Krist., A94, 249, (1963)
- 7) W.E. Hatfield, J.T. Yorke ; Inorg.Chem., 1, 463, (1962)
- 8) M. Goldstein, E.F. Mooney ; J.Inorg.Nucl.Chem., 27, 1601, (1965)
C.W. Frank, L.B. Rogers ; Inorg.Chem., 5, 615, (1966)
C.W. Reimann, S. Block,
A. Perloff ; Inorg.Chem., 5, 1185 (1966)
- 9) R.J. Kern ; J.Inorg.Nucl.Chem., 24, 1105 (1962)
- 10) G. Wulfsberg, A. Weiss ; J.C.S. (Dalton), 1640, (1977)
- 11) J.C. Barnes, C.S. Duncan ; J.C.S.(A), 1746, (1969)
- 12) G.W. Fowles, D.A. Rice,
R.A. Walton ; J.C.S.(A), 18-2, (1968)
- 13) J.C. Barnes ; J.Inorg.Nucl.Chem., 31, 95, (1969)
- 14) G.W. Fowles, D.A. Rice,
R.A. Walton ; Spectrochim.Acta., 26^A, 143, (1970)
- 15) J.C. Barnes, C.S. Duncan ; J.C.S.(A), 1442, (1970)
- 16) J.C. Barnes ; Inorg.Chim.Acta., 7, 404, (1973)
- 17) A. Ramsey ; Proc.Roy.Soc., 190A, 562, (1947)
- 18) O. Hassel, E. Viervoll ; Acta.Chem.Scand., 1, 149, (1947)
F.B. Malherbe, E.J. Berstein ; J.Amer.Chem.Soc., 74, 4408, (1952)
R.B. Marsh ; Acta Cryst, 8, 91, (1955)

- 19) P.J. Hendra, D.B. Powell ; J.C.S. 5105, (1960)
- 20) G.W. Fowles, D.A. Rice,
R.A. Walton ; J.Inorg.Nucl.Chem.,31,3119, (1969)
- 21) L.F. Hatch, G.D. Everett ; J.Org.Chem.,33, 2551, (1968)
- 22) R. Iwamoto ; "Structural Studies of crystalline complexes of Poly-(ethylene oxide) and its Oligomers with mercuric chloride", Government Industrial Research Institute Report No. 342, Osaka, (1972).
- 23) J.C. Barnes ; Inorg.Nucl.Chem.Lett, 13,153, (1977)
- 24) O. Hassel, J.Hvoslef ; Acta.Chem.Scand,8, 1953, (1954)
- 25) L.W. Daasch ; Spectrochim.Acta, 15,726, (1959)
- 26) R. Juhasz, L.F. Yntema ; J.Amer.Chem.Soc.,62,3522, (1940)
- 27) M. Goldstein, W.D. Unsworth; J.Mol.Struct., 14,451, (1972)
- 28) G. Wulfsberg ; Inorg.Chem., 15, 1791, (1976)
- 29) D.E.C. Corbridge, E.G. Cox,
J.S. Judge, W.M. Ruff,
G.M. Intille ; J.C.S., 594, (1956)
- 30) P. Ballway, W.A. Baker et al; J. Inorg.Nucl.Chem.,29,1711, (1967)
- 31) M. Gerloch ; J.Chem.Soc.(A), 1318, (1966)
- 32) J.S. Judge, W.A. Baker jnr.; Inorg.Chim.Acta,1, 239, (1967)
- 33) A. Ferrari, A. Braibanti,
G. Bigliardi ; Acta Cryst.,16, 498, (1963)
- 34) " , A.M. Lanfredi ; Acta Cryst., 18, 367, (1965)
- 35) K. Krishnan, R.A. Plane ; Inorg.Chem.,5, 852, (1966)
- 36) G. Newman, D.B. Powell ; J.C.S., 477, (1961)
- 37) A.B. Ablov, T.I. Malinovski; Dokl.Akad.Nauk.SSSR,123,677, (1958)
- 38) Y.N. Hsieh, G.V. Rubenacker,
T.L. Brown, C.P. Chang ; J.Amer.Chem.Soc., 99, 1384, (1977)

- 39) N.S. Gill, R.S. Nyholm ; J.Inorg. nucl.Chem., 18, 88, (1961)
- 40) D.H.Brown, R.N. Nuttall,
D.W.A. Sharp ; J.I.N.C., 26, 1151, (1964)
- 41) R.G. Snyder, G. Zerbi ; SpectrochimActa, 23A, 391, (1967)
- 42) R. Oswald ; Helv.Chim.Acta, 43, 77, (1960)
- 43) L. Guibe, M.C. Montabonel ; J.Magn.Res., 31, 419, (1978)
- 44) S. Basu ; Indian J.Chem., 16A, 245, (1978)
- S. Basu ; ibid., 16A, 246, (1978)
- 45) W. Fichtner, A. Weiss ; Z. Naturforsch, 31B, 1626 (1976)
- 46) R.W.G. Wyckoff ; "Crystal Structures", 2nd ed., Vol. I,
Interscience, New York, 1963

CHAPTER 6 - N.Q.R. INVESTIGATION OF GROUP IV TETRACHLORIDES -
REFERENCES

- 1) L.P. Brockway, F.T. Wall ; J.Amer.Chem.Soc., 56, 2373, (1934)
- 2) E.A.V. Ebsworth ; "Volatile Silicon Compounds",
Pergamon Press, Oxford, (1963)
- 3) F.G.A. Stone, D. Seyforth ; J.Inorg.Nucl.Chem., 1, 112, (1955)
- 4) D.P. Craig, A. McCall, ; J.Chem.Soc., 332, (1954)
R.S. Nyholm, L.E. Orgel,
L.E. Sutton
- 5) R. Livingston ; J.Phys.Chem., 57, 496, (1953)
- 6a) L. Pauling ; "The Nature of the Chemical Bond", (1948)
Cornell University Press, Ithaca, N.Y.
- 6b) A.L. Allred, E.G. Rochow ; J.Inorg.Nucl.Chem., 5, 264, (1958)
- 7) G.K. Semin, T.A. Babushkina, ; "The Application of Nuclear Quadrupole
G.G. Yakobson Resonance to Chemistry", (Russ.),
Khimiya, Leningrad, (1972)
- 8) R.Varma, A.G. MacDiarmid, ; Inorg.Chem., 3, 1754, (1964)
J.G. Miller
- 9) W.B. Goldfarb, S. Sujishi ; J.Amer.Chem.Soc., 86, 1679, (1964)
- 10) D.R. Jenkins, R.Kewley, ; Trans.Fara.Soc., 58, 1284, (1962)
T.M. Sugden
- 11) J.E. Griffiths, L.B. McAfee ; Proc.Chem.Soc., 456, (1961)
- 12) I.P. Biryukov, M.G. Voronkov, ; Akad.Nauk.Ukr. SSR., 1, 373, (1965)
I.A. Safin
- 13) I.P. Biryukov, M.G. Voronkov, ; Izvest.Akad.Nauk.Latv. SSR., 1, 115 (1965)
- 14) G.K. Semin, E.V. Bryuchova ; Chem.Comms., 605, (1968)
- 15) R.W. Taft ; J.Phys.Chem., 64, 1805, (1960)
- 16) H.O. Hooper, P.J. Bray ; J.Chem.Phys., 33, 334, (1960)
- 17) G.K. Semin, A.A. Boguslowskii ; Izv.Akad.Nauk.SSSR., 39, 2548, (1975)
E.V. Bryuchova, V.P. Kazakov
- 18) G.K. Semin, V.F. Kazakov, ; Teoreticheskaya i Eksperimental'naya
E.V. Bryuchova Khimiya, 13, 77, (1977)

- 19) N. Bloembergen ; Science, New York, 133, 1363, (1961)
- 20) R.W. Dixon, N. Bloembergen ; J.Chem.Phys., 41, 1720, (1964)
- 21) De Bertha ; PhD Thesis, West Virginia Univ., (1967)
- 22) T.A. Babushkina, V.I. Robas ; "Radiospektroskopia Tverdo o Tela",
G.K. Semin ; Atomizdat, (1967)
- 23) H. Gutowsky, D. McCall ; J.Chem.Phys., 32, 548, (1959)
- 24) T.A. Babushkina, V.V. Saatsazov; Yad.Kvadrupolnyi Reson, 1, 85, (1976)
T.L. Khotsyanova, G.K. Semin
- 25) J.D. Graybeal, P.J. Green ; J.Phys.Chem., 73, 2948, (1969)
- 26) Y. Morino, M. Toyama ; J.Chem.Phys., 35, 1289, (1961)
- 27) J.M. Mays, B.P. Dailey ; J.Chem.Phys., 20, 1695, (1952)
- 28) K. Shimomura ; J.Phys.Soc.Japan, 12, 657, (1957)
- 29) V.P. Brand, H. Sackmann ; Acta.Cryst., 16, 446, (1963)
- 30) S. Cohen, R.F. Powers, R.Rudman; Acta Crystallogr., Sec.B, 35B, 1670, (1979)
- 31) E.A. Lucken ; "Nuclear Quadrupole Coupling Constants"
Academic Press, New York, (1970)
- 32) J. Darville, A. Gerard et al. ; J.Mag.Res., 16, 205, (1974)
- 33) H.R. Brooker, R.B. Creel ; J.Chem.Phys., 61, 3658, (1974)
- 34) M.A. Whitehead, H. Jaffé ; Theor.Chim.Acta., 1, 209, (1963)
- 35) R. Bersohn ; J.Chem.Phys., 22, 2078, (1954)
- 36) J.R. Granada, G.W. Stanton, ; Mol.Phys., 37, 1297, (1979)
J.H. Clarke, J.C. Dore
- 37) S.F. Andrews, P.E.R. Badger, ; J.Chem.Res., 94, (1978)
P.L. Goggin, N.W. Hurst,
A.J.E. Rattray
- 38) M.A. Whitehead, H.H. Jaffé ; Theoretica Chim.Acta, 1, 209, (1963)
- 39) K. Shimomura ; J.Sci.Hiroshima Univ., Ser.A, 17, 383,
(1954)
- 40) Dinesh, P.T. Narasimhan ; J.Chem.Phys., 45, 2170, (1966)
- 41) K.V. Raman, P.T. Narasimhan ; Pure and Applied Chemistry, 32, 271 (1972)

- CHAPTER 7 -

THE ASYMMETRY PARAMETER IN THE P-Cl BOND - REFERENCES

- 1) D.L. McCall, R.S. Gutowsky ; J.Chem.Phys., 21, 1300, (1953)
- 2) H. Chihara, N. Ishimura, S. Seki ; Bull.Chem.Soc.Japan, 40, 50, (1967)
- 3) H. Kaplanky, L.A. Whitehead ; Canadian J. Chem., 45, 1669, (1967)
- 4) V.I. Svergun, V.G. Rozinov, ; Izv.Akad.Nauk SSSR., Ser.Chim., 8,
E.F. Greshkin, V.G. Titchkin, 1918, (1960)
U.A. Maksyumin, G.N. Semin
- 5) K.B. Dillon, R.J. Lynch, ; J.C.S. (Dalton), 1243, (1971)
T.C. Waddington
- 6) E.A.C. Lucken ; "Nuclear Quadrupole Coupling
Constants", Academic Press, London,
(1969)
- 7) R.J. Lynch ; PhD Thesis, Univ. of Warwick, (1972)
- 8) L. Desautel ; Ann.Phys., 14, 78, (1940)
- 9) R.J. Lynch, T.C. Waddington ; "Advances in n.o.r.", Ed. J.A.S.
Smith, Heyden and Son, London (1974),
Vol. 1, p. 40
- 10) K.B. Dillon, R.J. Lynch ; J.C.S. (Dalton), 1478, (1976)
T.C. Waddington

THE ⁵⁹Co N.M.R. OF η^5 -CYCLOPENTADIENYL-COBALT-DICARBONYL - REFERENCES

- 1) G.K. Semin, T.A. Babushkina ; "Application of E.R in Chemistry",
G.G. Yakobson Khimiya, Leningrad, (1972)
- 2) E.O. Fischer, K.S. Brenner ; Z. Naturforsch., B17, 774, (1962)
- 3) D.J. Cook, J.L. Davies ; J.Chem.Soc., (A), 1547, (1967)
R.D.W. Kemmitt
- 4) F. Rocquet, L. Berrely ; Spectrochim.Acta., 29A, 1101, (1973)
J.P. Marsault
- 5) I.W. Nowell, D.R. Russell ; J.C.S.(Dalton), 2393, (1972)
; ibid., 2396, (1972)

CHLOROMETHANES - REFERENCES

- 1) Dinesh, P.T. Narasimhan ; Proc.Nuclear Physics/ Solid State
Physics, 11th Symp., Kanpur, India (1967)
- 2) Dinesh, P.T. Narasimhan ; J.Chem.Phys., 49, 2519, (1968)
- 3) Y. Morino, M. Toyama ; J.Chem.Phys., 4, 1289, (1961)
- 4) J.D. Graybeal, P.J. Green ; J.Phys.Chem., 73, 2948, (1969)
- 5) H.S. Gutowsky, D.W. McCall ; J.Chem.Phys., 32, 548, (1960)
- 6) T.A. Babushkina, G.K. Semin; J.Struct.Chem., 7, 107, (1966)(Eng)
- 7) G.L. Minott, J.L. Ragle ; J.Mag.Res., 21, 247, (1976)
- 8) D.E. Woessner, H.S.Gutowsky; J.Chem.Phys., 39, 440, (1963)
- 9) J.L. Ragle ; J.Chem.Phys., 50, 3555, (1969)
- 10) M.P. Marzocchi, P.Manzelli ; J.Chem.Phys., 52, 2638, (1970)
- 11) J. Simmons, J. Goldstein ; J.Chem.Phys., 20, 122, (1952)

